Abstract

Cell migration is a highly coordinated process and any aberration in the regulatory mechanisms could result in pathological conditions such as cancer. The ability of cancer cells to disseminate to distant sites within the body has made it difficult to treat. Cancer cells also exhibit plasticity that makes them able to interconvert from an elongated, mesenchymal morphology to an amoeboid blebbing form under different physiological conditions. Blebs are spherical membrane protrusions formed by actomyosin-mediated contractility of cortical actin resulting in increased hydrostatic pressure and subsequent detachment of the membrane from the cortex. Tumour cells use blebbing as an alternative mode of migration by squeezing through preexisting gaps in the ECM, and bleb formation is believed to be mediated by the Rho-ROCK signaling pathway. However, the involvement of transmembrane water and ion channels in cell blebbing has not been examined. In the present study, the role of the transmembrane water channels, aquaporins, transmembrane ion transporters and lipid signaling enzymes in the regulation of blebbing was investigated. Using 3D matrigel matrix as an *in vitro* model to mimic normal extracellular matrix, and a combination of confocal and time-lapse microscopy, it was found that AQP1 knockdown by siRNA ablated blebbing of HT1080 and ACHN cells, and overexpression of AQP1-GFP not only significantly increased bleb size with a corresponding decrease in bleb numbers, but also induced bleb formation in non-blebbing cell lines. Importantly, AQP1 overexpression reduces bleb lifespan due to faster bleb retraction. This novel finding of AQP1-facilitated bleb retraction requires the activity of the Na^+/H^+ pump as inhibition of the ion transporter, which was found localized to intracellular vesicles, blocked bleb retraction in both cell lines. This study also demonstrated that a differential regulation of cell blebbing by AQP isoforms exists as knockdown of AQP5 had no effect on bleb formation. Data from this study also demonstrates that the lipid

signaling PLD2 signals through PA in the LPA-LPAR-Rho-ROCK axis to positively regulate bleb formation in both cell lines. Taken together, this work provides a novel role of AQP1 and Na^+/H^+ pump in regulation of cell blebbing, and this could be exploited in the development of new therapy to treat cancer.

Acknowledgements

First of all, I would like to express my profound gratitude to my supervisor Dr Phil Dash for painstakingly taking time to guide, support, encourage and inspire me in the course of my PhD in the Cell migration lab. This work would not have been possible without his inestimable help. I am grateful to my past lab member, Dr. Ibrahim Barnawi, and my current lab members: Mr Mahmoud A. Chawsheen, Ms Shirley Keeton, Miss Kelsey Huang, Mr Jonathan Rudge, Miss Ana Wass, Mr Dhurgham Al-Fahad and Mr Khatab Mawlood for their excellent support, understanding and friendship. A big thank you to Dr. Henry Collins-Hooper for all his support and help. The technical support and advice I got from Dr. Graham Luke, Mr Dave Butlin and Mrs Hong Lin is well appreciated. I am indebted to my supervisory committee members, Dr Sam Boateng and Dr Mike Fry for their time, advice and corrections. Thanks to Dr G.T. Charras (UCL) and Dr Matthew Conner (Sheffield Hallam University) for some of the plasmids used in this work. My warm regards also goes to the Molecular and Cellular Medicine (MCM) unit of the School of Biological Sciences, University of Reading for the unique opportunity to pursue my PhD at the Cell migration lab.

My special thanks go to my elder brother Mr Goodluck Ebelo, who believed in me, stood by me and made it possible for me to pursue my postgraduate studies in the United Kingdom. My sincere thanks also go to my parents, Hon. Aaron Ponuwei Ebelo and Mrs Deborah Ebelo, and to my siblings and friends for their prayers and encouragement.

Special thanks to my precious wife, Mrs Efe Ponuwei for her love, care, support and prayers in the course of my studies.

Above all, I am grateful to God for strengthening me and for the enabling grace to carry on in the midst of the challenges of PhD. This work is dedicated to my unborn children. I hope it inspires them to become better scientists in future.

Table of contents

List of Figures

List of Tables

List of abbreviations

2D	Two dimensional
3D	Three dimensional
ANOVA	Analysis of variance
APS	Ammonium persulphate
AQP(s)	Aquaporin(s)
Arf1/6	ADP-ribosylation factor 1/6
ASICs	Acid-sensing ion channels
BB-94	Batimastat
BMT	Bumetanide
BSA	Bovine serum albumin
CAF	Cancer associated fibroblast
CaM	Camodulin
Camodulin	Calcium-modulated protein
Cdc42	Cell division control protein 42
CHO	Chinese hamster ovary
DAG	Diacylglycerol

DAPI	4,6-diamidino-2-phenylindole
DAPK	Death associated protein kinase
DCPIB	4-(2-butyl-6,7-dichoro-2-cyclopentyl-indan-1-on-5-yl) oxobutyric acid
DIP	Diaphanous-interacting protein
DMEM	Dulbecco's modified eagle's medium
DMSO	Dimethyl sulfoxide
DNA	Deoxyribonucleic acid
ECL	Enhanced chemiluminescence
ECM	Extracellular matrix
EDTA	Ethylenediaminetetraacetic acid
EGF	Epidermal growth factor
EIPA	5-(N-Ethyl-N-isopropyl) amiloride
EMT	Epithelial-mesenchymal transition
ERK	Extracellular signal-regulated kinase
ERM	Ezrin radixin moesin
FAK	Focal adhesion kinase
FBS	Foetal bovine serum
FGF	Fibroblast growth factor

FH1/2	Formin homolog 1/2 domains
FIPI	5-fluoro-2-indolyl des-chlorohalopemide
FITC	Fluorescein isothiocyanate
FMNL1	Formin-like protein 1
GAP	GTPase activating protein
GDP	Guanosine diphosphate
GEF	Guanine nucleotide exchange factor
GFP	Green fluorescent protein
GFRs	Growth factor receptors
Go6976	5,6,7,13-tetrahydro-13-methyl-5-oxo-12H-indolo[2,3-α]pyrole[3,4-c] carbazole-12-propanenitrile
GPCRs	G-protein coupled receptors
Grb2	Growth factor receptor bound protein 2
GTP	Guanosine triphosphate
H-89	(N-[2-(p-bromocinnamylamino)ethyl]-5-isoquinolinesulfonamide)
HEK293	Human embryonic kidney 293
HEPES	4-(2-hydroxyethyl)-1-piperazineethanesulfonic acid
HGF	Hepatocyte growth factor

IGF-1	Insulin-like growth factor 1
IP_3	Inositol triphosphate
IR	Insulin receptor
LB	Luria-Bertani
LOK	Lymhocyte-oriented kinase
LPA	Lysophosphatidic acid
LPAR	LPA receptor
LY294002	2-(4-morpholinyl)-8-phenyl-4H-1-benzopyran-4-one hydrochloride
MAPK	Mitogen-activated protein kinase
mDia1	mammalian Diaphanous 1
MEF	Mouse embryonic fibroblasts
MLC	Myosin light chain
MLCK	MLC kinase
MMP	Matrix metalloproteinase
MRLC	Myosin regulatory light chain
MT1-MMP	Membrane-type 1 MMP
mTOR	Mammalian target of rapamycin
mTORC1/1	mTOR complexes 1/2

MTT	3-(4, 5-dimethylthiazolyl-2)-2,5-diphenyltetrazolium bromide
NCX1	Sodium calcium exchanger 1
NF-κB	Nuclear factor kappa B
NHE	Sodium Hydrogen Exchanger
NHERF	NHE regulatory factor
N-WASP	Neuronal Wiskott-Aldrich syndrome protein
OD_{600}	Optical density measured at 600 nm
PA	Phosphatidic acid
PAGE	Polyacrylamide gel electrophoresis
PAK	p27-activated kinase
PBS	Phosphate bovine saline
PC	Phosphatidylcholine
PDGF	Platelet-derived growth factor
PDZ	Postsynaptic density 95
PEI	Polyethylenimine
PFA	Paraformaldehyde
PH	Pleckstrin homology
PIC	Protease inhibitor cocktail

PI3K	Phosphoinsitide-3-kinase
PIP_2	Phosphoinositide 4,5-bisphosphate
PIP_3	Phosphoinsitide 3,4,5-triphosphate
PIP5K	Phosphatidylinositol 4-phosphate 5-kinase
PKA	Protein kinase A
PKB	Protein kinase B
PKC	Protein kinase C
$PLA_{1/2}$	Phospholipase A1/2
PLC	Phospholipase C
PLD	Phospholipase D
PMA	Phorbol 12-myristate 13-acetate
PTEN	Phosphatase and tensin homolog deleted on chromosome ten
PVDF	Polyvinylidene fluoride
Rac1	Ras-related C3 botulinum toxin substrate 1
RFP	Red fluorescence protein
Rheb	Ras homolog enriched in brain
RhoA/B/C	Ras homolog gene family, member A/B/C
RIPA	Radio-Immunoprecipitation Assay

RNA	Ribonucleic acid
RNAi	RNA interference
ROCK	Rho-associated, coiled-coil containing protein kinase
RSK	p90 ribosomal protein S6 kinase
RTKs	Receptor tyrosine kinases
SDF-1	Stromal cell-derived factor 1
SDS	Sodium dodecyl sulphate
siRNA	Small interfering RNA
Src	Sarcoma
TEMED	N N N'N'-tetramethylethylenediamine
TGFβ	Transforming growth factor β
TRITC	Tetramethylrhodamine
TSC	Tuberous sclerosis complex
U73122	(1-(6-((17β-3-methoxyestra-1,3,5(10)-trien-17-yl)amino)hexyl)-1H-pyrole-2,5-dione)
uPA	Urokinase plasminogen activator
uPAR	uPA receptor
VEGF	Vascular endothelial growth factor

VPC 32183	(S)-phosphoric acid mono-[2-octadec-9-enoylamino-3-(4-(pyridin-2-ylmethoxy)-phenyl)-propyl] ester
WASP	Wiscott-Aldrich syndrome protein
WB	Western blotting
Wnt	Wingless, integration
Y-27632	Trans-4-[(1R)-1-aminoethyl]-N-4-pyridinylcyclohexanecarboxamide dihydrochloride

Chapter 1: General Introduction

1.1 Introduction to Cancer

Cancer, a collection of diseases characterized by the common features of unregulated increase in cell number, invasion and metastasis remains a major health challenge in that the ability of the cells to spread to distinct anatomical sites has made it difficult to treat. Cancer is caused by activation of oncogenes or impaired tumour suppressor genes which result from somatic mutations (Steeg, 2006; Valastyan and Weinberg, 2011).

During multistep tumourigenesis, cancer cells acquire aberrant traits which confer on them the ability to defy normal growth regulatory mechanisms (Hanahan and Weinberg, 2000). Apart from cancer cells, contained within the tumour microenvironment are different cell types (stromal cells) such as cancer associated fibroblasts (CAFs), endothelial cells, pericytes and immune cells which interact together to promote the acquisition of the acquired traits. These acquired phenotypes, referred to as the hallmarks of cancer (Hanahan and Weinberg, 2011) (figure 1.1) are caused by either loss or gain of part or whole chromosomes giving rise to chromosomal instability or by a series of random mutations in DNA resulting in genomic instability. Similarly, immune cell-driven inflammation can lead to the acquisition of the cancer hallmarks (Negrini et al., 2010).

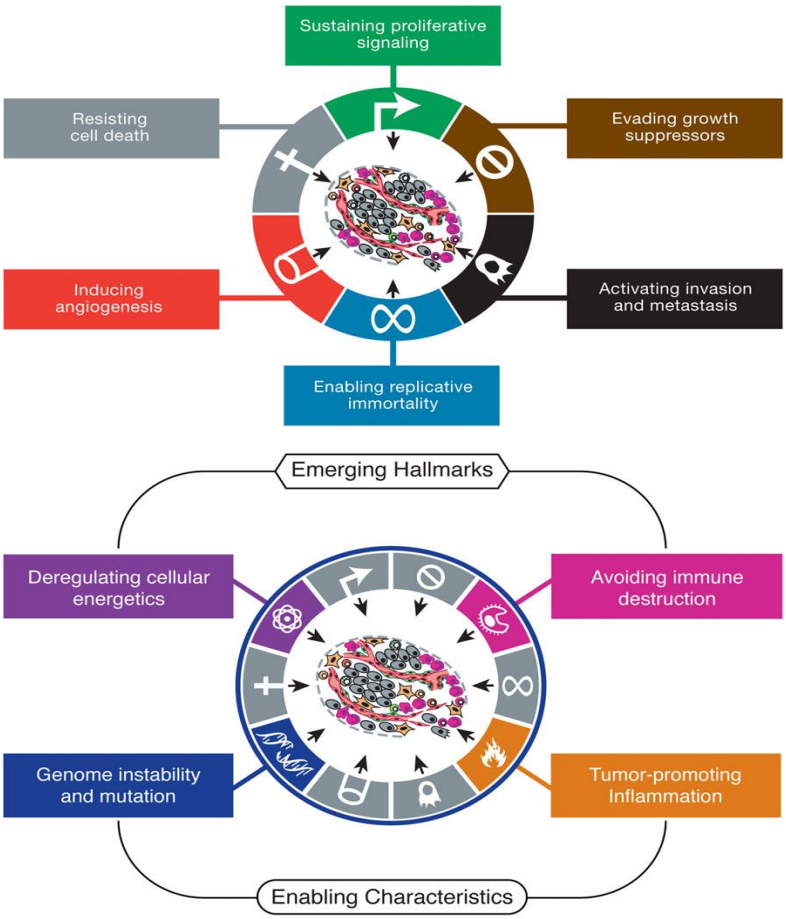

Figure 1.1: The Hallmarks of cancer. These acquired capabilities are changes in the physiological functions of a normal cell and are believed to govern the transformation of normal non-neoplastic cells into malignant tumour, and confer tumour cells the capabilities to metastasize and colonize their secondary site. Top and bottom figures represent the original six and two new emerging hallmarks respectively (Taken from Hanahan and Weinberg, 2011).

Normal cells and tissues proliferate in a controlled manner upon stimulation by mitogenic growth signals which dictate entry into the different phases of the cell cycle in order to ensure

a balance in cellular organization. These growth factors upon binding to their surface receptors such as the receptor tyrosine kinases (RTKs) coordinate biological processes such as apoptosis and energy metabolism via activation of cascade of intracellular pathways (Hanahan and Weinberg, 2011). In contrast, cancer cells show little or no dependence on normal growth signals and they not only produce their own growth factors but also acquire the ability to sustain this capability (Lemmon and Schlessinger, 2010). Cancer cells become independent of growth signal in a variety of ways. For instance, their ability to alter extracellular growth signals and thus, synthesize their own growth factors which constitutively act on their surface receptors (autocrine stimulation) rather than the heterotypic signaling found in normal cells (Cheng et al., 2008). Signaling by cancer cells to cells of the tumour microenvironment also results in release of growth factors that sustain the aberrant proliferation of cancer cells (Bhowmick et al., 2004). Similarly, in most cancer cells, there is overexpression of growth factor receptors (GFRs) which leads to amplification of growth signals that would not have caused proliferation in normal cells. Overexpression as well as modification of the structure of growth factors receptors by cancer cells could also result in signaling even in the absence of ligands (Hanahan and Weinberg, 2011). Growth factor autonomy leading to constitutive activation also results from mutations in downstream effectors of signaling pathways. For example, mutation of Raf protein can lead to aberrant signaling through the MAP kinase pathway (Davies and Samuels, 2010). Cancer cells can also modify their surface integrins to transmit only growth signals (Giancotti and Ruoslahti, 1999).

In cancer cells, there is inactivation of tumour suppressors which renders the cells insensitive to antigrowth signals. The retinoblastoma tumour suppressor (Rb) which directs and transduces most extracellular signals to regulate the restriction point of the cell cycle

(Burkhart and Sage, 2008; Deshpande et al., 2005), is defective in cancer cells thereby allowing excessive cell proliferation. Similarly, the P53 tumour suppressor protein which acts as a genotoxic stress sensor and an inducer of apoptosis and cell cycle arrest is often inactivated in most cancers (Levine, 1997), and this also results in hyper-proliferation. When a cell is exposed to genotoxic conditions such as DNA damage and chromosomal abnormalities, P53 activates pro-apoptotic proteins such as Noxa and PUMA which trigger the apoptotic program (Junttila and Evan, 2009). Besides inactivating the functions of P53, tumour cells also overcome programmed cell death by upregulating the levels of Bcl-2 and Bcl-x_L which are known anti-apoptotic proteins (Hanahan and Weinberg, 2011).

Usually, normal cells in the body only undergo a controlled number of successive cell divisions and replications due to tight regulatory mechanisms which impose two different hurdles for cells to proliferate. Firstly, constant cycles of cell division make normal cells go into senescence – a quiet and non-proliferative phase in which cells still remain viable, and secondly, cells that escape senescence go into crisis phase in which massive cell death occurs. In very rare situations, some of the cells may survive both barriers to acquire immortalization in which the cells demonstrate unlimited replicative potentials (Hanahan and Weinberg, 2011). This unlimited proliferation in normal non-immortalized cells is kept in check by telomeres that protects the ends of chromosomes. These telomeres gradually become decreased to an extent that they no longer possess the ability to protect the chromosomal ends from end-to-end fusion, and since non-immortalized cells lack telomerase (a DNA polymerase that maintains telomeric DNA by adding telomere repeats to telomeric DNA ends), the cells go into the crisis phase (Hanahan and Weinberg, 2011). However, in cancer cells the activity of telomerase is highly upregulated. Thus, the gradual reduction which occurs at telomeric DNA ends of normal cells is bypassed by cancer cells and this confers

them an indefinite replicative potential and immortalization (Bryan and Cech, 1999). TERT, a component of telomerase has been shown to stimulate the Wnt signaling pathway by activating β-catenin/LEF transcription factors, and this eventually leads to cell proliferation (Park et al., 2009).

Having acquired unlimited replicative potentials, cancer cells then acquire the ability to induce and sustain angiogenesis through upregulation of angiogenic factors such as vascular endothelial growth factor (VEGF) and fibroblasts growth factor (FGF), and downregulation of angiogenic inhibitors such as thrombospondin-1 and β-interferon (Baeriswyl and Christofori, 2009). This ensures the survival of cancer cells through the stimulation of formation and development of new blood vessels from preexisting ones which supply oxygen and other nutrients to the cells (Hanahan and Folkman, 1996). Upon formation of blood vessels from preexisting ones, cancer cells invade local tissues and then metastasize to distant sites mainly due to alterations in epithelial cadherin (E-cadherin), an adhesion molecule which not only mediates formation of cell-cell adhesion, but also keep the cells in their quiescent state (Hanahan and Weinberg, 2000).

It is now known that cancer cells not only have the capability to alter and reprogram the metabolic state of normal cells, but they also evade immune cells-mediated destruction (Colotta et al., 2009). Thus, it is imperative to elucidate the metastasis cascade as most death of cancer patients results from the ability of cancer cells to disseminate from their point of origin (primary tumour site) to distant tissues and organs where they acquire traits that make them adaptable to the new tissue microenvironment (Valastyan and Weinberg, 2011).

1.2 Cancer metastasis

Cancer metastasis is the dissemination of cancer cells from their original site (primary tumour) to distant anatomical organs and sites to form a secondary tumour. It is the outcome of series of molecular events that are linked not only through their reaction to different extracellular cues, but also through their association with the ECM and invasion of adjacent tissues (Brooks et al., 2010). It has been thought that metastatic potential is acquired at the later stages of tumourigenesis, however, recent reports have shown that from an early stage, a tumour can acquire metastatic competence (Glinsky, 2006; Glinsky et al., 2005; Weigelt et al., 2005).

1.2.1 The metastatic cascade

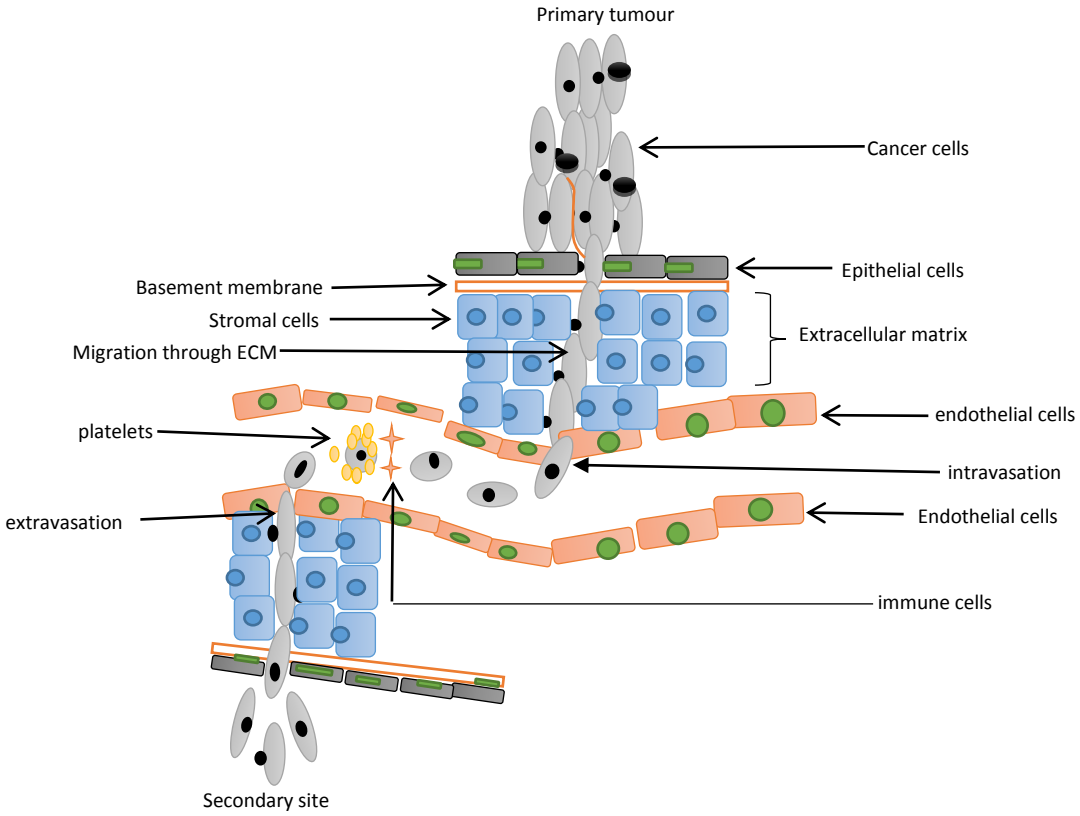

Figure 1.2: The metastatic cascade. Cancer cells in a primary tumour detach from adjacent cells in a tumour mass, they grow and then invade the basement membrane and traverse extracellular matrix surrounding tumour epithelium and subsequently invade endothelium of local blood vessel. The cells intravasate into blood vessel and are carried by the circulation. In the circulation, cancer cells may adhere to platelets and get protected from immune cell destruction. The circulating tumour cells adhere to lining endothelial cells at target organ before extravasation at a secondary site. The metastases then stimulate formation of new blood vessels, grow and expand for the next round of the cascade.

For tumour cells to become metastatic, they must undergo and complete the different sequence of events in the metastatic cascade. However, it is unclear how tumour cells successfully complete the cascade as different obstacles capable of halting the cascade are encountered in each step of the metastatic process (Chambers et al., 2002). One possibility could be due to the activities of cancer stem cells which are capable of self-renewal,

repopulating the metastatic tumour cells and even becoming resistant to unfavourable conditions (Wicha et al., 2006). Similarly, cancer cells avert immune cell destruction in the circulation by adhering to platelets which provide shielding for them.

1.3 Cell Migration

Cell migration is a crucial and highly coordinated phenomenon that occurs during physiological processes such as immune surveillance, wound healing, formation and maintenance of new tissues. A breach of regulation could result in pathological conditions such as osteoporosis, vascular diseases and cancer metastasis (Friedl and Wolf, 2010). Different modes of migration are adopted by cells, and several factors such as adhesion (Renkawitz et al., 2009; Sroka et al., 2002)009), contractility (Polte et al., 2004), Rho GTPases (Kolyada et al., 2003; Sanz-Moreno et al., 2008) and the integrity of the ECM components (Pelham and Wang, 1997) determine the form of movement adopted at any given time. During migration, cancer cells mimic normal, non-neoplastic cells not only in their morphology but in the way they remodel the ECM and generate contractile forces through the gliding action of myosin motors on actin filaments at the body and trailing edges of the cell (Friedl, 2004). However, cancer cells are insensitive to anti-migration signals that regulate normal non-neoplastic cells (Cox et al., 2001).

1.3.1 Modes of Cell Migration

Cancer cells migrate into and through the ECM by adopting two different modes of migration, depending on the tumour microenvironment and the type of cell. It could be collective or single cell migration (Friedl and Alexander, 2011). The basis in both modes of

migration is the interaction of cell surface receptors with neighbouring tissues and the underlying substratum (Ridley et al., 2003).

1.3.1.1 Collective Cell Migration

In collective cell migration, the cell-cell junction is kept intact in that the cells are connected together physically and functionally as a single larger cell migrating across a 2D or through 3D environment (Friedl, 2004; Ilina and Friedl, 2009). Collective cell migration is brought about by a combination of traction and protrusion forces generated as a result of concerted polarization of the different cells and the highly structured actin cytoskeleton (Friedl and Gilmour, 2009). The migrating cells clear a tunnel thereby subjecting the surrounding tissue along the migration path to structural modification (Friedl and Gilmour, 2009). In this mode of migration, tissue proteolysis and degradation is initiated by leader cells which have mesenchymal characteristics in generation of forward traction (Gaggioli et al., 2007; Khalil and Friedl, 2010).

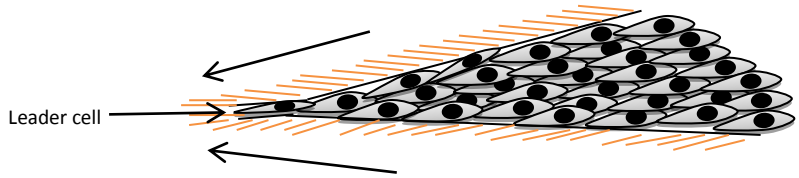

Figure 1.3: Collective cell migration. A leader cell with mesenchymal characteristics whose rear remains functional connected to adjacent and lateral cells generates integrin-mediated migratory traction via proteolytic activity. The path is then widened by follower cells as they migrate through the ECM (modified from Friedl and Alexander, 2011). Thick black arrows indicate direction of movement.

molecular mechanisms. In different epithelial, stromal and endothelial cells, intercellular interactions as well as association with the cytoskeleton are mediated by E-cadherin, N-cadherin and VE-cadherin respectively which are involved in development and angiogenesis

(Ewald et al., 2008; Gavert et al., 2008; van Kempen et al., 2000). Of critical importance is E-cadherin, the loss of which is responsible for reduced cell-cell association leading to the acquisition of an epithelial-mesenchymal transition (EMT) state and cancer invasiveness. Although, integrins connect cells to the ECM, they also strengthen cell-cell associations by binding to components of the ECM on intercellular surfaces. The binding of α6β1 and α5β1 to cell surface laminin and fibronectin respectively are a good example (Belvindrah et al., 2007). These integrins facilitate traction-mediated migration as more of them are expressed at the leading edge (Hegerfeldt et al., 2002; Vitorino and Meyer, 2008).

Collective migration is also attributed to loss of tight junction proteins such as desmocollins (Friedl and Gilmour, 2009; Khan et al., 2006), and there is a low expression of such tight junctions by cells at the leading edge compared to cells at the rear, an effect that results in polarized migration of cell collectives (Lecaudey et al., 2008). Similarly, within the tumour microenvironment, stromal cells may release chemokines such as the stromal cell-derived factor 1 (SDF1), fibroblast growth factor (FGF) and transforming growth factor β (TGF-β) which are capable of inducing polarized migration of cells (Lecaudey and Gilmour, 2006; Valentin et al., 2007).

Collective cell invasion is also made possible by the remodeling activity of MT1 MMP and MMP2 on the ECM both at the lamellipodia in 2D and in leader cells in 3D environments (Wolf et al., 2007). Cell polarization into leading edge and cell rear permits effective proteolytic degradation of the ECM by the tip cells giving rise to a narrow tunnel that is enlarged by follower cells and this result in force generation (Friedl and Wolf, 2008).

1.3.1.2 Single Cell Migration

Although, most cells migrate collectively either loosely or tightly packed, some do migrate individually. Usually, singly migrating cancer cells do not need cell-cell junctions, and they

move relatively short distances and then get incorporated into the surrounding tissue (Friedl and Wolf, 2010). The molecular mechanisms leading to individual cell migration could be considered as a cyclical event which eventually results in reorganization of the tissue architecture, changes in cellular morphology, as well as its position (Friedl and Gilmour, 2009; Friedl and Wolf, 2010; Lauffenburger and Horwitz, 1996; Sheetz et al., 1999).

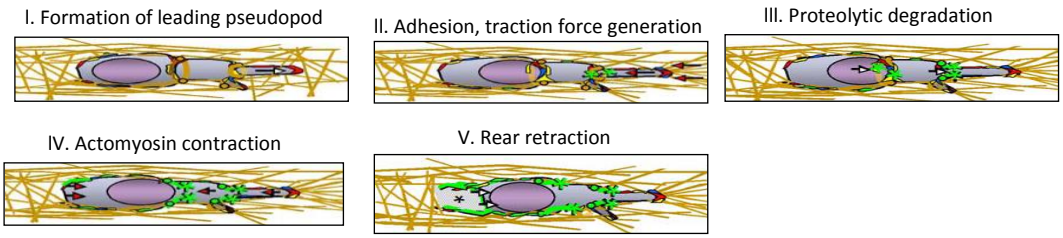

Figure 1.4: Molecular steps involved in single cell migration. Single cell migration is a cyclical event involving actin-driven formation of leading edge protrusions which interact with the substrate through integrins resulting in proteolytic degradation of the ECM. Cell contraction by actomyosin results in rear retraction and forward sliding of cell body. White and red arrows indicate migration and force generation respectively (Taken from Friedl and Wolf 2009).

Firstly, there is the formation of a leading membrane protrusion which is triggered by actin polymerization to form filaments and this subsequently results in polarization of the cell (Estecha et al., 2009; Poincloux et al., 2011). Binding of cell surface receptors due to interaction between the leading edge protrusion and extracellular substrates causes coupling of extracellular adhesion to intracellular traction and signaling cascades (Friedl, 2004; Friedl et al., 1997). Proteolytic degradation by cell surface MT1-MMP and the urokinase plasminogen activator (uPA) and uPA receptor (uPAR) system compromises the molecular integrity of the ECM and facilitates migration of the advancing cell body by widening the spaces within the ECM (Friedl and Wolf, 2009). Within the cell, tension is generated by

actomyosin-mediated contraction upon myosin II activation by Rho GTPase. Finally, there is the retraction of the rear end, while the leading edge translocates forward.

At the leading edge of many cell types, formation of lamellipodia or filopodia which interact with ECM proteins is dependent on the activity of the small Rho GTPases Rac and Cdc42 (Sanz-Moreno and Marshall, 2010). However, when the activity of Rac is reduced, some cells by-passed the formation of lamellipodia as well as generation of traction forces, instead they migrate by blebbing (Lorentzen et al., 2011; Poincloux et al., 2011).

Single cell migration could be either mesenchymal or rounded (amoeboid) migration.

1.3.1.2.1 Mesenchymal Migration

In mesenchymal migration, the invading cells which are usually small spindle-shaped, elongated and fibroblasts-like in morphology possess membrane protrusions and depend on integrin-mediated anchorage to the underlying cytoskeleton. There is high proteolytic cleavage and remodeling of ECM components by MMPs and serine and cysteine proteases which create microtracks that are widened by follower cells to migrate through (multicellular streaming) (Friedl and Alexander, 2011; Wolf et al., 2007). Tumour cells that adopt mesenchymal migration originate from the connective tissues and from dedifferentiated tumour cells that have lost their cell-cell junctions (Brabletz et al., 2001; Friedl and Wolf, 2009; Sanz-Moreno et al., 2008).

1.3.1.2.2 Amoeboid Migration

This mode of migration adopted by Dictyostelium discoideum, lymphocytes and tumour cells is characterized by low adhesion, and the contraction mediated by actomyosin is high (Friedl et al., 2001). However, contrary to amoeboid migration exhibited by Dictyostelium or leucocytes, amoeboid migration displayed by cancer cells lacks both cell-substrate adhesion

and Rho GTPases-driven lamellipodia and filopodia formation (Lorentzen et al., 2011). These amoeboid cells, through a process called blebbing, squeeze through gaps in the ECM even in the absence of matrix degrading enzymes (Wolf et al., 2003).

1.4 Blebbing

Blebbing is a mode of cell migration that involves the formation of spherical, dynamic protrusions on cell membranes in a cyclical manner. These spherical membrane protrusions which appear and disappear within a very short interval of time are formed by actomyosin-driven contraction of the cortex resulting in dissociation of the membrane from the underlying cortex, or by a local rupture in the cortex itself (Charras and Paluch, 2008). Although observed for a very long time in different cell types (Kubota, 1981; Trinkaus, 1973), blebbing migration was not given much attention as the interest of researchers was on the lamelliopodial based migration which was considered the ultimate mode of cell migration. Similarly, over the past decades, blebbing has been associated with and viewed only to be a hallmark of apoptosis in which during cell death dynamic blebs form at the execution phase (Mills et al., 1999). Blebs also formed in response to environmental insults such as acute oxygen levels, deficient energy levels and reactive oxygen species, processes which accompany a necrotic cell (Charras, 2008). It is imperative to note that whereas normal, healthy bleb formation is triggered by actomyosin contractility, apoptotic and necrotic blebs are not only bigger in size, but their formation is not mediated by actomyosin contractility (Barros et al., 2003). Blebbing is now known to occur during different normal physiological processes such as cytokinesis (Boucrot and Kirchhausen, 2007; Burton and Taylor, 1997), cell spreading (Bereiter-Hahn et al., 1990; Cunningham, 1995) and cell migration (Lammermann and Sixt, 2009). Cell migration through three dimensional matrices

was initially thought to be mediated primarily through the famous mesenchymal migration mode which is characterized by lamellipodia and filopodia formation, but it is now proven that blebbing migration can be used by different cells such as *Dictyostelium* (Lammermann and Sixt, 2009; Yoshida and Soldati, 2006), and tumour cells (Sahai and Marshall, 2003) to travel through 3D structures (Norman et al., 2010). During development, primordial germ cells from Drosophila melanogaster (Charras and Paluch, 2008) and zebrafish migrate by blebbing in response to stromal cell-derived factor 1, SDF-1 (Blaser et al., 2006). It is also known that Walker carcinoma cell lines can migrate not only on 3D structures but also on 2D using blebbing (Paluch and Raz, 2013). The growth of blebs, unlike other cellular protrusions such as lamellipodia and filopoda is mediated by cytoplasmic pressure, instead of polymerization of actin filaments (Pollard and Borisy, 2003), and certain metastatic cancer cells are unaffected by anti-tumour agents because of their ability to adopt blebbing motility (Friedl and Wolf, 2003; Sahai and Marshall, 2003). It is worthy of note that cell migration through blebbing does not exclude lamellipodia formation as both processes have been observed during gastrulation of prechordal plate precursor cells of zebrafish in an alternating manner, and also at different points of the leading edge on the cell membrane (Diz-Munoz et al., 2010). However, due to differences in the mechanical processes governing the formation of blebs and lamellipodia, the more the cell blebs, the less the lamellipodia formed and the reverse is also correct (Derivery et al., 2008). Lamellipodia formation depends on polymerization of actin which closely associates with the membrane, whereas during blebbing, the actin-membrane association is lost (Ridley, 2011).

1.4.1 The Life Cycle of a Bleb

The life cycle of a bleb involves the following phases: bleb initiation (nucleation), expansion, actin repolymerization and retraction (Charras and Paluch, 2008).

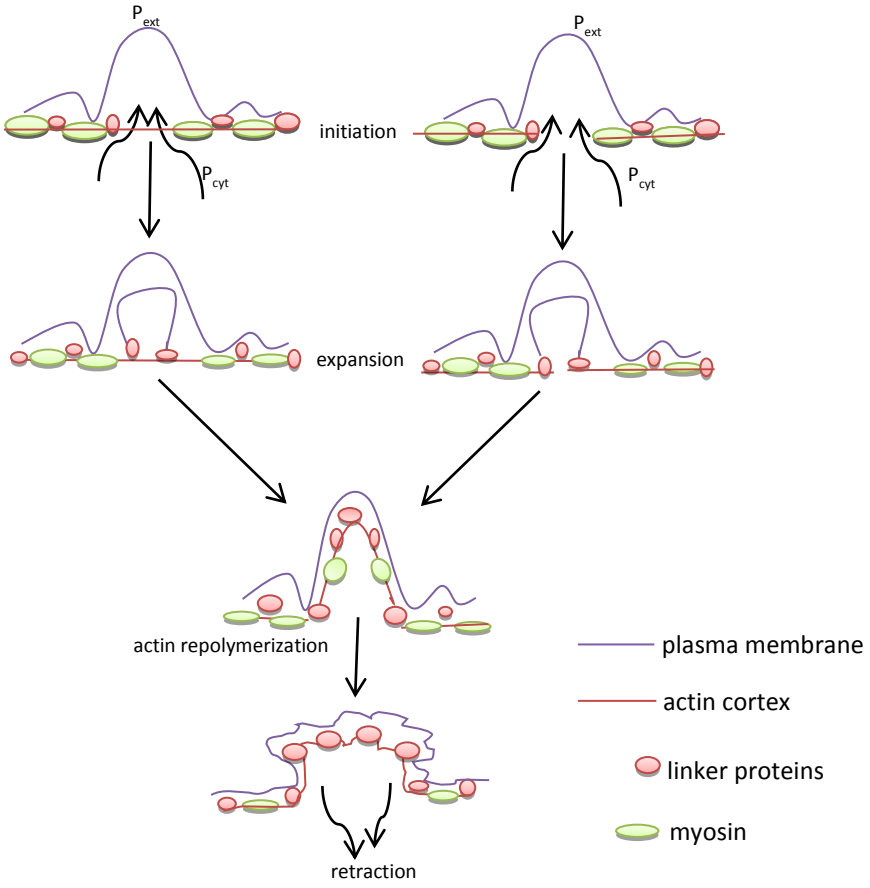

Figure 1.5: Life cycle of bleb. Bleb initiation is triggered by external stimuli which cause either delamination of the membrane from the cortex or local rupture of the cortical actin itself. The bleb expands as cytoplasmic pressure (P_{cyt}) causes flow of fluids and lipids via the bleb neck. Repolymerization of the actin cortex occurs as expansion decreases and bleb retracts upon recruitment of myosin and further assembly of actin (modified from Charras and Paluch, 2008). P_{cyt} – pressure in cytoplasm; P_{ext} – extracellular pressure.

1.4.1.1 Bleb Nucleation

Blebbing could be initiated by extracellular stimuli such as experimental techniques involving two-photon laser ablation of the cortex which creates a weaken cortex-membrane

interaction (Goudarzi et al., 2012) resulting in detachment of the plasma membrane from the underlying cortex (Norman et al., 2010) or a collapse of the actin cortex (Paluch et al., 2005) A bleb forms during nucleation if a portion of detached membrane grows to a size that is critical for blebbing, and this critical size is determined by the cytosolic pressure, membrane tension and adhesion energy between the membrane and cortex. From biophysical point of view, detachment of membrane from cortical actin, and cortex rupture could be exploited to determine the adhesion energy between membrane and the cortex, and tension along the cortex respectively (Charras et al., 2008).

1.4.1.2 Bleb Expansion

The growth phase which lasts between 5-30 seconds, is caused by the generation of hydrostatic pressure in the cytoplasm by actomyosin contractility. The bleb becomes enlarged in volume as cytosolic fluid and lipid flow through the bleb neck into the bleb resulting in an increase in the surface area of the bleb (Charras and Paluch, 2008). Thus, the plasma membrane gets delaminated from the cortex (Charras, 2008). Although, both migratory and non-migratory cells possess a submembranous cytoskeleton, a growing bleb lacks actin cortex (Blaser et al., 2006; Yoshida and Soldati, 2006).

1.4.1.3 Re-polymerization of Cortex and Retraction

Bleb expansion gradually subsides as the rate of actomyosin contractility-dependent fluid and lipid influx becomes inadequate to sustain a continuous growth (Charras et al., 2006). Thus, an expanding bleb gets to a stable point (bleb stabilization) before retracting their membranes. Bleb retraction is accompanied first by recruitment of membrane-cortex linker proteins (ezrin, radixin and moesin) within the bleb membrane. Then actin filaments reassemble at the bleb membrane, followed by the recruitment of motor proteins, especially myosin II (Charras et al., 2006). The bleb is then retracted by the newly formed cortex

towards the cell body (Norman et al., 2010). Retraction is the slowest process, and may last up to two minutes (Charras et al., 2008).

1.4.2 Molecular mechanism of Bleb formation

A weak interaction between the plasma membrane and actin cortex due to deficiency in actin polymerizing proteins such as filamin and membrane-cortex linker proteins such as the ERM (ezrin, radixin, moesin) proteins is largely responsible for blebbing of cells (Charras and Paluch, 2008). Bleb initiation by contractility of the actomyosin is induced by RhoA- and ROCK-mediated phosphorylation of myosin light chain which phosphorylates myosin II (Ridley, 2011) and this causes a rise in global and local hydrostatic pressure and subsequent inflation of the bleb (Tinevez et al., 2009). It is unclear which isoform of Rho (RhoA, RhoB or RhoC) is involved in blebbing. RhoA and its downstream effector ROCK have been shown to be activated by depolymerization of microtubule which resulted in membrane blebbing (Takesono et al., 2010). Death-associated protein kinase (DAPK) also stimulates phosphorylation of myosin light chain to induce membrane blebbing (Bovellan et al., 2010). Similarly, E-cadherin-dependent stimulation of Rac1 induces polymerization of actin which results in forward migration via lamellipodial membrane protrusions (Yap and Kovacs, 2003).

When overexpressed, the scaffolding protein diaphanous-interacting protein (DIP) interacts with and downregulates the activity of the formin, mDia2 which leads to membrane blebbing (Eisenmann et al., 2007). This is an indication that mDia2 could be a cortex-membrane linker protein that plays a role in preventing dissociation of the plasma membrane from the cortex, thus, stabilizing the actin cortex. There was a decrease in the size of ROCK1-induced blebs in cells overexpressing another kind of formin FH2 domain-containing protein 1 (FHOD1),

however, bleb number was increased (Hannemann et al., 2008). Bleb formation was also induced by the Formin-like protein 1 (FMNL1) in a ROCK-independent manner (Han et al., 2009).

Another protein that is critical for induction of blebs and blebbing migration is Dead end (Dnd) (Goudarzi et al., 2012) which binds RNA and promotes mRNAs translation by down-regulating microRNA activity (Weidinger et al., 2003). Knockdown of this protein in primordial germ cells of zebrafish not only resulted in reduction of actomyosin contractility – a process that triggers blebbing (Charras, 2008), but also strengthens membrane-cortex interaction by upregulating the levels of the membrane-cortex linker protein Annexin A5b (Goudarzi et al., 2012).

1.4.3 Bleb Polarization and Migration

It has been established that blebs are initiated by dissociation of the plasma membrane from the actin cortex. However, explanations for bleb polarization to the leading edge which results in migration are not clear. An increased contraction of the membrane-cortex interaction and its subsequent weakening at the front of a cell in response to chemoattractant might be a reason for polarization and bleb-based migration as observed in zebrafish germ cells (Blaser et al., 2006). Similarly, loss of integrity between membrane and cortex as well as a high hydrostatic pressure exerted on the membrane from the cytoplasm could be the trigger for polarized blebbing (Charras and Paluch, 2008). One possibility is that proteins linking the cortex and the membrane – the ERM (ezrin, radixin and moesin) proteins may be more concentrated at the cell rear, an effect that gives rise to dissociation of the membrane from the cortex at the leading edge as evidenced in Walker carcinoma cells (Gutjahr et al., 2005; Rossy et al., 2007).

The lipid second messenger phosphatidylinositol 4,5-bisphosphate (PIP_2) is known to stimulate the activity of the ERM proteins, and loss of PIP_2 activity may be responsible for the detachment of the membrane from the actin cortex (Franca-Koh and Devreotes, 2004; Sheetz, 2001). PIP_2 may function in a cell type-specific manner in that inhibition of PIP_2 activity was unable to prevent actin filaments repolymerization during retraction of blebs in filamin deleted cells (Charras et al., 2006). Similarly, the leading edge may have more myosin molecules which generate more contractile force at this region than the cell rear, and this may result in local rupture of the actin cortex (Paluch et al., 2005; Paluch et al., 2006). Increased intracellular calcium has been shown to precede blebbing in zebrafish germ cells (Blaser et al., 2006) and this generated the contractile force needed for cortex-membrane detachment and blebbing. Indeed, inhibition of intracellular calcium signaling inhibited bleb formation (Charras, 2008). The leading edge of cells is not only more pliable and younger than the rear but also has more concentrations of myosin and so blebbing mainly occurs at the front rather than the cell rear. However, in some cases, during blebbing migration, myosin motors can be found both at the cell front (Gutjahr et al., 2005) and rear (Stockem et al., 1982). Similarly, in some tumour cells, ROCK1, which mediate actomyosin contractility localizes to the trailing edge of migrating cells (Pinner and Sahai, 2008).

Usually, cell motility requires application of force by the cell body on the underlying substratum and this cause a change in the position and direction of the cell. In lamellipodial-based migration, the trailing edge first undergoes contraction, this is then linked together with interaction occurring between the underlying ECM and lamellipodia. In contrast, how cells migrate from one point to another via blebbing is not clearly understood as no examination of the proteins linking the cytoskeleton of a blebbing cell to the ECM has been carried out (Charras and Paluch, 2008). However, it might be that there are some forms of weak

interactions between focal adhesions and the ECM on one hand and with neighbouring cells on the other hand, and this results in blebbing motility (Grebecki et al., 2001). Such focal adhesions having connected to the ECM and the forming actin cortex, permits not only contraction of the cell rear but also cause the detachment of the cell-ECM interaction, and this subsequently leads to translocation of the cell mass (Sroka et al., 2002). Similarly, a cell may translate blebbing into migration through a process called chimneying which is independent of matrix adhesion and occurs either in 2D or 3D environment where a cell becomes flattened, and migration is achieved by applying a force perpendicular to the ECM (Charras and Paluch, 2008; Malawista et al., 2000).

Unlike lamellipodia protrusion, the growth of a bleb can occur in any direction of the cell and is usually faster. Because it is independent of matrix proteolysis, lesser energy is required for blebbing motility (Bereiter-Hahn et al., 1990). Blebs can conform more quickly to the external environment since they are deficient of cortical actin as well as reduced plasma membrane-cortex linker proteins at the leading edge (Charras and Paluch, 2008).

1.4.4 Significance of Blebbing

In general, the mode of migration a cell adopts at any given point is largely determined by the surrounding environment. While some cells could migrate using single protrusion type (Blaser et al., 2006; Svitkina et al., 1997), others could undergo plasticity which makes interconvertibility of migration modes possible. Most cancer cells have defied protease inhibitors which were designed to target the conventional mesenchymal migration as a result of their ability to switch from lamellipodia to bleb formation and this enables them to squeeze and migrate unperturbed through the pores of the ECM (Wolf et al., 2003). In times of unfavourable conditions such as in acute decreased in cell-ECM contact, neutrophils have

been found to migrate via blebbing (Sroka et al., 2002), while the amoeba, *Dictyostelium discoideum* uses blebbing as an escape mechanism in response to low osmolarity (Yoshida and Soldati, 2006).

1.5 The ERM Proteins (Membrane-cytoskeletal linker Proteins)

The ERM (ezrin, radixin and moesin) proteins are evolutionary conserved group of related proteins that possess band Four point one (4.1) as a common origin (Fehon et al., 2010). They interact with the plasma membrane through a common FERM (Four point one, ERM) domain (Arpin et al., 2011). The ERM proteins are located in cellular structures such as filopodia, apical microvilli, ruffling membranes, cleavage furrow of mitotic cells, retraction fibres, and adhesion sites, where the plasma membrane interacts with F-actin (Wakayama et al., 2009). ERMs are critical for maintaining the integrity of the cell cortex by coupling transmembrane proteins to the actin cytoskeleton as well as mediating signal transduction between the intracellular and extracellular compartments of the cell and also by interacting with other membrane phospholipids.

1.5.1 Structure of ERM Proteins

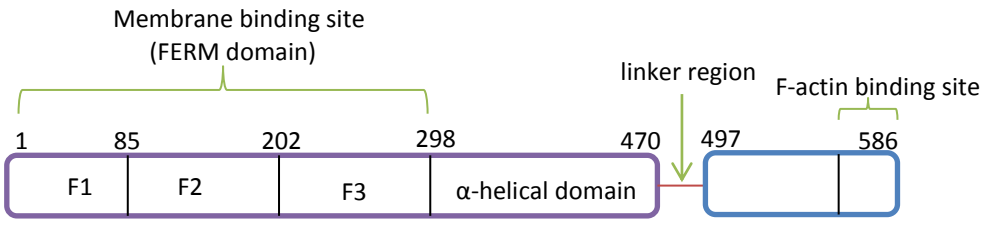

Figure 1.6: Domain structure of ERM Proteins. All ERM proteins display similar domain structure with the N terminus having F1, F2 and F3 subdomains. At the central portion of the protein is a α-helical domain which is followed by a linker region. At the last 30 carboxyl terminal end is the F-actin binding site.

Structurally, at the amino terminus of ERM proteins is an approximately 300 amino acid FERM domain through which they interact with cell membranes, and this domain consists of F1, F2 and F3 as subdomains. The FERM region is closely flanked by a central α–helical domain that mediate interaction with protein kinase A (PKA) (Dransfield et al., 1997), and then located at the carboxylic terminal end which is also called C-ERMAD (C-terminal ERM-Associated Domain) is a F-actin binding site which interacts with actin cytoskeleton as well as the FERM domain (Algrain et al., 1993).

ERMs exist in a dormant, inactive closed conformation in which the C-ERMAD stretches from the F-actin binding site through F2 and F3 to part of the FERM region, thereby concealing both the F-ctin and the membrane binding sites (Gary and Bretscher, 1995; Pearson et al., 2000). This covering of FERM by the C-ERMAD is bolstered by the central α-helical domain in that it is found to bind the FERM domain. Activation of the ERMs requires opening up the binding sites in the FERM domain and those of the F-actin biding sites in the C-terminal domain. This is achieved by phosphatidylinositol 4,5-bisphosphate (PIP_2)-mediated uncoupling of the C-terminal domain from the FERM domain (Fehon et al., 2010).

1.5.2 Regulation of ERM Proteins

ERM proteins are mainly regulated through conformational changes induced by phospholipids and kinases, and this results in activation of the proteins (Bonilha, 2007). Recruitment of ERMs to areas of the plasma membrane containing high amount of phosphoinositides such as PIP_2 exposes a conserved regulatory threonine phosphorylation residue (T567, T564 and T558 in ezrin, radixin and moesin respectively) located deep between the FERM domain and C-ERMAD domain (Nakamura et al., 2000). There are three lysine-rich consensus sites known to bind phosphoinositides on the FERM domain of ERM proteins and mutation on any of these sites inhibited PIP_2-ERM interaction and translocation

to the plasma membrane (Barret et al., 2000). Phosphorylation of the conserved threonine residue can be induced by different signaling protein kinases such as ROCK, protein kinase C (PKCα, PKCβ), NFκB-inducing kinase (NIK), lymphocyte-oriented kinase (LOK) thereby creating stearic hindrance that keeps the FERM and C-ERMAD domains apart (Nakamura et al., 1999; Pearson et al., 2000), and this stabilizes the active state of ERM proteins in their open conformation (Fievet et al., 2004; Yonemura et al., 2002). PIP_2-mediated recruitment of ERMs to the membrane is sufficient not only in the phosphorylation of these proteins by other kinases, but also in the formation of microvilli (Yonemura et al., 2002). Ezrin can be phosphorylated on threonine 235 which lies between the FERM and C-ERMAD domains by CDK5 (Yang and Hinds, 2003).

Binding of ERM proteins to the cytoskeleton in many cases is strengthened by phosphorylation of the proteins (Bretscher, 1999). Activation of the small Rho GTPase, RhoA and not Rac or Cdc42 was able to induce phosphorylation of both radixin and moesin, and this paralleled formation of membrane protrusions in Swiss 3T3 cells (Shaw et al., 1998). Also upon activation of platelets with thrombin, the phosphorylation status of moesin on threonine 558 (a residue also phosphorylated by PKCθ) was enhanced and this bolstered the interaction of moesin with the cytoskeleton, and moesin was found localized at the spreading filopodia (Nakamura et al., 1995). Phosphorylation of radixin on threonine 564 at the C-terminal half by Rho-kinase had no effect on the C-ERMAD to bind F-actin, but attenuated the ability of the C-ERMAD to bind N-ERMAD (Matsui et al., 1998) suggesting that the activated state of ERM proteins during which the intramolecular interaction between the N- and C- terminal domains is inhibited, can be sustained by the phosphorylation of threonine 564 in radixin (Bretscher, 1999), threonines 558 and 567 in moesin and ezrin respectively (Ivetic and Ridley, 2004).

ERM proteins can also be phosphorylated by receptor tyrosine kinases. Epidermal growth factor (EGF) receptor can phosphorylate ezrin at tyrosines 145 and 353 (Krieg and Hunter, 1992). Similarly, stimulation of ezrin-transfected LLC-PK1 cells with hepatocyte growth factor (HGF) resulted in increased phosphorylation of ezrin at the same tyrosine residues and this not only promoted cell migration, but also enhanced intracellular signal transduction (Crepaldi et al., 1997).

Regulation of ERM proteins could also be brought about by inactivation of the proteins. Moesin can be downregulated by myosin light chain phosphatase through dephosphorylation of threonine 558 (Fukata et al., 1998). Although, in phorbol 12-myristate 13 acetate (PMA)-stimulated leucocytes, ezrin is inactivated through calpain-mediated cleavage, moesin and radixin are insensitive to cleavage by calpain (Shcherbina et al., 1999) suggesting that distinct regulatory mechanisms exist for each protein in the same cell.

1.5.3 Interacting Partners of ERM Proteins

There are several proteins within the plasma membrane that interact with activated ERM proteins through the FERM domain. In a manner dependent on PIP_2, ERM proteins can associate with the cytoplasmic tails of intracellular adhesion molecules -1, -3 (ICAM-1 and -3) (Wang and Schey, 2011) and -2 (ICAM-2), as well as the hyaluronan receptor CD44 and CD43 (Yonemura et al., 1998). ERMs are also known to bind PDZ (postsynaptic density protein)-containing proteins such as transporters and ion channels through other anchoring proteins like NHERF1 (Na^+-H^+ exchanger regulatory factor) also known as ERM-binding phosphoprotein 50 (EBP50) and NHERF2 (Reczek et al., 1997; Weinman et al., 2006). They also interact with membrane glycoproteins such as P-selectin glycoprotein ligand-1 which tether white blood cells to injured tissues (Wang and Schey, 2011). The α-helical domain on

the central portion of ERMs can also bind subunits of HOPS complex (homotypic fusion and protein sorting) as well as the regulatory subunits RII of protein kinase A (Chirivino et al., 2011). Binding of ERM proteins to PKA tethers it to downstream targets to effect cAMP-mediated biological processes such as cell differentiation, proliferation, metabolism, apoptosis, exocytosis, T cell and B cell activation, muscle contraction (Dransfield et al., 1997). In COS-1 cells, ezrin was shown to bind and link syndecan-2 to the cortical cytoskeleton (Granes et al., 2000).

1.5.4 ERM Proteins and Cancer

Cancer cell migration is a coordinated process involving different steps that bring about loss of cell-cell adhesion and deregulation of cell-matrix interaction. In epithelial cells, interaction of ezrin with Fes kinase causes recruitment and activation of the later at the cell membrane where it facilitates HGF-mediated loss of cell-cell and cell-ECM contacts resulting in cell migration as revealed by wound healing assay (Crepaldi et al., 1997; Naba et al., 2008). In this interaction, ezrin not only localized to the leading edge of migrating epithelial cells (Naba et al., 2008), but also promoted the formation of membrane protrusions (Arpin et al., 2011).

Similarly, upon phosphorylation of the ERM proteins by PKCα, ERMs can act as downstream effector of PKC to mediate cell migration when the later was stimulated with phorbol-ester (Ng et al., 2001). PKC activation by phorbol ester also caused a switch in phosphorylation site of the transmembrane receptor CD44 from Ser325 to Ser29 and this phosphorylation regulated the association of ezrin with CD44 to promote directional cell migration triggered by CD44 (Legg et al., 2002). In radixin, phosphorylation of a conserved threonine 564 residue is sufficient to prevent the interaction of the FERM domain at the N-

terminus with the F-actin binding domain at the C-ERMAD terminus, and this results in constitutive opening of the membrane and F-actin binding domains (Louvet-Vallee, 2000). Indeed, in Madin-Darby canine kidney (MDCK) epithelial cells, phosphorylation of radixin on this site (T564) by the G protein-coupled receptor kinase 2 (GRK2) was able to induce membrane protrusions as well as increased migration of the cells as determined by wound healing assay (Kahsai et al., 2010).

Several reports have outlined different factors such as localization of ERMs within the cell, their level of phosphorylation as well as expression profile to be responsible for ERM proteins-mediated promotion of tumourigenesis (Arpin et al., 2011). In breast carcinoma, ezrin which was originally situated at apical structures in normal cell was found translocated to the cytoplasm and plasma membrane and this aberrant localization of ERM proteins could result in the acquisition of an EMT in which cells loss their normal differentiated, planar and apical-based polarity and anchorage dependent architecture and instead acquire metastatic phenotype that correlated with poor prognosis (Sarrio et al., 2006). Abnormal localization of ERM proteins may also lead to aberrant intracellular signal transduction triggered by growth factors. In the same vein, high level of moesin was also found in head and neck squamous cell carcinoma (Belbin et al., 2005). Ezrin binds cell-neural adhesion molecule (L1CAM) to promote progression of colorectal cancer in that RNA interference of ezrin activity inhibited tumour metastasis mediated by L1CAM (Gavert et al., 2010). Whereas both moesin and radixin were found upregulated in lymph node metastases of pancreatic cancer, the level of ezrin expression was unaffected, but its phosphorylation status did change (Cui et al., 2009).

1.6 Thesis Aims

As death of most cancer patients results from spread of cancer cells in the body, it has become imperative to understand the different mechanisms by which the metastatic process occurs and how these processes are regulated both at the molecular and cellular levels for successful therapy. For tumour cells to metastasize, the extracellular matrix is usually degraded by MMPs and other proteases secreted by cancer cells and other stromal cells surrounding tumours. However, use of inhibitors of matrix degrading enzymes has been largely unsuccessful in the fight against cancer. A large number of studies have attributed these futile attempts to the plasticity of tumour cells, and accordingly, upon inhibition of matrix proteolysis cancer cells switch from mesenchymal to protease-independent blebbing mode of migration (mesenchymal amoeboid transition, MAT) (Friedl and Wolf, 2010; Sanz-Moreno et al., 2008; Wolf et al., 2003). Blebs are spherical plasma membrane protrusions formed by Rho-ROCK-mediated actomyosin contractility resulting in increased hydrostatic pressure which cause delamination of membrane from the underlying cortex and subsequent flow of cytoplasmic fluids and water into the growing bleb through the bleb neck. There is now increasing evidence that water flow through transmembrane water channels called aquaporins is sufficient to drive lamellipodia formation, invasiveness and metastatic potential in different cancer cell lines (Papadopoulos and Saadoun, 2014; Papadopoulos et al., 2008; Saadoun et al., 2005a; Verkman et al., 2008). Therefore, the first aim of this study is to determine the role of aquaporins in cell blebbing in the ECM.

Usually, flow of water through aquaporins across the plasma membrane is in response to osmotic gradient created by ionic flow in and out of the cell through different ion transporters. Previous report (Illarionova et al., 2010), have shown functional interaction between aquaporins and ion channels; and it was also reported that tumour cells in a confined

environment exhibited polarized distribution of aquaporins and ion transporters at the plasma membrane which cause influx of water through the leading edge and efflux through the trailing edge, and the net effect is migration of cells (Stroka et al., 2014). And also, several reports have implicated different ion channels in tumourigenesis (Cuddapah and Sontheimer, 2011; Haas and Sontheimer, 2010; Reshkin et al., 2013; Schwab and Stock, 2014). Thus, the second aim of this thesis is to investigate the involvement of some of the transmembrane ion transporters in blebbing of cells.

Bleb formation resulting from delamination of the plasma membrane from the underlying cortex on one hand, and the fluxes of water and different ions across the plasma membrane on the other hand, will apparently impinge on the lipid composition of the plasma membrane. Lipid signaling enzymes and molecules have been implicated in different cancers and cancer-related abnormalities (Chen et al., 2012; Gomez-Cambronero, 2014; Henkels et al., 2013a; Wymann and Schneiter, 2008). Therefore, the third aim of this study is to investigate the role of lipid signaling molecules in cancer cell blebbing.

Chapter 2: Materials and Methods

2.1 Materials

2.1.1 Chemicals and Reagents

All chemicals and reagents used in the study were of analytical grade. Unless otherwise stated, all chemicals were purchased from Sigma-Aldrich (Dorset, UK). Acrylamide and bis-acrylamide were purchased from Bio-Rad Ltd, Hemel Hempstead, Hertfordshire, UK;. Ammonium persulphate (APS), bovine serum albumin (BSA), ethanol and methanol were obtained from Fisher Scientific, Loughborough, UK; Foetal bovine serum (FBS), L-glutamine, trypsin EDTA, and penicillin/streptomycin were purchased from Life Technologies, Paisley, UK; Fugene 6 was obtained from Promega, Madison, USA; Antibodies against human aquaporins 1, 3, 4 and 5 (AQP1, AQP3, AQP4 AQP5), phospholipases D1 and D2 (PLD1, PLD2), and phospholipase C (PLC) were purchased from Abcam Plc, Cambridge, UK; 5X siRNase buffer, DharmaFECT transfection reagent sets 1 and 4, RNase-free water, siRNAs to human AQP1, AQP3, AQP4, AQP5, PLC, PLD1, PLD2 were obtained from Fisher Scientific, Loughborough, UK; Growth factor-reduced phenol red-free matrigel was obtained from BD Biosciences, Oxford, UK; Butan-1-ol and tert-butanol were a kind gift from Prof Ketan's lab (University of Reading); PEI was a kind gift from Dr Keith Foster's lab (University of Reading); Phorbol-2-myristate-13-acetate (PMA) was purchased from Calbiochem (Merk Millipore), Nottingham, UK.

2.1.2 Inhibitors

Batimastat (BB-94) - a broad spectrum inhibitor of matrix metalloproteinases was obtained from Alexis-Enzo Life Sciences, Exeter, UK; Blebbistatin, caspase inhibitor set VI, cytochalasin D, FIPI, Go6976, H-89, latrunculin B, U73122, Y27632, LY294002 and the

protease inhibitor cocktail (PIC) set 1 which inhibits the activities of proteases such as serine, cysteine and tyrosine proteases as well as metalloproteases were purchased from Calbiochem (Merck Millipore), Nottingham, UK; Bumetanide, DCPIB, EIPA, Phenamil and zoniporide were obtained from Tocris Biosciences, Bristol, UK; Cariporide was purchased from Santa Cruz/Insight Biotechnology incorporated, Middlesex, UK; VPC32183 was a kind gift from Prof Ketan's lab, (University of Reading). All inhibitors, except PIC which was reconstituted in dH_2O, were dissolved in DMSO.

2.1.3 Plasma membrane dyes

The plasma membrane stains used in this study include BODIPY, calcein AM, calcein Blue AM, CellLight PM-RFP, CellMask orange and FM 4-64 FX. All were obtained from Life Technologies, Paisley, UK.

2.1.4 Plasmids

The plasmids and DNA constructs used for the study include GFP-lifeact and RFP-lifeact obtained from Addgene, Cambridge, MA, USA; GFP-ezrin, moesin-GFP, myrstoylated-GFP (myr-GFP), MRLC-RFP, constitutively active ezrin-T567D-GFP, and a dominant negative ezrin-T567A-GFP were a kind gift from Dr Guillaume Charras (University College London); GFP-AQP1 was a kind gift from Dr Matthew Conner (Sheffield Hallam University). All plasmids were reconstituted in dH_2O.

2.2 Methods

2.2.1 Cell culture

2.2.1.1 Cell lines

The cell lines used in this study include:

A172 (human glioblastoma cell line)

A549 (human lung adenocarcinoma cell line)

ACHN (human renal adenocarcinoma cell line)

HT1080 (human fibrosarcoma cell line)

MDA-MB-231 (human invasive breast cancer cell line)

Panc-1 (human pancreatic cancer cell line)

The cell lines were obtained from HPA culture collections, Salisbury, UK.

2.2.1.2 Culture media

The growth and maintenance of cell lines was performed using sterile techniques in the tissue culture room. The culture media contains the nutrients, minerals, organic and inorganic salts, growth factors and proteins required for the healthy growth of the cells. The media used for all cell lines was made with Dulbecco's modified Eagle's medium (DMEM) supplemented with 10% (v/v) FBS, 1% (2 mM) L-glutamine, 1% (100 µg/ml) streptomycin, 1% (100 units/ml) penicillin.

2.2.1.3 Freezing Buffer

The freezing buffer was routinely used to preserve the cells for longer storage in the liquid nitrogen whenever the need arises. It was prepared in the tissue culture room from 10% (v/v) sterile DMSO and 90% (v/v) FBS.

2.2.1.4 Thawing of frozen Cells

To start growth and culturing of cells for experiments, cells previously frozen down and stored in liquid nitrogen needs to be liquefied. Cryovials of frozen cells from liquid nitrogen were rapidly defrosted in warm water bath and decontaminated by wiping with 70% (v/v) ethanol. Thawed cell suspension was then added to 10 ml of pre-warm cell culture media and spun at 200 x g for 5 minutes. Media was aspirated and cell pellet was resuspended in 5 ml of fresh cell culture media. Cell suspension was then transferred into a 75 cm^2 tissue culture flasks containing 15 ml of fresh media. Cells were then incubated at 37^oC until they are grown to confluent. The cell lines were operated in class II laminar flow cabinet and kept in the incubator at 37^oC with 5% carbondioxide at an atmospheric humidity of 95%.

2.2.1.5 Passaging of cells

To ensure continuous growth and maintenance of the cell lines, cells are passaged every two to four days, depending on cell line. Old media from confluent cells was removed and cells washed with 10 ml PBS and then trypsinized with 1.5 ml trypsin-EDTA for 3-5 min in the incubator at 37^oC. When cells have detached, the action of trypsin was inactivated with 10 ml of culture media and then resuspended before splitting into 1:2, 1:3 or 1:4. Flasks were appropriately labeled with name, cell type and date before incubating at 37^oC.

2.2.1.6 Cryopreservation of cells

After trypsinizing cells as previously described above**,** cells were collected in culture media into 15 ml falcon tubes and spun for 10 minutes at 200 x g. Media was aspirated and cell pellet was resuspended with freezing buffer and then aliquoted into cryovials. Cryovials were neatly placed in Nalgene Mr Frosty freezing containers and temporarily kept at -80^{o}C overnight before taking into liquid nitrogen for long-term storage.

2.2.2 Cell Counting

Cells were washed with PBS, trypsinized and resuspended in culture media. A clean glass coverslip was properly set on top of haemocytometer and about 20 µl of healthy cell suspension was taken with a pipette and a drop of the cell suspension was placed at the edge of the coverslip. By capillary action, the drop flows into the counting chamber of the haemocytometer and become evenly distributed. Haemocytometer was taken to the microscope and number of cells in four squares (two squares from each chamber of the haemocytometer) was counted. The average number of cells per square was determined by dividing the total number of cells counted in the four squares by four.

Number of cells/ml (cell concentration/ml) was determined by: $\frac{\text{Average No cells per square}}{10^{-4}}$

However, when some of the cells appear unhealthy, trypan blue was used. 100 µl of cell suspension was taken and mixed properly with 100 µl of 0.4% (w/v) trypan blue. 20 µl of cell-trypan blue mixture was introduced into each counting chamber. The number of cells per ml (cell concentration/ml) was determined.

Number of cells/ml: Average No cells per square x dilution factor x 10^4

2.2.3 Determination of cell viability (MTT Assay) and Spectrophotometry

The viability of cells after treatment with different conditions was determined by the reduction of yellow tetrazolium salt, 3-(4,5-dimethylthiazolyl-2)-2,5-diphenyltetrazolium bromide (MTT) by metabolically active cells into intracellular purple formazan which is subsequently solubilized and quantified spectrophotometer. Briefly, ACHN and HT1080 cells (5×10^4 cells/well) were seeded on 24-well plate using phenol red-free media supplemented with 10% FBS and 1% each of glutamine and penicillin/streptomycin and then incubated 24 h at 37^{o}C for cells to adhere to plates. Culture media was removed and cells stimulated with hypotonic solutions of different osmolarities for 5 min, while in another instance, media was replaced and cells cultured for 30 min with media of different pH values. Solutions and media were replaced with 500 µl of pre-warmed media. MTT stock (5 mg/ml) was added (1:10 dilution) to a final concentration of 0.5 mg/ml. Cells were wrapped in aluminium foil and incubated for 3 h at 37^{o}C in humidified atmospheric condition with 5% CO_2 supply. 550 µl of solubilizing buffer (27 ml isopropanol, 3 ml triton x-100 and 2.5 µl 35% HCl) was added and content mixed properly at room temperature. Content was transferred to eppendorf tubes and mixed by vortexing and then incubated for 10 min at room temperature. Samples were mixed again by vortexing and absorbance values recorded using Jenway spectrophotometer. For determination of viability of cells induced to bleb with BB-94 and PIC, the drugs were added as the cells were being plated on the wells before the 24 h incubation. Percentage cell viability was calculated as:

$$\%V_C = \frac{A_{TC} - A_{BG}}{A_{CC} - A_{BG}} \times 100$$

where V_C = cell viability; A_{TC} = absorbance of treated cells; A_{CC} = absorbance of control cells; A_{BG} = absorbance of background

2.2.4 Wound Healing Assay (WHA)

Cells were plated on a 6-well plate at a density of $2.5x10^5$/well using normal cell culture media and incubated at 37ºC for 24 h. Cells in duplicate wells were treated with human AQP1 siRNA and scrambled siRNA, while in other two wells media was only replaced with fresh media. Cells were then incubated again for another 24 hours before scratching a wound through the middle of each well with a 200 µl tip. Cells were gently rinsed twice with culture media to remove any floating cell debris. Media was replaced with fresh one and then first image acquisition (t = 0 h) was done using phase contrast inverted microscope. Cells were then incubated 24 h before next image acquisition (t = 24 h).

2.2.5 Transfection

2.2.5.1 siRNA transfection

The transfection of HT-1080 and ACHN cell lines was performed using DharmaFECT transfection reagent set 4 (T-2004-02) according to the manufacturer's instruction. Briefly, confluent cells on 75 cm tissue culture flasks were washed with PBS, trypsinized and resuspended with complete media. Cells were seeded in 6-well plates at a density of 2×10^5 cells/well and incubated at 37ºC with 5% CO_2 for 24 h before transfection. From a 20 µM stock siRNA, 5 µM siRNA solution was prepared in 1X siRNA buffer (20 mM KCl, 6 mM HEPES (pH 7.5), and 0.2 mM $MgCl_2$). The 1X siRNA buffer was prepared from 5X siRNA buffer (300 mM KCl, 30 mM HEPES (pH7.5), 1.0 mM $MgCl_2$) and RNase-free water at a ratio of 1:4. Two tubes were set up. To the first and second tubes, an appropriate volume of the 5 µM siRNA solution and DharmaFECT transfection reagents were respectively introduced. A media supplemented with only L-glutamine (antibiotic- and serum-free media)

was introduced into each tube and both tubes were incubated for 5 min in the hood. After incubation, the content of the first tube was added to the second tube and the resulting mixture was resuspended and allowed to complex for 20 min. An antibiotic-free media was finally added to the mixture. Culture media from 6-well plate was removed and 2 ml of the total transfection medium was added into each well and then incubated for 24, 48, 72, and 96 h. The final siRNA concentration used was 25 nM, and knockdown of proteins was confirmed by western blot. The siRNAs used are shown below:

Table 2.1: SMARTpool siRNAs with the different target sequences. A scrambled ON-TARGETplus (Non-targeting) siRNA was used as a control.

SMARTpool siRNA	**Target Sequences**
AQP1	GAGAUGAAGCCCAAAUAGA, GAACUCGCUUGGCCGCAAU, GGAUCAAGCUGCCCAUCUA, CCACGACCCUCUUUGUCUU
AQP3	GGAUCAAGCUGCCCAUCUA, CUUCUUGGGUGCUGGAAUA, UAUGAUCAAUGGCUUCUUU, GAGCAGAUCUGAGUGGGCA
AQP4	GAAUUUCUGGCCAUGCUUA
AQP5	GCUCCGGGCUUUCUUCUAC
SLC9A1/NHE1	UGAUCAAGGGUGUAGGCGA,GCCUUCACCUCCCGAUUUA, GGACAAGCUCAACCGGUUU, GAGGAGGAGAUCCGCAAAA
PLCβ	GAGAAUAGCAGUUUAUGAA,GCACUUAAUUUCCAGACAA, GAACACACUACCAAGUAUA, CAUCGAAGCUUUAUCAAAC

PLD1	CAACAGAGUUUCUUGAUAU,GGUAAUCAGUGGAUAAAUU,
	CCAUGGAGGUUUGGACUUA, CCGGGUAUAUGUCGUGAUA
PLD2	GGACCGGCCUUUCGAAGAU, CAGCAUGGCGGGACUAUAU,
	CAAGGUGGGCGAUGAGAUU, ACAUUAUGCUCAAGAGGAA

2.2.5.2 Transfection with GFP- and RFP-tagged proteins

The transfection of cells with GFP- and RFP-labeled plasmids was done using Fugene transfection reagents according to the manufacturer's instructions. Briefly, prior to start of experiment, cells were seeded in 6-well plate at a density of 2 x 10^5 cells/well and incubated at 37ºC with 5% CO_2 supply overnight. Eppendorf tubes corresponding to the number of plasmid DNAs were set up, and serum-free media was introduced into each tubes. Optimized volumes of Fugene transfection reagent was directly added to the serum-free media without touching the sides of the tubes and mixed by gentle 'flicking'. Tubes were incubated for 5 min in the hood. Optimized amounts of plasmid DNAs were added to the tubes and the contents carefully mixed before incubating for another 15 min. Media of cells in 6-well plate was removed, and in a drop-wise manner, the DNA-Fugene complex in the tubes was evenly distributed into the wells. Cells were then incubated at 37ºC for 24 h or 48 h for uptake of DNA and expression of the GFP-tagged proteins. For AQP1-GFP transfection in ACHN and HT1080 cells, the ratio of DNA:fugene was respectively 1:6 and 2:5. Percentage transfection efficiency was determined using AxioImager epifluorescent microscope (Zeiss). The optimized amounts of plasmids, volumes of Fugene transfection reagent and serum-free media used for the experiments are shown on the table below:

Table 2.2: Optimized amounts of different plasmids and fugene 6 reagent used.

Plasmid DNA	**Concentration**	**Amount used**	**Fugene 6 (µl)**	**SFM (µl)**
AQP1-GFP	1263.87 µg/ml	2 µg	5	96
GFP-lifeact	900 µg/ml	1 µg	3	96
RFP-lifeact	680 µg/ml	1 µg	3	96
Ezrin-GFP	5,506.9 ng/µl	1 µg	6	94
Moesin-GFP	16,544 ng/µl	2 µg	3	97
myrGFP	18.5 µg/µl	1 µg	6	94
MRLC-RFP	4,990 ng/µl	1 µg	3	97
Ezrin T567A-GFP	6,502 ng/µl	1 µg	6	94
Ezrin T567D-GFP	5,167.4 ng/µl	1 µg	6	94
NMHCIIA	5,140 ng/µl	1 µg	6	94
NMHCIIB	4,820 ng/µl	1 µg	6	94

2.2.6 Microbiological Techniques

2.2.6.1 Reagents

2.2.6.1.1 Ampicillin stock

This was prepared by weighing 0.2 g ampicillin into 10 ml dH_2O. Solution was then filtered through a 0.22 µm filter in a tissue culture hood. It was then aliquoted into sterile eppendorf tubes and kept at -20^oC until needed.

2.2.6.1.2 LB Agar

A litre of this solution was made by dissolving 1% (w/v) bacto-tryptone, 0.5% (w/v) yeast extract, 1% (w/v) NaCl and 1.5% (w/v) granulated agar in ultrapure water. The solution was then autoclaved for 15 min at 120^oC. When solution was cooled to about 50^oC, 1 ml of antibiotics prepared in session 2.2.6.1.1 was added to 1 L of the solution.

2.2.6.1.3 LB Media

This was prepared by dissolving 1% (w/v) bacto-tryptone, 0.5% (w/v) yeast extract, 1% (w/v) NaCl in dH_2O. Solution was autoclaved at 120^oC for 15 min and kept at 4^oC until needed.

2.2.6.1.4 LB SOC Media

A litre of SOC media was prepared by dissolving 2% (w/v) bacto-tryptone, 0.5% (w/v) yeast extract and 0.05% (w/v) NaCl in dH2O. The solution was shaken until all solutes dissolved. The following solutions were then added: 10 ml 250 mM KCl (1.86g KCl in 100 ml dH_2O, pH 7, then make up to 1 L with dH_2O); 5 ml 2 M $MgCl_2$ (19 g $MgCl_2$ in 90 ml dH_2O, make up to 100 ml with dH_2O); 20 ml of 1 M glucose solution (18 g glucose in 90 ml of dH_2O,

adjust volume to 100 ml with dH_2O and then filter sterilized through a 0.22 µm filter). The media was stored at 4°C.

2.2.6.1.5 80% Glycerol

This was prepared from 80 ml glycerol and 20 ml dH2O, then autoclaved at 120°C for 15 min.

2.2.6.2 Techniques

2.2.6.2.1 Preparation of Agar Plates

In order to prepare agar plates for bacterial transformation, 25 µl of LB agar prepared in session 2.2.6.1.2 was evenly poured and distributed to cover the surface of a 9 cm petri dish, and allowed to cool for 30 min. Lids were placed, and plates inverted and properly sealed with parafilm. Plates were stored in plastic bags and kept at 4°C.

2.2.6.2.2 Transformation of competent E. coli cells

The competent E. coli strain, XL10 gold used for this experiment was a kind gift from Dr Keith Foster (University of Reading, UK). All procedures were performed under standard aseptic conditions. XL10 gold bacterial strains previously stored at -80°C were thawed on ice and 50 µl of bacteria was placed in a falcon tube before gently adding and mixing with 2 µl of GFP-tagged AQP1 plasmid and then incubated on ice for 30 min. Samples were heat-shocked at 42°C for 30 seconds on a water bath without shaking, and then back to ice for 2 min. Bacterial cells were added to 450 µl of SOC media and shaken at 37°C for 1 h for transformation. 100 µl of this transformation was spread on LB agar plates containing

ampicillin and incubated in the normal position at 37^{o}C for 2 min. Plate was then inverted upside down and incubated overnight at 37^{o}C for transformed colony growth.

2.2.6.2.3 Plasmid DNA Purification

Following transformation, a single bacterial colony was picked from the plate into a falcon tube containing 5 ml LB medium and the antibiotic, and then mixed vigorously. The content was incubated by shaking at 285 rpm for 10 h at 37^{o}C until the mixture becomes cloudy. 400 µl of transformed cell suspension was added to 200 ml LB media containing 20 µl of ampicillin in a sterilized flask and shaken at 285 rpm for 16 h at 37^{o}C. Culture was transferred into 250 ml tube and centrifuged at 6000 x g for 20 min at 4^{o}C. Supernatant was discarded and pellet frozen down at -80^{o}C or used immediately for plasmid DNA amplification and purification using Qiagen HiSpeed Plasmid Maxi kit.

Briefly, bacterial pellet was resuspended in 10 ml buffer P1 and mixed with 10 ml buffer P2 by inverting 4-6 times before incubating at room temperature for 5 min. Buffer P3 was added and then mixed thoroughly by inverting 4-6 times until the solution turns colourless. Lysate was collected through QIAfilter Cartridge by incubating for 10 min and then filtered through a HiSpeed tip previously equilibrated with 10 ml buffer QBT. The HiSpeed Tip was washed with 60 ml buffer QC before eluting DNA with 15 ml buffer QF and precipitated by incubation for 5 min with 10.5 ml isopropanol. Eluate-isopropanol mixture was filtered through a QIAprecipitator, and DNA contained in the QIAprecipitator was washed with 2 ml 70% ethanol. QIAprecipitator was dried and DNA was finally eluted with 1 ml buffer TE into a 1.5 ml collection tube.

2.2.6.2.4 Determination of DNA concentration and Purity

The concentration of plasmid DNA was determined using NanoDrop spectrophotometer which measures at wavelengths of 260 nm and 280 nm and determines absorption spectrum from 220-350 nm. Briefly, in order to establish a blank, 1 µl of buffer TE was placed on the bottom pedestal, arm was lowered and reading was noted. Blank was gently wiped and 1 µl of DNA sample was placed on the measurement pedestal of the instrument and measurement taken. Sample was wiped off the pedestal and the procedure repeated three times to obtained three values (in ng/µl). The average of the three measurements was obtained as the DNA concentration in ng/µl, and a purity of A260/280 = 1.89 was obtained.

2.2.7 Blebbing Assay

This assay is designed to explore how cells form and use blebs to migrate through the ECM in an in vivo setting. Hence, it utilizes growth factor reduced (GFR) phenol red free matrigel (BD Biosciences) to mimic an in vivo ECM environment. GFR matrigel is a soluble preparation of basement membrane obtained from Engelbreth-Holm-Swarm mouse sarcoma, a tumour known to contain important ECM proteins such as laminin, collagen IV, proteoglygycans and enactin. It also contain little amount of growth factors such as EGF, IGF, FGF and TGFβ. Thus, it is efficient in studying tumour cell invasion and migration assays in vitro.

Prior to start of experiment, matrigel was thawed overnight at 4^{o}C and kept on ice. Tips, pipettes, plates, glass coverslips, µ-dishes and tubes were chilled at -20^{o}C for at least 30 min. Confluent cells were rinsed with 10 ml PBS, trypsinized and then resuspended in 10 ml cold serum-free media. Cell suspension was carefully added on ice to matrigel in an equivalent

ratio and mixed properly. 200 µl of cell-matrigel suspension was plated on glass coverslips in 6-well plates, and on 35 mm glass-bottomed plates and then incubated at 37^{o}C for 30 min for matrigel to set before adding 2 ml of cell media into each wells and glass-bottomed plates. In order to induce blebs, the activity of MMPs and proteases was inhibited by treating cells with BB-94 (1 µM) and PIC (1:100 dilution) respectively in the presence of caspase inhibitor set VI (10 µM) which prevents cell death due to apoptosis. Plates were incubated at 37^{o}C for bleb formation. Cells were then challenged with specific inhibitors known to target key signaling pathways.

For bleb induction in siRNA-treated cells, after confirmation of a specific time point (24, 48, 72, 96 h) for effective knockdown of proteins by western blotting, cells were seeded on the plates and transfected with specific siRNAs for the specific knockdown-time points as described in session 2.2.5.1 before embedding in matrigel.

2.2.8 Three Dimensional On-Top Assay

The 3D on-top assay was a modification of a previously developed protocol (Lee et al., 2007). Briefly, matrigel was thawed in the cold room and 100 µl was evenly spread from the centre of pre-chilled coverslips without reaching the outer edges of the coverslips. Coverslips were carefully placed in 6-well plates and incubated for 30 min at 37^{o}C for matrigel to set. Cells were trypsinized, resuspended in normal media and 25,000 cells were carefully laid and spread on top the matrigel and then incubated again for another 30 min before adding 2 ml of normal media containing PIC (1:100) and BB-94 into each well and then incubated overnight. Cells were then immunostained for confocal microscopy

2.2.9 Monitoring AQP1 flow During Bleb Expansion and Retraction

AQP1-GFP overexpressing cancer cells induced to bleb were seeded on ibi-treated µ-dishes and mounted on a pre-warmed scanning laser confocal microscope chamber heated at 37^{o}C and connected to 5% CO_2 supply. Cells were imaged using x60 oil-immersion objective of a Nikon A1-R confocal microscope. For each blebbing cell, phase contrast-bright field and fluorescence time-lapsed movies were simultaneously generated using the TD and 488 lasers respectively. The time-lapse movies were generated at a rate of one frame every 2 seconds for an experimental period of 10 minutes.

To quantify the levels of AQP1-GFP during expansion and retraction, bright field and AQP1-GFP fluorescence movies from the two lasers were opened on ImageJ, and then merged to give a clear overlay of AQP1-GFP on the bright field movie. Blebs were tracked by manually controlling the 'forward' and 'backward' buttons of the time-lapse movies. As the combined movie was played, the fluorescence intensities (used as a read-out for AQP1-GFP levels) at the 'preinitiation point' (the frame just before bleb initiation and expansion began) was quantified by drawing three short straight lines across the membrane using the 'straight' tool, and the three peak values from each line was recorded before taking their average (P_{fi}). At the preinitiation point, there was no frame movement, hence, time was zero. As the movie progresses, the fluorescence intensities of every frame during bleb expansion and retraction were carefully monitored and quantified as described for 'preinitiation point' above. The average fluorescence intensities of expansion (E_{fi}) and retraction (R_{fi}) were then obtained. The number of frames moved during bleb expansion and retraction were multiplied by 2 seconds since movies were generated every frame for 2 seconds. The fluorescence intensities which represent the AQP1-GFP level during bleb expansion and retraction were then normalized to the preinitiation values, and then expressed as percentage as shown:

$$\% \text{ AQP1level (during expansion or retraction)} = \frac{E_{fi} \text{ or } R_{fi}}{P_{fi}} \times 100$$

where E_{fi}, R_{fi} and P_{fi} represent average fluorescence intensities during bleb expansion, retraction and preinitiation.

Finally, the different percentage AQP1-GFP levels during the different bleb phases were plotted against the corresponding times in seconds (figures 3.14a and b).

2.2.10 Preparation and calibration of various pH media

The determination and adjustment of pH values of solutions was performed in a sterile tissue culture hood using pre-calibrated Orion 3 star benchtop pH meter (Thermo Scientific). 30 ml of normal cell culture media was introduced into six sterile falcon tubes, and to the first three tubes, 35% HCl was gently added in drop-wise and mixed carefully to obtain pH of 5.5, 6.0 and 6.5. The pH values of the next three tubes were gradually adjusted with 10 M NaOH to obtain 8.0, 8.5 and 9.0, while the pH of the normal cell culture media was also measured and found to be 7.4. All tubes were then incubated at 37ºC in an atmospheric condition with 5% CO_2 supply. The pH values were checked and adjusted twice a day for six days when the values became stable. The acidic media turned bright yellow while the alkaline media turned bright pink.

2.2.11 Incubation of Cells with pH media

Culture media of blebbing cells previously embedded in matrigel on µ-dishes at 37ºC was removed and fresh media with the different pH values was introduced into the dishes and

cells incubated for 30 min. Where necessary, the activity of Na^+/H^+ pump was inhibited with EIPA for 15 min at 37^{o}C. Fixed and live cells were acquired using an inverted phase contrast microscopy and Nikon TE200 time-lapse system respectively.

2.2.12 Immunocytochemistry

Cells were seeded on coverslips in 6-well plates and incubated at 37^{o}C with an atmospheric condition of 5% CO_2 supply for 24 hours for cells to adhere to coverslips. After incubation, culture media was aspirated and cells were rinsed twice with pre-chilled PBS before fixing for 20 min with 4% (v/v) paraformaldehyde (PFA). Cells were rinsed twice (10 min each) with PBS before permeabilizing with 0.2% (v/v) triton X-100 for 15 min at room temperature. Cells were blocked with 10% (v/v) goat serum (Sigma) in PBS for 30 min and then incubated at room temperature with human AQP1, AQP5, NHE-1, PLD1 and PLD2 antibodies (1:200 dilution) in 1% (v/v) goat serum for 1 h. Primary antibodies were removed and cells were rinsed 3 times (10 min each) with pre-chilled PBS, and further incubated for 1 h with secondary antibodies (1:500) conjugated with Alexa fluor 488 (Invitrogen). When necessary, to distinguish actin cytoskeleton from other proteins of interest, cells were co-incubated with the secondary antibodies and phalloidin. Cells were counter-stained with Vectashield/DAPI mounting medium and allowed to set before taking for confocal microscopy.

2.2.13 Microscopy

2.2.13.1 Plasma Membrane (PM) staining

In order to investigate whether specific proteins of interest such as AQP1, AQP5 and NHE1 are localized to bleb membrane or to other intracellular compartments, the plasma membrane

(PM) of cells was labelled with different PM dyes, as these dyes clearly stain and distinguish the PM from the rest of the cell. The dyes used included CellMask orange PM stain, FM 4-64 and CellLight PM-RFP. All dyes were purchased from Invitrogen (Life technologies) UK, and staining with each dye was performed according to the manufacturer's instruction. Briefly, for staining with CellMask orange, culture media in cells previously transfected with AQP1-GFP was removed and pre-warmed media containing 4 µg/ml CellMask orange was added and cells incubated at 37ºC for 20 min; For FM 4-64, cells were incubated at 37ºC for 10 min with cold magnesium- and calcium-free DMEM containing 17 µM FM 4-64; For CellLight PM-RFP, after removing media from AQP1-GFP transfected cells, 2 ml fresh media containing 2 µl of the dye was added and then cells incubated at 37ºC for 18 h. Cells in all conditions were then trypsinized and resuspended with serum-free media before embedding in matrigel, and then challenged with BB-94 and PIC. Cells were incubated for 18 hours before image acquisition using confocal microscopy.

2.2.13.2 Imaging of fixed Cells

After incubation of cells with BB-94 and PIC, media was aspirated and cells were rinsed twice with pre-chilled PBS and then fixed for 30 min with 2.5% (v/v) glutaraldehyde. Fixative was removed and cells permeabilized with 0.2% (v/v) triton X-100 for 30 min. Acquisition of images of fixed cells was done with a x40/0.60 phase contrast objective lens of a Zeiss A1 inverted epifluorescent microscope. For examination of actin cytoskeleton, after fixing and permeabilization, cells were stained with phalloidin (1:100 dilution) in PBS for 30 min. Cells were then rinsed with PBS and mounted for microscopy using fluorescence microscope.

2.2.13.3 Live-cell Imaging

To investigate the dynamics of blebs, unfixed, live-blebbing cells were imaged using both phase contrast and confocal microscopy. Cells previously treated with bleb-inducing agents mounted on a microscope stage that was pre-warmed and maintained at 37ºC with 5% CO_2 supply system. Images of live-cells were acquired with Nikon A1R confocal microscope (60x oil immersion objective lens) while phase contrast live-cell images were acquired using 40x objective lens. When necessary, time-lapse movies of blebbing cells were generated at an interval of every 2 seconds per frame for an experimental length of 10 min. In all cell imaging experiments, fluorophores were excited at 488 nm for GFP-tagged proteins or FITC and 543 nm for RFP-tagged proteins or TRITC.

2.2.14 Sodium dodecyl sulphate-polyacrylamide gel electrophoresis (SDS-PAGE)

2.2.14.1 Whole cell lysates

Culture media of cells in 6-well plate previously transfected with different siRNAs was removed and each well rinsed with 1 ml chilled PBS before scrapping cells into tubes on ice. Samples were spun in a fast-cooled centrifuge at 4ºC for 10 min at 15000 x g. Supernatant was removed and pellet resuspended on ice in 200 µl radioimmunoprecipitation assay (RIPA) buffer (50 mM Tris-HCl (pH 8.0) with 150 mM sodium chloride, 1.0% (v/v) NP-40, 0.5% (w/v) sodium deoxycholate and 0.1% (w/v) SDS) containing PIC (1:100). To ensure shearing of DNA, the mixture was further resuspended with 21-guage needles 2-3 times before incubating on ice for 30-60 min. Samples were centrifuged and supernatant was collected into new sets of cold eppendorf tubes and kept at -20ºC until needed for experiment.

2.2.14.2 Bradford Assay

The Bradford assay is a biochemical technique used to estimate protein concentration in a solution. It is based on the principle that absorbance of Brilliant Blue G dye shifts from 465 nm to 595 nm when it binds proteins. The amount of dye bound is proportional to the concentration of protein present.

The concentration of BSA standards used to plot a standard curve included: 25 µg/ml, 125 µg/ml, 150 µg/ml, 250 µg/ml, 500 µg/ml, 750 µg/ml, 1000 µg/ml, 1500 µg/ml and 2000 µg/ml.

The assay was performed using a 96-well plate in which the first column (blank column) contains only 195 µl Bradford reagent while the second and third columns contained 5 µl of the BSA standards ranging from 25 µg/ml - 2000 µg/ml (from the first row to the last); while the remaining columns contained 5 µl test samples (cell lysates) in triplicate. 195 µl of Bradford reagent was added into both standards and test samples, and plates were gently and carefully swirled avoiding bubbles, and when formed, bubbles are carefully removed with 20 µl pipette. Plate was taken to a precision microplate reader and absorbance values at 595 nm were recorded.

2.2.14.3 SDS-PAGE gel preparation

SDS-PAGE allows the separation of proteins according to their migration during electrophoresis, and this mobility usually depends on the molecular weight of the protein. A recipe for 12% and 15% SDS gel is shown below:

Table 2.3. Recipe for resolving and stacking gels.

Reagents	12% Running gel (15 ml)	15% Running gel (15 ml)	5% Stacking gel (4 ml)
30% Acrylamide mix	6.0 ml	7.5 ml	0.67 ml
1.5M Tris-HCl (pH 8.8)	3.8 ml	3.8 ml	-
1.0M Tris-HCl (pH 6.8)	-	-	0.5 ml
Distilled H_2O	4.9 ml	3.4 ml	2.7 ml
10% (w/v) SDS	150 µl	150 µl	40 µl
TEMED	6 µl	6 µl	4 µl
10% (w/v) APS	150 µl	150 µl	40 µl

The resolving gel was first poured to an appreciable level and overlaid with water on two glass plates 1.5 mm apart and allowed to set for 20 min. Water was removed and stacking gel was poured on top of the resolving gel and a comb was inserted. The setup was left for another 20 min for the gel to set. When stacking gel was set, the gel plate was taken to an electrophoresis tank containing 1x electrophoresis running buffer. Comb was removed and precision plus prestained protein markers (BioRad) of known molecular weight (5-175 kDa) were loaded in the first well. Samples to be analyzed were prepared by mixing protein samples (cell lysates) previously harvested with 5x SDS loading buffer (5:1). Samples were

vortexed and incubated on a heating block for 6 min at 90ºC before loading 10 µg unto gel. Gel was initially run at 50 mA and later 30 mA from stacking through resolving gels respectively. When samples migrated to the bottom of the gel, the gel was removed from glass plates for western blotting

2.2.15 Western Blotting

2.2.15.1 Reagents used:

Table 2.4. Buffers and solutions used in western blotting. Where possible, these solutions were made up to the final volume by dissolving in dH_2O.

Transfer buffer (1L)	38.6 mM glycine, 23.11 mM Tris-base, 20% (v/v) methanol
10x TBS (1L)	18.98 mM Tris-base, 1.36 mM NaCl, 26.83 mM KCl. pH adjusted to 7.4 with HCl
1x TBS (1L)	100ml 10X TBS plus 900ml ddH_2O
TBS_T (1L)	1XTBS plus 0.1% Tween 20
Blocking solution	5% dried skimmed milk in TBS_T
5% BSA solution	5% BSA in TBS, 0.1% Tween 20
5x SDS sample buffer	10% (w/v) SDS, 20% (v/v) glycerol, 1% (v/v) β-mercaptoethanol, 0.2M Tris-HCl (pH 6.8), 0.05% (w/v) bromophenolblue
5x Running buffer (1L)	15.1g Tris base, 94g glycine, 50ml of 10% (w/v) SDS

2.2.15.2 Transfer of Proteins to membranes

Upon completion of SDS-PAGE, PVDF membranes (9 cm x 9 cm) were immersed in methanol for 10 seconds and then placed in transfer buffer for 15 min to equilibrate. Similarly, six filter papers (10 cm x 10 cm) were soaked in transfer buffer for 5 min. Membranes were placed on top of three of the filter papers followed by the gel. The remaining three papers were placed and air bubbles were rolled away from the sandwich before placing on a Trans-blot semi-dry electrophoretic transfer cell (Bio-Rad). The proteins were transferred at a constant current of 50 mA for 1 h 45 min.

2.2.15.3 Blocking of membrane and antibody incubation

After protein was transferred, the membrane was blocked in blocking solution at room temperature for 1 hour. Membrane was washed with TBS_T and incubated overnight with primary antibody (1:1000 in 5% milk TBS_T or in 5% BSA) at 4^{o}C in a shaker. The membrane was washed three times for 10 min each with TBS_T and then incubated with an appropriate secondary (1:2000 in 5% milk TBS_T) for 1 hour with gentle shaking.

2.2.15.4 Enhanced chemiluminescence (ECL)

Membrane was washed three times with TBS_T for 10 min each and treated with ECL reagents A and B at ratio 1:1 for 5 min. Membrane was wrapped and bands were developed using ImageQuant LAS 4000 machine.

2.2.15.5 Stripping and reprobing

In order to investigate another protein of interest, membrane was washed three times with TBS_T for 10 min each on a rocker, and then incubated for another 20 min on a rocker with 10% (v/v) re-blot solution (Millipore) in dH_2O. Membrane was blocked with 5% milk, rinsed with TBS_T and re-incubated with the new primary and secondary antibodies.

2.3 List of antibodies

Table 2.5: Different primary and secondary antibodies with the manufacturer, sources and concentration used.

Primary antibody	**manufacturer**	**Cat. No**	**Source**	**Dilution**
Human aquaporin 1	Abcam	ab65837	Rabbit	1:1000
Human aquaporin 3	Abcam	ab125219	Rabbit	1:1000
Human aquaporin 4	Abcam	ab46182	Rabbit	1:1000
Human aquaporin 5	Abcam	ab85905	Rabbit	1:1000
Human NHE1	Abcam	ab67314	Rabbit	1:1000
Phospholipase D1	Abcam	ab10583	Rabbit	1:1000
Phospholipase D2	Abcam	ab123663	Rabbit	1:1000
Phospholipase C	Abcam	ab21824	Mouse	1:1000
anti-tubulin	Sigma	T9026	Mouse	1:500
Secondary antibody	**Manufacturer**		**Source**	**Dilution**
Ant-rabbit HRP-linked	Sigma	A-9169	rabbit	1:2000
Ant-mouse HRP-linked	Sigma	A-8924	mouse	1:2000

2.4 Analyses and Quantifications of images and movies

All movies, images and cell morphologies were analyzed using freeware package ImageJ (version 1.4.3) open source software from the National Institute of Health, Bethesda, MD, USA, (http://rsb.info.nih.gov/ij). The following analyses were performed:

2.4.1 Analysis of Wound Healing Assay (WHA)

To quantify the percentage of wound closure, images were opened on ImageJ and a thin line was drawn three different times to cover the entire surface areas of the initial wound (t = 0 h) and the final wound (t = 24 h) in two different wells of a 6-well plate using the 'polygon' tool. The procedure was repeated for untreated control, scrambled control and siRNA-treated cells in three different plates at three different times (n=3), and the overall average of each experimental conditions was then taken. The percentage of wound closure was calculated as the difference between the average initial wound area and average final wound area, divided by the initial wound area and then multiplying the quotient by 100 as shown below:

$$\% \text{ wound closure} = \frac{(\text{Average initial area, } t = 0 \text{ h}) - (\text{Average final area, } t = 24 \text{ h})}{\text{Average initial area at } t = 0 \text{ h}} \times 100$$

where t = 0 h and t = 24 h are the wound areas before and after siRNA treatments respectively.

2.4.2 Quantification of Percentage Blebbing Cells

For quantification of the percentage of blebbing cells, plates and µ-dishes were properly fitted on the stages of a phase contrast Zeiss A1 inverted and Nikon A1-R confocal microscopes, and the total number of cells (all blebbing and non blebbing cells) were visualized using x40 objective lens, and manually counted. The percentage of blebbing cells

was obtained by dividing the number of blebbing cells by the sum of blebbing and non blebbing cells, and then multiplying the result by 100 as shown below:

$$\% \text{ blebbing cells} = \frac{\text{number of blebbing cells}}{\text{blebbing + blebbing cells}} \times 100$$

2.4.3 Measurement of Bleb Size/Circumference

The sizes of blebs in each individual cell were measured by manually drawing a thin circular line round the entire circumference with the 'polygon' tool in ImageJ. This was followed by 'analyze > measure', and from the dropdown result list, the perimeter values in pixel were recorded. Because images were acquired with a x40 objective, values in pixel were normalized by multiplying with a pre-calibrated factor of 0.11 µm (a factor which corresponds to 1 pixel, and which was obtained when the x40 objective lens was calibrated with a graticule). For all other quantification of bleb size and distance/length where necessary, values in pixels were converted into µm by multiplying with 0.11 µm.

2.4.4 Analysis of Bleb Speed

For determination of bleb speed, images were opened in imageJ, and a straight line was drawn across the center of each bleb from one end to the other using the 'straight' tool and expressed in µm. This was termed 'bleb distance'. Similarly, the time it took each bleb to expand and retract was quantified by manually tracking the frame numbers during expansion and retraction, and then multiplied by 2 as movies were generated at 2 seconds per frame (i.e the time elapsed between the first frame in which bleb expansion/retraction was observed and the last frame in which expansion/retraction ceased).

The bleb speed was calculated as:

$$\text{Bleb speed } (\mu m/s) = \frac{\text{bleb distance } (\mu m)}{\text{time (sec)}}$$

2.4.5 Analysis of Bleb Dynamics

For analysis of bleb dynamics, blebbing cells cultured in 3D matrigel matrix in µ-dishes were monitored in TiE200 microscope whose chamber was pre-warmed at a temperature of 37^{o}C with 5% CO_2 supply. Time-lapse movies of blebbing cells were then generated at a rate of one frame every 2 seconds for an experimental period of 10 minutes using x40 objective lens. Time-lapse movies were opened in imageJ and played manually by controlling the 'forward' and 'backward' buttons of the movie. As the movie progresses, the number of frames it took blebs to expand, stabilize and retract were carefully manually monitored, counted and recorded, and then multiplied by 2 (since movies were generated 2 seconds/frame). Bleb lifespan was calculated as the summation of bleb expansion, stabilization and retraction.

2.4.6 Determination of Percentage of AQP1 in Bleb and Cellular membranes

The percentage of AQP1 in bleb membrane with respect to that in other parts of cellular membrane was quantified by drawing three short straight lines to cut across three different points of bleb and cellular membranes using the 'straight' tool. The three highest fluorescence intensity values of each line was noted, and the averages taken. The percentage of AQP1 in bleb membrane or cell membrane was obtained by dividing the fluorescence

intensities of bleb membrane (B_{fi}) or cellular membrane (C_{fi}) by the sum of B_{fi} and C_{fi}, and then multiplying the result by 100:

$$\% \text{ AQP1 Bleb or Cell membrane} = \frac{B_{fi} \text{ or } C_{fi}}{B_{fi} + C_{fi}} \times 100$$

where B_{fi} and C_{fi} are the fluorescence intensities of bleb and cellular membranes respectively.

2.4.7 Analysis of Western Blot

Immunoblot bands were developed using ImageQuant LAS 4000 machine (G.E Healthcare). Briefly, after treating membranes with ECL reagents A and B for 5 minutes, membranes were neatly wrapped in clean self-sealed cellophane bags before taken to the machine. Membranes were placed on a particular tray (tray 2 for this work) and then focused on computer screen. Image brightness was adjusted to get the best focus before exposing for different times.

To quantify and normalize band intensities to loading controls, images (test samples and loading controls) were opened one at a time in freeware imageJ. From the toolbar, the 'rectangular' tool was selected and a rectangle was drawn round the first lane before going to 'analyze>gels>select first lane. The first lane got selected with '1' at the centre. Rectangle on first lane was clicked on and gently dragged to the second lane before going to 'analyze>gels>select next lane'. This process was done for all available lanes, and then going to 'analyze>gels>plot lanes to generate profile plots which represent the intensities of each band in the rectangular regions. To enclose off each peak, a straight line was drawn across the base of each peak using the 'straight line' tool. With the 'wand' tool, beginning with the first lane, the inside of each peak was clicked on. At this point, measurements popped up on a result window that appeared. Going to 'analyze>gel>label peaks' labels the size of each peak which is expressed as percentage of total size of all peaks highlighted. These percentage

values are the densities of the bands. The test sample (arbitrary units) were then normalized to control by dividing the test sample densities by the loading control densities. The result gives the relative density values.

2.5 Statistical analysis

Statistical significance was performed by one-way analysis of variance after Tukey's post hoc multiple comparison for three or more variables, while unpaired, two-tailed student's t test was performed for two variables. GraphPad prism 5 software (GraphPad software, San Diego, CA) was used to perform all comparisons. All data were generated from at least three independent experiments in triplicate (n=3), and P values < 0.05 were considered statistically significant.

Chapter 3. Regulation of Blebbing by Aquaporins

3.1 Introduction

Aquaporins (AQPs) are integral membrane proteins (28-30 kDa) which act as channels that facilitate transport of either water or both water and other solutes such as glycerol or urea across cell membranes of plants and animals (Isokpehi et al., 2009). Since their discovery in the 1980s, thirteen aquaporins (AQP0-AQP12) have been identified in different mammalian tissues and organs (Verkman, 2011). AQP-expressing cells such as endothelial and epithelial cells display greater water permeability than the non AQP-expressing cell membranes in which the lipid bilayer acts as the main means of water transport. AQPs, other than transport of water across membranes, have been implicated in pathological conditions such as brain edema, cancer, renal failure, cataracts, infertility and impaired fat metabolism (Verkman, 2008).

3.1.1 Structure of Aquaporins

Structurally, in cell membranes, the AQPs exist as homotetramers consisting of six α-helical transmembrane regions (I-VI) with five loops (A-E) linking them together. Loops B and E which have short α-helices folding backwards into the membrane, possess a conserved asparagine-proline-alanine (NPA) motifs. Loop B goes into the membrane through the cytoplasmic domain while loop E enters from the extracellular compartment (Fujiyoshi et al., 2002), and this gives rise to the functional water pore (Kruse et al., 2006).

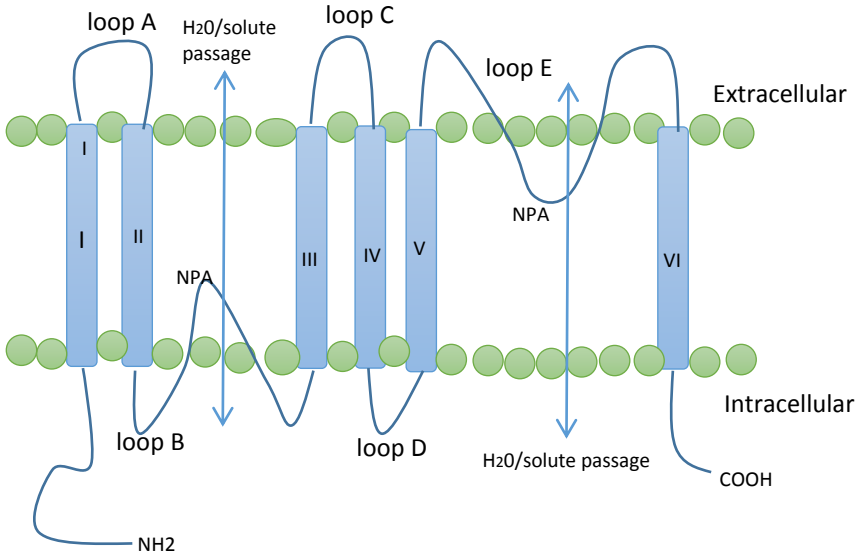

Figure 3.1: Aquaporin structure within the membrane. The protein contains five loops A-E linking the six transmembrane helices together. Contained within loops B and E is asparagine-proline-alanine motifs that facilitate passage of water and other solutes.

In mammals AQP0, AQP1, AQP2, AQP4, AQP5, AQP6 and AQP8 exclusively transport water in a bidirectional manner. As selective water transport requires the single-file passage of water molecules through the aquaporin pore, the density of aquaporins on the plasma memebrane must be high for efficient water permeability, usually several thousand AQPs in 1 μm^2 of membrane. (Yang and Verkman, 1997). Some aquaporins such as AQP3, AQP7, AQP9 and AQP10 transport both water and glycerol and are referred to as aquaglyceroporins (GLPs) (Gonen and Walz, 2006).

Apart from water and glycerol, AQPs can also transport molecules such as NO, ammonia (NH_3), hydrogen peroxide (H_2O_2) and carbon dioxide (CO_2) (Miller et al., 2010; Musa-Aziz et al., 2009) . Whereas the role of AQPs 11 and 12 in transmembrane transport is not known, AQP6 can also specifically transport chloride ions (Yasui et al., 1999) while AQP9 transports

amino acids, arsenite and sugars in addition to glycerol (Carbrey et al., 2009; Tsukaguchi et al., 1998).

A mechanism by which the aquaporins structures permit water passage has been earlier proposed (Fu et al., 2002). According to this proposition, since the pores in all contain a common conserved hydrophobic sequence that allows passage of water molecules through the channel as a single-file hydrogen bonded chain, a conserved arginine residue and the NPA motifs at loops B and E act as filters that mediate water interaction with the asparagine side chains. This effect results in rotation of water molecule through 180^{o} as it passes rapidly through the pores.

Although several investigations are on-going, the exact mechanism(s) by which AQPs facilitate cell migration are still poorly understood. It has been proposed that it might involve targeted influx of water into the leading edge which cause recruitment of actin nucleating factors and the subsequent formation of lamellipodia via actin polymerization. This was consistent with polarization of the AQPs towards the leading edge of migrating cells (Bisi et al., 2013). It was also proposed that rapid water influx and efflux through AQPs accompany a migrating cell, and this helps in facilitating rapid changes in cell shape as the migrating cell squeeze through preexisting gaps in the ECM (Papadopoulos and Saadoun, 2014). Similarly an osmotic engine model was recently postulated in which tumour cell migration was said to be driven in confined microchannels due to exhibition of polarized distribution of AQPs and Na^{+}/H^{+} ion transporters with the net effect of water and ions inflow and outflow through the leading and trailing edges respectively, and this results in net displacement of cells (Stroka et al., 2014).

3.1.2 Tissue Distribution of Aquaporins

Although most AQPs are localized in the plasma membrane, some are found in the cytosolic compartment. However, for rapid and efficient water passage, aquaporins on the cytoplasmic compartment must translocate to the membrane (Verkman, 2011). The different aquaporins display different expression pattern within different tissues, organs, cellular and subcellular compartments (Krane and Goldstein, 2007).

Table 3.1: Distribution of different aquaporins in different mammalian tissues. CSF: cerebrospinal fluid; GIT: gastrointestinal tract; ND: not determined (unknown).

Aquaporins	Tissue Distribution	Functions	References
AQP 0	Lens fibres, kidney	Maintenance of fluid balance in eye lens	(Charras et al., 2005; Verkman et al., 2014)
AQP 1	Kidney, lungs, brain choroid plexus, GIT, ear, corneal epithelium, RBCs, skeletal and heart muscles	Urine concentration, hydration, water and CSF maintenance	(Tournaviti et al., 2007; Wang et al., 2008)
AQP 2	Kidney	Regulation of antidiuretic hormone	(Kawaguchi et al., 2014; Yang et al., 2001)
AQP 3	Kidney, epidermis, bladder, lung, trachea	Maintain glycerol homeostasis, skin hydration, water reabsorption	(Ma et al., 2000; Madsen et al., 2015)
AQP 4	Kidney, brain, lung, GIT, salivary gland , astrocytes	Water reabsorption, maintain CSF level, osmoregulation	(Li and Verkman, 2001; Saadoun et al., 2002b)

AQP 5	Salivary and lacrimal glands, pancreas, airways, eye, placenta	Regulates saliva and tears levels, water balance	(Hidalgo-Carcedo et al., 2011; Sanz-Moreno et al., 2011)
AQP 6	kidney	Chlorides and anions transport	(Krane and Goldstein, 2007)
AQP 7	Adipocytes, testis and sperm, kidney	Transports glycerol, urea, water and arsenite	(Hara-Chikuma et al., 2005; Maeda et al., 2009)
AQP 8	Testis and sperm, liver, GIT, kidney, placenta, pancreas	Water, urea and ammonium transport	(Krane and Goldstein, 2007)
AQP 9	Hepatocyte, Erythrocytes, Spleen, leucocytes, lung, liver, testis, brain	Glycerol, urea and water transport	(Gaggioli et al., 2007; Sahai, 2005; Wang et al., 2005)
AQP 10	Small intestinal enterochromaffin cells (duodenum and jejunum)	Water, glycerol and urea transport	(Verkman et al., 2014)
AQP 11	Kidney, brain, liver	ND	(Sahai, 2002)
AQP 12	Pancreas	ND	(Vial et al., 2003)

3.1.3 Aquaporins and Cell Migration

Several reports have implicated the aquaporins in promoting cell migration. For instance, in aortic endothelial cells from AQP1 knockout mice, migration in response to chemoattractant was greatly reduced compared with wild type cells, and in a similar manner, in cultured endothelial cells, expression of AQP1 and AQP4 resulted in faster wound healing (Papadopoulos et al., 2008; Saadoun et al., 2009). In fast migrating AQP-expressing cells, AQP1 was found polarized to the leading edge and showed a direct correlation with formation of protrusions at the cell membrane (Verkman et al., 2008). Similarly, AQPs promote tumour metastasis in that in AQP1-deleted mice, injected melanoma tumour cells not only failed to form new blood vessels, but became less infiltrative, and a drastic reduction in growth of these cells was observed (Saadoun et al., 2005a).

In AQP4 null astrocytes, delayed migration was observed and this also paralleled a deficient formation of glial scar (Saadoun et al., 2005b). Overexpression of aquaporins has been found in many human tumours and these correlated with higher tumour grade and poor prognosis (Hoque et al., 2006; Liu et al., 2007). Knockdown of AQP3 decreased both fibroblasts motility (Cao et al., 2006) and proliferation of keratinocytes (Hara-Chikuma and Verkman, 2008) while its expression promotes wound healing in both skin and cornea (Hara-Chikuma and Verkman, 2008; Levin and Verkman, 2006). AQP3-mediated movement of glycerol enhances the elastic strength of the skin as well as epidermal and stratum corneum hydration (Ma et al., 2002), and lack of this protein was shown to cause dehydration due to impaired permeability of glycerol which aids in retention of water (Hara et al., 2002). Similarly, overexpression of AQP9 resulted in filopodia formation and increased water influx through plasma membrane (Loitto et al., 2007).

The water and glycerol transporting ability of the AQPs is responsible for most of their biological effects in the cell (Verkman, 2011). Thus, this ability of the aquaporins to transport H_2O, NO, H_2O_2, and CO_2 across plasma membranes could be exploited to investigate the potential roles of these water channels in cancer cell blebbing. As a mode of cell migration, blebbing is associated with rapid changes in cell shape which is facilitated by fluctuations in cell volume arising from aquaporins-mediated influx and efflux of water and lipids from the cell across the membrane (Papadopoulos et al., 2008). In addition to enhanced shape changes, cell volume fluctuations also aid actomyosin-mediated cell motility. Therefore, the AQPs, by transporting water across biological membranes, are likely to play a role in promoting changes in cell shape observed in blebbing cells.

3.2 Chapter Aim

The aquaporins were thought to facilitate transport of water across the plasma membrane in response to osmotic gradient. However, the discovery of the involvement of AQP1 (Saadoun et al., 2005a) and several other AQPs in cell migration, angiogenesis and cancer metastasis (Papadopoulos et al., 2008; Saadoun et al., 2005b; Verkman et al., 2008) has shown that these transmembrane proteins could play potential roles in physiological and pathophysiological processes other than water transport.

Thus, the aim of this chapter was to investigate the potential roles of specific AQPs and aquaglyceroporins in the blebbing of cancer cells in the extracellular matrix. The study utilized matrigel as an in vitro model for investigating blebs in the ECM upon perturbation of AQPs activity by RNA interference. A characterization of the dynamics of blebs in AQP-knocked down and wild-type HT1080 cells was performed. The effects of overexpression of AQPs by transfecting cells with GFP-tagged AQPs was also investigated in both HT1080 and ACHN cell lines.

3.3 Results

3.3.1 Bleb induction in cancer cells

At the normal uninhibited state, cancer cells including the human fibrosarcoma HT1080 and human renal adenocarcinoma ACHN cell lines when plated on plastic or in 3D matrices such as matrigel and collagen migrate as elongated mesenchymal cells using lammellipodia and filopodia at the leading and trailing edges respectively and degrade the ECM with invadopodia expressing matrix metalloproteinases (Ridley, 2011). Previous reports have shown that tumour cells can migrate using blebbing as an alternative mode of cell migration through the ECM upon inhibition of proteolytic activities (Charras and Paluch, 2008; Wolf et al., 2003). Thus, to study blebbing of cancer cells in the ECM, the study employed matrigel, a basement membrane component rich in ECM components, and six different human cancer cell lines, A172 (glioblastoma cells), A549 (lung carcinoma cells), ACHN (renal adenocarcinoma cells), HT1080 (fibrosarcoma cells), MDA-MB-231 (breast cancer cells) and Panc-1 (pancreatic cancer cell) lines were induced to bleb in matrigel by blocking the activities of MMPs with the general MMP inhibitor batimastat BB-94 (1 μM) and other surface proteases with protease inhibitor cocktail PIC (1:100) in the presence of caspase inhibitor set VI (10 μM). As shown in figure 3.2 only the ACHN and HT1080 cell lines were found to bleb after inhibition of matrix degradation.

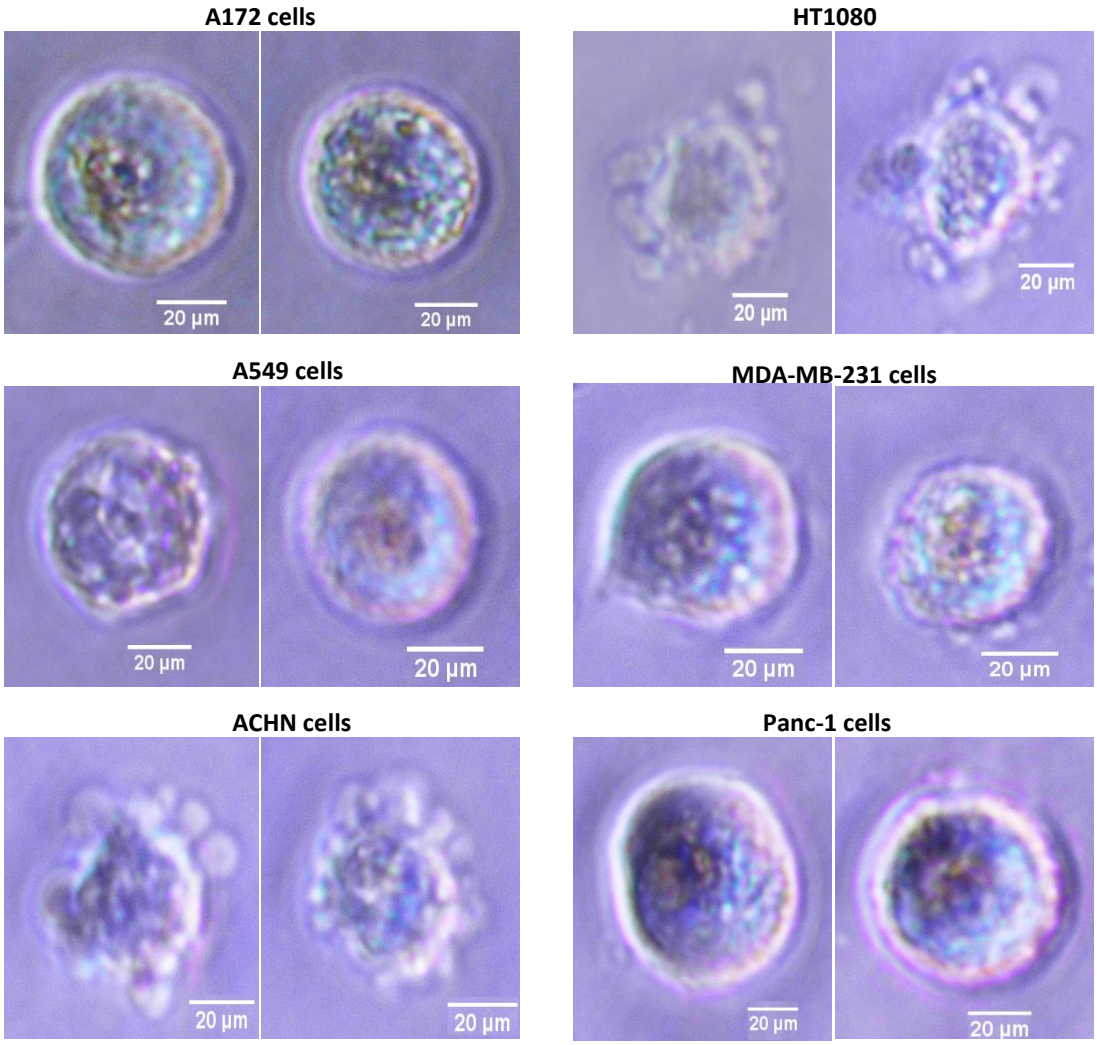

Figure 3.2: Bleb induction in cancer cells: The ability of cancer cells to bleb in the ECM was assessed by embedding each cell line in 3D matrigel matrix in 3 wells of a 6-well plate using serum-free media, and then blocking proteolytic degradation with BB-94 (1 µM) and PIC (1:100) in presence of caspase inhibitor set VI. Data is a representative of three independent experiments in which 75 cells were counted in each cell line for each experiment.

3.3.2 Bleb induction has no effect on cell viability

To further confirm the blebs were not due to apoptosis, and that the treatments with the inhibitors did not impinge on the viability of cells, an MTT assay was performed in which metabolically active cells were separated from dead ones due to the capability of the former

to reduce yellow tetrazolium salt, 3-(4,5-dimethylthiazolyl-2)-2,5-diphenyltetrazolium bromide (MTT) into intracellular purple formazan which is subsequently solubilized and quantified spectrophotometrically. As shown in figure 3.3, bleb induction did not significantly affect the viability of the two cell lines. Therefore, this study was carried out using these two blebbing cell lines.

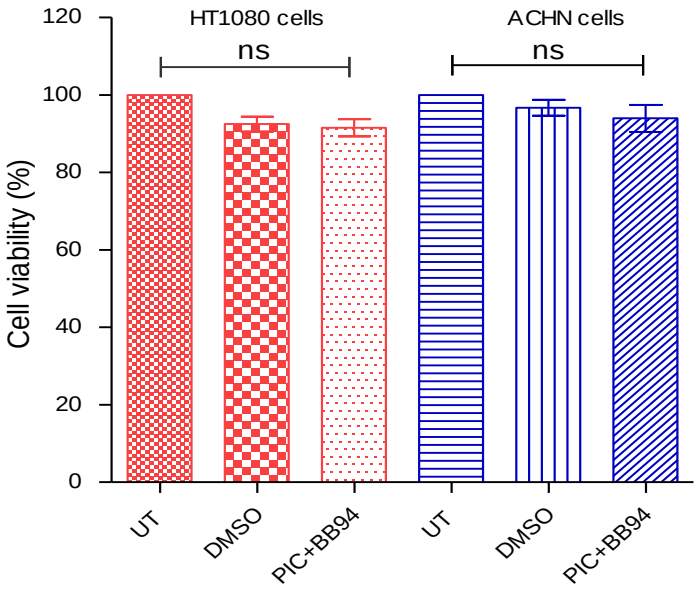

Figure 3.3: Cell viability. Viability of BB-94- and PIC-treated ACHN and HT108 cell lines was determined by incubating cells with MTT (0.5mg/ml) in the dark at 37^{o}C for 3 h before solubilizing with solubilization buffer. After thorough resuspension, samples were incubated at RT for 10 min and then vortexed before taking absorbance values using spectrophotometer. Data is a representative of three independent experiments. UT = untreated control; ns = non-significant; RT = room temperature.

3.3.3 Formation of membrane blebs is mediated by Rho-ROCK signaling and is dependent on myosin II activity

As formation of blebs is thought to be triggered by ROCK-mediated activation of myosin light chain that drives myosin II-stimulated contraction of the cortical actin which results in

increased hydrostatic pressure and subsequent delamination of the plasma membrane from the underlying cortex (Paluch and Raz, 2013), the involvement of the Rho-ROCK pathway in blebbing of ACHN and HT1080 cell lines was tested using the ROCK inhibitor, Y27632. 5 μM of the drug potently ablated cell blebbing (figures 3.4a and b, middle panel). The requirement of myosin II was tested by inhibiting the ATPase activity of myosin II with blebbistatin, an effect that will lead to relaxation of the actin cortex. Again, pretreatment with 50 μM of blebbistatin sufficiently blunted bleb formation in both cell lines (figures 3.4a and b, bottom panel), with only 12% and 14% respectively of HT1080 and ACHN cells blebbing upon blebbistatin treatment (figure 3.4d). This data demonstrates that ROCK-driven activation of myosin II activity is critical for blebbing and that the ACHN and HT1080 cells used in this study were blebbing normally in the well-understood manner.

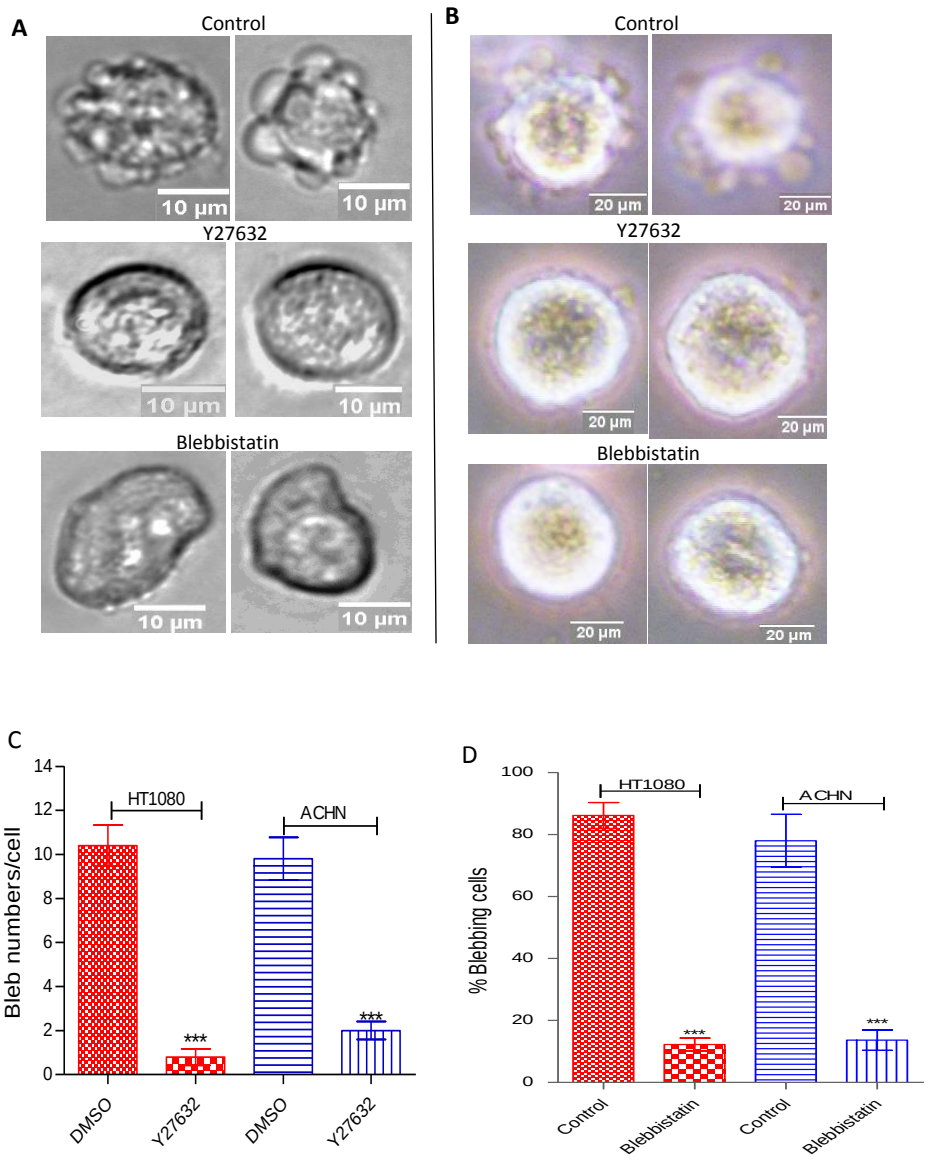

Figure 3.4: Myosin II activity is required for cell blebbing. HT-1080 and ACHN cells cultured in matrigel were treated with BB-94 and PIC plus caspase inhibitor VI. **A.** and **B.** HT1080 and ACHN cells treated with only BB-94 and PIC (upper panel), while bottom panels show cells in which myosin II activity has been blocked with blebbistatin (50 µM); **C.** Quantification of bleb numbers; **D.** Quantification of percentage of blebbing cells in control and blebbistatin treated cells. Data are a representative of the means ± SEM of three independent experiments performed in triplicate in which 75 cells were analyzed for each case. ***:P < 0.001, using one-way ANOVA after Tukey's multiple comparison test.

3.3.4 Expression of cortex-membrane linker proteins

The interaction between the actin cortex and the plasma membrane is firmly mediated by the ERM proteins (Arpin et al., 2011), Thus, for cells to bleb, there must be a destabilization of the cortex-membrane interaction. To test the proposition that the ERM proteins strengthens the cortex-membrane interaction which prevents membrane blebbing, HT-1080 cells were transfected with different amounts of ezrin and moesin using Fugene 6 transfection reagent as described in the materials and methods section. As anticipated, no blebs were formed by cells overexpressing ezrin-GFP and moesin-GFP (figures 3.5b and 3.5d respectively). Whereas cells transfected with a dominant negative ezrin-T567A-GFP were blebbing (figure 3.5c), overexpression of a constitutively active ezrin-T567D-GFP inhibited cell blebbing (figure 3.5e). Upon quantification, it was revealed that over 60% of cells expressing the dominant negative ezrin-T567A were blebbing, whereas only 12% and 7% of cells expressing the dominant active ezrin-T567D and ezrin-GFP respectively were blebbing (figure 3.5f). This data suggests that ERM proteins-mediated cortex-membrane interaction prevents cell blebbing.

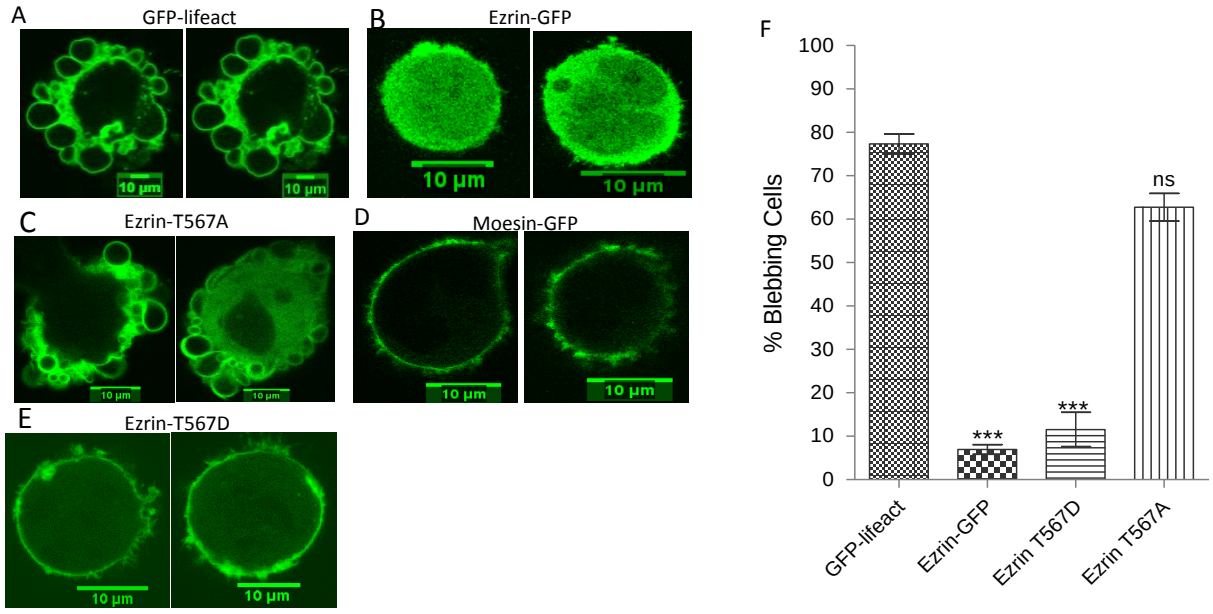

Figure 3.5: Expression of ERM proteins. HT-1080 cells were grown to confluent and transfected with: **A.** 1 µg GFP-lifeact, **B.** 1 µg ezrin-GFP; **C.** 1 µg GFP-ezrin T567A; **D.** 2 µg moesin-GFP; **E.** 1 µg ezrin-T567D. Thereafter, cells were embedded in matrigel and treated with BB-94, PIC and caspase inhibitor VI and then incubated at 37ºC. **F.** Quantification of percentage of blebbing cells transfected with ezrin-GFP, ezrin-T567D (constitutively active ezrin) and ezrin-567A (dominant negative form of ezrin). 50 cells were scored in each case. Data represents mean ± SEM for three separate experiments performed in triplicate. P values were obtained using one-way ANOVA followed by Tukey's multiple comparison test. ***:$P < 0.001$.

3.3.5 Detection of expression levels of Aquaporins (AQPs) in cancer cells

To investigate the role of AQPs in cancer cell blebbing, the expression levels of multiple AQPs previously shown to be involved in cancer was assessed in HT1080 cell line. Cells were seeded on a 6-well plate at a density of $2.5x10^5$ cells/well and incubated at 37ºC overnight. Cells were rinsed with prechilled PBS and lysed with RIPA buffer in the presence of PIC (1:100). Proteins were resolved on a 12% SDS gel and then western-blotted with human AQPs 1, 3, 4 and 5. As shown in figure 3.6a, whereas there was little or no expression

of AQPs 3 and 4, there was a high expression of AQPs 1 and 5 in HT1080 cells, thus, these two proteins were further investigated. Similarly, the expression levels of AQP1 across the six different cancer cell lines was assessed and the protein was found expressed in all the cell lines tested (figure 3.6b).

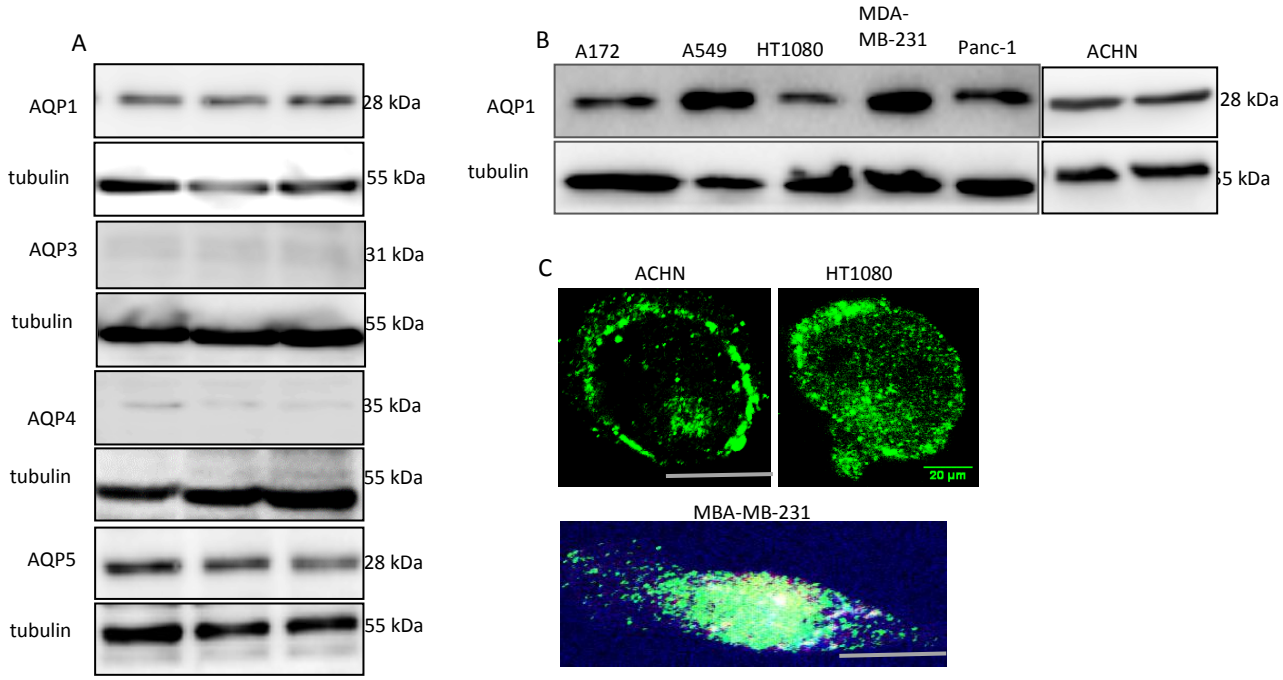

Figure 3.6: Expression of aquaporins in cancer cells. A. HT1080 cells grown to confluent were lysed in RIPA buffer in presence of PIC. Proteins were resolved on a 12% SDS gel before immunoblotting with human anti-AQP1, 3, 4 and 5 antibodies; **B.** Expression levels of AQP1 in different human cancer cell lines by western blotting. In both cases tubulin was used as a loading control; **C.** Immunocytochemistry shows AQP1 expressed at the plasma membrane of ACHN and HT1080 cells, while it is mainly cytosolic in MDA-MB-231 cell line (bottom image). Data is a representative of three separate experiments. Scale bar – 20 µm.

3.3.6 siRNA-mediated knockdown of AQP1 gene

To investigate the role of AQP1 in the blebbing of cancer cells, HT1080 and ACHN cells were grown at density of 2 x 10^5 cells/well. Cells were transfected with human AQP1 siRNA using Dharmacon transfection reagent set 4 according to manufacturers' instructions as

described in the materials and method. To ensure effective knockdown, AQP1 was targeted at four different sequences and knockdown in both cell lines occurred at 24 h, which in the case of ACHN cell line persisted up to 48 h post transfection as confirmed by western blot analysis (figures 3.7a, b and c). In this, and subsequent RNAi experiments, to ensure knockdowns were not due to non-specific effects, non-targeting scrambled siRNAs were used as control.

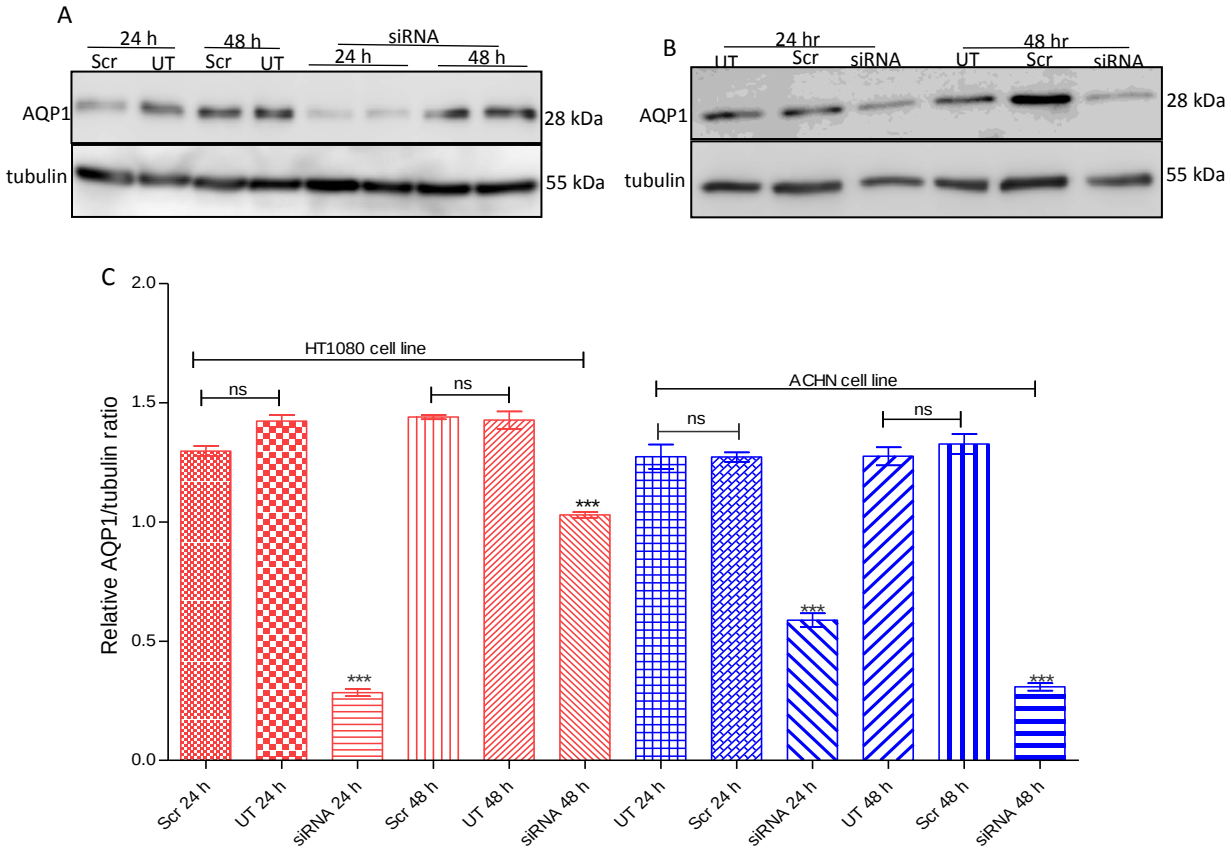

Figure 3.7: siRNA depletion of AQP1 in HT1080 and ACHN Cell lines. HT1080 and ACHN cells were grown to confluent on 6 well plate and transfected with human AQP1 siRNA using Dharmafect transfection reagent (set 4). Cells were lysed using RIPA buffer with protease inhibitor cocktail PIC (1:100 dilution). Proteins were resolved on a 12% SDS gel and immunoblotted with human AQP1 antibody (1:1000 dilution). Tubulin was used as a loading control. **A.** Immunoblot of AQP1 knockdown in HT-1080 cells; **B.** Immunoblot of AQP1 knockdown in ACHN cells; **C.** Densitometric quantification of AQP1 levels in HT-1080 and ACHN cell lines after normalization to tubulin loading control; Data is a representative of the mean ± SEM for three independent experiments; ***:P<0.001; UT = untreated control; Scr = scrambled control; ns = non-significant.

3.3.7 AQP1 knockdown inhibits cell blebbing

To investigate the effect of siRNA-mediated knockdown of AQP1 on the blebbing of cells in a 3D environment, AQP1 siRNA-transfected cells were cultured in growth factor reduced

matrigel using serum-free media. To induce blebs, the activities of MMPs and proteases were blocked with BB-94 (1 µM) and PIC (1:100) respectively, and to prevent apoptotic bleb formation, cells were treated with 10 µM caspase inhibitor set VI. As seen in figures 3.8a, in HT1080 cells, knockdown of AQP1 at 24 h abrogated blebbing. However, at 48 h post transfection of the cell line, a recurrence of blebs was observed. Similarly, AQP1 gene knockdown at 48 h in ACHN cell line abrogated blebbing of the cells (figure 3.8b).

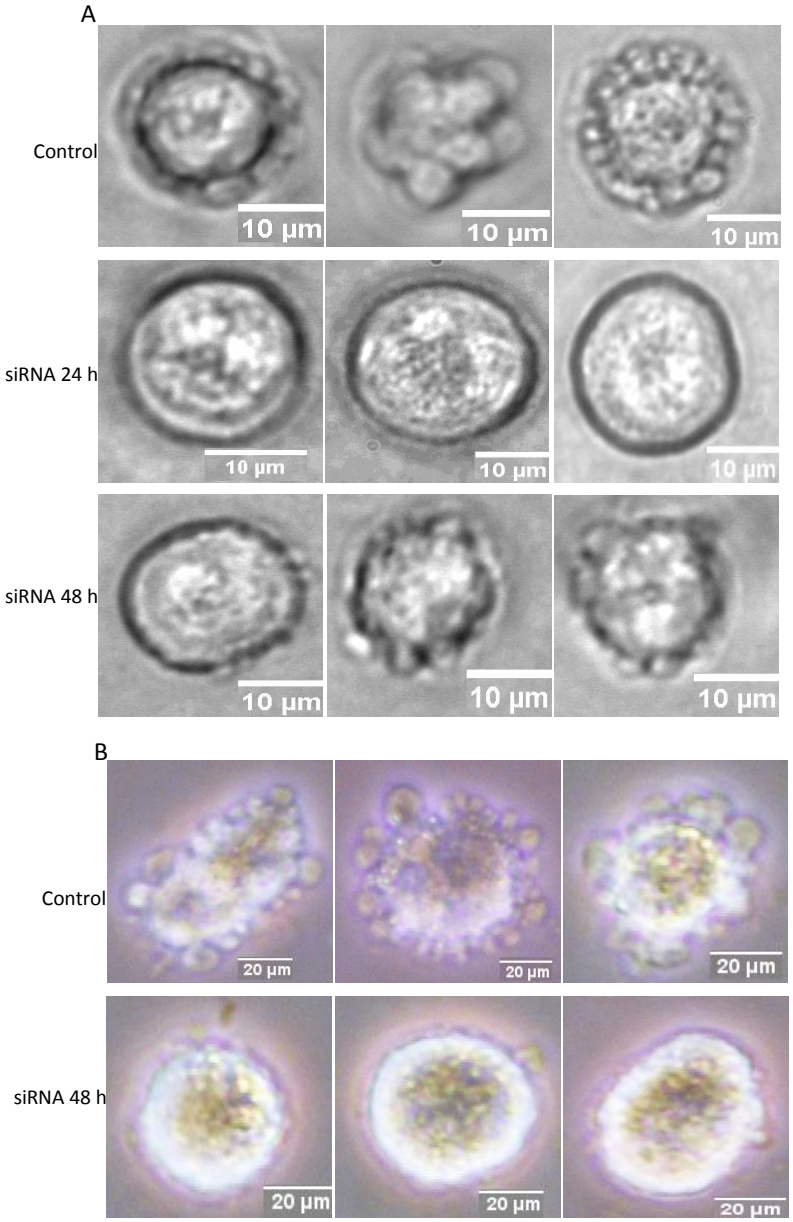

Figure 3.8: AQP1 knockdown inhibits blebbing. AQP1 siRNA transfected HT1080 and ACHN cells were embedded in matrigel and challenged with 1 µM BB-94 and PIC (1:100 dilution) in the presence of 10 µM caspase inhibitor set VI. **A.** HT1080 cells (upper panel - control, middle panel - AQP1 siRNA 24 h, bottom panel - AQP1 siRNA 48 h); **B.** ACHN cells (upper panel - control, bottom panel - AQP1 siRNA 48 h). Data represent the mean ± SEM of three independent experiments performed in triplicate in which 75 cells were scored for each treatment.

3.3.8 Assessment of Bleb Numbers and Size upon AQP1 knockdown

To further assess the impact of AQP1 siRNA on cancer cells, the number of blebs as well as their sizes were quantified. Quantification of bleb numbers indicates that AQP1 knockdown at 24 h in HT1080 cells completely blocked the cells from blebbing with no visible quantifiable bleb number. Although blebs appeared 48 h post transfection, there was a drastic reduction in their number and size as compared to wild-type cells (figure 3.9a). Similar effect was found in ACHN cells upon AQP1 knockdown (figure 3.9b). This data suggests that AQP1 promotes cancer cell blebbing.

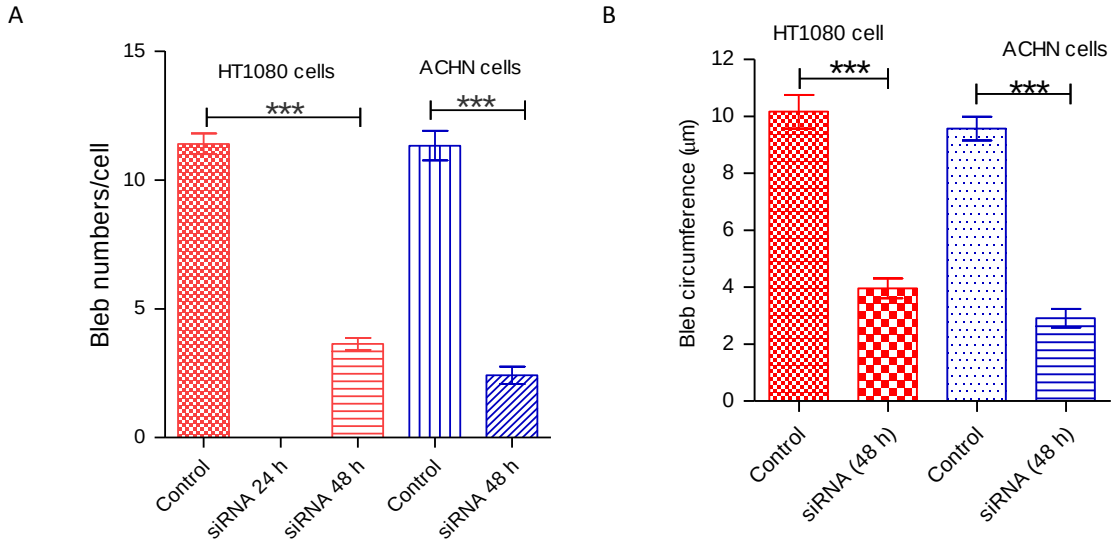

Figure 3.9: Bleb numbers and size after AQP1 knockdown. A. Quantification of bleb numbers in HT1080 and ACHN cells; **B.** Quantification of bleb size of HT1080 and ACHN cells. Data represent the mean ± SEM of three independent experiments in which 75 cells were tracked for each parameter. ***:P < 0.001, using one-way ANOVA after Tukey's multiple comparison test.

3.3.9 Impairment of AQP1 activity in HT1080 cells prolongs bleb lifespan

Although AQP1 knock down was confirmed at the 24 h time point in HT1080 cells (an effect that correlated with abrogation of blebs in the cells (figures 3.7a and 3.8a, middle panel),

AQP1 expression did reappear at 48 h (figure 3.7a) and this paralleled the recurrence of blebs at that time point (figure 3.8a, bottom panel). Thus, it was imperative to undertake a comparative examination of the bleb life cycle in wild-type and 48 h AQP1-transfected cells. Upon detailed analysis of the bleb dynamics by tracking time-lapse movies of live blebbing cells, it was revealed that blebs in AQP1-impaired cells expand, stabilize and retract much more slowly (9.7, 3.9 and 14.3 seconds respectively) than the wildtype cells (7.0, 3.0 and 10.3 seconds respectively) (figure 3.10a, b and c). The net effect is a longer lifespan on the AQP1-deficient blebs (28.1 seconds) than the wild-type cells (figure 3.10d). This data demonstrate that impairment of AQP1 activity increases the lifespan of a bleb.

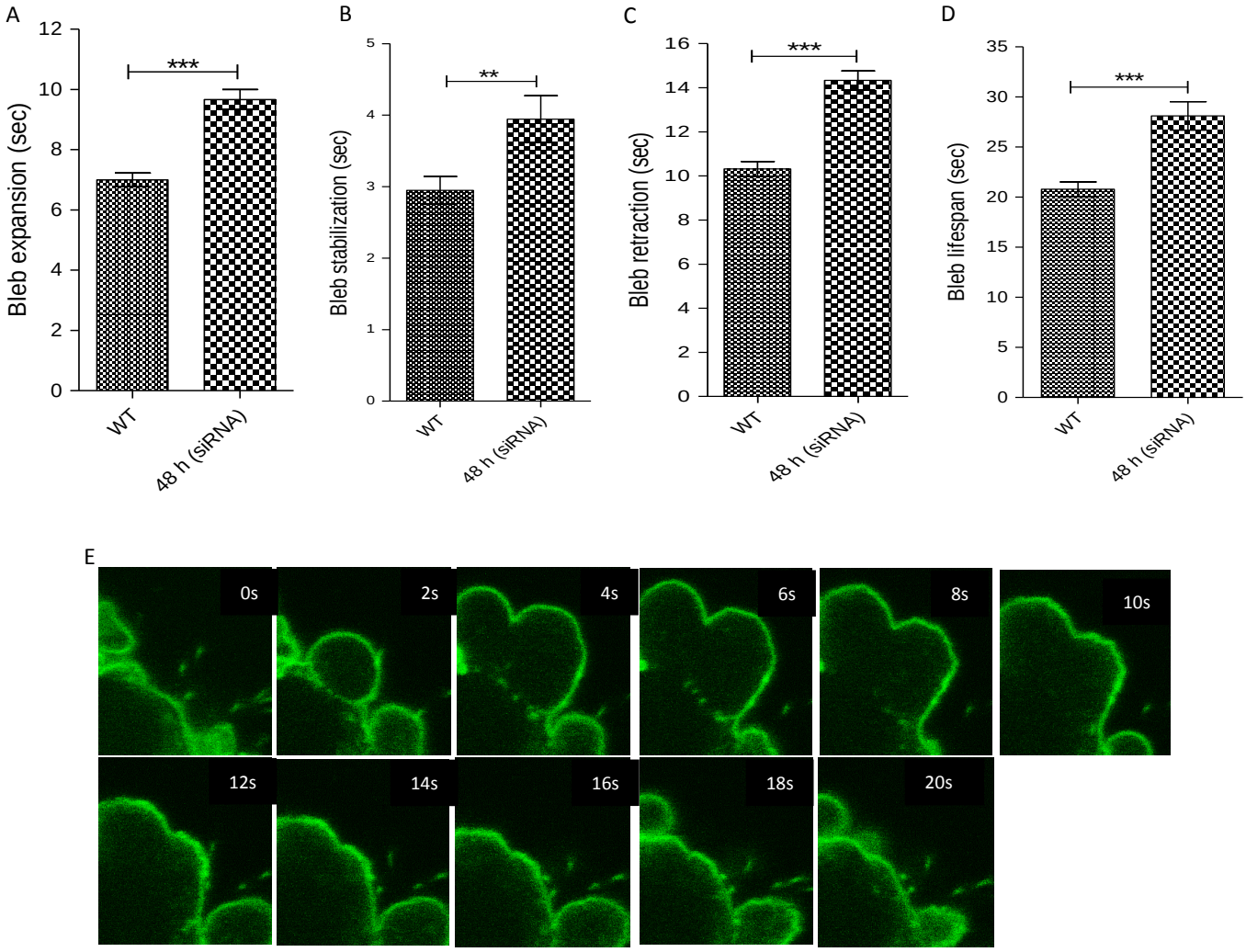

Figure 3.10: Bleb dynamics upon AQP1 perturbation. The dynamics of blebs was determined by manually tracking time-lapse movies of blebbing cells using ImageJ. **A, B and C.** Impaired AQP1 activity significantly increased time of bleb expansion, stabilization and retraction respectively; **D.** Impaired AQP1 activity confers longer bleb lifespan. **E.** A cropped confocal montage showing bleb life cycle in GFP-lifeact-transfected HT1080 cells. Data are the means ± SEM of three independent experiments performed in triplicates in which 75 cells were tracked in each case. **:$P < 0.01$; **:$P < 0.001$, using two-tailed unpaired student's t test.

3.3.10 AQP1-GFP overexpression in cancer cells

AQP1-mediated water passage has been reported to enhance cell migration by facilitating lamellipodia formation at the leading edge (Papadopoulos and Saadoun, 2014). Thus, to

further study the role of AQP1 in cell blebbing, AQP1 was overexpressed in cells by transfecting them with AQP1-GFP as described in materials and methods. Upon overexpression, more AQP1 was found localized to bleb membranes than the other remaining cellular plasma membranes as shown by quantification of fluorescence intensity along bleb and cellular membranes (figure 3.11a and b) as well as intensity profile data generated using freeware imageJ (figure 3.11c).

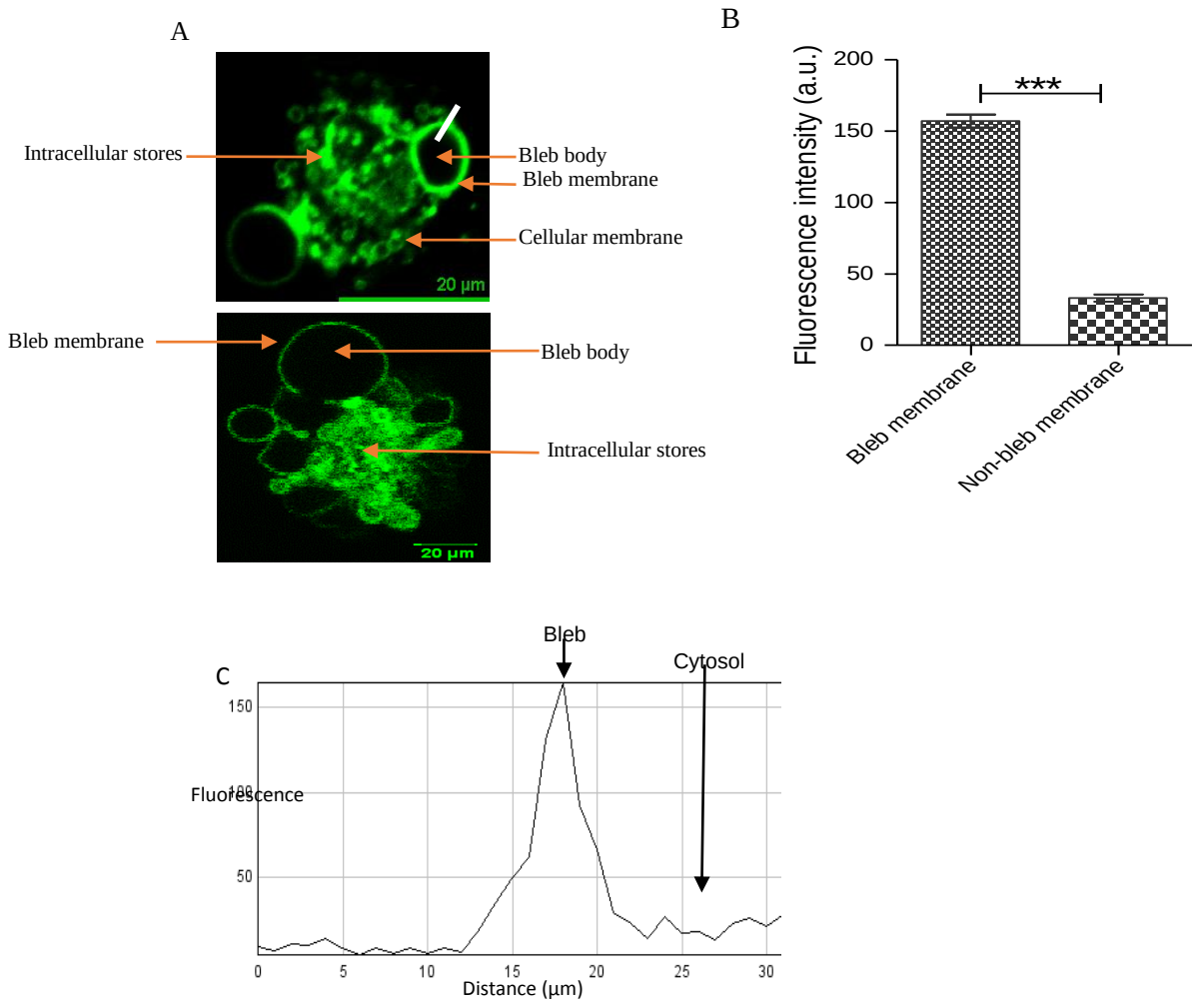

Figure 3.11: AQP1-GFP overexpression. A. AQP1-GFP overexpression in ACHN (top panel) and HT1080 (bottom panel) reveals more localization of the protein at bleb membranes than other parts of cellular membrane; **B.** Quantification of fluorescence intensity of AQP1-GFP expression in bleb and cellular membranes; **C.** Intensity profile diagram. Data is a representative of three independent experiments performed in triplicate in which 25 cells were scored. **:$P < 0.001$, using two-tailed unpaired student's t test.

3.3.11 Increased Bleb Size upon AQP1-GFP Overexpression

To further study the morphological changes induced by AQP1-GFP overexpression, the sizes of blebs in AQP1-transfected cells were quantified using the 'freehand selection' tool of imageJ. It was discovered that AQP1-GFP overexpression in both cell lines induced a nearly two-fold increase in the size of blebs. However, overexpression of the channel protein significantly decreased the number of blebs in both cell lines as compared to wild-type cells (figures 3.12a, b, c and d).

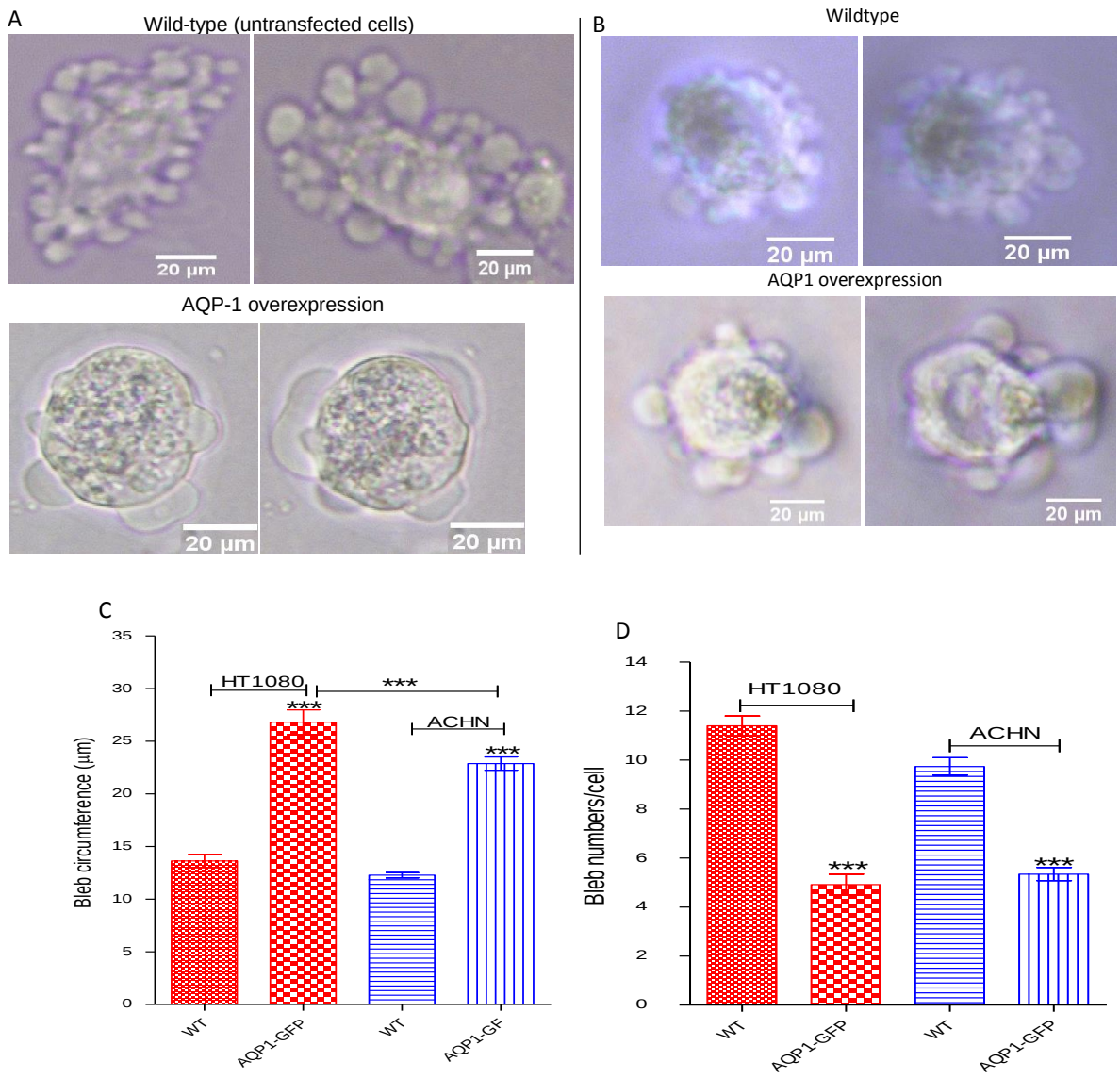

Figure 3.12: AQP1-GFP overexpression increases bleb size. HT1080 and ACHN cell lines transfected with AQP1-GFP were cultured in matrigel and then challenged with BB-94 (1 µM) and PIC (1:100) in presence of caspase inhibitor set VI (10 µM). **A** and **B (lower panels).** AQP1 overexpression significantly increased bleb size, but decreased bleb numbers; **C.** and **D.** Quantification of bleb size and numbers respectively in AQP1-transfected HT1080 and ACHN cell lines. Data represents the means ± SEM of three independent experiments done in triplicate. ***:$P < 0.001$, using one-way ANOVA after Tukey's multiple comparison test.

3.3.12 AQP1 Overexpression Increased Bleb Expansion and Retraction Speed

Since AQP1 overexpression resulted in an increase in bleb size but decreased bleb numbers, it was first asked how active those blebs were, and whether they behave like the wild-type blebs. Therefore, phase contrast time-lapse movies of live-blebbing AQP1-overexpressing HT1080 cells cultured in 3D matrigel were generated and the different phases of a bleb life cycle were tracked. A detailed analysis of the bleb dynamics revealed that the time of expansion and stabilization phases of blebs in AQP1-overexpressing and wild-type cells were similar as no significant difference existed between them (figures 3.13a and b). However, it was found that AQP1-overexpressing cells retracted their blebs in a much more shorter time than wild-type cells (figure 3.13c), an effect that conferred the former a shorter lifespan (figure 3.13d).

As blebs in AQP1-GFP overexpressing cells were much larger, it was necessary to determine the speed of expansion and retraction rather than simply the time taken to expand and retract. Upon quantification of speed (ratio of bleb distance to time of expansion or retraction), it was revealed that in wild-type cells, speed of bleb expansion was higher than that of retraction (albeit, not significantly). Although, overexpression of AQP1-GFP significantly increased bleb expansion speed, it is interesting to note that upon AQP1 overexpression, the speed of bleb retraction became elevated to an extent that it was significantly higher than that of bleb expansion (figure 3.13e). Taken together, this data demonstrate that AQP1 regulates cell blebbing by increasing bleb retraction speed.

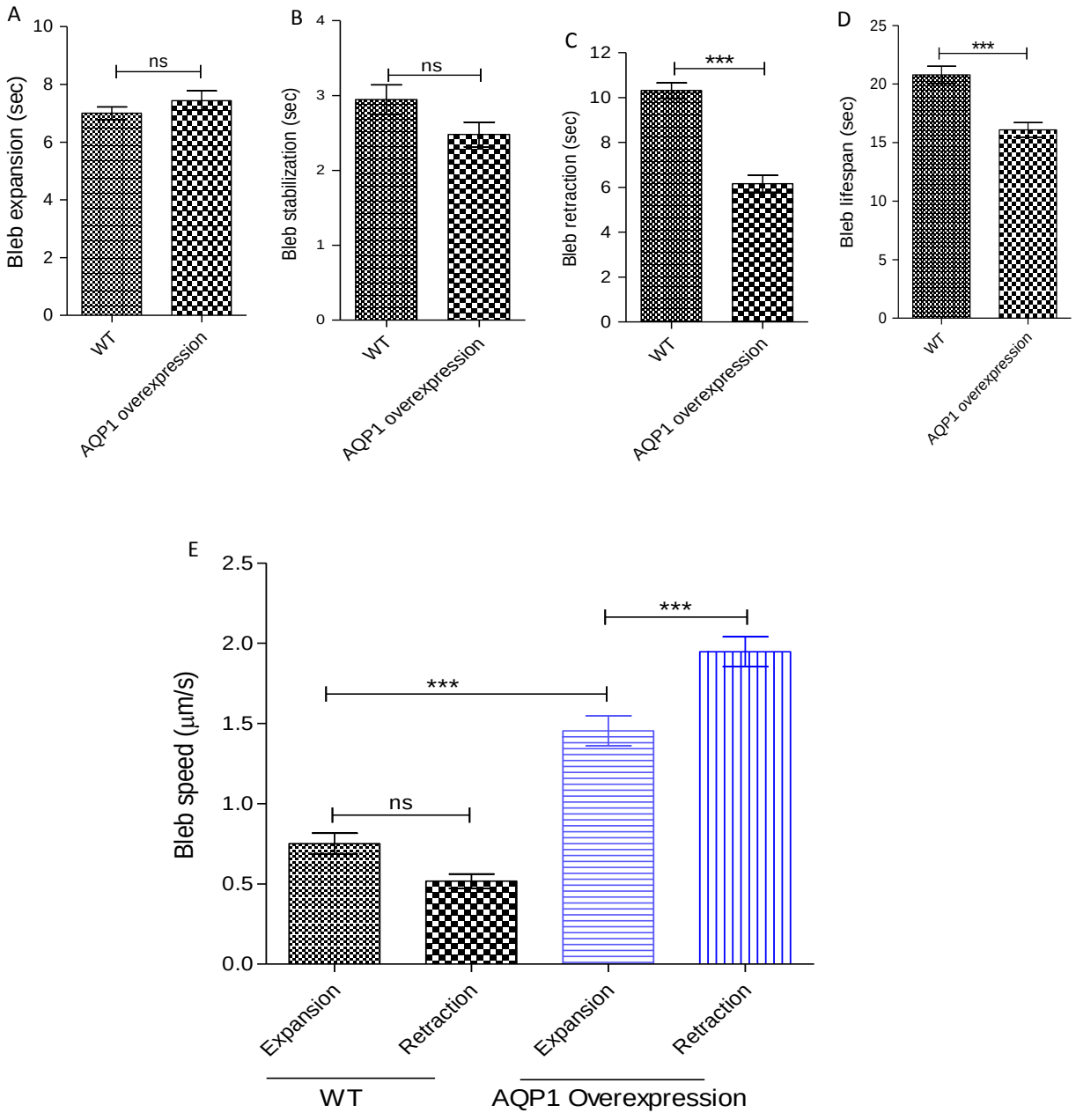

Figure 3.13: AQP1 overexpression facilitates bleb retraction speed. HT1080 cells transiently overexpressing AQP1-GFP were cultured in matrigel and treated with bleb-inducing agents before incubating at 37ºC overnight before making phase contrast, time-lapse movies at 2 sec/frame for an experimental length of 10 min. **A. and B.** Quantification of bleb dynamics in HT1080 cells showed that bleb expansion and stabilization in wild-type and AQP1 overexpressing cells are not significantly different; **C.** AQP1 overexpressing cells retract their blebs faster than wild-type cells; **D.** AQP1 overexpressing cells have shorter bleb lifespan than wild-type blebs; **E.** Whereas speed of bleb expansion and retraction was not significantly different in wild-type HT1080 cells, AQP1 overexpression significantly increased speed of bleb retraction than bleb expansion speed. Data represents the means ± SEM of three independent experiments in triplicate. ***:P < 0.001, using two-tailed unpaired student's t test, and one-way ANOVA after Tukey's multiple comparison test.

3.3.13 AQP1 levels Accumulate during Bleb Retraction

Since AQP1 localizes to membrane blebs, and facilitates both bleb expansion and retraction, the flow and levels of the protein during the different phases of bleb life cycle of AQP1-GFP transfected HT1080 cells was monitored by generating time-lapse confocal movies of AQP1-GFP expressing cells using 488 laser channel, and bright field movies using the TD channel of a Nikon AIR confocal microscope. The GFP movies were then overlaid on the bright field movies, and AQP1 levels were determined by quantifying the fluorescence intensities during bleb expansion and retraction. As shown in figures 3.14a and b, there was a continuous flow and rise of AQP1 levels during initiation and expansion of bleb. Moreover, the AQP1 levels always accumulate to a peak during the retraction phase before dropping, when the bleb is fully retracted.

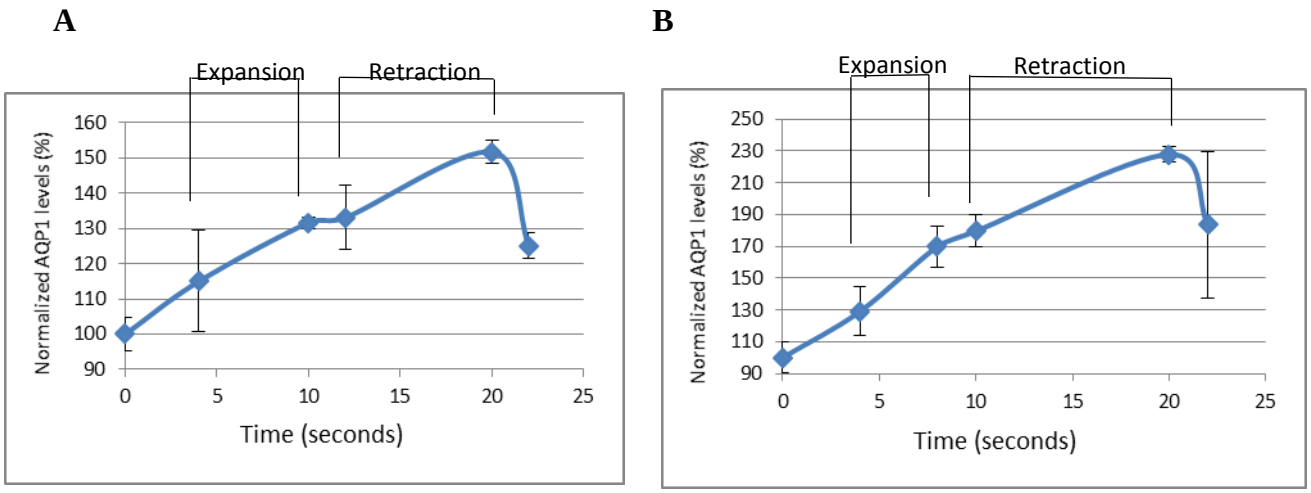

Figure 3.14: Accumulation of AQP1 levels during bleb retraction. A and B. AQP1 levels of blebbing HT108 cells were monitored for different phases of bleb cycle by quantifying the fluorescence intensities of live confocal time-lapse movies of AQP1-GFP overlaid on bright field movies. Intensities values were normalized to preinitiation values and expressed as percentage. The time elapsed between the first and last frames of each bleb phase was manually tracked. Normalizes fluorescence intensities at the different bleb phase were the plotted against the times. 7 of such movies were generated and tracked. Data is the means ± SEM of three independent experiments performed in triplicates.

3.3.14 AQP1 Overexpression induces blebbing morphology in non-blebbing cell line

Since AQP1-GFP overexpression resulted in enlarged bleb sizes in both HT1080 and ACHN cell lines, an investigation into its overexpression in non-blebbing cells was sought. The metastatic breast cancer cell line, MDA-MB-231 when embedded in 3D matrigel matrices and challenged with bleb-inducing agents and caspase inhibitor, do not bleb. They only possess tiny plasma membrane protrusions (figure 3.15, upper panel). Therefore, the cell line was transfected with AQP1-GFP and then phase contrast images of AQP1-transfected and non-transfected cells (controls) were captured. As shown in figure 3.15 (bottom panel), AQP1 overexpression sufficiently induced blebbing in this non-blebbing cell line.

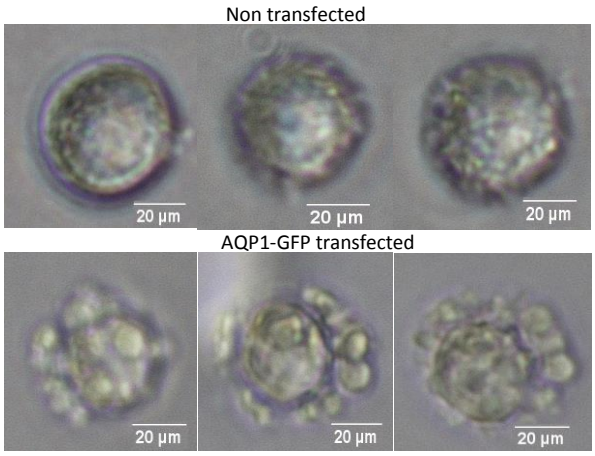

Figure 3.15: AQP1-GFP overexpression induces blebbing phenotype. Non blebbing MDA-MB-231 cells overexpressing AQP1-GFP were embedded in 3D matrigel in the presence of BB-94 (1 µM), PIC (1:100) and caspase inhibitor set VI (10 µM). Overexpression of AQP1 induces blebbing (bottom panel).

3.3.15 siRNA-mediated down-regulation of AQP1 reduces migration of HT1080 cells

Different reports have previously shown the involvement of AQP1 in cell migration in different cell types (Jiang, 2009; Nico and Ribatti, 2010; Verkman, 2011). To test the hypothesis that AQP1 promotes migration of HT1080 cells, a wound healing assay was performed. Briefly, AQP-knockdown cells seeded on a 6 well plate were grown to confluent at 37^{o}C, and with the aid of a sterile pipette a single straight line was drawn across the centre to make a scratch. Media was removed and cells rinsed twice with pre-warm media to remove any debris from the scratched surface after which images where captured (t = 0 h). Cells were then incubated 24 h before the next image acquisitions. As anticipated, AQP1 knockdown by siRNA significantly reduced the ability of cells to cover up the wound when compared to untreated and scramble controls (figures 3.16a and b).

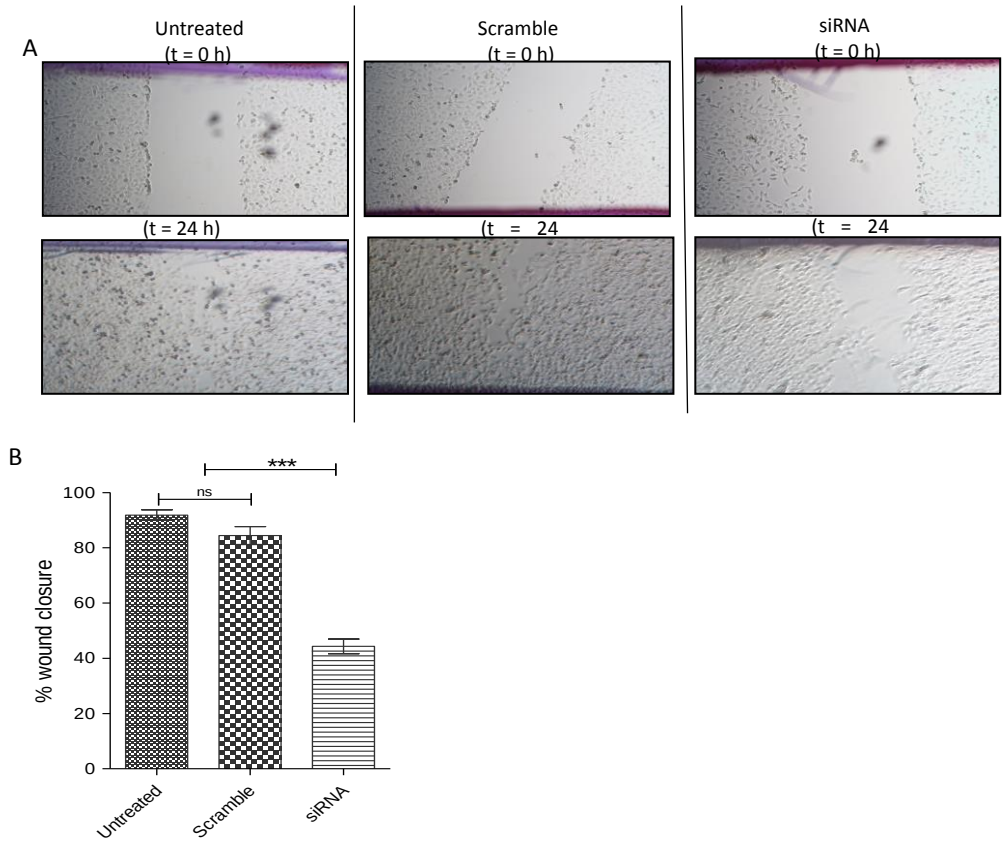

Figure 3.16: AQP1 knockdown reduces cell migration. HT1080 cells (untreated, scramble- and APQ1 siRNA treated) were cultured to confluent at 37^{o}C before scratching a wound. After first image acquisition, cells were incubated again for 24 h before the next acquisition. **A.** Migration of AQP1 siRNA-treated HT1080 cells was significantly impaired; **B.** Quantification of percentage wound closure by the controls and siRNA-treated HT1080 cells. Data is a representative of the means ± SEM of three independent experiments performed in triplicate. **:P < 0.01, using one-way ANOVA after Tukey's multiple comparison test.

3.3.16 Differential involvement of AQP isoforms in cancer cell blebbing: Cell blebbing is independent of AQP5

As the HT1080 cell line was found to also express AQP5 (figure 3.6a), and with the effect of AQP1 knockdown on HT1080 and ACHN cells, namely abrogation of membrane blebs, it was anticipated that other aquaporins might also regulate blebbing. To test this hypothesis, the effect of siRNA-mediated down-regulation of AQP5 on blebbing was investigated.

HT1080 cells were transfected with human AQP5 siRNA as previously described in materials and methods. AQP5 knockdown was confirmed by western blot (figures 3.17a and b) before embedding cells in growth factor-reduced matrigel. As shown in figures 3.17c and 3.17d, blebbing was unaffected in both wild-type and AQP5 knocked down cells. An analysis of bleb numbers per cell and bleb size (figures 3.17e and 3.17f respectively) in wild-type and AQP5-deleted cells revealed no significant difference. This suggests that cancer cell blebbing might be differentially regulated by the AQPs, and that blebbing of HT1080 cells is independent of AQP5 activity.

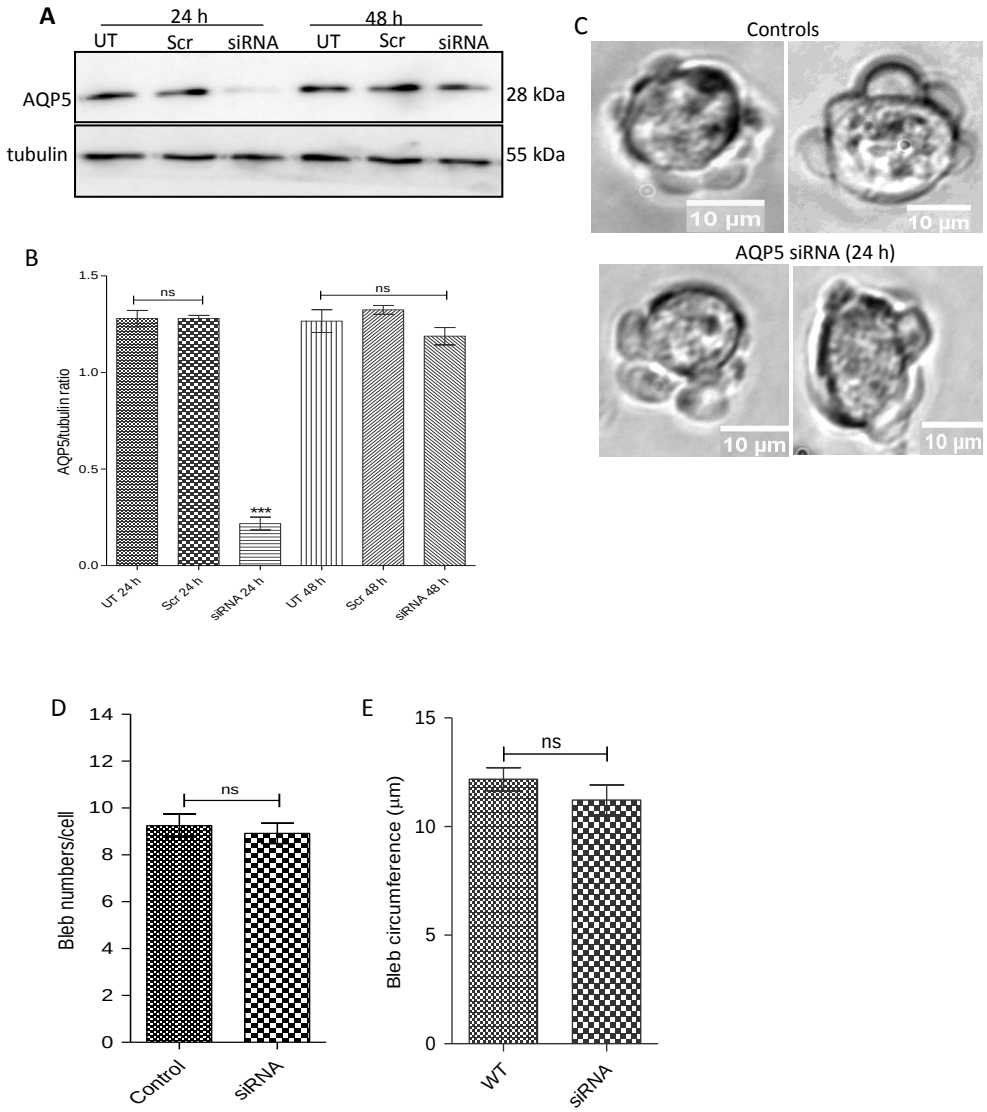

Figure 3.17: AQP5 RNA interference has no effect on cell blebbing. HT-1080 cells were grown to confluent on 6 well plate and transfected with human AQP5 siRNA using Dharmafect transfection reagent (set 4). Cells were lysed using RIPA buffer with protease inhibitor cocktail PIC (1:100 dilution). **A.** Proteins were resolved on a 12% SDS gel and immunoblotted with human AQP5 antibody (1:1000 dilution) using tubulin as a loading control; **B.** Densitometric analysis of AQP5 levels in HT1080 cells after normalization to tubulin loading control; **C.** wild-type and AQP5-knocked down HT1080 cells were seeded in matrigel and treated with BB-94 and PIC in the presence of caspase inhibitor set VI; **D**. No significant difference exists in the number of blebs per cell (25 cells tracked); and **E.** the bleb size of wild-type and AQP5-knocked down cells (25 cells tracked). Data represents mean ± SEM for three separate experiments performed in triplicate. $^{***}P < 0.001$, using one-way ANOVA after Tukey's multiple comparison test. UT = untreated control; Scr = scrambled control; ns = non significant.

3.4 Discussion

The aquaporins are transmembrane water channels that facilitate the flow of water and other molecules in and out of the cell in response to an osmotic gradient arising from salts and ions (Papadopoulos and Saadoun, 2014). These proteins are particularly important as they perform transcellular and transepithelial water transport as well as maintaining body water homeostasis (Krane and Goldstein, 2007). Out of the 13 aquaporins found in mammals, extensive studies have been carried out on AQP1 which is the best characterized and most widely expressed in a variety of tissues throughout human and other mammalian systems (Belge and Devuyst, 2006; Isokpehi et al., 2009). Several pathological conditions have been attributed to impaired aquaporins functions. For instance, AQP2 deficiency has been linked to defective vasopressin-dependent water transport in collecting duct (Deen et al., 1994) as well as nephrogenic diabetes insipidus (Khanna, 2006); AQP3 knock-out in mice has been reported to result in decreased stratum corneum hydration and skin elasticity due to low glycerol in the skin (Verkman, 2012). AQP4 overexpression correlated with brain oedema (Yang et al., 2008a) while its deficiency caused impaired hearing, vision and olfaction (Verkman, 2012). High expression of both AQP4 and AQP9 have been reported in astrocytomas (Jelen et al., 2013). AQP7 deficiency resulted in obesity due to accumulation of glycerol and triglycerides (Hara-Chikuma et al., 2005; Hibuse et al., 2005). Of interest is the discovery that the AQP1 water channel not only facilitates water passage, but is involved in angiogenesis, cell proliferation, cell migration, cell adhesion and carcinogenesis (Moon et al., 2003; Papadopoulos and Saadoun, 2014; Saadoun et al., 2005a). Thus, there is the need for a critical evaluation of not only its role, but the role of other AQPs in cancer metastasis and other pathological conditions. However, despite their involvement in the lamellipodial-based cell migration and tumourigenesis, the role of the AQPs in bleb formation and blebbing of cell has not been investigated.

These blebs are believed to be spherical membrane protrusions produced when the plasma membrane detaches from the underneath cortex which comprises actin, myosin and other proteins. Contractility of actomyosin is said to increase intracellular pressure which drives membrane delamination and blebbing (Charras and Paluch, 2008). As an alternative mode of cell migration, cell blebbing has been studied using the M2 melanoma cell line that is deficient of the actin binding protein filamin-A, and that blebbing of this cell line occurs downstream of the Rho-ROCK signalling pathway (Charras et al., 2006).

Therefore, the present study started to investigate blebbing by screening six different human cancer cell lines: A172 (gliomablastoma), A549 (lung carcinoma), ACHN (renal adenocarcinoma), HT1080 (fibrosarcoma), MDA-MB-231 (breast adenocarcinoma) and Panc-1 (pancreatic cancer) cell lines for blebbing. The screening which was performed by inhibiting the activities of MMPs and other surface proteases, found only the ACHN and HT1080 cells blebbing upon inhibition of matrix proteolysis (figure 3.2). These blebs were non apoptotic as the activity of caspases which are known to execute programmed cell death were inhibited (figure 3.2). The cells were further confirmed to survive bleb induction as determination of cell viability through MTT assay showed 91.53% and 93.98% viability for the HT1080 and ACHN cells respectively (figure 3.3).

Furthermore, it was imperative to establish whether these blebs formed conform to, and are under the influence of the Rho-ROCK signaling pathway reported to govern normal cell blebbing (Paluch and Raz, 2013). Inhibition of ROCK with its known inhibitor, Y27632 effectively blocked blebbing in both cell lines. In a similar vein, this report established the fact that bleb formation in HT1080 and ACHN cell lines was dependent on myosin II-mediated contractility of the actin cortex as relaxation of the cortex via blebbistatin inhibition of the ATPase activity of myosin II drastically reduced the percentage of blebbing cells

(figures 3.4a, b, c and d), suggesting these blebs were under the influence of the Rho-ROCK-MLC signaling pathway.

In previous cell lines used in the study of blebbing, it has been reported that bleb formation requires a weakening and detachment of the membrane-cortex linkage (Paluch et al., 2005; Paluch and Raz, 2013; Tinevez et al., 2009). Usually the plasma membrane of cells is linked to the underlying cortex by the ERM proteins which can exist either in a dormant conformation in which the F-actin binding site is closed or in an active state mediated by phosphoinositides (PIP_2) activation and by phosphorylation of threonine residues at the C-terminus. ERMs interact with the plasma membrane and the actin cytoskeleton through their N-terminal and C-terminal domains respectively. Thus, bleb formation requires dissociation of the membrane from the cortex which could be achieved by among other factors, a destabilization of the cortex-membrane linker proteins. To test the hypothesis that the ERM proteins firmly cement the cortex and membrane, and so are inhibitory to bleb formation, different forms of ezrin (best characterized ERM protein) were overexpressed in HT1080 cells. Indeed, overexpression of GFP-tagged ezrin and moesin inhibited blebbing of HT1080 cells (figures 3.5b and 3.5d). However, cells overexpressing a dominant negative ezrin-T567A-GFP were found blebbing while overexpression of a constitutively active form of ezrin, ezrin-T567D-GFP completely inhibited cell blebbing (figure 3.5c and e). This is in agreement with previous reports in which transfection of cells with ezrin-T567A promoted blebbing while cells overexpressing the dominant active mutant, ezrin-T567D inhibited blebbing (Charras et al., 2006). Therefore, having confirmed that both cell lines conform to the basic properties of bleb formation viz: viability of the cells, Rho-ROCK-mediated actomyosin contractility and the requirement of the ERM proteins for membrane-cortex interaction, this study proceeded to investigate the role of the aquaporins in blebbing.

Three of the aquaporins (AQPs 1, 4 and 5) which selectively transport water, and the aquaglyceroporin (AQP3) which transport glycerol in addition to water, all of which have been previously implicated in cancer (Hara-Chikuma and Verkman, 2008; Jiang, 2009; Jung et al., 2011; Saadoun et al., 2002b; Verkman, 2012; Warth et al., 2004) were investigated. Western blot analysis indicated that the profusely blebbing HT1080 cells expressed only AQPs 1 and 5, (figure 3.6a), hence, only these two AQPs were further investigated in this cell line. AQP1 was also found expressed in the ACHN cells as well as in the other non-blebbing cell lines (figure 3.6b). Interestingly, a higher AQP1 expression was found in the non-blebbing A549 and MDA-MB-231 cell lines, implying that expression levels of AQP1 does not necessarily correlate with a cell's ability to bleb. The AQP water channels are mainly localized in the plasma membrane, although they are also found localized in cytosolic compartments, and they do translocate to the plasma membrane in response to activation by hormones and kinases (Conner et al., 2013). For instance, a PKA-dependent AQP1 phosphorylation and plasma membrane translocation has been reported in oocytes (Han and Patil, 2000), in astrocytes, hypotonicity-induced AQP1 translocation has been shown (Conner et al., 2012). Similarly, in HEK293 cells, it has been reported that AQP1 was trafficked to the plasma membrane in a PKC-dependent mechanism (Conner et al., 2010). It might therefore be that most of the AQP1 in the non-blebbing MDA-MB-231 and A549 cells could be localized to the cytosol, and that a plasma membrane translocation mechanism might be required for these cells to bleb. Indeed, immunocytochemical staining with human anti-AQP1 antibody indicated AQP1 expression at the plasma membranes of both ACHN and HT1080 cells, whereas, the protein was mainly expressed in the cytosolic compartment of MDA-MB-231 cell line (figure 3.6c).

Having found AQP1 being expressed in both blebbing cell lines, the AQP1 gene was knocked down using smartpool siRNA that targets AQP1 from four different sequences and knockdown was confirmed by western blot. Specifically, knockdown of AQP1 in HT1080 cells occurred at 24 hours (80.02%) post siRNA transfection (figure 3.7a and c), and this completely blocked the cells from blebbing (figure 3.8a, middle panel). In the renal ACHN cell line, AQP1 knockdown also occurred at 24 hours (53.79%) and this persisted until 48 hours (75.83%) post transfection (figure 3.7b and c). Again, AQP1 knockdown in this cell line at 48 hours sufficiently suppressed cell blebbing (figure 3.8b, bottom panel), drastically reducing both bleb numbers and size from 11 blebs/cell and 9 µm to 2 blebs/cell and 3 µm respectively (figures 3.9a and b).

However, at 48 hours post AQP1 siRNA transfection of HT1080 cells, it was observed that blebs started emerging from the cells (4 blebs/cell) (fig 3.8a, bottom panel), and upon quantification, it was observed that a more than two-fold decrease in both numbers and size of blebs occurred at the 48 hour time point (4 blebs/cell; 3.96 µm) as compared to wild-type (11 blebs/cell; 10.16 µm) (figures 3.9a and b). Importantly, the reappearance of blebs at 48 hours post AQP1 siRNA transfection paralleled the expression of AQP1 protein levels at this time point as revealed by immunoblot analysis (figure 3.7a). A comparative analysis of bleb life cycle which is the entire lifespan of a bleb, between wild-type and 48 hour AQP1 siRNA transfected cells revealed that blebs re-emerging 48 hour post-AQP1 knockdown had longer lifespan (28.1 seconds) as compared to wild-type blebs (20.8 seconds) (figure 3.10d). Since a bleb lifespan consists of expansion, stabilization and retraction (Charras and Paluch, 2008; Collins-Hooper et al., 2012), it was imperative to examine the bleb dynamics in wild-type cells and the blebs reappearing after 48 hour AQP1 knockdown. Upon detailed analysis of bleb dynamics by time-lapse microscopy, it was discovered that blebs re-emerging post-

AQP1 knockdown took a relatively longer period (9.7 seconds) of expansion than wild-type blebs (7.0 seconds; figure 3.10a) possibly because of defective mechanism of water flow across the plasma membrane, and cytoplasmic lipids from the cytosol into the growing bleb. It was also noted that the AQP1-deficient blebs had a longer time of stabilization than the wild-type blebs (3.9 seconds and 3.0 seconds respectively) (figure 3.10b). Similarly, the time of retraction did differ significantly. It took wild-type blebs 10.3 seconds to retract the membrane, whereas the AQP1-deficient blebs retracted their membrane for a longer period of 14.3 seconds (figure 3.10c). Bleb retraction is associated with recruitment of cortex-membrane binding proteins as well as repolymerization of actin (Norman et al., 2011). Thus, one possible explanation for the observed slow bleb retraction in the AQP1-deficient cells could be that deficiency of AQP1 negatively affected the recruitment and reassembly of the membrane-cortex linker proteins as well as reducing the repolymerization of cortical actin, events known to orchestrate bleb retraction. This suggests AQP1 might also function in facilitating recruitment of actin nucleation factors such as the Arp2/3. In a similar vein, impaired AQP1 function might have weakened the efflux of fluid out of the retracting bleb, thereby resulting in the protracted retraction phase.

It is worthy of note that, similar to previous reports where AQP1 deficiency resulted in decreased membrane ruffles (Hara-Chikuma and Verkman, 2006), in the present study, siRNA-mediated down-regulation of AQP1 caused a drastic reduction in the number and size of membrane blebs. The large bleb size in the wild-type cells may be due to rapid water influx through AQP1 into the cytoplasm leading to increased hydrostatic pressure that caused a rapid expansion of blebs in these cells, whereas the AQP1-deficient cells are defective in water transport mechanism thereby leading to slower water passage that results in longer duration of bleb expansion, stabilization and retraction, an effect that resulted in prolonged

lifespan in the AQP1-deficient cells. It is not out of place to speculate that the few minute membrane ruffles found in the AQP1-null cells may be probably due to membrane lipid bilayers which they themselves can also transport water, albeit , at a very slow rate.

To get further insights into the roles of AQP1 in cancer cell blebbing, a GFP-tagged AQP1 was overexpressed in both blebbing ACHN and HT1080 cell lines, and it was found that in both cell lines, AQP1 localized to membrane blebs (figure 3.11a). To compare the level of AQP1 expression in bleb membranes and the remaining cellular membrane, fluorescence intensities at the bleb and cellular membranes were quantified. The result showed more than a two-fold concentration of AQP1 in bleb membranes than the cellular membranes (figure 3.11b). In accordance with previous reports that AQP1 could also be cytoplasmic (Conner et al., 2013), a high intracellular stores of AQP1 was also observed in the HT1080 cell line (figure 3.11a, bottom panel). AQP1 overexpression has been previously associated with cell swelling and volume increase (Conner et al., 2012; Zhang et al., 2013), thus, it was anticipated that AQP1 overexpression might modulate bleb morphology. Indeed, live cell imaging with phase contrast microscopy to assess the morphological alterations upon AQP1 overexpression revealed that AQP1 overexpression significantly increased the sizes of blebs (figure 3.12a, b and c) with a decrease in the number of blebs (figure 3.12d) in both cell lines. The effect of AQP1 overexpression on bleb size was more profound in the HT1080 cells as those blebs are significantly larger than blebs in the ACHN cell line (figure 3.12c). Whether the HT1080 cells express more aquaporin water channels than the ACHN is not clear, however, western blotting and immunostaining with human anti-AQP1 antibody from this study showed no difference in the expression levels of AQP1 in both cell lines.

An analysis of the dynamics of the blebs between AQP1-overexpressing and wild-type HT1080 cells showed no significant difference in bleb expansion and stabilization (figure

3.13a and b). However, AQP1-overexpresing cells retracted their blebs much more faster (6.2 seconds) than the wild-type cells (10.3 seconds), an effect that conferred the former a shorter lifespan (figure 3.13c and d). A track of the speed with which the blebs expanded and retracted their membrane revealed that, although, in the wild-type cells, no significant difference existed in the speed of bleb expansion and retraction, speed of expansion was higher than retraction speed. However, upon AQP1 overexpression, bleb retraction speed became significantly higher than that of expansion despite the fact that there was an increase in expansion speed when compared to wild-type cells (figure 3.13e). This unexpected finding is quite novel as the AQPs were thought to mediate bleb expansion by allowing water influx into a growing bleb, while bleb retraction was due to actin repolymerization. This novel finding suggests that AQP1 is critical for the retraction phase of cell blebbing, and that perhaps other AQPs could regulate cell blebbing in similar manner.

To probe into the AQP1-facilitated increase in bleb retraction speed, the flow of AQP1 during the different phases of the bleb cycle was monitored by generating and tracking an overlay of time-lapse confocal movies of AQP1-GFP overexpressing HT1080 cells which were excited using 488 laser channel for GFP and TD for bright field movies. Analysis of the fluorescence intensities, which was used as a read-out for AQP1 levels at the different phases of the bleb cycle revealed that AQP1 flows, and gradually increased from bleb initiation through expansion and subsequently accumulated and peaked during bleb retraction (figures 3.14a and b). However, it remains unresolved whether the increased fluorescence intensity observed during retraction was actually due to AQP1 accumulation or due to thickening of the membrane curvature as attempts to stain the plasma membrane with membrane dyes (FM4-64 and CellMask orange) to distinguish it from the bleb membrane were not successful as the dyes stained every part of the cells. In cell lines previously studied, the retraction phase

of bleb cycle is the longest (Charras, 2008; Charras et al., 2008), so it was anticipated that speed of expansion would be higher than that of retraction as AQP1 overexpression would enhance more water influx into the growing bleb. Therefore, the unexpected increase in bleb retraction speed could be in part due to influence of activity of plasma membrane ion channels which might affect the extracellular and intracellular ionic states as well as generation of pH gradients across the membrane.

As the aquaporins have been shown to promote formation of plasma membrane protrusions, for instance, AQP9-mediated induction of filopodia (Loitto et al., 2007), and AQP1-facilitated lamellipodia polymerization (Papadopoulos and Saadoun, 2014), and most importantly, because overexpression of AQP1 increased the size of blebs in the two cell lines tested in this study, the effect of its overexpression in non blebbing cells was sought. The metastatic human breast cancer cells MDA-MB-231 were detected by western blotting to have a high endogenous expression of AQP1 levels (figure 3.6b), yet they do not bleb, suggesting that in this cell line, most of the AQP1 might be mainly cytosolic as confirmed by immunostaining with human anti-AQP1 antibody (figure 3.6c), and that in general terms, the level of AQP1 expression does not necessarily correlate with blebbing. Interestingly, AQP1 overexpression sufficiently induced bleb formation in this cell line (figure 3.15). This suggests that the overexpression of AQP1 in this cell line, in part, caused a rise in the intracellular stores of the proteins and its subsequent translocation to the plasma membrane, an effect that resulted in blebbing of the cells.

The AQP1 water channel has been previously ascribed a positive role in lamellipodial-based cell migration. It was reported to facilitate actin polymerization that powers formation of lamellipodia and the subsequent inflow of water through the leading edge, and the net effect was cell migration (Papadopoulos and Saadoun, 2014; Papadopoulos et al., 2008). Thus, the

involvement of AQP1 in migration of HT1080 cells was tested by performing *in vitro* wound healing assay in which cells were plated on 12-well plates and treated in triplicate with either AQP1 siRNA, scrambled siRNA or untreated. As previously reported, AQP1 knockdown at 24 hours by siRNA impaired migration of the cells to cover up the scratched wound (figure 3.16a). An analysis of wound closure indicated that AQP1 knocked down cells were only able to cover up 44.31% of the wounds as compared to 84.42% and 91.85% for scrambled and untreated controls respectively (figure 3.16b).

A further investigation into the role of the AQPs in blebbing was carried out with a probe into the involvement of the water-selective AQP5 which was detected by western blotting to be expressed by the HT1080 cell line (figure 3.6a). Located at the apical membrane of epithelial cells in mammalian tissues, this water channel is also expressed in salivary and lacrimal glands where it mediates sweat secretion necessary for thermoregulation (Krane and Goldstein, 2007; Nejsum et al., 2002; Sidhaye et al., 2012). AQP5 has been previously reported to promote cell proliferation and migration (Zhang et al., 2010), and is upregulated in various human cancers such as breast, colorectal and lung cancers (Chae et al., 2008; Jung et al., 2011; Kang et al., 2008b). However, results from this study showed no apparent effect of AQP5 knockdown (82.95%) on the blebbing of HT1080 cells as both bleb numbers and size of wild-type and AQP5-knockdown cells were similar with no significant difference (figures 3.17a, b and c). Why AQP5 played no role in the formation of blebs in this cell line is unknown. It might be that the amount of AQP5 left after knockdown (17.05%) is still enough to exert its normal function, if this is the case, then gene knockout may be necessary to study its role. However, as a molecular mechanism, AQP5 has been previously reported to possess a diproline peptide sequence similarity to SH3 binding consensus site, and this confers it the capability to bind SH3 domain-containing proteins. Indeed, AQP5 was found

bound to the SH3 domains of lyn, Grap2 and c-Src, a non-receptor cytoplasmic tyrosine kinase in human lung cancer cells, an event that triggered downstream signaling to promote tumourigenesis and metastasis (Chae et al., 2008). Whether AQP5 has an absolute requirement for binding SH3 domains to perform it functions is not known, however, if that is the case, then the non-involvement of AQP5 in blebbing of HT1080 cells might be due to impaired binding or that lyn, Grap2 or c-Src are not expressed in these cells. It might also be that AQP5 regulates cell blebbing in a cell type-specific manner. This calls for investigating the role of AQP5 in other blebbing cell lines. Because the ACHN cell line was only acquired recently, the present study was out of time to study AQP5 knockdown in this cell line.

The present study also attempted to investigate the role of the aquaglyceroporins which transport glycerol in addition to water in cancer cell blebbing. The aquaglyceroporins include AQP3, AQP7, AQP9 and AQP10. Of these, AQP3 has been reported to promote skin tumourigenesis (Verkman, 2012) and proliferation of epidermal cells (Hara-Chikuma and Verkman, 2008), deficient AQP7 expression correlates with obesity (Hibuse et al., 2005), while AQP9 is reported to regulate glycerol metabolism (Carbrey et al., 2003). In three separate experiments to probe for AQPs 3 and 4, the expression levels of these proteins in HT1080 cells were found to be so low (barely detectable) (figure 3.6a) that it was difficult to knock them down by siRNA.

Data presented in this chapter have demonstrated that HT1080 and ACHN cells express AQP1, and is localized to membrane blebs and most importantly, the novel findings here are that i) siRNA-mediated knockdown of AQP1 gene inhibits blebbing of ACHN and HT1080 cell lines; ii) AQP1-deficient HT080 cells have relatively longer bleb lifespan possibly due to defective mechanism of AQP1-facilitated water flux; iii) overexpression of AQP1-GFP increases bleb size, but decreases bleb number; iv) AQP1 regulates cancer cell blebbing by

facilitating bleb retraction speed; v) overexpression of AQP1 can induce blebbing morphology in non-blebbing cell lines; vi) there exists a differential regulation of cell blebbing by the different AQP isoforms as AQP5 knockdown had no effect on cell blebbing.

Chapter 4. Involvement of Ion Channels in Cancer Cell Blebbing

4.1 Introduction

Ion channels are integral transmembrane proteins located in the plasma membranes of different mammalian tissues and they permit the influx and efflux of ions across the membrane in a passive manner in that ion passage through the channels is dependent only on their electrochemical gradient. Their gating (opening and closure) can be directed by specific external stimuli, they are selective in the transport of specific ions and have the capacity to detect regulatory signals (Prevarskaya et al., 2010). There are several evidences that ion channels and transporters play vital roles in cancer, and are thus promising novel targets in the fight against cancer (Cuddapah and Sontheimer, 2011). Ion channels such as Ca_v, K^+, Cl^-, Na^+, TRPC6, TRPM1, TRPM8, TRPV5, TRPV6 channels have been reported to be pivotal drivers of neoplastic transformation through their involvement in uncontrolled growth, insensitivity to antigrowth signals, decreased apoptosis, dis-regulated angiogenesis, aggressive migration, invasion and metastasis, which are the classical hallmarks of cancer (Hanahan and Weinberg, 2011).

Normally, cell migration is a complex process involving a cyclic events of actin polymerization and de-polymerization at the leading and trailing edges respectively with different components that are tightly regulated in a spatiotemporal manner (Schwab and Stock, 2014). The process involves joining of actin monomers, severing and branching of actin filaments which then interact with cytoskeletal motor proteins like myosin to generate forces transmitted to the ECM through focal adhesion complexes (Le Clainche and Carlier, 2008). Cytoskeletal dynamics and cell adhesion dynamics are regulated by transmembrane ion transporters, some of which regulate the intracellular and extracellular pH as well as Ca^{2+} homeostasis. Migration of tumour cells is largely influenced by the intracellular and

extracellular pH in that the functions of the intracellular and extracellular proteins in physiological and pathophysiological conditions as well as their ionization state is regulated by pH (Paradise et al., 2013; Webb et al., 2011). For instance, the actin binding protein, cofilin, in a pH-dependent manner regulates cell migration by severing actin filaments to create free barbed filaments ends to which new filaments are assembled resulting in not only actin polymerization, but formation of membrane protrusions at tip of invasive structures and at the leading edge of migrating cells (Bravo-Cordero et al., 2013; Schwab and Stock, 2014). The activity of cofilin is inhibited by PIP_2 binding, however, this inhibition is relieved upon intracellular alkalinization induced by NHE1 (Frantz et al., 2008) which not only accumulates at leading edge of tumour cells (Clement et al., 2013), but is required for migration of melanoma, breast cancer and cervical carcinoma cells (Stock et al., 2012). Increase in intracellular pH by NHE1 also causes release of cortactin-bound cofilin which then promote actin polymerization by creating barbed end formation (Magalhaes et al., 2011).

Cell migration is also regulated by intracellular Ca^{2+} in a spatiotemporal manner via modulation of cytoskeletal dynamics. The Ca^{2+}-sensitive actin-binding protein, α-actinin is required for lamellipodia formation and cell migration, and its activity is inhibited by increased intracellular Ca^{2+} ion (Hamill et al., 2013). Contractile force required for retraction of cell rear during cell migration is generated by stimulation of myosin II activity by intracellular Ca^{2+} ion (Schwab and Stock, 2014).

Cell adhesion to the ECM mediated by different subunits of integrin is regulated by pH. Acidic extracellular pH leads to increased cell adhesion due to conformational change which enhances interaction of integrins and the ECM proteins (Schwab and Stock, 2014). Focal adhesions maturation and turnover is regulated by intracellular Ca^{2+} due to more concentration of Ca^{2+} at the trailing edge thereby limiting Ca^{2+}-sensitive calpain phosphatase-

mediated disassembly of focal adhesions to the rear of a migrating cell (Chan et al., 2010). Similarly, increase in Ca^{2+} levels results in phosphorylation of focal adhesion kinase (FAK) on tyrosine residues leading to modulation of focal adhesion dynamics (Giannone et al., 2004).

The passage of osmotically active ions through plasma membrane ion channels may facilitate cell migration with the net effect of osmotic water transport that generates osmotic gradient and regulate cell shrinkage, swelling and other cellular processes. Ions are considered as osmolytes that trigger two dimensional migration in that the transport of ions across the plasma membrane increases osmotic water influx through aquaporins leading to the protrusion of cell leading edge, and a subsequent release of ions at the cell rear that cause a corresponding release of osmotic water and cell shrinkage (Schwab et al., 2007).

Among other ion transporters, there are two that have been implicated in cell migration: the sodium hydrogen exchanger isoform 1 (NHE1) and the sodium, potassium chloride co-transporters (NKCC) (Cuddapah and Sontheimer, 2011).

4.2 The Sodium Hydrogen (Na^+/H^+) Exchangers (NHEs)

The NHEs are transmembrane transporters that catalyze the electroneutral transport of extracellular sodium (Na^+) into and an intracellular proton (H^+) out of the cell at a ratio of 1:1 in an ATP-independent manner (Donowitz et al., 2013). The human NHEs are encoded by the SLC9 gene which comprises three subfamilies SLC9A, SLC9B and SLC9C.

Structurally, the NHEs consist of an N-terminus which has approximately 450 amino acid residues and 12 transmembrane spanning domains, and this terminus is actively responsible for the exchange of H^+ for Na^+, while the intracellular C-terminus which plays regulatory

roles of the exchange activity of the N-terminus, is made up of approximately 125-440 amino acids residues (Donowitz et al., 2009). Interactions between the C-terminus and phospholipids such as phosphotidylserine (PS), phosphatidylinositol-4,5-bisphophate (PIP_2), and phosphatidylinositol-3,4,5-triphosphate (PIP_3) couples the C-terminus to the N-terminus intracellularly and with the inner leaflet of the plasma membrane (Ikeda et al., 1997). A funnel organization has been proposed for the NHEs in which a two inverted funnel area consisting of two transmembrane helices that sometimes cross one another exist at the centre of the N-terminus, and it contains charged residues that form dipoles that are modulated by residues of opposite charges, and that a change in conformation at this region drives Na^+ and H^+ transport (Donowitz et al., 2013). The NHE structures also contain a pH sensor that regulates the exchange function by the H^+. Although the NHEs transport ions as dimers, they exist as dimers and the dimerization bolster the molecules (Padan et al., 2009).

4.2.1 Sodium Hydrogen Exchanger 1 (NHE1)

The 815 amino acids long human NHE1 is encoded by the SLC9A1. It has N-terminal membrane that is hydrophobic and contains 500 amino acid that transports ions across the membrane. The intracellular C-terminus, which is 315 amino acid long is hydrophilic and is concerned with regulating the ion exchange activity of the pump (Donowitz et al., 2013). NHE1 is expressed in diverse mammalian tissues and found mainly resident in plasma membrane and its levels at this site is regulated by ubiquitination (Simonin and Fuster, 2010). It may also accumulate in discrete microdomains of the plasma membrane. In polarized epithelial cells and cardiac myocytes, NHE1 is localized to basolateral membranes and intercalated disks respectively. Localization to intercalated discs and T-tubules in myocytes is necessary to affect local pH, and hence regulate the activities of pH-sensitive proteins like connexin 43 and ryanodine-sensitive Ca^{2+} release channel. Whereas in resting fibroblasts, it is

localized to focal adhesions, it is localized to the borders of lamellipodia in migrating fibroblasts (Simonin and Fuster, 2010). NHE1 not only help in intracellular alkalinization by extruding H^+ resulting from metabolism, and provide a mechanism for Na^+ influx into the cell, but it also play a regulatory role by bringing cell volumes to normal levels after contraction of cells (Donowitz et al., 2013).

4.2.2 NHE1 in Cancer

There are now different reports that almost all tumours exhibit a common feature of abnormal regulation of hydrogen ion dynamics (Cardone et al., 2005; Harguindey et al., 2009), and that tumour cells have a completely different acid-base balance from normal tissues and this aberrant condition is directly proportional to the neoplastic state. The result is an acidic extracellular pH (pHe) in tumour microenvironment and an alkaline malignant intracellular pH (pHi) (Reshkin et al., 2013). Thus, alkaline pHi values of 7.12-7.7 exists in tumour cells as compared to 6.99-7.05 in normal cells, and acidic pHe values of 6.2-6.9 as against 7.3-7.4 in normal tissues. This means that the pH gradient across the plasma membrane is reversed and this phenomenon increases with tumour progression. This aberrant pathological alteration and reversal of pH gradient in cancer cells compared to normal cells is now considered a defining hallmark in all tumour cells irrespective of their genetic origins (Cardone et al., 2005; Porporato et al., 2011). NHE1 contributes to neoplastic transformation and promotes tumourigenesis using different mechanisms. Usually, in normal healthy cells, NHE1 is dormant and inactive, but is activated when the cytosol becomes acidic (Harguindey et al., 2013). However, in cancer cells the cytosol is always alkaline due to hyperactivity of NHE1, even at resting intracellular pH (pH_i). High cytosolic pH which implies increased intracellular alkalinization is associated with malignant transformation (Reshkin et al., 2000b), uncontrolled growth (Rich et al., 2000), DNA synthesis and spontaneous mutations,

induction of oncogene expression, growth factors stimulation (Lee et al., 2003) and metastasis (Vahle et al., 2014). Dysregulated proliferation, migration and invasiveness of cancer cells which are attributable to hyperactive NHE1 activity have been reported in non-small lung cancers (Provost et al., 2012), melanoma (Ludwig et al., 2013) and breast cancer (Lauritzen et al., 2012). The neoplastic transformation is now known to be governed by initiation and maintenance of intracellular alkalinization, with the ensuing extracellular acidosis (Harguindey et al., 2005). Moreover, tumour invasiveness and metastasis is driven by H^+ efflux along concentration gradient into the surrounding normal cells and tissues which produces an acidic microenvironment (Harguindey et al., 2005). This capability of tumour cells to extrude H^+ which increases with a corresponding increase in tumour aggressiveness is responsible for the reversed pH gradient. Among other membrane transporters such as carbonic anhydrases (CAs), vacuolar H^+-ATPases, H^+/Cl^- symporter, the monocarboxylate transporter 1 (MCT1, also called lactate-proton symporter), Na^+-dependent Cl^-/HCO_3^- exchangers and ATP synthase, the NHE1 is the primary driver of tumour acidosis right from earliest pre-cancer stage of oncogene-driven neoplastic transformation. Thus, increase and decrease of intracellular and extracellular pH respectively correlate with increased NHE1 activity (Reshkin et al., 2000b).

4.2.3 Regulation of NHE1 Activity

The regulation of NHE1 activity is usually mediated at a long c-terminal cytoplasmic tail which is rich in serine and threonine residues that can be phosphorylated by protein kinases. For instance, although most Akt-mediated phosphorylations lead to substrate inhibition and inactivation, the exchanger activity of NHE1 was found to be increased by the serine/threonine kinase, Akt, which acts as an upstream regulator of the pump by phosphorylating it on a specific serine 648 residue (Meima et al., 2009). Similarly,

phosphorylation of NHE1 at serine 703 by p90 ribosomal S6 kinase (p90Rsk) upon serum stimulation has been shown to activate channel activity (Takahashi et al., 1999). It also functions downstream of Rho-activated kinase, ROCK which activates it by phosphorylation to regulate stress fibres (Tominaga et al., 1998); it is also reported to be directly phosphorylated by the stress-activated p38 mitogen-activated protein kinase (MAPK) (Khaled et al., 2001). Upon stimulation by platelet-derived growth factor (PDGF), the ste20-like Nck-interacting kinase NIK, phosphorylates and activates NHE1 (Yan et al., 2001). In quiescent cells, some of the serine/threonine sites in NHE1 are constitutively phosphorylated (Reshkin et al., 2013).

The activity of NHE1 in both normal and tumour cells is regulated by several extracellular stimuli such as soluble growth factors, hormones and cytokines which bind receptors and activate receptor tyrosine kinases as well as G-protein coupled receptors. Regulation of NHE1 is also mediated by Cell-ECM binding proteins such as integrins (Tominaga and Barber, 1998) and CD44 (Bourguignon et al., 2004). Physical stimuli such as cell shrinkage induced by osmotic gradient across the plasma membrane, and shear stress (Hoffmann and Pedersen, 2011).

An important factor that contributes to regulation of NHE1 activity is the possession of multiple proteins binding sites on the cytoplasmic tail which confers the pump the ability to assemble different signaling proteins and relay intracellular signals (Baumgartner et al., 2004; Meima et al., 2007). It interacts with PIP_2 (Aharonovitz et al., 2000), calcineurin homologous protein (CHP) 1 (Pang et al., 2001) and the ERM (ezrin, moesin and radixin) family of proteins (Denker et al., 2000) at the cytoplasmic-membrane interface. p90Rsk-mediated direct phosphorylation promotes binding of NHE1 with the 14-3-3 adaptor protein (Lehoux et al., 2001). Also at the c-terminal of NHE1, there are binding sites for Camodulin (CaM) at a

site distal to the NIK binding domain (Wakabayashi et al., 1997). The heat shock protein 70 (HSP70) and carbonic anhydrase II also bind NHE1 at the c-terminus (Baumgartner et al., 2004).

There is now evidence that factors such as low serum, acidic extracellular pH, and hypoxia which are attributable to the tumour microenvironment can also activate the activity of tumour NHE1 (Busco et al., 2010; Cardone et al., 2007; Lucien et al., 2011). NHE1 was also shown to be activated by the $Na_v1.5$ channel which leads to acidification of the extracellular environment and subsequent degradation of the ECM by activated extracellular cathepsin B (Brisson et al., 2011).

NHE1 has the ability to detect pHi due to the possession of a unique internal allosteric proton binding regulatory site such that when pHi plummet to a threshold level, the pump becomes activated. This set-point in normal cells is usually at their physiological resting pHi in which the cells re quiescent. Upon intracellular acidification, the pump is activated, and functions to restore the normal resting state. However, during neoplastic transformation, this process is mimicked by tumour cells to constitutively activate NHE1 which leads to a rise in pHi through an aberrant elevation of the affinity of the regulatory allosteric binding site (Reshkin et al., 2000b). Serum deprivation in tumour cells was shown to increase NHE1 activity by increasing the affinity of the allosteric binding site in a PI3K-dependent manner (Reshkin et al., 2000a). The activity of NHE1 has been shown to be increased by direct interaction with carbonic anhydrase II (Li et al., 2006). Similarly, NHE1 was found colocalized and regulates pHi with bicarbonate transport systems, Na^+-CO_3^- cotransporters, and Na^+-dependent HCO_3^-/Cl^- exchangers (Reshkin et al., 2013).

4.3 Aims of Chapter

The transport of ions across the plasma membrane normally creates an osmotic gradient and this dictates the direction of flow of water and liquids. Ion channels and transporters are involved in physiological and pathophysiological conditions such as cancer. It is also known that they do interact with other proteins in the membrane to exert their biological effects. An osmotic engine model (OEM) was recently postulated by Kimberly and colleagues (Stroka et al., 2014) in which they postulated that tumour cells in a confined microchannel exhibit polarized distribution of the Na^+/H^+ pump and AQPs at the plasma membrane, and this leads to water influx through the cell leading edge and efflux through the trailing edge. The net effect is a displacement of the cell (cell migration) from one point to another. Therefore, the aim of this chapter is to investigate the possible involvement of the Na^+/H^+ pump and other channels in AQP1-mediated regulation of cancer cell blebbing. Similarly, the effects of modulation of tumour extracellular pH in relation to the inhibition of Na^+/H^+ pump activity shall be examined. To this end, the activity of different ion channels shall be blocked with specific and potent inhibitors.

4.4 Results

4.4.1 AQP1-facilitated increase in bleb retraction requires Na^+/H^+ pump activity

Recent studies have demonstrated that when tumour cells are confined in a microchannel, they establish a polarized distribution of aquaporins and Na^+/H^+ pump with the net influx and efflux of water through the leading and trailing edges respectively, and this drives migration of cell from one point to another (Stroka et al., 2014). Therefore, it was anticipated that the unexpected increase in bleb retraction upon AQP1 overexpression (figure 3.10) could be in part due to either influx of Na^+ with the accompanying intracellular alkalinization or extracellular acidification by proton extrusion or both, by the activity of the Na^+/H^+ pump. To test this proposition, the channel activity of the pump in ACHN and HT1080 cells cultured and induced to bleb in 3D matrigel matrix was blocked for 15 min with the general Na^+/H^+ pumps inhibitor, 5-(N-Ethyl-N-isopropyl) amiloride (EIPA) , an effect that will result in intracellular acidification due to proton accumulation. As shown in figures 4.1a and b (bottom panel), pretreatment of cells with 100 µM EIPA blocked bleb retraction. Blebs were found only expanding without any visible retraction, resulting to more than a four-fold increase in bleb size as compared to vehicle control cells. This suggests that Na^+ influx through the NHEs with the ensuing intracellular alkalinization or/and extracellular protein release with the accompanying acidification could be involved in AQP1-facilitated bleb retraction.

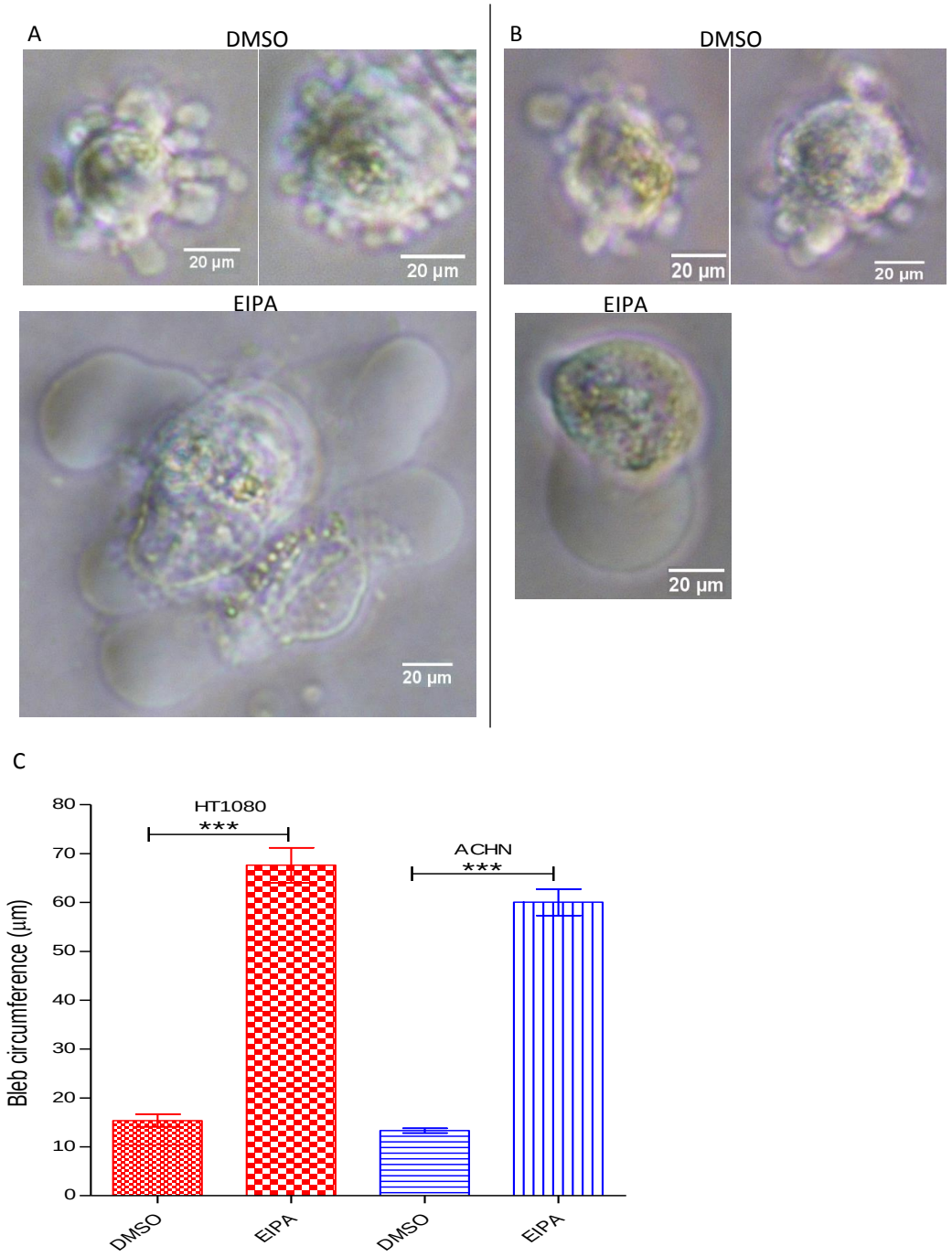

Figure 4.1 EIPA inhibits bleb retraction. HT1080 and ACHN cell lines were cultured in 3D matrigel and then challenged with BB-94 and PIC in presence of caspase inhibitor set VI. Cells were then pretreated with EIPA (100 µM). **A. and B.** EIPA blocked bleb retraction in HT1080 and ACHN cells respectively. Blebs were only expanding; **C.** Quantification of bleb size upon EIPA treatment of cells. Data is a representative of the means ± SEM of three independent experiments performed in triplicate in which 75 cells were scored. ***:P < 0.001, using one-way ANOVA after Tukey's multiple comparison test.

4.4.2 Effect of Timing of EIPA inhibition of Na^+/H^+ pump

As inhibition of NHEs with EIPA for 15 min resulted in expansion of blebs which never retracted, it was thought that bleb retraction may be slowed and that longer time periods would allow retraction to be observed. This assertion was tested by inhibiting the activity of the NHEs in HT1080 and ACHN cell lines for 30, 60 and 90 min with EIPA before phase contrast microscopy. Data presented in figure 4.2 indicate that in the HT1080 cell line, although no significant difference was found in the sizes of bleb at the different time points, there was an increase in size from 30 min to 60 min, which then remained stable throughout the 90 min time point. However, in the ACHN cell line, a gradual time-dependent increase in size occurred, and the size difference became significant at the 90 min time point. In both cell lines, blebs were only expanding without any observable retraction.

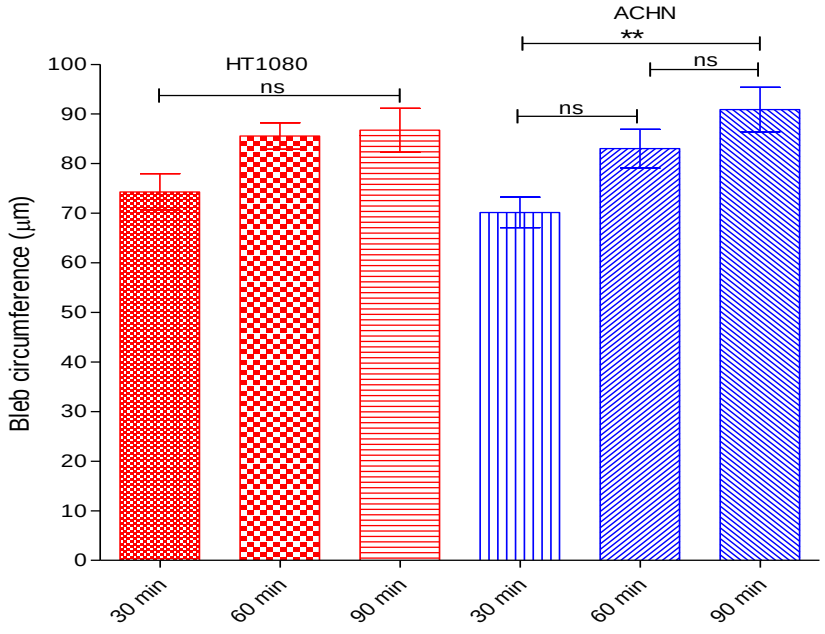

Figure 4.2: Time course of EIPA treatment. Cells were cultured in matrigel and challenged with BB-94 (1 µM) and PIC (1:100) in presence of caspase inhibitor set VI (10 µM) before inhibiting NHEs with EIPA for different time points. Data is a representative of the means ± SEM of three independent experiments performed in triplicate. **:$P < 0.01$, using one-way ANOVA after Tukey's multiple comparison test.

4.4.3 Detection of NHE1 expression

NHE1 is the best characterized and extensively studied isoform of the nine NHE isoforms that have been characterized in mammalian tissues, and it is reported to be ubiquitously expressed and most biological processes mediated by the NHEs have been attributed to NHE1. Therefore, the expression level of the protein was investigated in HT1080 and ACHN cell lines using western blotting and immunohistochemistry. As shown below, western blot analysis (figure 4.3a) and immunostaining (figure 4.3b) show that both cell lines expressed the ion channel.

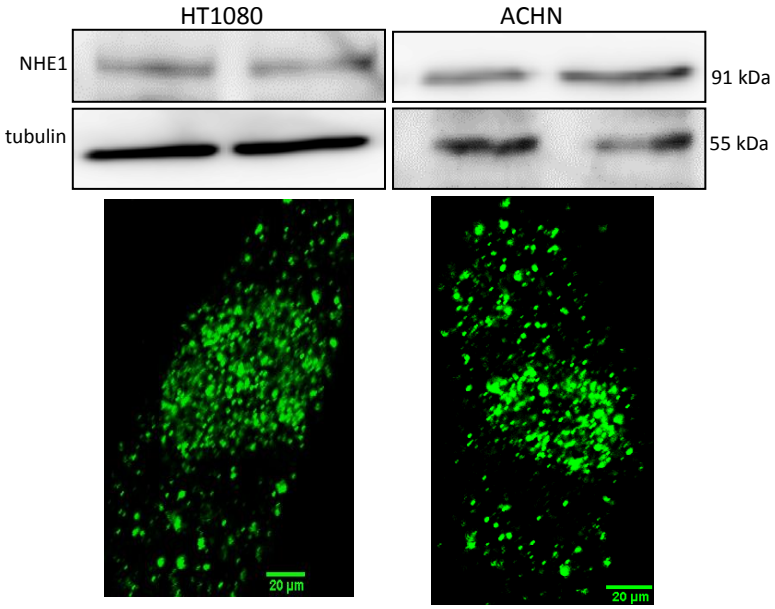

Figure 4.3: Detection of NHE1 expression. Upper panel: HT1080 and ACHN cells were lysed with RIPA buffer in presence of PIC (1:100). Proteins were resolved on 10% SDS gel before western blotting with anti-NHE1 antibody (1:1000). Tubulin was used as loading control; **Bottom panel**: cells seeded on coverslips were rinsed and fixed with 4%v formaldehyde before permeabilizing with triton-X 100. Cells were incubated with human ant-NHE1 antibody and then with alexa flour 488 fluorescent antibody. Data is a representative of three independent experiments.

4.4.4 NHE1 localizes to cytosolic compartment

To determine whether NHE1 localizes to bleb membrane or to other intracellular organelles, immunohistochemical staining was performed on ACHN cell line seeded on round-bottomed dishes, and then induced to bleb with BB-94 and PIC. Confocal microscopy of immuno-stained ACHN cells shown in figures 4.4a, b and c revealed that NHE1 localizes to the cytosol.

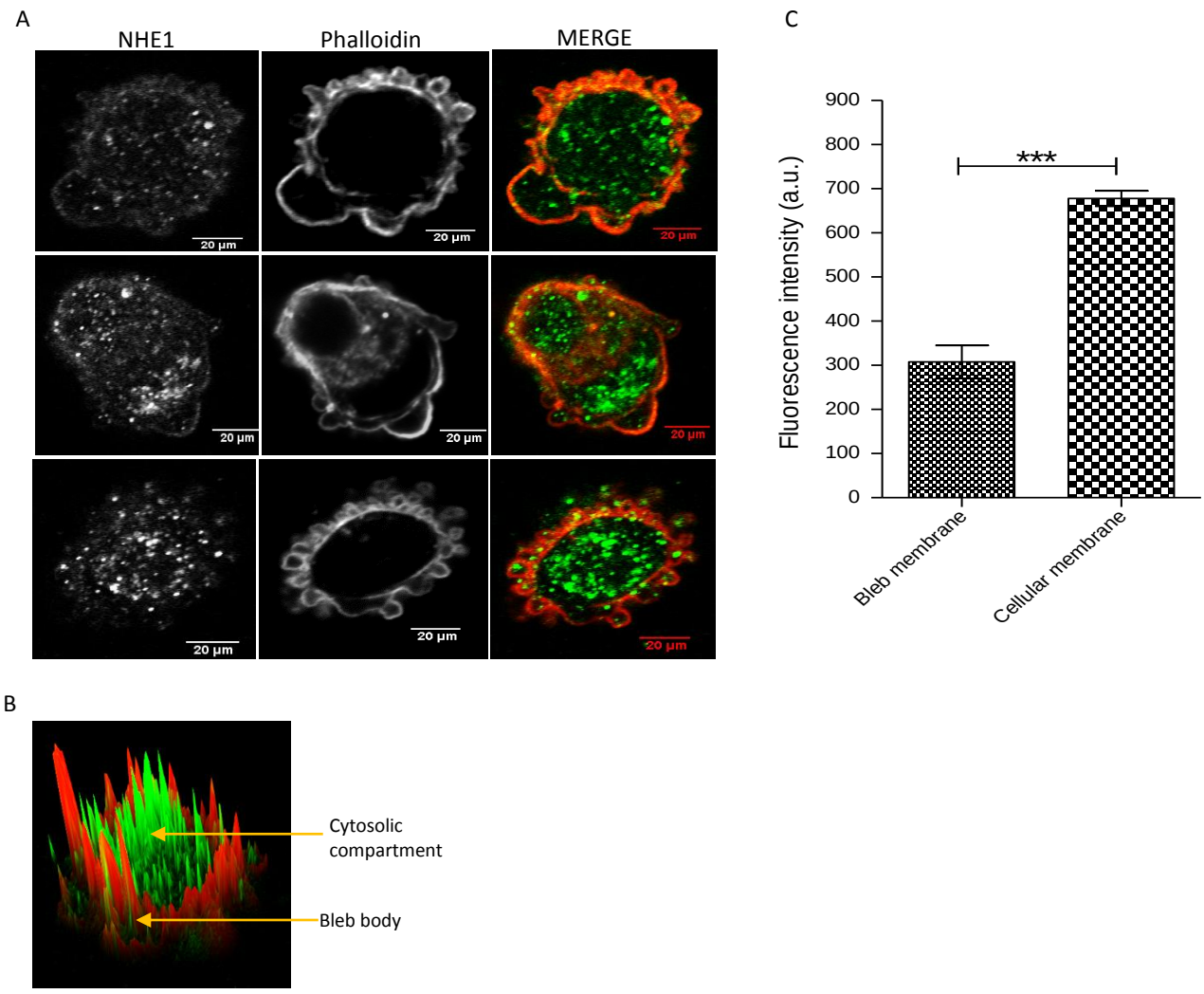

Figure 4.4: NHE1 localizes to cytosolic compartment. A. ACHN cells seeded on coverslips in a 6-well plate containing 2 ml media to which BB-94 (1 µM), PIC (1:100) and caspase inhibitors (10 µM) have been previously added. Cells were incubated overnight and rinsed with PBS. Cells were fixed, permeabilized and stained with anti-NHE antibody. F-ac-actin was revealed with phalloidin; **B.** Intensity surface plot using imageJ shows more NHE1 (green) at the cytosol than at the blebs; **C.** Quantification of fluorescence intensity across the bleb and cell membranes. Data is a representative of the means ± SEM of three independent experiments. **:$P < 0.001$, using two-tailed unpaired students' t test.

4.4.5 AQP1-facilitated increase in bleb retraction is independent of NHE1 activity

Most biological processes by the sodium hydrogen exchangers are mediated by the ubiquitously expressed NHE1. Thus, it was anticipated that the involvement of the NHEs in AQP1-facilitated bleb retraction might be through NHE1. In different cancer cells, the activity of NHE1 is reported to be specifically and potently inhibited by cariporide (HOE-642) (Amith and Fliegel, 2013; Lucien et al., 2011). Therefore, in the present study, increasing concentrations of the drug was used to inhibit NHE1 activity, and as shown in figures 4.5a and b, neither bleb expansion, retraction nor bleb size was affected. Blebs were dynamically expanding and retracting. Another inhibitor of NHE1, zoniporide which was reported to be more specific and potent than cariporide (Gao et al., 2011) was tested. In a manner similar to cariporide, in the HT1080 cell line, use of different doses of zoniporide had no effect on bleb size, in addition to that, blebs were dynamically expanding and retracting (figure 4.5c). However, in the ACHN cell line, zoniporide caused a dose-dependent increase in bleb size but again, the blebs were dynamically expanding and retracting (figure 4.5d), suggesting that AQP1-facilitated increase in bleb retraction was not due to NHE1 activity

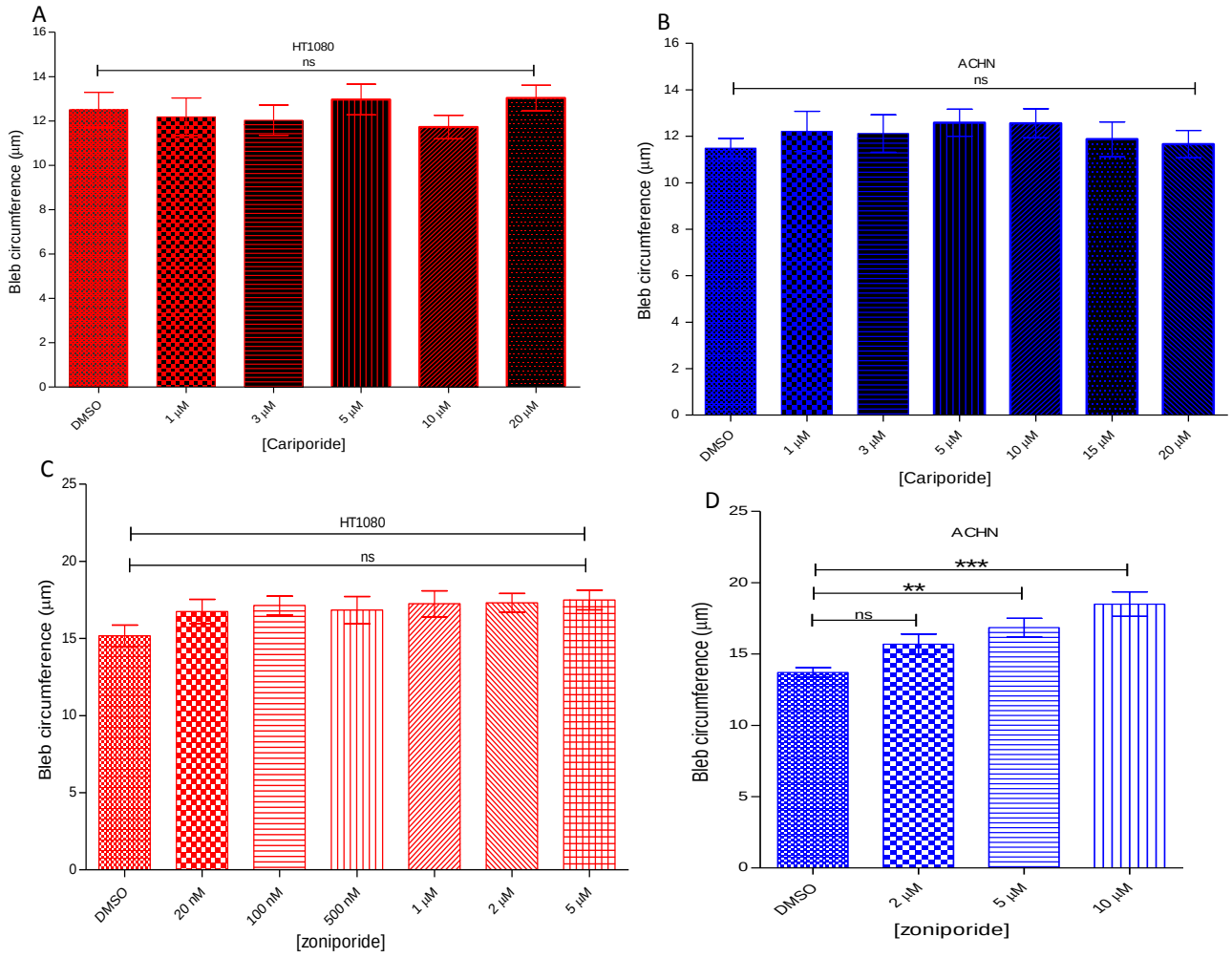

Figure 4.5: AQP1-faclitated bleb retraction is independent of NHE1 activity. A and **B**. inhibition of NHE1 activity in HT1080 and ACHN cells respectively with different doses of cariporide; **C** and **D.** use of different concentrations of zoniporide in inhibition of NHE1 activity. Data represents the means ± SEM of three separate experiments. **:P < 0.01, ***:P < 0.001 using one-way ANOVA after Tukey's multiple comparison test.

4.4.6 The TRPP3 channel is not involved in AQP1-facilitated bleb retraction

To further probe into the blockage of bleb retraction by EIPA, the involvement of TRPP3, a member of the transient receptor potential (TRP) family of cation channels was investigated as this channel has been previously reported to be also blocked by EIPA (Dai et al., 2007). Therefore, a specific and potent TRPP3 blocker, phenamil was used at different doses. As seen in figure 4.6, in HT1080 cell line (red columns), use of 5, 10 and 20 µM phenamil produced no significant change in bleb size as compared to vehicle treated cells. However, although not significantly different, there was increase in bleb size with concentrations of 50, 70 and 100 µM. In the ACHN cell line (blue columns), only 100 µM phenamil yielded a significant difference in bleb size, while the other doses had effects that were statistically insignificant (figure 4.6a). Furthermore, the effect of timing channel inhibition in both cell lines for up to 2 hours with 100 µM phenamil could also not mimic the effect observed with EIPA (figure 4.6b). In both experimental conditions, there was no blockage of bleb retraction in the two cell lines as blebs were expanding and retracting actively. This suggests that the effect of EIPA was not through inhibition of the TRPP3 channel.

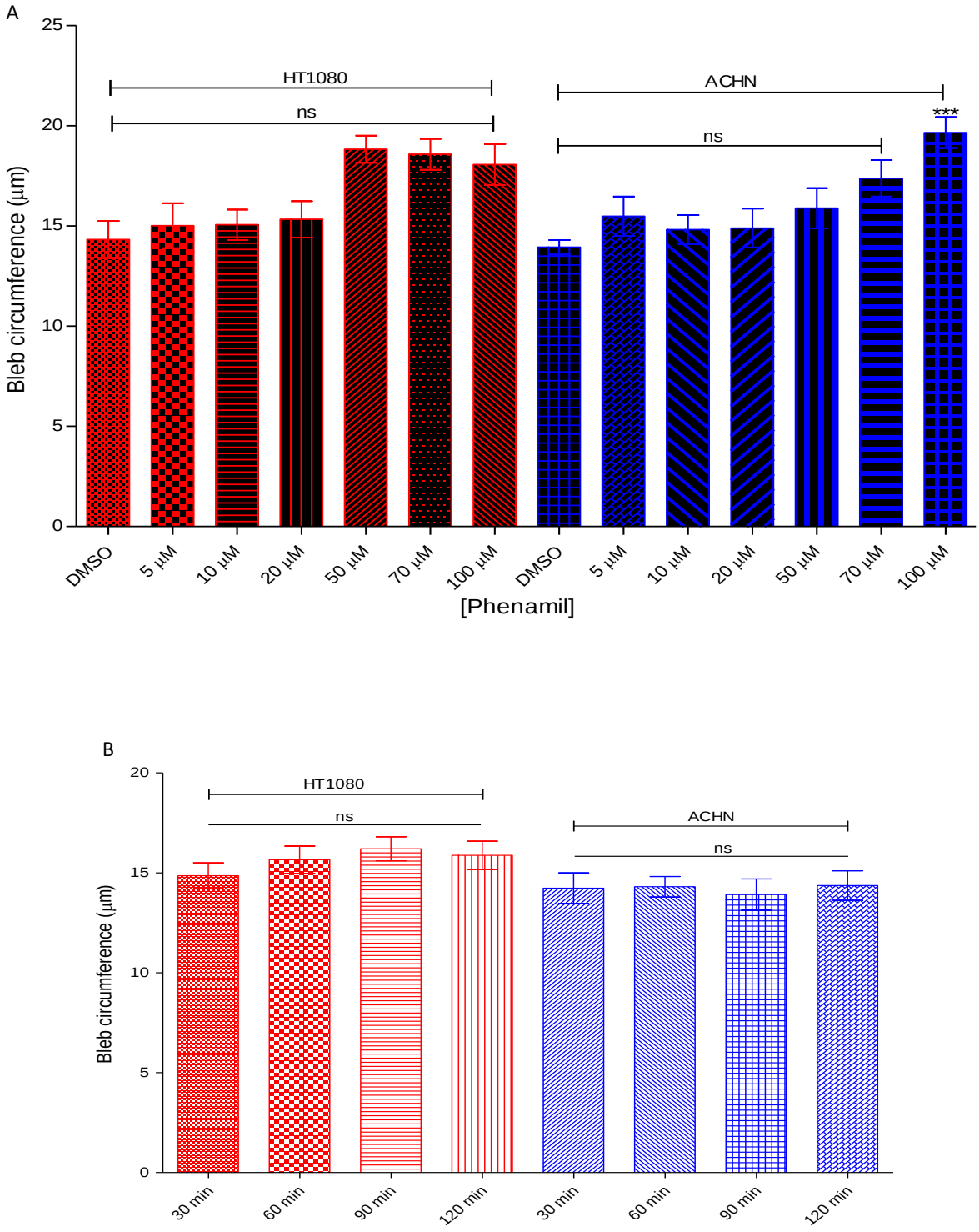

Figure 4.6: Non-involvement of TRPP3 channel in AQP1-facilitated bleb retraction. HT1080 and ACHN cells were cultured in matrigel and treated with bleb-inducing agents before incubating overnight. **A.** Cells were then challenged with different concentrations of phenamil, the TRPP3 selective blocker; **B.** Time course of phenamil treatment of cells at dose of 100 µM. Data is a representative of the means ± SEM of three separate experiments. ***:$P < 0.001$, using one-way ANOVA after Tukey's multiple comparison test.

4.4.7 Extracellular pH modulation and inhibition of NHE regulate bleb morphology

As the Na^+/H^+ pump activity results in intracellular alkalinization and its inhibition results in intracellular proton accumulation and hence, to intracellular acidosis, the effects of modulating the extracellular pH in the absence or presence of EIPA on bleb morphology was examined by incubating cells in 3D matrigel matrix and cultured with media of different pH values, and when necessary, activity of the Na^+/H^+ pump inhibited by adding EIPA to the media before incubating cells for 30 min at 37^{o}C. Data shown in figure 4.7a indicates that incubation of HT1080 cells in all different pH media (5.5-9.0) resulted in a decrease in bleb size (albeit, not significant) as compared to control. However, inhibition of Na^+/H^+ pump at 5.5 and 6.0 resulted only in an insignificant increase in bleb size, but this became significant from 6.5-9.0 (figure 4.7a). Similar to the HT1080 cells, in ACHN cells, incubation of cells at acidic pH of 5.5-6.5 resulted in decrease in bleb size (albeit, not significant), however, at the alkaline pH values of 8.0-9.0, the bleb size in this cell line became identical to that of control. Also in the ACHN cell line, inhibition of Na^+/H^+ pump at all pH conditions led to significant increase in bleb size when compared to the respective uninhibited pH values (figure 4.7b). In both cell lines, similar to previous observation, EIPA treatment blocked bleb retraction, but these blebs were less in size compared to those in which ion transporter was inhibited in normal media.

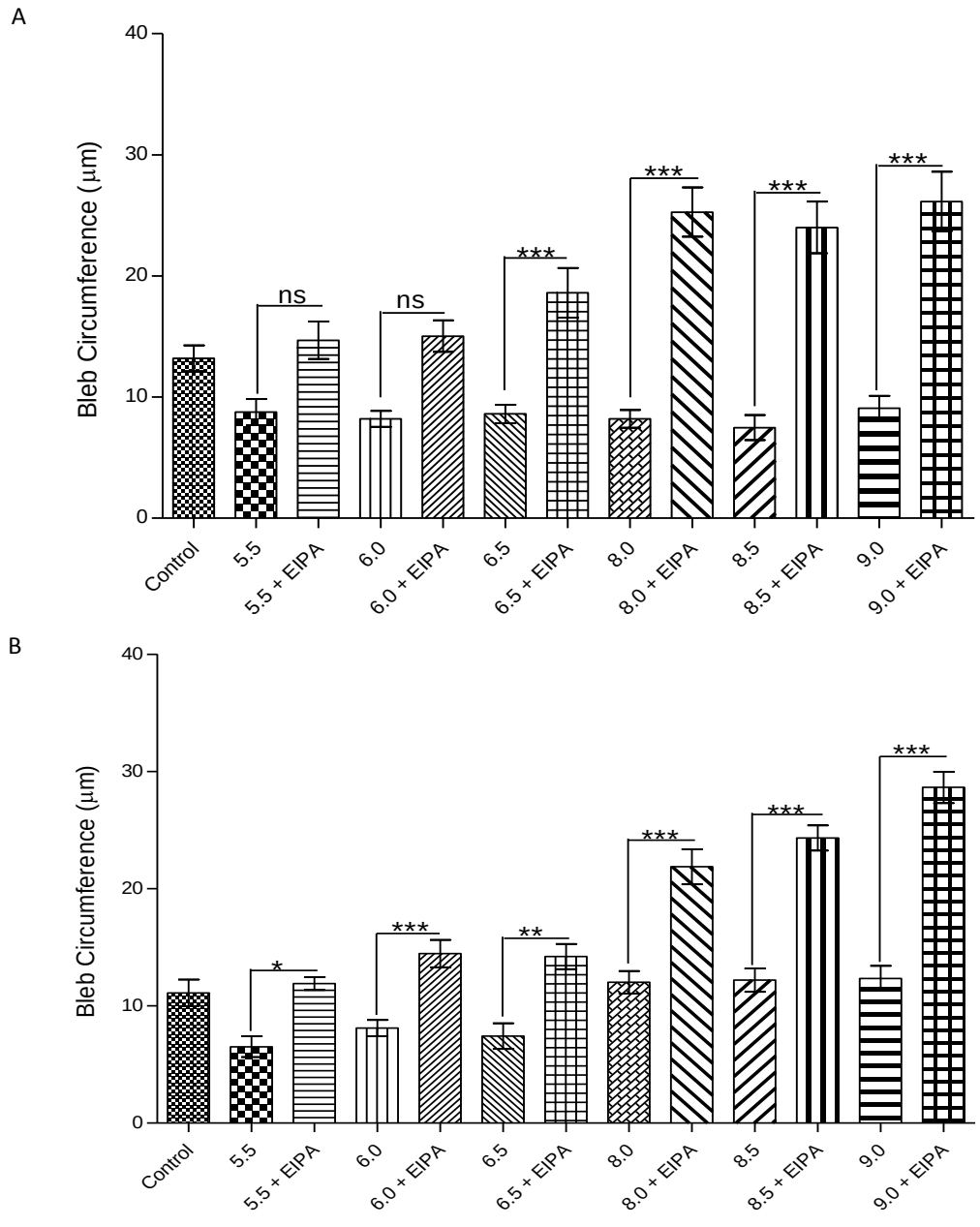

Figure 4.7: Extracellular pH modulation and cell blebbing: A. HT1080 and **B.** ACHN cells were cultured in 3D matrigel and challenged with bleb-inducing agents and then incubated at 37ºC overnight. Media was removed before incubating with media of different pH and when necessary NHEs activity was inhibited with EIPA. Data represent three independent experiments done in triplicate and is the SEM ± SEM of three separate experiments. *:$P < 0.05$, ***:$P < 0.001$, using one-way ANOVA after Tukey's multiple comparison test.

4.4.8 Effect of Inhibition of Sodium Potassium Chloride co-transporter 1 (NKCC1)

To further unravel the mechanism behind AQP1-mediated increase in bleb retraction, and because inhibition of Na^+ influx and proton efflux through the Na^+/H^+ pump with EIPA resulted in continuous bleb expansion without any observable bleb retraction, suggesting that either Na^+ influx with the accompanying intracellular alkalinization or H^+ efflux with the accompanying extracellular acidification might play a crucial role in AQP1-mediated increase in bleb retraction, other membrane channels that transport Na^+ as well as other cations in and out of the cell across plasma membrane were investigated. One of such transporters is the NKCC1 which is widely expressed in several mammalian tissues. This channel which mediate the electroneutral transport of Na^+ and K^+, tightly coupled to Cl^- transport in and out of the cell, plays an important role in regulating cell volume (Markadieu and Delpire, 2014). NKCC1 has been implicated in the promotion of cell cycle progression and cell proliferation (Shiozaki et al., 2014), cell migration and invasive capabilities of glioblastoma cells (Garzon-Muvdi et al., 2012). Therefore, the effect of inhibition of NKCC1 on bleb morphology was investigated with the potent loop diuretic bumetanide (BMT). As shown in figure 4.8a, in HT1080 cells, bumetanide at a dose of 5 µM had no significant effect on bleb size, but a concentration of 10 µM induced a significant increase in bleb size, and this effect remained constant and was maintained up to 100 µM dose. However, in ACHN cell line, although not significantly different from vehicle control, blebs started increasing in size from 5 µM, and the increase became significant from 10 µM BMT treatment and remains stable up to 20 µM dose. Blebs further increased in size from 50 µM and again remained stable up to 70 µM dose. Finally, a further expansion in bleb size was observed at a concentration of 100 µM. In both cell lines, there was a drastic decrease in bleb numbers as the concentration of the inhibitor increased (figure 4.8b). This suggests that although, the

blebs were dynamically expanding and retracting, either intracellular alkalinization or extracellular acidification or both plays a key role in bleb retraction.

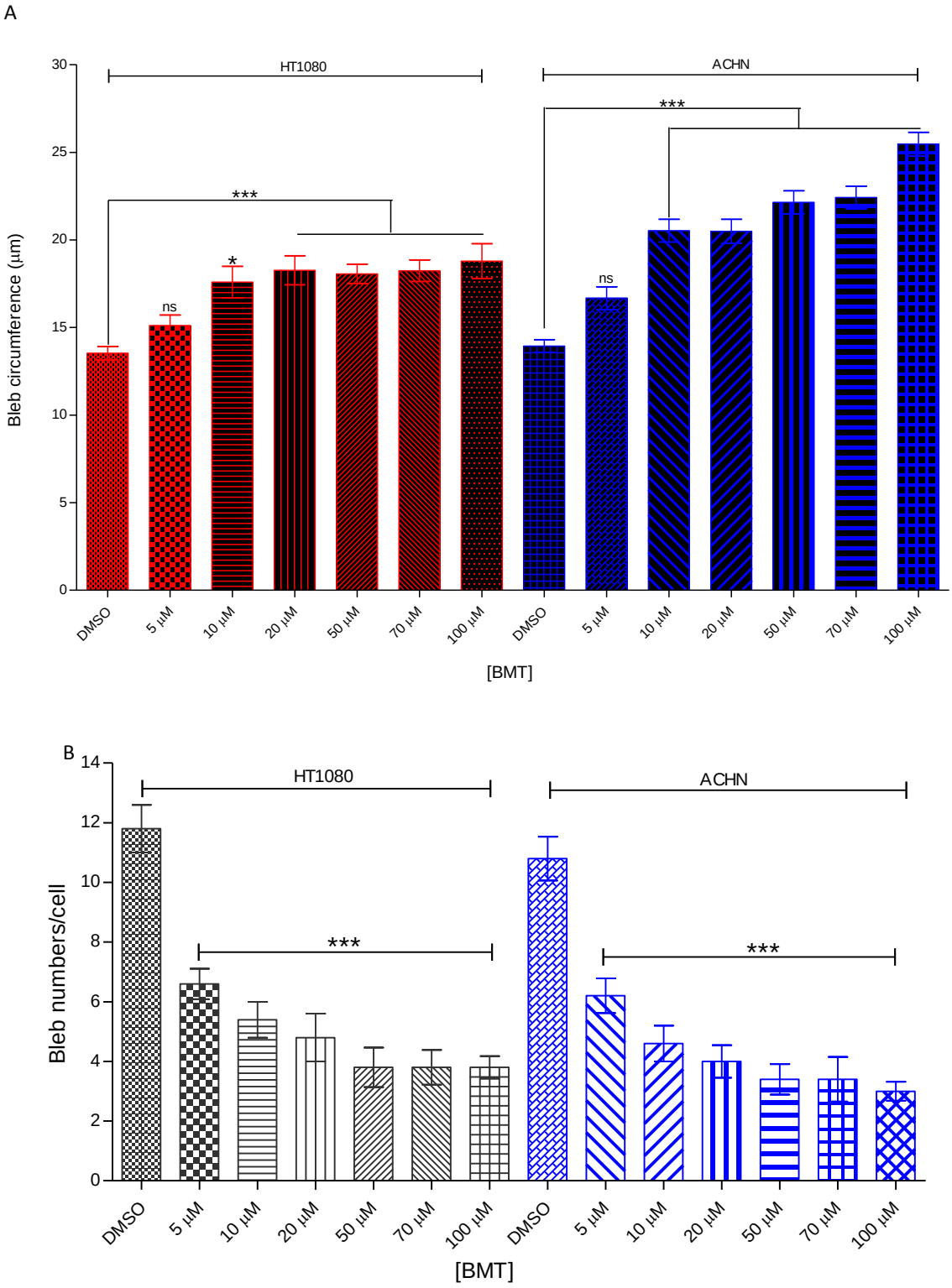

Figure 9: Effect of bumetanide on bleb morphology. HT1080 and ACHN cells cultured in 3D matrigel matrix were induced to bleb and incubated at 37ºC. **A.** Cells were then challenged with different concentrations of the NKCC inhibitor, bumetanide for 15 min; **B.** Bleb numbers per cell upon treatment with different doses of BMT. Data is a representative of the means ± SEM of three separate experiments. *:P < 0.05, ***:P < 0.001, using one-way ANOVA after Tukey's multiple comparison test.

4.4.9 Bleb Dynamics upon NKCC1 inhibition

As maximum bleb size in both HT1080 and ACHN cell lines was obtained upon inhibition of NKCC1 with 100 µM BMT (figures 4.8), it was imperative to determine whether the blebs behaved like normal blebs in wild-type cells. Thus, time-lapse movies of live-blebbing control and BMT-treated HT1080 and ACHN cells were generated, and the dynamics of the blebs was analyzed using ImageJ. Data from the analysis of bleb dynamics revealed that treatment of both cell lines with BMT significantly increased the lifespan of blebs (figure 4.9a). Further examination of the bleb cycle showed that inhibition of NKCC1 in HT1080 cells had no significant effect on bleb expansion, whereas in the ACHN cell line, channel inhibition significantly increased bleb expansion time (figure 4.9b). In both cell lines, BMT had no significant effect on the time it took bleb to stabilize (figure 4.9c). However, in both cell lines, channel inhibition with BMT significantly increased the time it took blebs to retract (figure 4.9d). Taken together, the data suggests that influx of Na^+ and possibly other ions across the plasma membrane results not only in water and fluids inflow into an expanding bleb, but is also crucial for bleb retraction.

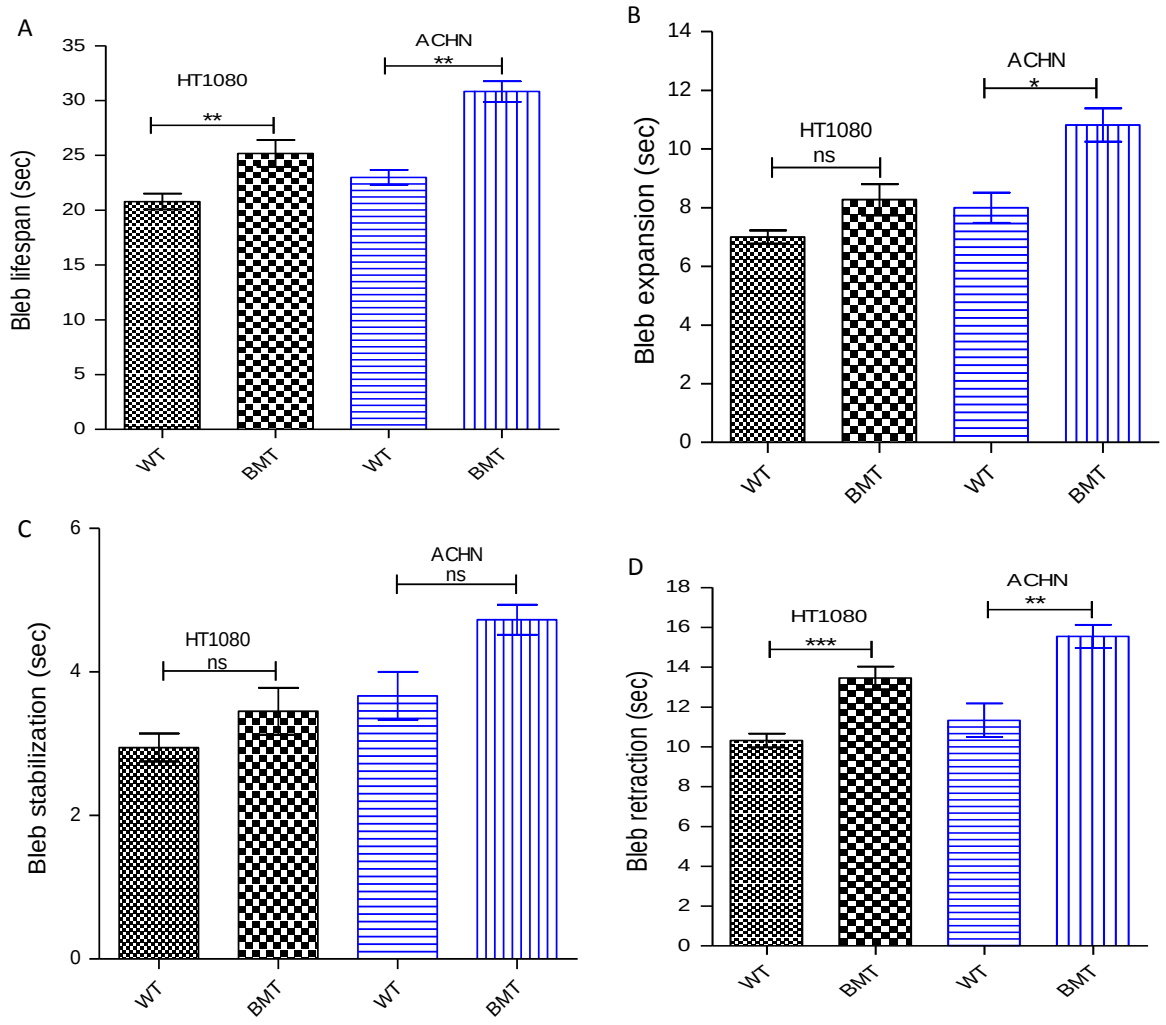

Figure 10: Inhibition of NKCC1 and bleb Dynamics. ACHN and HT1080 cells were cultured in matrigel and induced to bleb with BB-94 (1 µM) and PIC (1:100) before incubating at 37°C overnight. The activity of the NKCC channel was then blocked with bumetanide BMT (100 µM) for 30 min. Phase contrast, time-lapse movies were than generated at 2 sec/frame for an experimental length of 10 min. **A.** NKCC inhibition elongated the lifespan of blebs in both cell lines; **B.** BMT caused slow bleb expansion in ACHN cells whereas there was no significant change in HT1080 cells; **C.** No significant difference in bleb stabilization in both cell lines upon BMT treatment; **D.** NKCC inhibition caused significant decrease in bleb retraction time. Three movies were tracked in each case. Data is a representative of the means ± SEM of three separate experiments. *:P < 0.05, **:P < 0.01, ***:P < 0.001, using one-way ANOVA after Tukey's multiple comparison test.

4.4.10 Effect of inhibition of the volume-regulated anion channel (VRAC) on cell blebbing

Usually, a rapid water flow occurs when there is an increase in intracellular osmolarity due to transport of osmotically active ions across the plasma membrane into the cell. Similarly, decrease in extracellular osmolarity will lead to water influx into the cell, and these two processes results in cell swelling, and the pressure from such water influx contributes to bleb expansion. Normally, swelling is negated by several mechanisms put in place by cells, and these cause regulatory volume decrease (RVD) resulting in outflow of osmotically obligated water, an event that is preceded by ion efflux across the plasma membrane (Hoffmann et al., 2009). The eventual shrinkage in cell size may have a regulatory effect on bleb size. One of such mechanisms by which cells maintain RVD is through the ubiquitously expressed volume-regulated anion channel (VRAC) which maintain cellular homeostasis by sustaining constant cell volume in response to osmotic changes in the extracellular or intracellular environment (Qiu et al., 2014).

To test the hypothesis that AQP1-facilitated increase in bleb retraction is due to a change in osmotic gradient induced by ion transport mediated by VRAC, blebbing HT1080 and ACHN cells were incubated for 15 min with different doses of VRAC specific blocker, 4-(2-butyl-6,7-dichloro-2-cyclopentyl-indan-1-on-5-yl) oxo-butyric acid (DCPIB). As shown in figure 4.10a, inhibition of VRAC in HT1080 cells with 10 µM, 15 µM and 20 µM DCPIB caused a significant increase in bleb size and this persisted in all the doses, whereas in the ACHN cell line, although an increase in bleb size was observed with 10 µM, 15 µM, the difference was insignificant. However, a significant change in size was found with 20 µM DCPIB. To further study the contribution of VRAC to cell blebbing, the effect of timing DCPIB treatment of cells was examined. Data from the study shown in figure 4.10b revealed that

incubation of cells with 50 μM DCPIB significantly increased bleb size when compared to vehicle control, and this increased bleb size was sustained up to 90 min of incubation with DCPIB. In both cell lines, blebs were expanding and retracting. Again, inhibition of VRAC with DCPIB could not produce similar effect to that which was observed with EIPA inhibition of Na^+/H^+ pump.

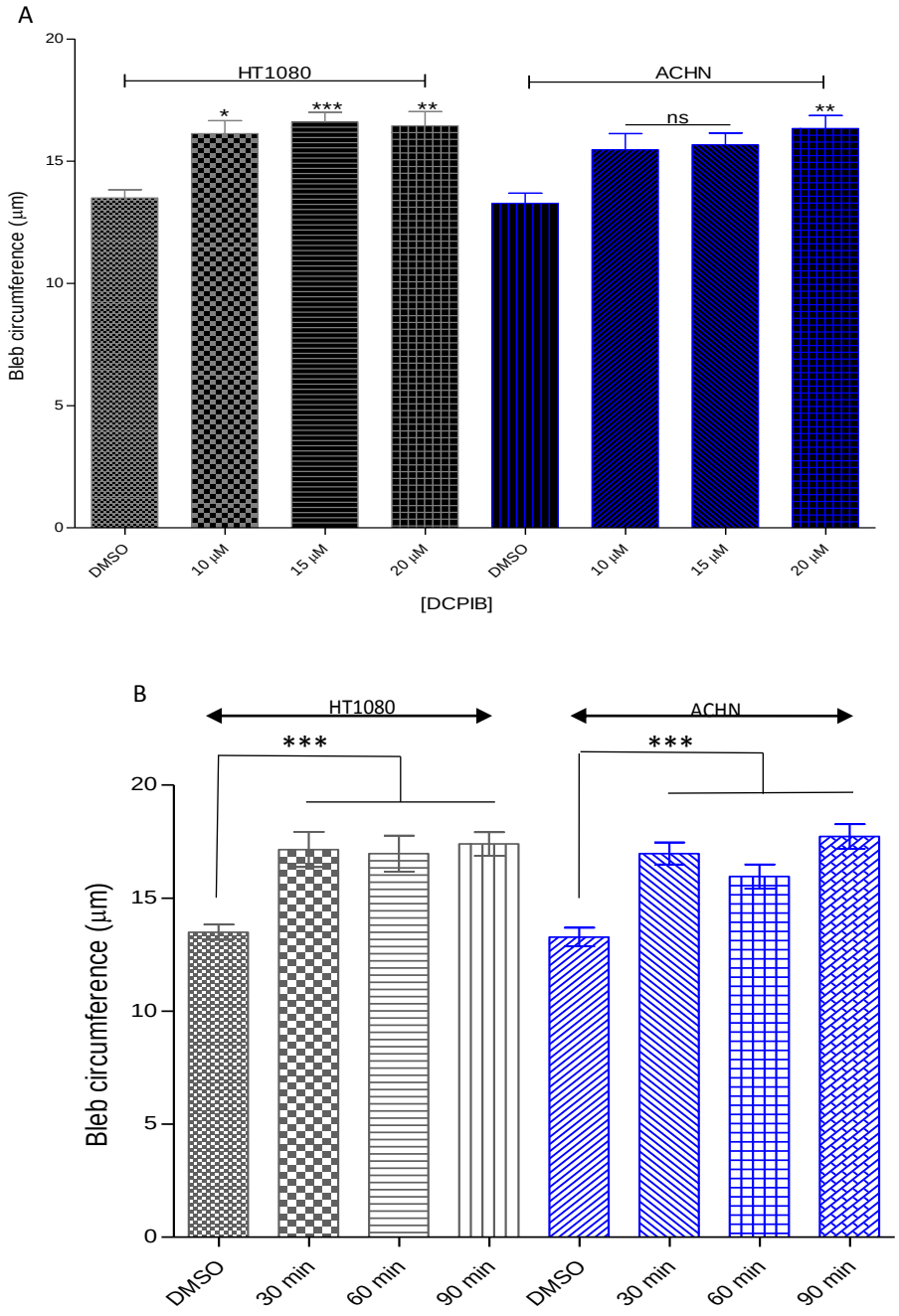

Figure 4.10: Effect of inhibition of VRAC on blebbing. ACHN and HT1080 cells were cultured in matrigel and challenged with BB-94 (1 µM) and PIC (1:100) before incubating at 37°C **A.** Cells were treated with different concentrations of the VRAC blocker, DCPIB for 15 min before phase contrast microscopy; **B.** Time course of DCPIB inhibition of VRAC in HT1080 and ACHN cells. Data represent the means ± SEM of three independent experiments in which 30 blebbing cells were quantified for each cell line. *:$P < 0.05$, **:$P < 0.01$, ***:$P < 0.001$, using one-way ANOVA after Tukey's multiple comparison test. All comparisons are between control and test treatments.

4.5 Discussion

The plasma membranes of all mammalian tissues contain numerous ion channels and transporters that mediate passage of osmotically active ions in and out of the cell, and this imposes an osmotic gradient across the membrane. These channels are critical regulators of cell shape and volume, intra- and extracellular pH, membrane potential, calcium signaling and interaction with the ECM and other intracellular signaling cascades (Becchetti et al., 2013). There is now ample evidence that has implicated these integral membrane proteins in playing positive roles in cell proliferation (Becchetti et al., 2013), tumour vascularization (Fiorio Pla et al., 2012), tissue invasion (Becchetti and Arcangeli, 2010) and evading apoptosis (Lehen'kyi et al., 2011), processes that characterize the multistep neoplastic progression.

Previous studies have demonstrated the involvement of different ion channels in cell migration and metastasis (Haas and Sontheimer, 2010; Lauritzen et al., 2012) and one such membrane transporters that has attracted interest over the past decades is the Na^+/H^+ pump (NHEs) that catalyze the electroneutral exchange of intracellular H^+ for an extracellular Na^+. Of the nine NHE isoforms identified in mammalian tissues, NHE1 is the best and most extensively studied, and it has been reported to mediate most of the physiological and pathophysiological effects of these ion transporters (Amith and Fliegel, 2013; Donowitz et al., 2013). The NHE1 interacts with different binding proteins at the plasma membrane to effect several biological processes, some of which are exerted through intracellular signaling molecules, while others are exerted extracellularly (Baumgartner et al., 2004). An interesting finding was the demonstration that the NHE1 also regulates the formation and activities of membrane protrusions such as pseudopodia (Lagana et al., 2000) and invadopodia (Busco et al., 2010) which are used in motility. This implies that the NHE1 might also promote cell

migration by playing a regulatory role in the formation of other plasma membrane protrusion such as blebs, although, the involvement of the channel pump in cancer cell blebbing has not been investigated.

This chapter investigated the involvement of the Na^+/H^+ pump and other membrane ion transporters in cancer cell blebbing. The study identified a requirement for Na^+/H^+ pump activity in AQP1-facilitated increase in bleb retraction. Usually, in mammalian tissues, in response to osmotic gradient, the AQP water channels facilitate water passage across plasma membranes. The water influx leads to a rise in intracellular pressure that results in flow of water and cytosolic fluid into a growing bleb to cause its expansion. However, for AQP1 overexpression to simultaneously increase bleb retraction as observed in the preceding chapter (figure 3.13) was quite unexpected, and that raised the question whether the effect was due to the activity of plasma membrane ion transporters. One principal ion transporter that regulates intracellular pH and cell volume is the Na^+/H^+ pump. This pump together with AQPs has been recently reported to be polarized to lamellipodia of migrating tumour cells (Stroka et al., 2014), and that inhibition of the pump was reported to result in increased cytosolic acidification at the leading edge of migrating cells (Martin et al., 2011), suggesting that the Na^+/H^+ pump contributes to generation of intracellular pH gradients. Thus, in the present study, blocking the activity of the Na^+/H^+ pump with the broad spectrum NHE inhibitor, EIPA induced continuous expansion of blebs while completely shutting down bleb retraction in both ACHN and HT1080 cell lines (figures 4.1a and b), and this effect persisted up to the maximum time (90 min) of incubation with the inhibitor (figure 4.2). This suggests that extracellular acidosis due to H^+ extrusion (reduced pH), and Na^+ entry into the cell with the accompanying increase in intracellular pH (intracellular alkalinization) by the Na^+/H^+ pump plays a critical role in regulating the retraction phase of cell blebbing.

In mammalian tissues, nine isoforms of the NHE antiporters have been cloned. Of these, NHE1 is ubiquitously expressed, and its functions are well-characterized. Indeed, both western blotting and immunohistochemical analyses confirmed NHE1 expression in both HT1080 and ACHN cells (figure 4.3). A probe to determine its localization with respect to the bleb membrane using confocal microscopy revealed that contrary to previous reports that NHE1 is localized to bleb membranes (Yi et al., 2012), in the present study, the antiporter was found localized to intracellular vesicles, with few punctate of the protein in the bleb body (figure 4.4). This observed difference in the localization of NHE1 might be due to the cell line used, as Yi and colleagues used Chinese hamster ovary cells expressing integrin$_{\alpha IIb}$ and integrin$_{\beta 3}$ (CHO$_{\alpha IIb\beta 3}$), which possibly upon binding ECM substrates get activated, and target NHE1 for translocation to the plasma membrane.

To investigate whether the effect of EIPA was due to inhibition of NHE1, a selective and potent NHE1 inhibitor, cariporide (HOE642) (Harguindey et al., 2013) was used to block the activity of this ion transporter. However, a dose response of the drug had no effect on bleb expansion and retraction as both cell lines were dynamically expanding and retracting with no significant difference in the size of blebs when compared to vehicle treatment (figure 4.5a and b). To rule out the involvement of NHE1, zoniporide, a more potent inhibitor that possesses greater selectivity towards NHE1 (Clements-Jewery et al., 2004; Gao et al., 2011) was applied. Similar to cariporide, use of different concentrations of zoniporide had no inhibitory effect on bleb retraction in HT1080 cells (figure 4.5c). Although in the ACHN cell line, zoniporide induced dose-dependent increase in bleb size (figure 4.5d), like the HT1080 cell line, retraction was not inhibited. Although, data from this study showed non-involvement of the widely reported NHE1, it is however obvious that the NHEs are required for AQP1-facilitated bleb retraction as demonstrated by EIPA inhibition. How the Na^+/H^+

pump actually regulate bleb retraction is not understood, however, one possible explanation is that reduction in extracellular pH due to proton efflux and accumulation with the resulting extracellular acidosis could activate acid signaling via plasma membrane acid-sensing ion channels (ASICs) to mediate rapid outflow of water from expanding bleb, thereby increasing bleb retraction through AQP1 water channel. Although, it is not known whether ASICs which are reported to be predominantly found in neurons (Kapoor et al., 2009) are involved in cell blebbing, they are known to mediate physiological processes such as synaptic plasticity, learning/memory and fear, and in pathological conditions such as depression, anxiety, neurodegeneration, epileptic seizures, brain ischemia, multiple sclerosis and malignant glioma (Chu and Xiong, 2012; Mari et al., 2014). In D54-MG human glioblastoma multiforme cell line, knockdown of ASIC1 reduced cell migration (Kapoor et al., 2009) and in SMMC-7721 hepatocellular carcinoma cell line, downregulation of ASIC1a activity by RNA interference inhibited migration and invasion (Jin et al., 2015). It has been reported that acidosis-mediated activation of ASIC1a during ischemia in neuronal cells triggers calcium release from intracellular pools (Mari et al., 2010), and interestingly, calcium efflux via the sodium-calcium exchanger 1 (NCX1) has been previously shown to regulate bleb retraction (Yi et al., 2012). Therefore, one possible mechanism by which the Na^+/H^+ pump is involved in AQP1-facilitted bleb retraction could be that extracellular acidosis by the Na^+/H^+ pump activates plasma membrane ASIC1a to raise intracellular calcium levels whose efflux through the NCX1 facilitates bleb retraction through AQP1. The Na^+/H^+ pump could also regulate cell blebbing independently of ASICs activation as it was reported that NHE1 is functionally coupled to NCX1 (Yi et al., 2009), and that Na^+ influx through the former directly activates the latter to triggered intracellular calcium release, and this modulation of intracellular calcium levels was capable of mediating bleb retraction (Yi et al., 2012). Similarly, the increased bleb retraction upon AQP1 overexpression could be that a high intracellular pH by

Na^+/H^+ pump enhances recruitment of actin nucleation factors such as Arp2/3 and mDia together with the ezrin/moesin/radixin which are essential for bleb retraction (Charras et al., 2006; Paluch and Raz, 2013). On the other hand, it was previously reported that talin, an actin binding protein which strengthens interaction between integrins, actin filaments and the extracellular matrix was pH-sensitive in that increased intracellular pH decreases the affinity of talin binding to F-actin thereby promoting cell migration (Srivastava et al., 2008). Thus, it is speculated that the intracellular accumulation of protons upon inhibition of NHEs could be responsible for the continuous bleb expansion. Attempts to probe the involvement of some other NHE isoforms were not successful due to inability to get specific inhibitors. It will be interesting in the future to perform gene knockdown using specific smartpooled siRNAs directed at the different NHE isoforms or to take mass-knockdown of some of the isoforms as this will indicate the specific isoform(s) that is involved in AQP1-regulated cell blebbing.

It was previously reported that EIPA inhibited the activity of transient receptor potential polycystin 3 (TRPP3), a nonselective cation channel activated by Ca^{2+}, and is permeable to Na^+, K^+, Ca^{2+}, Rb^+, NH_4 and Ba^{2+} (Dai et al., 2007). This raised the question whether the effect of EIPA was due to TRPP3 channel inhibition. Inhibition of this channel in both HT1080 and ACHN cells with different doses of the TRPP3 channel-specific blocker, phenamil, could not halt blebs retraction (figure 4.6a). In a time course experiment to study the effect of timing of phenamil treatment, inhibition of TRPP3 for up to two hours at intervals of thirty minutes had no effect on bleb retraction, and there was no observable difference between each treatments and vehicle controls (figure 4.6b), suggesting this ion channel might not be involved in AQP1 regulation of cell blebbing.

The fact that EIPA is a blocker of the Na^+/H^+ pump which mediate Na^+ influx into the cell, is an indication that at least Na^+ influx and increased intracellular pH could be involved in

AQP1-mediated regulation of cell blebbing. Different Na^+ transporting channels are found in the plasma membranes of mammalian tissues. One of such transporters that is ubiquitously expressed is the active cotransporter, NKCC1, that permits the influx of Na^+, K^+ and $2Cl^-$ into the cell, and has been implicated in cell migration (Haas and Sontheimer, 2010). Pharmacological inhibition of NKCC1 with the loop diuretic bumetanide displayed concentration-dependent and cell line-specific effects. In the HT1080 cells, 5 µM BMT induced an insignificant increase in bleb size which became significant and stable from 10 µM up to maximum 100 µM; however, in the ACHN cell line, 5 µM BMT again caused an insignificant increase in bleb size which gradually increased and became significant and steady between 10 and 20 µM of BMT treatment. A further steady significant increase in bleb size was observed between 50 and 70 µM and then a final increase at maximum 100 µM dosage of BMT was detected, and there was a significant difference in the sizes of the blebs between the maximum dosage used and each of the other treatments in this cell line (figure 4.8a). However, in both cell lines, there was a progressive decrease in bleb numbers with increasing dosage of BMT treatment (figure 4.8b).

This dose-dependent effect on the cells thus called for analysis of the dynamics of the bleb. A detailed investigation of time-lapse movies of blebbing ACHN and HT1080 cells in which the activity of the NKCC1 was inhibited with 100 µM BMT revealed that channel blockade conferred the blebs longer lifespans (figure 4.9a), and a further probe into the bleb phases indicated that whereas inhibition of NKCC1 in HT1080 cells had no significant effect on bleb expansion, in ACHN cell line, bleb expansion was significantly slower than wild-type (figure 4.9b), suggesting that Na^+ plays a role in expansion of blebs in this cell line. Although, in both cell lines, no significant difference in bleb stabilization was observed (figure 4.9c), inhibition of Na^+ flux significantly slowed down bleb retraction (figure 4.9d). Thus, there

exists differential mechanisms of bleb regulation in the two cell lines, whereby in HT1080 cells, the longer bleb lifespan upon BMT treatment was due to the effect of Na^+, K^+ and Cl^- flux on bleb retraction, while in the ACHN cells, a longer bleb lifespan was due to the effects of the ions on both bleb expansion and retraction. It is tempting to speculate that the increase in bleb size with a corresponding decrease in bleb number induced by NKCC1 inhibition is consistent with the result of the EIPA inhibition of Na^+/H^+ pump, which further implicates Na^+ in regulating cell blebbing. The NKCC1 regulates intracellular volume by mediating passage of Na^+, K^+ and Cl^- across plasma membrane utilizing the energy stored in the Na^+ gradient produced by the Na^+/K^+ ATPase, and intracellular accumulation of Cl^- by NKCC1 has been previously reported to drive not only proliferation, but migration of glioma cells (Habela et al., 2009). It would therefore be interesting in future to investigate the roles of Cl^- as well as K^+ ions by using specific inhibitors of chloride and potassium channels or by knocking down the channels with specific siRNAs.

The above observations opened up the hypothesis that numerous cation and anion channels on mammalian plasma membranes regulate cell blebbing. Normally, increased intracellular osmolarity due to ion influx results in inflow of obligated water which cause cell swelling and subsequent fluid flow into blebs. To put excessive swelling in check, mammalian cells have pathways which are swelling-activated Cl^- currents for regulatory volume decrease (RVD) (Hoffmann et al., 2009). One of such pathways mediating swelling-activated Cl^- currents is via the volume-regulated anion channels (VRAC), also called the volume-sensitive organic anion channels (VSOAC) which are ubiquitously expressed in mammalian plasma membranes and permit the passage of small organic and inorganic anions. The activity of VRAC as well as glutamate release and uptake through connexin hemichannels and glutamate transporter GLT-1 respectively in rat glial cells were reported to be selectively, and

potently blocked by DCPIB (Bowens et al., 2013; Min et al., 2011). Thus, the present study tested the involvement of VRAC in blebbing of ACHN and HT1080 cells by inhibition of the channel with this selective blocker. In both cell lines, although the different doses of DCPIB used induced significant increase in the size of blebs as compared to vehicle controls (figure 4.9a), neither bleb expansion nor retraction was halted. Although, this drug was reported to completely block VRAC activity at 20 µM and said to have a solubility limit in physiological solutions at 50 µM (Decher et al., 2001), in a further experiment to determine the effect of timing of DCPIB treatment of blebbing cancer cells, pretreatment of cells with 50 µM DCPIB for up to 90 minutes showed no inhibitory effect on bleb retraction.

Therefore, it is apparent from these findings that blebbing of cells, as a biological process, goes beyond the old-held traditional belief of Rho-ROCK signaling activation of actomyosin contractility. It is rather a process that is regulated by complex cascade of water and ions flow through different aquaporins and transmembrane ion transporters as well as generation of pH gradients and acid signaling, which apparently impinge on the plasma membrane lipids architecture to cause delamination and expansion of the plasma membrane from the underlying cortex and then the subsequent reincorporation of the membrane into the cortex.

Chapter 5. Regulation of Blebbing by Lipids

5.1 Lipid Signaling

The cell membrane of plants and animals is composed of different lipids which are vital for the architectural integrity of the cell as well as in metabolic activities. In animals, these signaling lipids mediate a plethora of biological processes ranging from signal transduction, membrane trafficking, cell proliferation, cytoskeletal dynamics, apoptosis and cell migration (Wang, 2004; Wymann and Schneiter, 2008) and are crucial for cell survival, growth and differentiation (Wang, 2002). The level of the lipid mediators in the cell is regulated in a spatiotemporal manner by lipid signaling enzymes such as phospholipases, lipid kinases, prostaglandin synthase and phosphatases. The activity of these signaling enzymes itself is regulated by extracellular signals such as growth factors, nutrients and cytokines. These lipid signaling events mainly occur by binding specific receptors at the plasma membranes which are composed of several aquaporin water and ion channels, the activities and regulation of which interfere with the interaction between plasma membrane and the underlying cortical actin as well as the membrane lipid composition, eventually resulting in membrane ruffling and cell blebing.

5.2 Phospholipase D

Phospholipase D (PLD) is an enzyme abundantly expressed in a wide variety of organisms including bacteria, yeast, plants and mammals. PLD enzymes catalyze the hydrolysis of the phosphodiester bond of membrane phospholipid phosphatidylcholine (PC) to yield phosphatidic acid (PA) and free choline (Su et al., 2009a). They can also catalyze a transphosphatidylation reaction involving the transfer of the aliphatic chain of a primary

alcohol to the phosphatidyl group of PA product (Morris et al., 1997). Whereas the freed choline diffuse away from the membrane, the versatile lipid second messenger PA remains in the membrane to mediate cell biological processes such as signal transduction (Zhao et al., 2007), cell proliferation (Oude Weernink et al., 2007), membrane vesicle trafficking (Shen et al., 2001), lipid metabolism (Wagner and Brezesinski, 2007), actin cytoskeletal reorganization (Du and Frohman, 2009), phagocytosis and exocytosis (Corrotte et al., 2006; Shen et al., 2001) cell survival (Foster, 2009) and cell migration (Scott et al., 2009; Su et al., 2009b). Thus, impairment of PLD activity has been correlated with pathological conditions such as cancer, neurodegeneration, diabetes and inflammation (Selvy et al., 2011).

5.2.1 Structure of PLD Isoforms

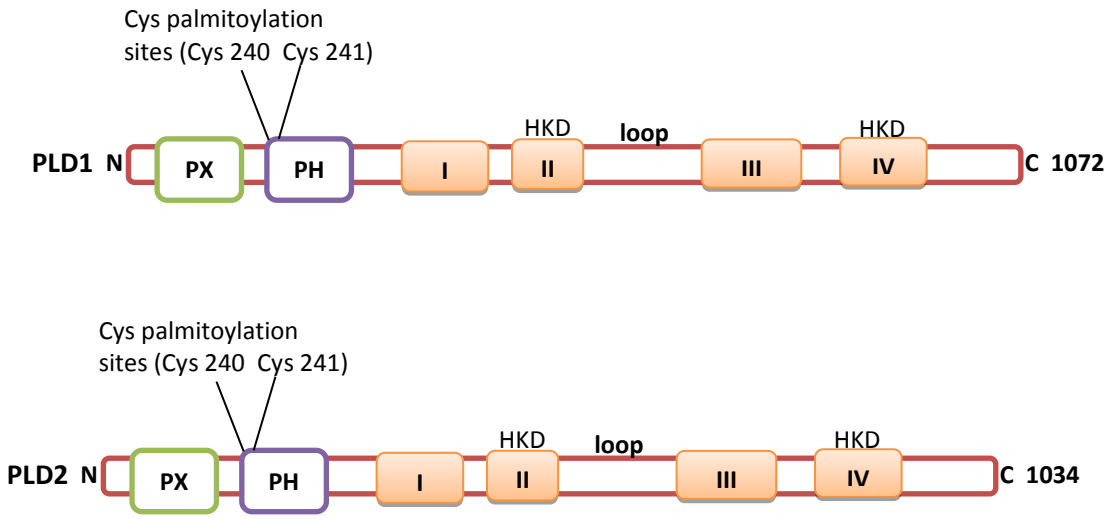

Figure 5.1: Domain structure of mammalian PLD isoforms. The two mammalian isoforms are highly homologous with both isoforms possessing the PH and PX domains at the N terminus. At the PH domain are two cysteine residues, and the two conserved HKD motifs are located both at the central portion and C terminus at domains II and IV of the enzymes.

In mammals, there are two PLD genes PLD1 and PLD2 (Cao et al., 1997; Lopez et al., 1998) with approximately 50% identity, and these isoforms are characterized by the possession of two highly conserved HKD motifs which are essential for the catalytic activity of the enzyme as revealed from point mutation of PLD genes in a variety of species both in vitro and in vivo (Frohman and Morris, 1999).

Both isoforms contain two regulatory motifs at the N-terminal domain. The phox (PX) motif mediates protein-protein interactions as well as binding polyphosphoinositides (Stahelin et al., 2004). It also facilitates protein activation and translocation by binding regulatory proteins such as Growth receptor bound protein 2 (Grb2) (Di Fulvio et al., 2006; Selvy et al., 2011). The pleckstrin homology (PH) domain contains two cysteine residues which are palmitoylated, and this domain is known to promote localization of the enzyme to plasma membranes of different subcellular compartments (Selvy et al., 2011). Despite the similarities between the two mammalian PLD isoforms, in PLD1, downregulation of the PX domain and truncation of part of the PH domain resulted in an increased activity of the enzyme, suggesting a probable autoinhibitory role of the N-terminus of PLD1 (Sugars et al., 1999), while perturbation of the N-terminus of PLD2 leads to reduced enzymatic activity, indicating that this domain is important for catalytic activity of this isoform (Selvy et al., 2011).

In both mammalian PLD1 and PLD2, the C-terminal end is homologous, and the integrity of the conserved residues at this domain must be kept constant as these residues interact with the catalytic core of the enzyme (Liu et al., 2001), and impairment of one of the residues abrogate catalytic activity, implying that the C-terminus is critical for the catalytic activity of the enzymes (Liu et al., 2001; Steed et al., 1998).

Although the classical mammalian PLDs generate PA as a major product using PC, phosphatidylserine (PS), phosphatidylethanolamine (PE), lysophosphatidylcholine (LPC) as

substrates, they cannot hydrolyze cardiolipin and phosphatidylinositolamine (PI) (Selvy et al., 2011).

5.2.2 Subcellular localization of PLD

The expression of classic mammalian PLDs cuts across a wide variety of cells and tissues, though, with differences in expression levels (Colley et al., 1997; Zeniou-Meyer et al., 2007). Although PLD2 is not expressed in peripheral leucocytes, there is high expression of PLD1 and PLD2 in most mammalian tissues such as in the spleen, brain and heart (Su et al., 2009a). Whereas PLD2 constitutively localizes to the plasma membrane (Du et al., 2004), cytosol (Yang et al., 2008b) and golgi apparatus (Yang et al., 2008b), PLD1 is specifically found localized in perinuclear structures such as endoplasmic reticulum, golgi apparatus, secretory vesicle (Huang et al., 2005).

However, depending on the kind of stimulant, PLD1 may also translocate to the plasma membrane when stimulated (Du et al., 2003). Upon treatment of Cos 7 cells with PMA, PLD1 translocates to the plasma membrane, while serum treatment results in translocation to both the early endosome and plasma membrane (Du et al., 2003; Selvy et al., 2011). PIP_2 binding to PLD1 is believed to be the cause of plasma membrane translocation (Du et al., 2003).

5.2.3 Regulation of Phospholipase D activity

The regulation of PLD activity involves a complex array of signals from different signaling pathways which either work together to activate or act in an antagonistic manner to

downregulate the activity of the enzyme. The enzyme is activated upon stimulation by both the G-protein coupled receptors (GPCRs) and the receptor tyrosine kinases (RTKs).

Growth factors such as EGF stimulate the activity of ADP-ribosylation factor (ARF) which causes not only its translocation to the plasma membrane, but also to the colocalization and activation of mammalian PLD (Su et al., 2009a). PLD activity is directly activated when bound to the Rho family of GTPases (RhoA, Rac and Cdc42) which regulate the spatial production of PA (Santarius et al., 2006). Rho GTPases also activate phosphatidylinositol-4-phosphate 5-kinase (PI4P5K) to regulate PIP_2 levels. GPCRs-mediated stimulation of PKC results in activation of PLD (Santarius et al., 2006). In contrast, phosphorylation of PLD1 by PKC has also been shown to play no role in activating the lipase activity both in vitro and in vivo (Hu and Exton, 2003). Post-translational palmitoylation at two cysteine sites at the PH domain has no effect on catalytic activity, but rather promotes translocation of proteins to lipid rafts (Sugars et al., 1999). Hydrogen peroxide (H_2O_2) stimulation leads to increased phosphorylation and lipase activity of PLD1 (Min et al., 2001).

5.2.4 Phospholipase D and Cancer

During the past decades, several reports have implicated Phospholipase D activity to have direct correlation with the hallmarks of cancer (Foster and Xu, 2003). Overexpression of PLD has been found in gastric, colon, kidney and breast cancers (Foster, 2009; Huang and Frohman, 2007; Su et al., 2009a). Elevated PLD activity is responsible for abnormal dissemination of cancer cells to distant sites, a process that is characterized with loss of adhesion to ECM, increased motility, intravasation and surmounting of barriers in circulation, extravasation and colonization of new site (Brooks et al., 2010; Geiger and Peeper, 2009).

Interestingly, PLD activity has been shown not only to facilitate tumour invasion (Chen et al., 2012), but is also required for EGF-stimulated formation of membrane ruffles and protrusions as evidenced in v-src-transformed fibroblasts that required PLD2 activity (Honda et al., 1999; Shen et al., 2002). In stressed, serum-starved MDA-MB-231 cells, there was high expression of PLD activity and this corresponded to aggressive invasion in matrigel (Zheng et al., 2006). Similarly, PLD2 activity promoted cell spreading, cell elongation, increased migration, activation of Akt activity and metastasis in EL4 lymphoma cells (Knoepp et al., 2008). PLD1 is involved in matrix degradation and metastasis in that cell surface matrix metalloproteinase secretion in response to PMA was abrogated when PLD1 activity was downregulated in HCT116 colon cancer cell (Kang et al., 2008a). PLD1 not only promoted tumour angiogenesis in zebrafish (Zeng et al., 2009), but in addition stimulated vasculogenesis in mice (Chen et al., 2012).

5.3 Phospholipase C (PLC)

Phospholipases C are a group of lipid metabolizing enzymes that specifically catalyze the hydrolysis of membrane phosphatidylinositol 4,5-bisphosphate (PIP_2) to generate diacylglycerol (DAG) and inositol 1,4,5-triphosphate (IP_3), two intracellular second messengers that trigger other signal transduction cascades by activating PKC and intracellular calcium ion release respectively (Suh et al., 2008). PIP_2 is a versatile intracellular second messenger that regulates the activity and subcellular localization of PLD, ion channels and other actin regulatory proteins by interacting with their PH and PX domains (Niggli, 2005; Suh and Hille, 2005) to affect biological processes such as vesicle trafficking, gene expression, membrane ruffling, actin reorganization and cell migration (Ling et al., 2006; Oude Weernink et al., 2004). PI3K-mediated phosphorylation of PIP_2 results in the plasma

accumulation of PIP_3 which recruits and activates proteins involved in downstream signaling events.

In mammals there are thirteen PLC isozymes which are grouped into six subtypes that include PLC-β (1-4), -γ (1-2), -δ (1,3,4), -ε, (1) –ζ (1) and –η (1-2).

Structurally, PLC enzymes consist of the catalytic X and Y domains located between EF-hand motif and C2 domain. The EF-hand motif and C2 domain contain binding sites for Ca^{2+}, and this increases the activity of the enzyme (Nakashima et al., 1995). At the N-terminal of β-, γ-, δ- PLC is the PH domain that binds PIP_2, it also facilitates interaction with PIP_3 (Falasca et al., 1998). In PLC-γ1 and -γ2, there are two Src homology 2 (SH2) and one SH3 domains that separate an additional PH domain just between the X and Y domains, and the split PH domain at the C-terminal end of this enzyme has been reported to associate with TRPC3 calcium channel (Wen et al., 2006).

The mammalian PLC isozymes are distributed in different tissues as shown below:

Table 5.1: Tissue distribution of PLC isozymes. The mammalian PLC consists of six subgroups that are classified into thirteen isozymes and are distributed in various tissues as shown:

PLC Isozymes	Tissue Distribution	Reference
PLC-β1	Cerebral cortex, hippocampus	(Homma et al., 1989)
PLC-β2	Haematopoietic cells	(Sun et al., 2007)
PLC-β3	Brain, liver, paratoid glands	(Jhon et al., 1993)
PLC-β4	Cerebellum, retina	(Adamski et al., 1999)
PLC-γ1	Neurons, astrocytes, oligodendrocytes	(Mizuguchi et al., 1991)
PLC-γ2	Anterior pituiutary, granule cells	(Tanaka and Kondo, 1994)
PLC-δ1	Brain, heart, lung, testis, skeletal muscles	(Lee et al., 1999)
PLC-δ3	Brain, skeletal muscle, heart	(Lin et al., 2001)
PLC-δ4	Brain, skeletal muscle, testis, kidney	(Lee and Rhee, 1996)
PLC-ε	Heart, brain, lung, colon	(Lopez et al., 2001)
PLC-ζ	Testis	(Saunders et al., 2002)
PLC-η1	Brain, kidney, lung, spleen, intestine, pancreas	(Hwang et al., 2005)
PLC-η2	Brain, intestine	(Zhou et al., 2005)

5.4 Phosphoinositide 3-kinase (PI3K)

The PI3K belongs to a family of enzymes involved in the phosphorylation of membrane phospholipids at the 3-OH positions to produce phosphoinositide 3-phosphate, phosphoinositide 3,4-bisphosphate, phosphoinositide 3,5-bisphosphate, and phosphoinositide 3,4,5-triphosphophate which are capable of binding downstream proteins possessing special binding sites such as PH, PX, FYVE and ENTH domains (Ellson et al., 2002; Itoh et al., 2001) thereby recruiting them to the cell membrane. On the basis of their structures, regulation, and substrate specificity, they are classified into three groups consisting of eight different isoforms (Foster et al., 2003). Isoforms in class I which is further divided into class Ia and class Ib include p110α, p110β, p110δ and p110γ; Class II includes PI3K-C2α, PI3K-C2β and PI3K-C2γ, while class III has Vps34 as the only member (Fry, 2001).

The PI3K pathway which regulates a lot of cellular processes such as cell growth, migration, proliferation and survival (Weigelt and Downward, 2012) is often found upregulated in a variety of human cancers. Upon stimulation by growth factors and hormones, receptor tyrosine kinases activate the PI3K pathway resulting in the formation of PIP_3 from PIP_2, and the action of PI3K can be directly opposed by the tumour suppressor, phosphatase and tensin homologue deleted on chromosome ten (PTEN) (Sarbassov et al., 2005). Downstream signaling events are triggered by the accumulation of PIP_3 which recruits phosphoinositide-dependent kinase 1 (PDK1) to phosphorylate Akt on threonine 308. Akt phosphorylates and inactivates tuberous sclerosis complexes 1 and 2 (TSC1/2) thereby liberating the small Ras homologue enriched in brain (Rheb) from TSC2-mediated down-regulation, thus, mammalian target of rapamycin complex 1 (mTORC1) becomes constitutively active. Similarly, Akt can stimulate mTORC1 by either directly stimulate the kinase activity of mTOR protein or inhibit PRAS40 (Sabatini, 2006). The net effect is cell growth, proliferation and protein translation.

Therefore, development and use of effective and isoform-specific inhibitors of PI3K, Akt (the most crucial downstream target of PI3K), PLC as well as inhibitors of mTOR look promising in the fight against cancer.

5.5 Chapter Aim

Previous studies have linked the lipid signaling enzyme PLD1 to angiogenesis, cell proliferation and metastasis in different cell types. Similarly, PLD2 has been shown to increase migration of cells and cell spreading. Most of these effects are mediated through the versatile second messenger PA either directly or by stimulating other signaling pathways that promotes tumour progression. Therefore, this chapter is aimed at investigating the role lipid signaling enzymes (PLD1, PLD2 and PLC) and their metabolites as well as the PI3K signaling pathway play in the blebbing of cancer cells.

5.6 Results

5.6.1 Pharmacological inhibition of Phospholipase D (PLD) activity

To investigate the role of lipid signaling mediated by PLD enzymes in blebbing of cancer cells induced to bleb in 3D matrigel matrix, the activity of these enzymes was inhibited with 5-fluoro-2-indolyl des-chlorohalopemide (FIPI), a drug that has been shown to potently block PLD1 and PLD2 activity both in vitro and in vivo (Su et al., 2009b). As shown in figure 5.2a and b, pretreatment of cells with 750 nM of FIPI for 30 min sufficiently suppressed blebbing of HT1080 and ACHN cells.

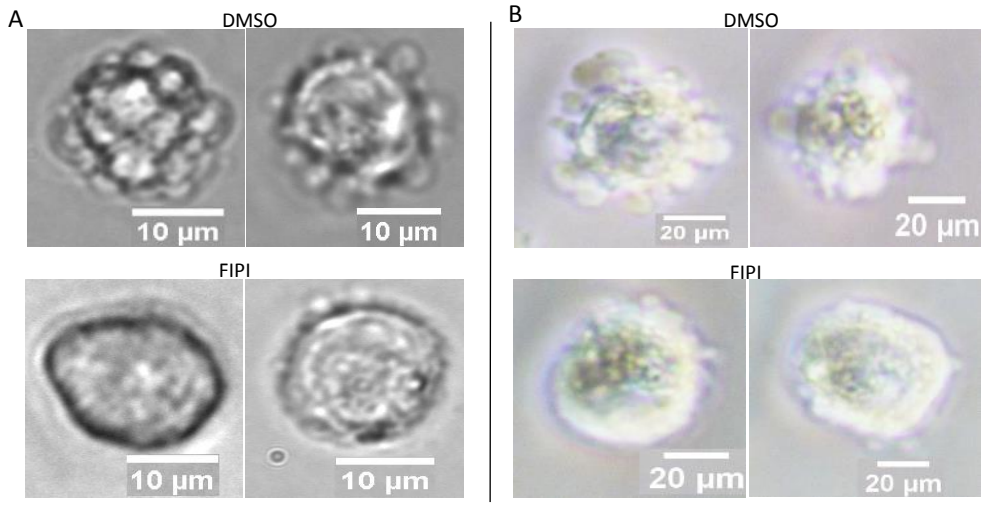

Figure 5.11 FIPI inhibits blebbing. A. HT1080 cells **B.** ACHN cells were cultured in 3D matrigel and blebs were induced with BB-94 (1 µM) and PIC (1:100) in presence of caspase inhibitor set VI (top panel). Pretreatment of cells with 750 nM FIPI suppressed cell blebbing (bottom panel). Data is a representative of three separate experiments done in triplicate in which 75 cells were scored.

5.6.2 Impact of inhibition of PLD activity

To assess the impact of inhibition of PLD activity with FIPI, the percentage of blebbing cells as well as the number of blebs in each cell and bleb size were analyzed. Upon quantification, it was revealed that inhibition of PLD activity reduced the percentage of blebbing HT1080 and ACHN cells to 12% and 13% respectively as compared to 83% and 88% respectively for vehicle controls (figure 5.3a). Furthermore, in both cell lines, the number of blebs in each cell upon FIPI treatment was significantly reduced to 3 blebs/cell (figure 5.3b). Finally, analysis of the bleb size indicates that PLD inhibition significantly reduced bleb size to 2 µm in both cells as compare to vehicle controls (figure 5.3c). Taken together, this data suggest that both PLD1 and PLD2 positively regulate blebbing of cancer cells.

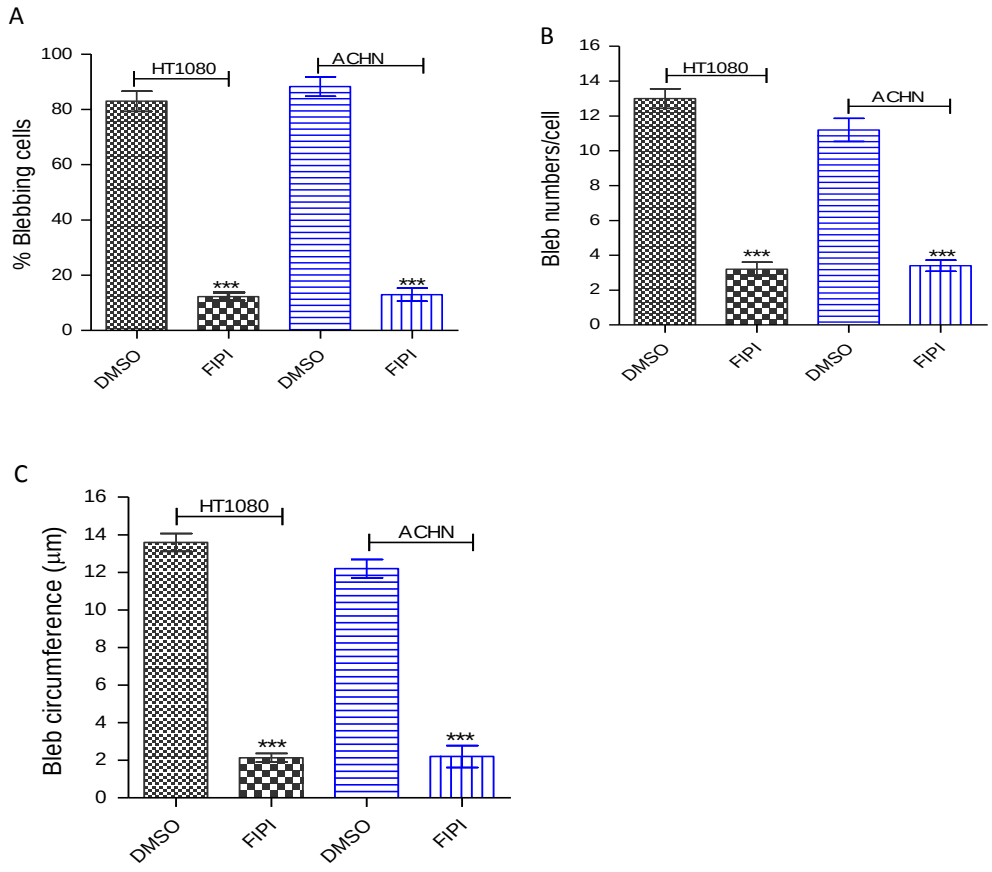

Figure 5.3: Impact of inhibition of PLD activity with FIPI A. Quantification of percentage of control and FIPI treated HT1080 and ACHN cells; **B.** Analysis of numbers of blebs in each of control and FIPI treated HT1080 and ACHN cells; **C.** Size of blebs in control and PLD inhibited HT1080 and ACHN cells. Data are the mean ± SEM for three separate experiments. ***:P < 0.001, using one-way ANOVA followed by Tukey's multiple comparison test.

5.6.3 Impairment of PLD1 activity by siRNA Suppresses Blebbing of HT1080 Cells

To investigate whether inhibition of cell blebbing by FIPI was due to inhibition of PLD1, the involvement of this isoform was probed by siRNA-mediated gene knockdown. HT1080 cells were seeded in 6 well plate at a density of 2 x 10^5 cells/well and incubated at 37^{o}C for 24 h for cells to adhere to plate. Cells were transfected with human PLD1 siRNA and a scrambled non-targetting siRNA as a control using Dharmacon transfection reagent set 4 according to

the manufacturers' instruction. Protein knockdown was effective at 24 h (91.85%) post-PLD1 siRNA transfection as confirmed by western blotting and densitometric analysis (figures 5.4a and b). Upon confirmation of PLD1 knockdown at 24 h time point, wild-type and PLD1 knocked down cells were cultured in 3D matrigel matrix and challenged with BB-94 (1 µM) and PIC (1:100) in presence of caspase inhibitor as described in materials and method. As shown in figure 5.4c, similar to FIPI treatment, PLD1 RNA interference suppressed blebbing of HT1080 cells.

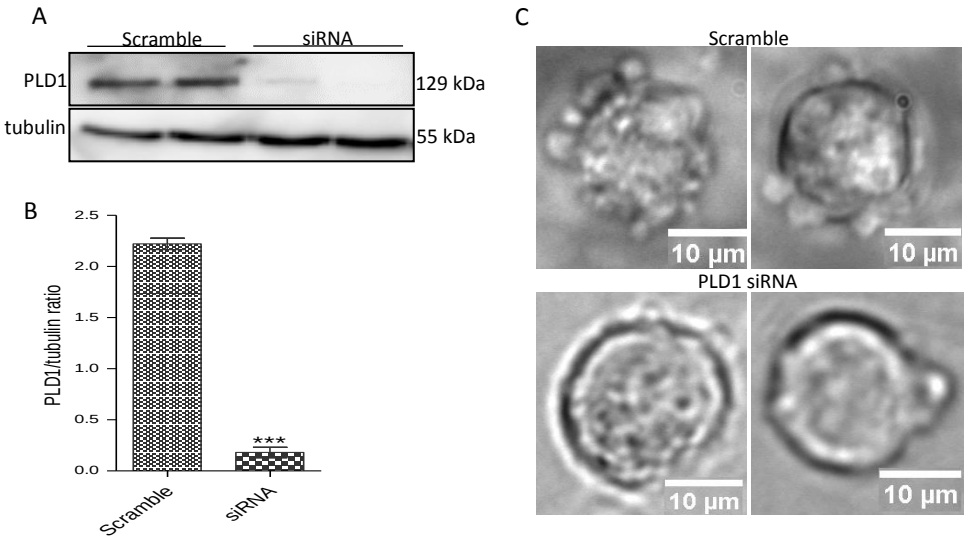

Figure 5.4: Impairment of PLD1 activity suppresses cell blebbing: A. HT1080 cells were grown to confluent on 6 well plate and transfected with human PLD1 siRNA using Dharmafect transfection reagent (set 4). Cells were lysed using RIPA buffer PIC (1:100). Proteins were resolved on a 10% SDS gel and immunoblotted with human anti-PLD1 antibody (1:1000). Tubulin was used as a loading control; **B.** Densitometric quantification of PLD1 levels in HT1080 cells after normalization to tubulin loading control; **C.** Scrambled control and PLD1 siRNA-treated HT1080 cells were cultured in matrigel followed by treatment with BB-94 and PIC and caspase inhibitors. Data is a representative of the mean ± SEM for three independent experiments; ***:$P < 0.001$, using two-tailed unpaired students' t test.

5.6.4 Knockdown of PLD2 by siRNA Negatively Regulates Cell Blebbing

Since mammalian PLD exists in two isoforms, the involvement of PLD2 in blebbing was also investigated. Firstly, the PLD2 gene was knocked down (89.65%) by siRNA as confirmed by western blot analysis after 24 h post siRNA transfection (figures 5.5a and b) before embedding cells in matrigel, followed by treatment with BB-94 and PIC in the presence of caspase inhibitor. As shown in figure 5.5c, in a manner similar to PLD1 knockdown, blebbing was attenuated by PLD2 down-regulation. Quantification revealed that both PLD1 and PLD2 siRNAs significantly decreased not only the number of blebs in each cell but the sizes of the blebs as well (figures 5.5d and e).

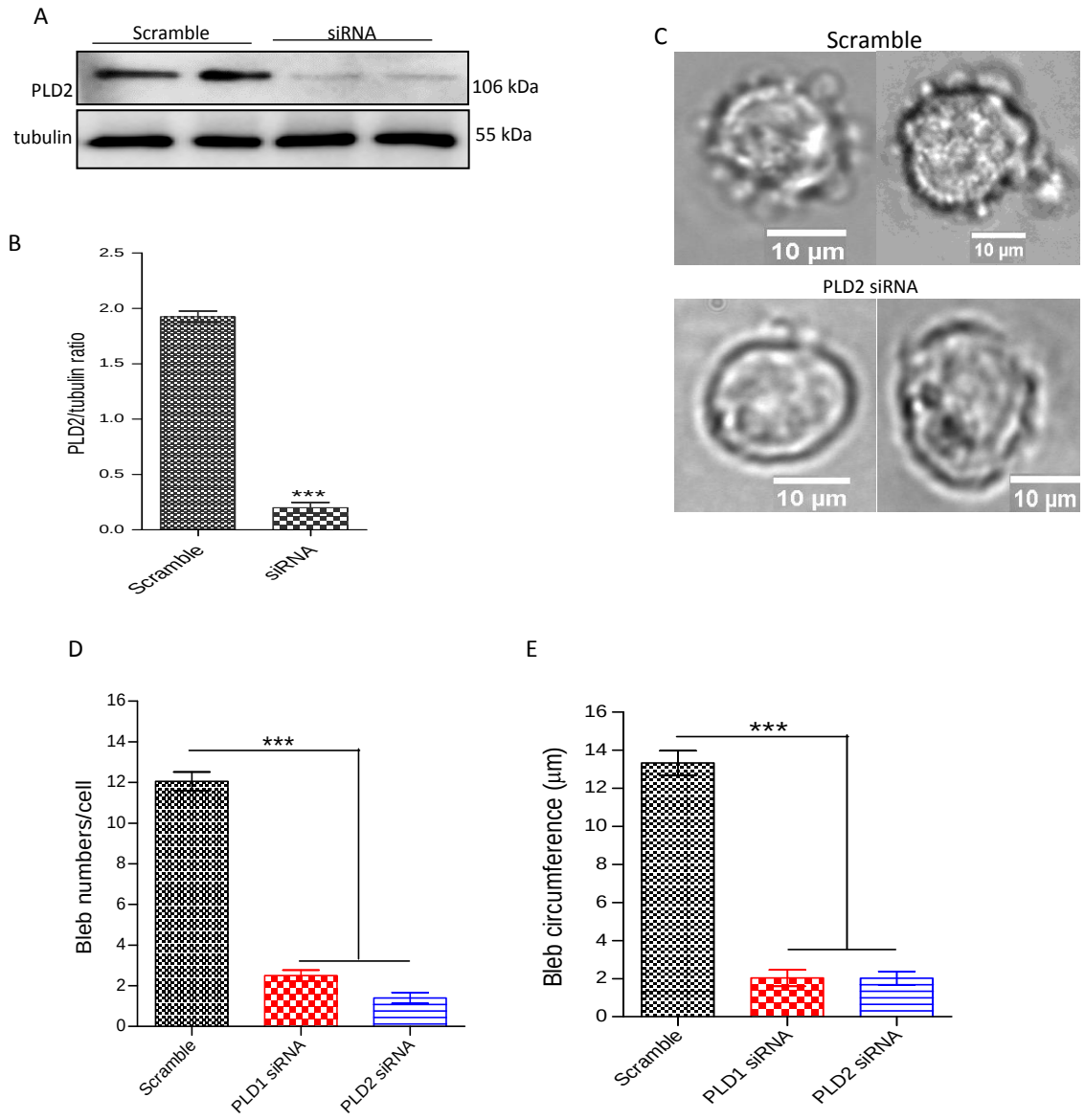

Figure 5.5: PLD2 knockdown attenuates membrane blebbing. HT1080 cells were seeded on 6 well plate and transfected with human PLD2 siRNA using Dharmafect transfection reagent (set 4). Cells were lysed using RIPA buffer with protease inhibitor cocktail PIC (1:100). **A.** Proteins were resolved on a 10% SDS gel and western-blotted with human anti-PLD2 antibody (1:1000) using tubulin as a loading control. **B**. Densitometric quantification of PLD2 levels in HT1080 cells after normalization to tubulin loading control; **C**. Control and PLD2 knocked down HT1080 cells embedded in matrigel before challenging with BB-94, PIC and caspase inhibitor; **D.** Analysis of bleb numbers/cell of controls, PLD1 and PLD2 knocked down cells; **E.** Analysis of bleb size in control, PLD1 and PLD2 knocked down cells. 50 cells were quantified for each case. Data is the mean ± SEM for three separate experiments; ***:P < 0.001, using one-way ANOVA followed by Tukey's multiple comparison test.

5.6.5 PLD2, but not necessarily PLD1 is involved in blebbing of HT1080 cells

The suppression of bleb formation upon siRNA-mediated knockdown of both isoforms of the PLD raised the question whether the knockdown of a particular isoform is negatively impacting on the other isoform. To confirm the isoform-specificity of the different PLD siRNAs, PLD1 knocked down cell lysates were probed with anti-PLD2 antibody, while the PLD2 siRNA samples were immunoblotted with an anti-PLD1 antibody. Data from this study (figure 5.6a and b) indicates that the PLD1 siRNA used was not specific for this protein as knockdown of PLD1 also negatively affected PLD2. On the contrary, knockdown of PLD2 had no effect on PLD1 activity (figure 5.6c and d). Taken together, this data suggests that the effect of PLD on blebbing of HT1080 cells could be mediated by PLD2.

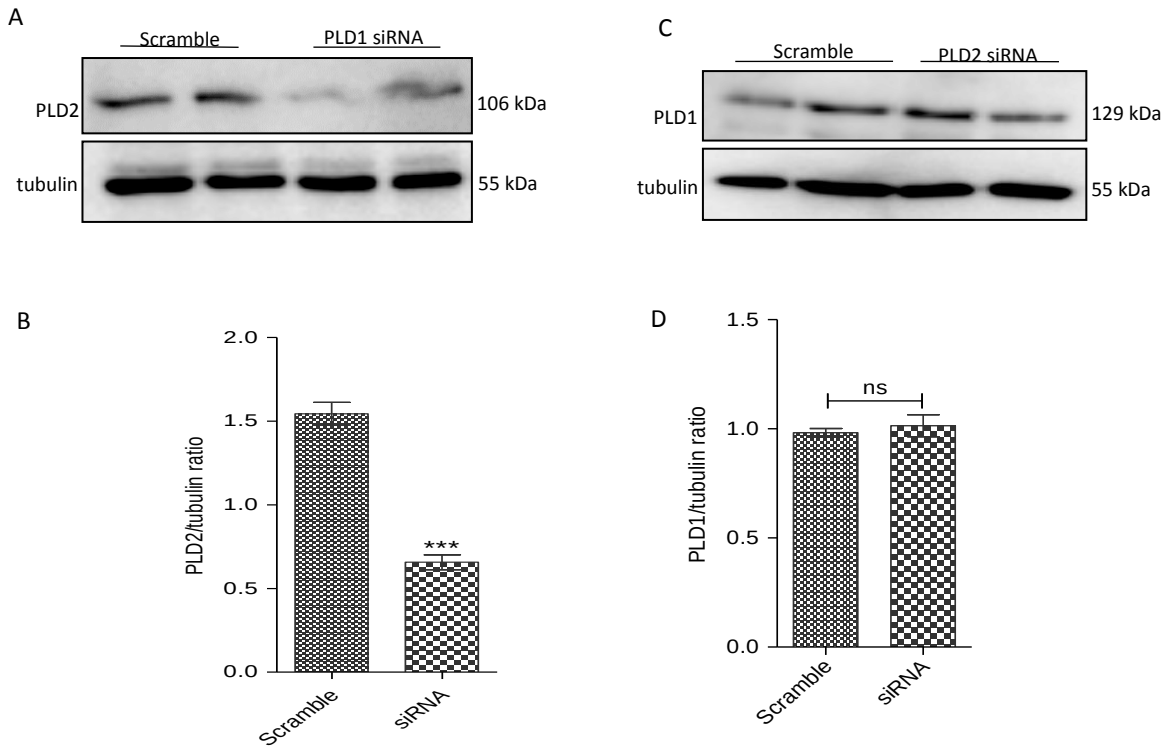

Figure 5.6: Specificity of PLD knockdown in HT1080 cells. A. HT1080 cell lysates transfected with human PLD1 siRNA were probed with human anti-PLD2 antibody; **B**. Densitometric quantification of PLD2 levels in PLD1 siRNA-treated HT1080 cell lysates after normalization to tubulin loading control; **C.** HT1080 cell lysates transfected with human PLD2 siRNA were probed with human anti-PLD1 antibody; **D**. Densitometric quantification of PLD1 levels in PLD2 siRNA-treated HT1080 cell lysates after normalization to tubulin loading control. Data represents the mean ± SEM for three independent experiments; ***:$P < 0.001$, using two-tailed unpaired students' t test.

5.6.6 PLD2 signals through Phosphatidic acid (PA) to promote cell blebbing

As most biological processes by the PLD enzymes are mediated by the lipid second messenger, phosphatidic acid (PA), it became imperative to investigate whether PLD2-mediated cell blebbing was via PA production. The involvement of PLD in most biological processes is tested for by using primary alcohols which are capable of undergoing transphosphatidylation reaction to block PA formation (Zouwail et al., 2005). Indeed, addition of 1% butan-1-ol to blebbing HT1080 and ACHN cells for 5 min almost completely abolished blebbing (figures 5.7a and b, middle panel), whereas addition of 1% tertiary butanol had no significant effects (figures 5.7a and b, bottom panel). In both cell lines, treatment with butan-1-ol drastically reduced the percentage of blebbing cells and number of blebs per cell (figure 5.7c and d).

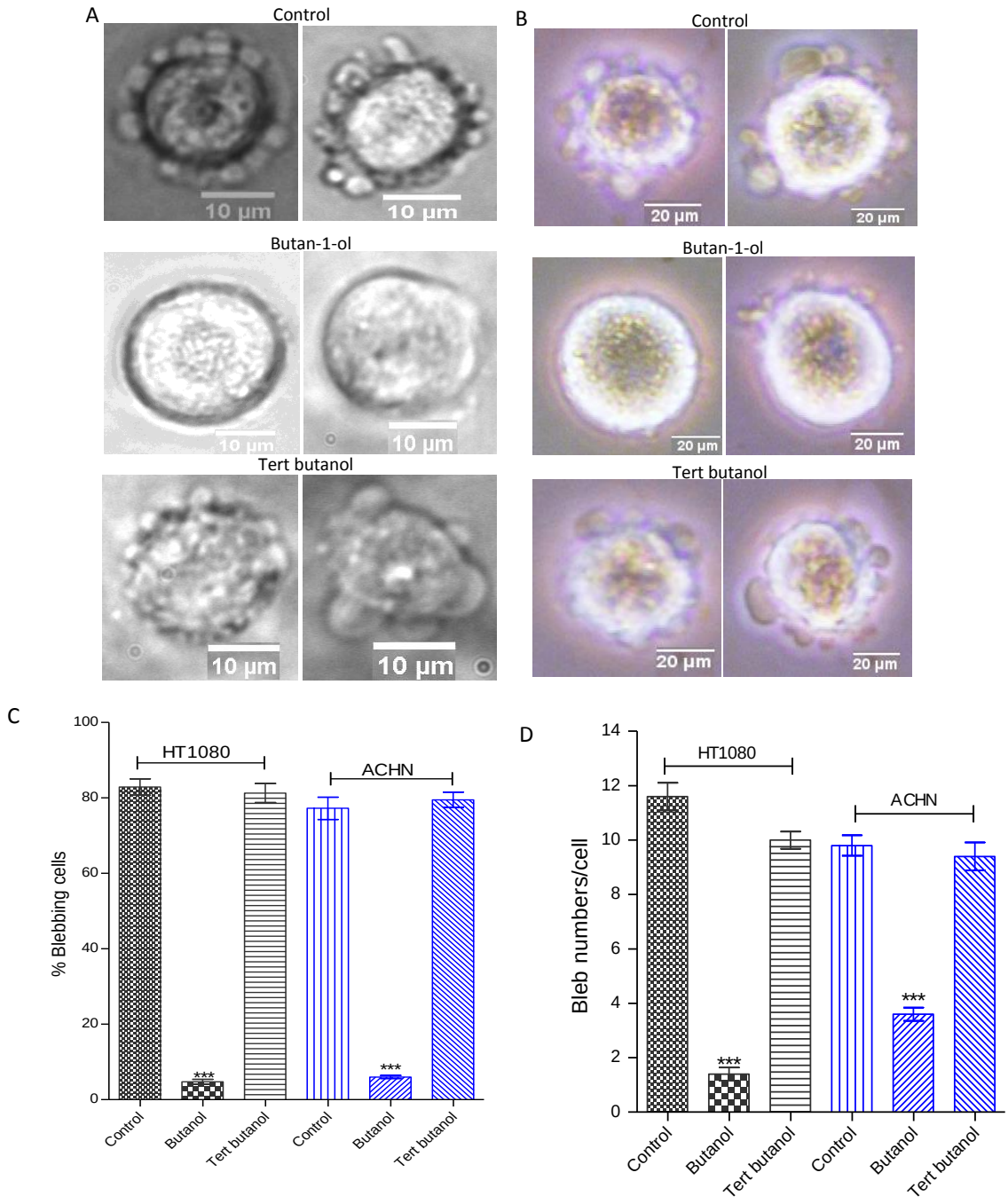

Figure 5.7: PLD2 Promotes cell blebbing through PA: A. and B. Incubation of HT1080 and ACHN cells with 1% butan-1-ol and tert-butanol for 5 min; **C.** Quantification of percentage blebbing cells in butan-1-ol and tert-butanol treated HT1080 and ACHN cells as compared to control; **D.** Number of blebs/cell in butan-1-ol and tert-butanol treated HT1080 and ACHN cells. Data are the mean ± SEM for three independent experiments. **:P < 0.01, ***:P < 0.001, using one-way ANOVA after Tukey's multiple comparison test.

5.6.7 PA signals through lysophosphatidic acid (LPA) to activate the LPAR-Rho-ROCK pathway

To further unravel the mechanism by which PA signals to mediate bleb formation, it was anticipated that PA could possibly promote bleb formation through its product lysophosphatidic acid (LPA) which binds its receptors (LPAR) at the plasma membrane. LPAR has been previously reported to function upstream the Rho-ROCK pathway to regulate blebbing in osteoclasts (Panupinthu et al., 2007). Thus, the receptor was blocked with 1 µM VPC-32183 for 30 min, and as anticipated, both the number of blebs per cell and the percentage of blebbing cells was significantly inhibited in both HT1080 and ACHN cell lines (figures 5.8), suggesting the involvement of the PA-LPAR-ROCK signaling pathway in cell blebbing.

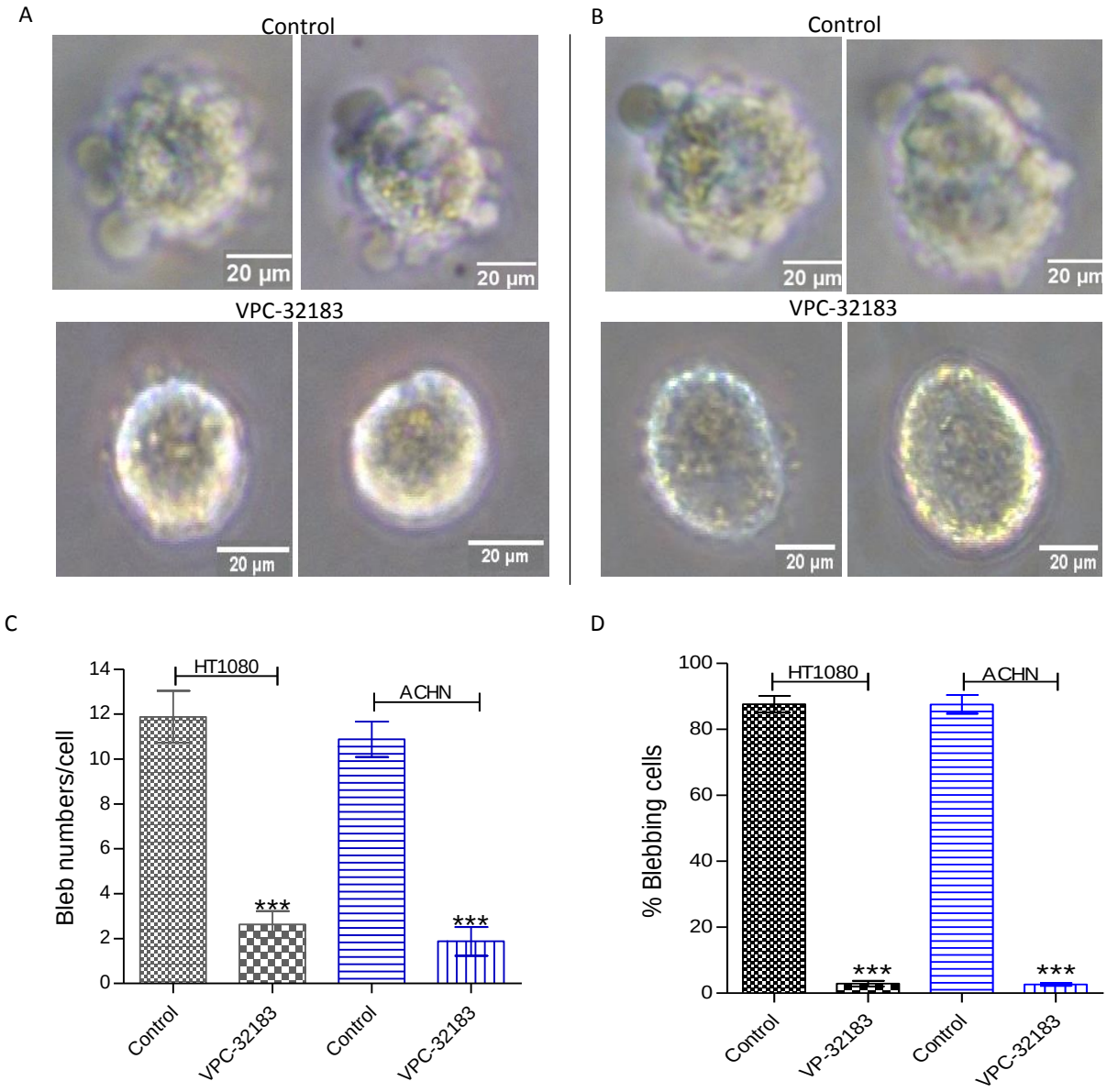

Figure 5.8: PA signals through LPAR to promote bleb formation: A. and **B.** HT1080 and ACHN cell lines respectively were cultured in 3D matrigel and induced to bleb before pretreatment with LPAR inhibitor, VPC-32183 for 30 min at 37°C; **C.** and **D.** Quantification of bleb numbers and percentage blebs respectively in each cell line upon LPAR inhibition. Data is a representative of the mean ± SEM of three independent experiments. ***:$P < 0.001$, using one-way ANOVA after Tukey's multiple comparison test.

5.6.8 Effect of inhibition of key signaling pathways on bleb formation

To ascertain the contribution of different signaling pathways in blebbing of cancer cells, different inhibitors known to inhibit key lipid signaling pathways were used. The involvement of PLC was tested using U73122, a drug reported to inhibit PLC activities in different cell lines (Ward et al., 2003). Use of 20 µM of U73122 significantly reduced the size of blebs without any significant change in bleb numbers (figures 5.9b, e and f). The involvement of PLC led to analysis of PKC which is stimulated by PLC-generated diacylglycerol (DAG). Thus, use of 5 µM of the PKC inhibitor, Go6976 also resulted in significantly diminished bleb size (figure 5.9c and e), but no effect on the number of blebs formation (figure 5.9f). The PI3K inhibitor, LY294002 was used to test for the requirement of this enzyme in blebbing. Again, use of 5 µM of the PI3K inhibitor LY294002 suppressed bleb formation (figure 5.9d and e), but no significant difference in bleb numbers (figure 5.9f) when compared to vehicle controls.

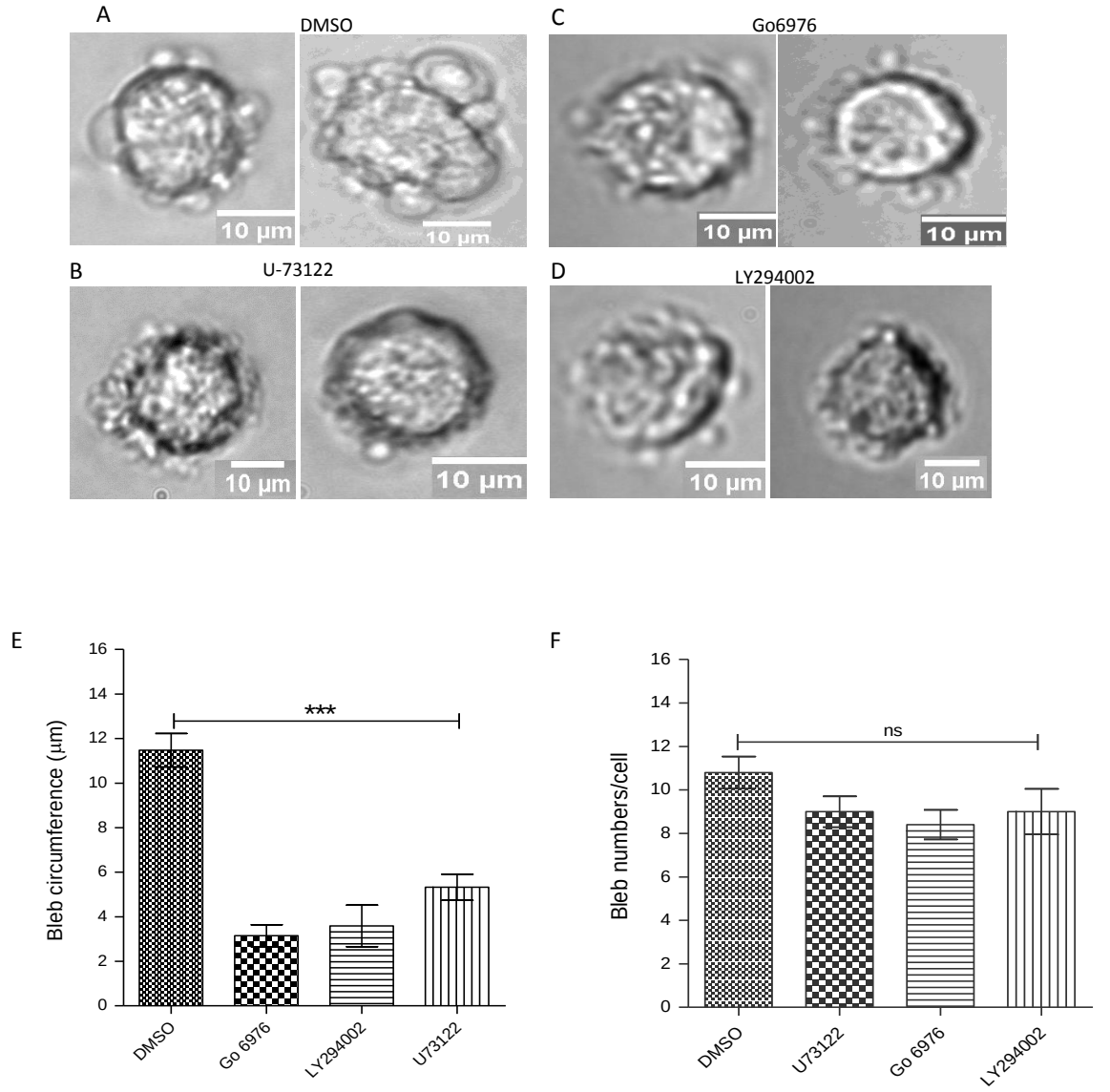

Figure 5.9: inhibition of bleb formation via inhibition of signaling pathways. A. HT-1080 cells embedded in matrigel and treated with BB-94 and PIC in presence of caspase inhibitor before challenging with DMSO; **B.** Pretreatment of blebbing cells with 20 µM PLC inhibitor, U73122 for 30 min; **C.** Pretreatment of cells with 5 µM PKC inhibitor, Go6976; **D.** Inhibition of PI3K pathway with 5 µM LY294002; **E.** Quantification of bleb size in inhibitors treated and vehicle control cells; **F.** Quantification of number of blebs/cell of inhibitors and vehicle control treated HT1080 cells. Data are mean ± SEM of three separate experiments. ***:P < 0.001 using one-way ANOVA followed by Tukey's multiple comparison test. Comparisons are between inhibitors and controls.

5.7 Discussion

In different cell lines, the lipid signaling PLD enzymes are known not only to preserve the architectural integrity of cellular or intracellular membranes, but mediate a plethora of biological processes including cell proliferation, cytoskeletal dynamics, protein trafficking, cell migration and cancer metastasis (Chen et al., 2012; Gomez-Cambronero, 2014). In this chapter, the role of the PLDs in cancer cell blebbing was investigated by first blocking the activities of both isoforms of mammalian phospholipase D, PLD1 and PLD2 by using a small molecule inhibitor, FIPI which has been previously shown to inhibit the activity of the enzymes both in vitro and in vivo (Zouwail et al., 2005). In the present study, it was found that pretreatment with FIPI for 30 min sufficiently suppressed blebbing of ACHN and HT1080 cell lines (figures 5.2a and b). The effects of FIPI in the two cell lines were comparable as the percentage of blebbing cells was drastically brought down to 12.30% and 13% respectively for the HT1080 and ACHN cells as against vehicle treated controls which had 82.95% and 88.25% (figure 5.3). FIPI inhibition of PLD also suppressed bleb numbers and size in both cell lines in a comparable manner. This suggests that either PLD1 or PLD2, or both promote cell blebbing. The mechanism by which FIPI inhibits blebbing of cells via inhibition of PLD1 and PLD2 is not known, but it was previously reported that the drug acts directly to inhibit the phosphodiesterase activity of both PLD1 and PLD2 (Su et al., 2009b)

As FIPI is known to potently inhibit the activity of both PLD isoforms, next, siRNA-mediated gene knockdown was performed using smart pooled small interfering RNAs that were directed against human PLD1 and PLD2, and which target the proteins at four different sequences. Upon gene knockdown, which was confirmed by western blotting, it was observed that treatment of HT1080 cells with PLD1 and PLD2 siRNAs strongly inhibited bleb formation in a manner akin to FIPI treatment as the number of blebs per cell as well as

the size of blebs were comparable in the two different treatments. Furthermore, comparison of the bleb numbers and size between PLD1- and PLD2-deficient HT1080 cells showed no significant difference (figures 5.5d and e), suggesting that these enzymes might probably be regulating bleb formation through a common mechanism. However, it must be stated at this point that, because the ACHN cell line was acquired towards the end of this study, the study ran out of time and resources to investigate PLD knockdown in this cell line. Thus, in future, siRNA-mediated knockdown of the PLDs should be performed on the ACHN cells and perhaps on other cell lines to investigate their roles on blebbing of these cell lines.

As knock down of both PLD1 and PLD2 seemed to negatively regulate cell blebbing, it was anticipated that PLD1 siRNA might be impacting negatively on PLD2 activity and vice versa. The specificity of the siRNAs used was tested in HT1080 cells by probing PLD1 knocked-down samples with anti-PLD2 antibody and vice versa. Immunoblotting with human anti-PLD2 antibody of HT1080 cell lysates in which the activity of PLD1 was knocked down revealed that PLD1 siRNA also down-regulated PLD2 activity (figure 5.6a and b), whereas PLD2 siRNA had no effect on PLD1 activity (figures 5.6c and d), raising the possibility that it was actually PLD2, and not PLD1 that might be involved in bleb formation.

Interaction of PLD2 with different adaptor proteins is known to regulate plasma membrane protrusions. For instance, PLD2 binding to Grb2 has been implicated in formation of plasma membrane ruffles, an event that preceded lamellipodia formation and enhanced cell migration and chemotaxis (Gomez-Cambronero, 2011; Mahankali et al., 2011a). PLD2 promotes phagocytosis through an interaction in which growth receptor bound protein 2 (Grb2) acts as a docking protein between PLD2 and Wiscott-Aldrich syndrome protein (WASP) (Kantonen et al., 2011). Similarly, in a microtubule-dependent manner, formation of membrane protrusions in v-Src-transformed fibroblasts has been attributed to PLD2 (Shen et al., 2002).

Since bleb formation, unlike formation of lamellipodia, filopodia and other membrane protrusions is independent of actin polymerization, it is possible that PLD2 might be signaling to stimulate actomyosin contractility. Whether PLD2 interacts with, and stimulates the activities of aquaporins and ion channels is not known, however, the PLD2 is widely reported to interact with a wide range of other proteins to mediate cancer cell migration (Gomez-Cambronero, 2011).

In an attempt to elucidate the mechanism by which PLD2 promotes cell blebbing, the present study implicated PA, the catalytic product of the lipase reaction of PLD2 and which acts as an intracellular second messenger, as the signaling molecule through which PLD2 could be mediating cell blebbing. Usually, in most biological systems, the intracellular levels of PA is used as a read-out for PLD activity. Although mammalian PLDs could also exert their physiological functions by either signaling through protein-protein interactions or through a unique GEF activity (in the case of PLD2) (Gomez-Cambronero, 2014). On the other hand, the involvement of PLD in most biological processes is detected by use of primary alcohols which are preferentially used instead of water by PLD to generate stable phosphatidylalcohol which unlike PA, is unable to yield DAG and lysophosphatidic acid (LPA), and is also unable to recruit and activate downstream target proteins (Oude Weernink et al., 2007). Thus, in the presence of primary alcohol such as butan-1-ol, PA production is not only blocked, but other downstream signaling events are halted. Indeed, pretreatment of HT1080 and ACHN cells with 1% (v/v) butan-1-ol resulted in a near total loss of membrane blebs (figures 5.7a and b, middle panel) with only 5% and 6% respectively of HT1080 and ACHN cells blebbing (figure 5.7c), whereas pretreatment with same concentration of tertiary butanol had no effect on blebbing of cell (figure 5.7a and b, bottom panel). Butan-1-ol-mediated depletion of PA also significantly suppressed the number of blebs appearing in both cell lines (figure 5.7d).

This suggests that PLD2-mediated cell blebbing is via PA. PA has been previously linked to leucocyte cells migration through regulation of lamellipodia structures and membrane ruffles (Gomez-Cambronero, 2014).

Furthermore, the mechanism as well as the downstream signaling pathway by which PLD2-derived PA promotes cell blebbing was investigated. One possible mechanism could be via the hydrolytic activity of phospholipase A_1 or A_2 (PLA_1/PLA_2) on PA to produce the ubiquitously expressed lysophosphatidic acid (LPA) which binds its receptors (LPAR) at the plasma membrane to trigger downstream effectors (Stoddard and Chun, 2015). LPAR has been reported to be involved in matrix degradation by upregulating MMP activities, cell proliferation, tumour progression and metastasis of different cancers via stimulation of Rho activity to activate ROCK (Gotoh et al., 2012; Jeong et al., 2013; Jeong et al., 2012). Importantly, LPAR has been shown to induce membrane blebbing in osteoclast via the ROCK signaling pathway (Panupinthu et al., 2007). Indeed, inhibition of LPAR with VPC-32183, a potent LPAR inhibitor abrogated bleb formation in both HT1080 and ACHN cell lines. It is worth mentioning that LPA can also be produced by the action of lysophospholipase D (autotaxin) on lysophosphatidylcholine (LPC) which itself is produced from phosphatidylcholine (PC) by PLA_2. Whether this pathway was involved in cell blebbing was not confirmed by the present study. However, it was previously reported that the pathway was not likely to be involved in ATP-induced blebbing of osteoclast as autotaxin is not inhibited by butan-1-ol (Panupinthu et al., 2007). It is also not known whether the GEF activity of PLD2 is involved in its role in cell blebbing.

There is a great deal of cross-talks between PLD signaling and other lipid signaling pathways that regulate cytoskeletal reorganization, cell proliferation, survival and cell migration. One such pathway which is upregulated in most human cancers is the phosphoinositide-3 kinase

(PI3K) pathway that signals via activation of Akt (Weigelt and Downward, 2012) which has been previously reported to be an upstream regulator of PLD activation (Kang et al., 2008a). Indeed, data from the present study revealed significant attenuation of cell blebbing upon treatment of HT1080 cells with the PI3K inhibitor, LY294002. Specifically, inhibition of PI3K pathway resulted in significant reduction of bleb size without a significant effect on bleb numbers. Bleb formation is said to be triggered by Rho recruitment and activation of ROCK which phosphorylates and relieves MLCP of its activity leading to activation of MLCK that phosphorylates MLC thereby resulting in myosin contraction (Charras, 2008). Thus, a role for the Rho-ROCK signaling pathway which is also activated by and signals downstream of LPAR was examined in ACHN and HT1080 cells using the ROCK inhibitor, Y27632. Inhibition of ROCK effectively ablated bleb formation, suggesting the involvement of the LPA-LPAR-Rho-ROCK signaling axis in cell blebbing.

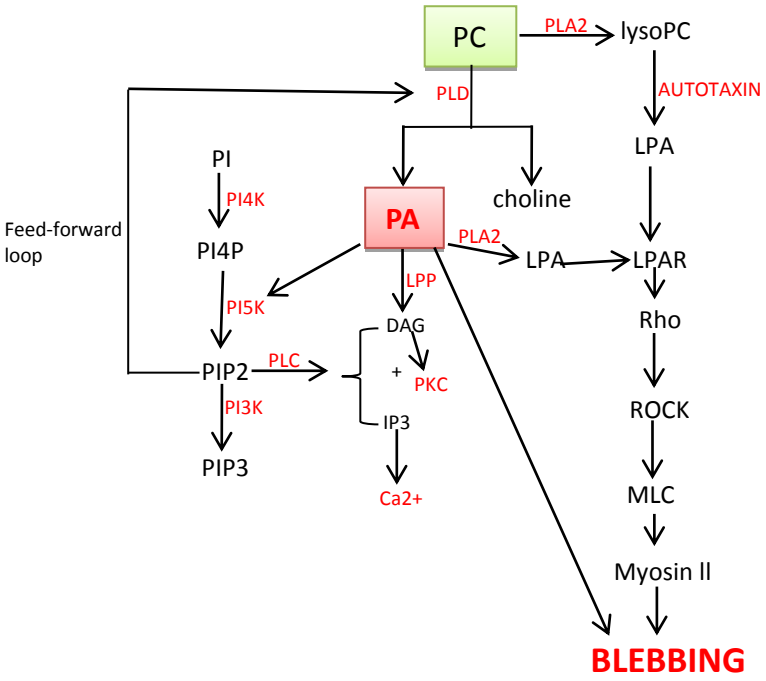

Figure 120: Lipid signaling and blebbing. Membrane phospholipids such as phosphatidylcholine (PC) is hydrolyzed by phospholipase D (PLD) to generate phosphatic acid (PA) and choline. PA could be hydrolyzed either by lipid phosphate phosphohydrolase (LPP) to yield diacylglycerol (DAG) which stimulate PKC activity or by phospholipase A (PLA) to yield lysophosphatidic acid (LPA) which binds its receptor (LPAR) in cell membrane to stimulate the activity of Rho which then activates ROCK, eventually resulting in cell blebbing. PA can stimulate phosphatidylinositol 4-phosphate 5-kinase (PI5K) to generate phosphatidylinositol 4,5-bisphosphate (PIP_2) from phosphatidylinositol 4-phosphate (PI4P aka PIP). PIP_2, through a positive feedback loop can stimulate PLD to generate PA and then cell blebbing. PC can also be partially hydrolyzed by PLA2 to form lysoPC which is acted upon by autotaxin to generate LPA which again binds LPAR to trigger blebbing via the Rho/ROCK axis. On the other hand, PIP_2 could be acted upon by phospholipase C (PLC) to generate DAG which activates PKC and inositol 1,4,5-triphosphate (IP_3) which triggers calcium release from intracellular stores.

Another pathway through which PLD-generated PA could also mediate its biological effects in cells is by stimulating the activity of phosphatidylinositol 4-phosphate 5-kinase (PI4P5K aka PI5K), an enzyme which synthesizes phosphatidylinositol 4,5-bisphosphate (PIP_2) from phosphatidylinositol 4-phosphate (PIP). PIP_2 can on its own right function as a second messenger to trigger signaling cascades, and its signaling effects can be terminated through dephosphorylation by inositol polyphosphate 5-phosphatases such as synaptojanin (Majerus et al., 1999). Interestingly, PIP_2 can act as cofactor to stimulate the activity of PLD through a feed-forward loop, and receptors that increase PLD activity have been reported to upregulate the activity of PLC which is known to regulate PIP_2 levels (Oude Weernink et al., 2007).

Therefore, the contribution of PLC in blebbing of HT1080 cells was investigated with the PLC-specific inhibitor, U73122. Inhibition of PLC activity with U73122 negatively impacted on bleb formation, causing a significant decrease in bleb size, albeit, bleb numbers was not significantly affected when compared to vehicle controls. The observed decrease in bleb size upon inhibition of PI3K and PLC activities were consistent with the fact that inhibiting the activities of these proteins result in accumulation of intracellular PIP_2 levels which not only aid in strengthening the plasma membrane architecture, but also bolsters the membrane-cortex interaction, and hence, prevents membrane detachment and cell blebbing (Ridley, 2011). Previous reports (Klein et al., 2011), in an attempt to give further insight into the molecular interactions between U73122 and PLC isoforms, have shown that U73122 did not inhibit, but rather activates several isoforms of PLC. It will be therefore interesting in future to investigate whether the observed bleb attenuation with U73122 was actually due to PLC inhibition or it was due to inhibition of other proteins. Thus, in future, a critical reevaluation of the use of U73122 as PLC inhibitor is required. It is worth mentioning that attempts by the present study to determine by confocal microscopy whether PIP_2 or/and PIP_3 localize to bleb

membrane by transfecting cells with the PH domain of PLC and Btk respectively yielded no fruitful results as the cells were difficult to transfect with these plasmids.

However, since U73122 suppressed bleb formation, the involvement of PLC was further investigated by blocking the activity of PKC which is stimulated by DAG, one of the byproducts of PLC catalytic breakdown of PIP_2 (Oude Weernink et al., 2007). Therefore, a requirement for DAG-mediated activation of PKC which has been previously reported to function upstream and stimulate PLD activity (Foster and Xu, 2003) in cell blebbing was probed. In a manner similar to PI3K and PLC inhibition, inhibition of PKC with its known inhibitor, Go6976 inhibited cell blebbing, significantly reducing bleb size in HT1080 cell line (figure 5.9e and f). The present study was not able to determine mechanisms by which Go6976 exerts its inhibitory effect on cell blebbing. But PKC has been reported to strengthen the enzymatic activity of PLD1 by physically interacting with it (Park et al., 1998). It might be that Go6976 is interfering with the PLD-PKC association thereby decreasing the activity of the enzyme. As IP_3 released by PLC activity can trigger intracellular calcium release, in future, it will be interesting to test whether calcium ions are involved in the PLC-mediated effect on cancer cell blebbing.

Therefore, the data from this chapter identified PLD2 as a positive regulator of cell blebbing in a mechanism that involves cascade of different downstream signaling molecules. Specifically, this study identified that PA derived from PC by PLD2 lipase activity is hydrolyzed by PLA1/2 to yield LPA which then binds its receptor, LPAR at the plasma membrane. LPAR then stimulates Rho activity which results in activation of ROCK and then MLC to stimulate myosin II activity and contractility, eventually leading to cell blebbing. Thus, a proposed mechanism by which PLD2 promotes cell blebbing is shown below:

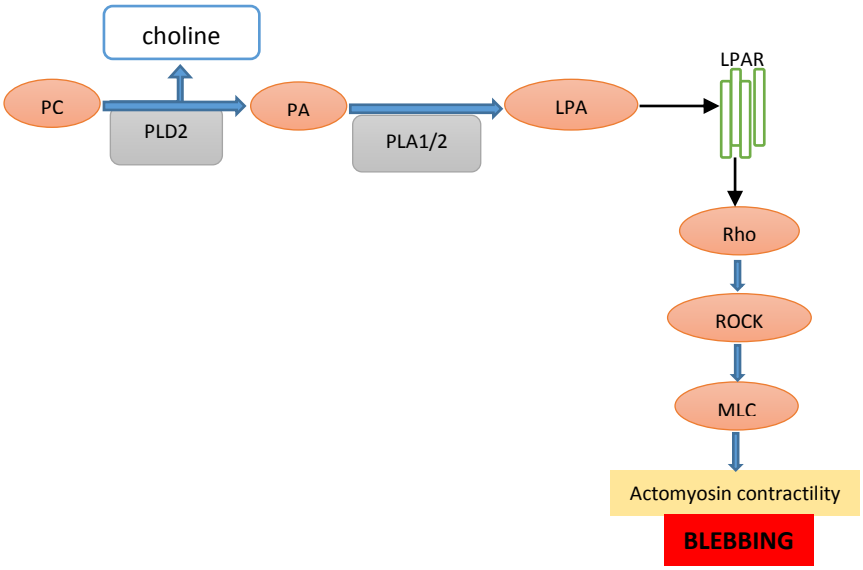

Figure 5.11: Mechanism of PLD2-mediated bleb formation. PLD2 hydrolyze membrane phosphatidylcholine generate choline and phosphatidic acid. The latter is acted upon by either phospholipase A1 or 2 to produce lysophosphatidic acid which binds its receptors at the plasma membrane and then stimulate Rho to activate its substrate, ROCK. Activated ROCK further stimulate myosin II activity inducing actomyosin contractility and subsequently bleb formation.

Chapter 6. General Discussion

Cell migration is a critical biological process required in both physiological and pathophysiological conditions such as immune cell trafficking, embryogenesis and cancer (Blaser et al., 2006; Friedl and Gilmour, 2009; Ridley, 2011). Although cancer cells have been described to possess unlimited replicative potentials as a common feature, the ability of these cells to invade local tissues and migrate to distant sites has made the disease intractable, thereby resulting in death of most cancer patients. Tumour cells could metastasize as a collective functional entity in which the constituent cells are firmly held together by cell-cell and cell-matrix adhesions or as a single unit in the absence of cell-cell junctions. Over the past decades, much considerable research has been investigating the molecular mechanisms underlying cell migration as the basis for cancer metastasis (Friedl et al., 1997; Sanz-Moreno et al., 2008; Schmidt and Friedl, 2010). Much of these works were focused on the mesenchymal mode of cell migration in which cancer cells secrete surface MMPs and proteases in plasma membrane structures such as invadopodia to degrade and migrate through the ECM in an elongated, spindle morphology (Friedl and Wolf, 2010; Lauffenburger and Horwitz, 1996) using lamellipodia and filopodia formed by actin polymerization driven by Rac1 and Cdc42 respectively (Small et al., 2002). Usually, mammalian cell plasma membranes undergo persistent reorganization due to cytoskeletal remodeling resulting from intracellular and extracellular cues (Fackler and Grosse, 2008).

Different attempts at using therapies targeted at these matrix degrading enzymes have not yielded the desired results in combating cancer. It is now known that tumour cells have the ability to switch from the protease-dependent mesenchymal mode of cell migration to an amoeboid mode in which cells migrate through preexisting gaps in the ECM by blebbing which is independent of proteolytic activity (Wolf et al., 2003). Thus, blebbing as an

emerging alternative mode of cell migration has generated interest from different research groups over the past few years. Blebs have been observed in different cell kinds during embryogenesis, mitosis, cell spreading and cell migration; and they are believed to be Rho-ROCK-stimulated actomyosin contractility-mediated plasma membrane protrusions (Charras et al., 2008). At the molecular level, apart from the well-known Rho-ROCK signaling pathway, blebbing has been observed in filamin-deficient M2 cells (Charras et al., 2005), talin-deficient megakaryocytes (Wang et al., 2008), SH4 overexpression in CHO cell line (Tournaviti et al., 2007), and overexpression of FilGAP in MDA-MB-231 cells (Saito et al., 2012). In zebrafish primordial germ cells, the microRNA binding protein, dead end (dnd) promoted myosin contractility and blebbing motility by inhibiting repression of MLCK by miR-430. (Goudarzi et al., 2012). However, it is not known whether transmembrane water and ion channels play a positive role in the blebbing of cancer cells.

Therefore, firstly, the present study investigated the role of the aquaporin water channels which function in mediating water passage across plasma membrane in response to osmotic gradient, and which have been previously implicated in tumourigenesis, in the blebbing of cells. However, before investigating the AQPs in cell blebbing, and because not all cells bleb upon induction, the study screened six different human cancer cell lines by blocking matrix proteolysis with a combination of the general MMP inhibitor, batimastst (BB-94) and protease inhibitor cocktail (PIC), in the presence of caspase inhibitor set V1, an effect that effectively convert cells from an elongated mesenchymal mode of migration into an amoeboid protease-independent blebbing mode (Wolf et al., 2003). Two of these cell lines tested, the human fibrosarcoma HT1080 and human renal adenocarcinoma ACHN cell lines were identified to be blebbing. Although, the activities of caspases were inhibited, it was further confirmed that the blebs were non-apoptotic as the cells were tested to be viable after

treatment with bleb-inducing agents. To further verify that these blebs conformed to the basic principles that have been widely reported to govern normal bleb formation (Charras and Paluch, 2008; Charras, 2008; Charras et al., 2008; Sahai and Marshall, 2003), the present study not only confirmed that the formation of these blebs was mediated by the Rho-ROCK signaling pathway and required myosin II activity for actin cortex contractility, but also confirmed that a weakening of the cortex-membrane linkage is required for formation of these blebs.

Having established the facts that the blebs were normal, healthy blebs in healthy cell lines, the study proceeded to examine the expression of AQP1, AQP3, AQP4 and AQP5, which have been previously implicated in different cancers (Deb et al., 2012; Jung et al., 2011; Lee et al., 2014; Nico and Ribatti, 2010; Papadopoulos and Saadoun, 2014; Saadoun et al., 2002a) in the profusely blebbing HT1080 cells and detected expression of only AQP1 and AQP5 in this cell line. Furthermore, by using western blotting, AQP1, which is the best characterized of all known AQP isoforms was found expressed across the other five different cancer cell lines, with the non-blebbing MDA-MB-231 and A549 cell lines showing highest endogenous expression levels, suggesting that the expression levels of AQP1 does not necessarily confer blebbing capabilities in cells. One possibility is that in the MDA-MB-231 and A549 cells, most of the AQP1 expression could be cytosolic, and that plasma membrane translocation might be required. It could also be that AQP1 is not sufficient and that other regulators are also required, but are absent in these cell lines.

Investigation of the involvement of AQP1 in blebbing by siRNA-mediated gene knockdown revealed that AQP1 promotes blebbing of both HT1080 and ACHN cells as knockdown of protein in HT1080 cells (24 hour post transfection) abrogated bleb formation, and in a similar manner, in the ACHN cell line, AQP1 knockdown occurred 24 hours and persisted up to 48

hours post transfection to give the best knockdown, and this also inhibited blebbing of the cells. Importantly, in the HT1080 cells, it was discovered that blebs started reappearing 48 hours post-AQP1 siRNA transfection, and this paralleled expression of AQP1 protein at this time point as evidenced from western blot analysis. An investigation of the dynamics of blebs reemerging at 48 hour post-AQP1 siRNA transfection and those in wild-type HT1080 cells was performed by taking a detailed analysis of bleb lifespan. It was found that blebs re-emerging after 48 hours had longer lifespan than blebs in wild-type cells due to the longer time it took the former to expand, stabilize and retract their membranes. One possible explanation for this observation could be that although, blebs re-emerged at 48 hour post-AQP1 siRNA transfection, the siRNA treatment negatively impacted on AQP1 activity resulting in a defective water transport mechanism that impeded the rapid influx of water across plasma membrane, an effect that delayed flow of cytosolic fluids into the growing bleb. As actin repolymerization and recruitment of cortex-membrane linker proteins are factors reported to mediate bleb retraction (Charras et al., 2006), the impaired AQP1 activity could also hinder actin repolymerization as well as recruitment of cortex-membrane linker proteins such as the ERM proteins. An important implication of this finding is that impairment of AQP1 activity in blebbing cells will result in longer time to complete the bleb cycle, and so such cells will undergo a slow and awkward blebbing migration, whereas, in wild-type cells where there is faster rate of water and fluid passage, bleb cycle will be completed in a relatively short period of time, and thus, the cells will not only migrate faster, but also become more aggressive and invasive. Consistent with previous reports where AQP1 deficiency resulted in decreased plasma membrane protrusions (Hara-Chikuma and Verkman, 2006), the present study discovered a significant decrease in size and number of blebs after perturbation of AQP1 activity.

The role of AQP1 in cell blebbing was further investigated by transfecting both HT1080 and ACHN cells with a GFP-tagged AQP1 to overexpress the water channel. AQP1 was found clearly localized to bleb membranes, but in the case of HT1080 cells, there was also high intracellular stores of the protein. In accordance with previous reports where transfection of HEK293 and Schwann cells with AQP1 upregulated cell size (Conner et al., 2012; Zhang et al., 2013), in the present study, AQP1 overexpression in both HT1080 and ACHN cell lines significantly increased bleb size with a corresponding decrease in bleb numbers. It would be interesting in future to perform water permeability test to investigate whether the increased bleb size upon AQP1 overexpression correlates with increased water fluxes.

This morphological change in bleb size in response to AQP1 overexpression called for a detailed comparative examination of the blebs in AQP1 transfected cells and blebs in non-transfected wild-type cells. Analysis of AQP1-overexpressing HT1080 cells revealed that AQP1 overexpression significantly reduced bleb lifespan due principally to faster time of bleb retraction as there was no significant difference in expansion and stabilization time of the blebs in wild-type and AQP1 overexpressing cells. A further probe into the speed with which the blebs expanded and retracted their membranes revealed that AQP1 overexpression simultaneously increased bleb expansion and retraction speed. This unexpected novel finding is quite interesting as AQP1 overexpression significantly increased bleb retraction much faster, to an extent that it became significantly faster than bleb expansion which was previously faster in wild-type cells. This novel finding demonstrates that the traditional view and notion of bleb retraction being mediated by actin repolymerization as well as recruitment of cortex-membrane linker proteins may not always be the case, as AQP1 and perhaps other AQPs can function simultaneously to expand a growing bleb by allowing fluid influx, and on the other hand, permitting rapid efflux of fluid out of the bleb to cause retraction.

The mechanism of AQP1-facilitated bleb retraction is not known. Whether AQP1 aids recruitment of actin nucleation factors such as Arp2/3 complex and mDia1, and cortex-membrane linker proteins is yet to be determined. An investigation to monitor the flow of AQP1 in the course of a bleb cycle by quantifying the fluorescence intensities of AQP1 overexpressing HT1080 cells revealed that AQP1 flows and gradually increases right from bleb initiation through the expansion phase and subsequently accumulate to a peak during the retraction phase. Thus, it is not out of place to speculate that the accumulation of AQP1 during the retraction phase might partly explain the unexpected increased faster bleb retraction that was earlier observed. However, further studies need to be done to stain the plasma membrane of AQP1-oversexpressing cells with membrane dyes as this would clearly resolve whether the increased fluorescence intensity during bleb retraction was actually due to AQP1 accumulation or membrane curvature. It is also anticipated that the faster bleb retraction could be due to activity of transmembrane ion channels.

To further explore the effects of AQP1 overexpression in cancer cell blebbing, I took advantage of the observed morphological increase in bleb size upon AQP1 overexpression, coupled with previous reports that aquaporins can induce formation of plasma membrane protrusions such as filopodia (Loitto et al., 2007), on non blebbing MDA-MB-231 breast cancer cells. In this cell line, a high endogenous expression of AQP1 was found by western blotting, yet they do not bleb. When embedded in 3D matrices, they only possess tiny, spike-like membrane protrusion. However, AQP1 overexpression effectively induced a blebbing phenotype in this cell line, further confirming that AQP1 could promote cell migration in the extracellular matrix. Whether AQP1 can induce bleb formation in other non-blebbing cells, or whether the effect is cell type-specific, is yet to be addressed.

From the perspective of cell migration on flat surfaces, AQP1 involvement in lamellipodial-based cell migration on 2D was examined by performing the famous wound healing assay by making a scratch along cells treated with either AQP1 siRNA, scramble siRNA or untreated controls. It was discovered that AQP1 knockdown by siRNA at 24 hours significantly reduced the ability of the cells to migrate and fill up the scratched wound. This ability of AQP1 to increase cell migration has been attributed to its ability to facilitate lamellipodia formation by mediating actin polymerization at the leading edge of migrating cells (Papadopoulos and Saadoun, 2014)

The present study did identify differential regulation of cell blebbing by different aquaporin isoforms in that siRNA-mediated knockdown of AQP5 which was earlier detected by both western blotting and immunostaining to be expressed in the HT1080 cells had no effect on cell blebbing as neither bleb size nor bleb number was significantly altered. AQP5 has been implicated in cell migration, cell proliferation as well as in different human cancers such as breast, colorectal and lung cancers (Chae et al., 2008; Kang et al., 2008b; Zhang et al., 2010). Why AQP5 appeared to have no apparent effect on cell blebbing is not known. However, one possibility is that the amount of the protein left after knockdown might be still sufficient to perform the normal functions of the protein, in which case a complete knockout of the gene might be required. The protein has been also reported to bind SH3 domain of c-Src to effect downstream intracellular signaling and promote tumourigenesis (Chae et al., 2008). Whether this is an absolute requirement for the protein to perform its functions is not clear, if that is the case, it then implies that the cells might not express SH3 domain of c-Src. Another possible explanation is that AQP5 could function in a cell-type specific manner.

The actual mechanisms by which the aquaporins regulate cell blebbing is not understood, however, a novel finding from this study revealed that AQP1 regulate cell blebbing by

simultaneously facilitating bleb expansion and retraction. For this to occur, a possible involvement of transmembrane ion channels was anticipated. One of such ion channels recently implicated to have a polarized distribution along with the AQPs in tumour cells to mediate water and ion fluxes across the membrane to facilitate cell migration, was the Na^+/H^+ pump (NHE) (Stroka et al., 2014). Normally, Na^+ influx into the cell by this pump is expected to be accompanied by obligated water inflow through AQP1 and this leads to an increase in cytoplasmic pressure to drive bleb expansion. Strangely and interestingly, the present study identified a requirement for the Na^+/H^+ pump in AQP1-facilitated bleb retraction as blockage of Na^+ influx and proton extrusion by inhibiting activity of the antiporter with its known general inhibitor, EIPA completely blocked bleb retraction as well as formation of new blebs in both HT1080 and ACHN cell lines. Cells were found continuously expanding up to 90 minutes (maximum pre-incubation time) without any observable bleb retraction. This suggests that extracellular acidification as well as intracellular alkalinization due to increased intracellular pH could facilitate not only actin polymerization, but recruitment of ERM proteins required for bleb retraction.

Since NHE1 is the best characterized, and known to be mediator of most biological processes of the nine known human NHE isoforms, the present study investigated this isoform. NHE1 was found expressed in both cell lines, and it was found localized to intracellular vesicles rather than bleb membranes. However, other studies have previously reported localization of NHE1 to the bleb membranes of CHO cells overexpressing integrin$_{\alpha IIb}$ and integrin$_{\beta 3}$ ($CHO_{\alpha IIb\beta 3}$) (Yi et al., 2012). This discrepancy is attributable to signaling events downstream of ($CHO_{\alpha IIb\beta 3}$) which targets NHE to the plasma membrane. The effect of EIPA on blebbing is unlikely due to inhibition of NHE1 as blocking the activity of NHE1 with two drugs, zoniporide and cariporide which have been reported to specifically and potently block NHE1

activity (Gao et al., 2011; Harguindey et al., 2013) failed to halt bleb retraction as blebs in both cell lines were dynamically expanding and retracting. Although, the present study was unable to investigate some of the other NHE isoforms due to unavailability of specific inhibitors, and because the study was also out of time and resources, it is obvious the Na^+/H^+ pump is involved in AQP1-facilitated bleb retraction. A possible mechanism speculated is via acid signaling where extracellular acidosis due to proton accumulation (reduced pH) activates plasma membrane acid-sensing ion channels (ASICs) which then triggers increase in Ca^{2+} from intracellular pools, and release of Ca^{2+} through activated NCX1 causes bleb retraction by either mediating actin polymerization or recruiting the ERM proteins. Similarly, intracellular alkalosis activates pH-sensitive cytoskeletal proteins such as talin to stimulate actin filaments polymerization as well as rapid water efflux from the bleb. One future direction here is to further investigate the actual mechanism by which both ASICs and other cytoskeletal proteins could mediate bleb retraction. Also, a further probe of NHE1 and other NHE isoforms with use of specific siRNAs directed against them will be required.

As NHEs requirement in AQP1-mediated bleb retraction could also be through generation of pH gradient, this study examined effects of modulating extracellular pH on bleb morphology in 3D matrigel matrix. Incubation of HT1080 cells in pH 5.5-9.0 resulted only in a decrease in bleb size which was not significant when compared to control, whereas in ACHN cells, a decrease in bleb size was only found at pH 5.5-6.5. However, once again, addition of EIPA in all different pH conditions in both cell lines resulted in bleb expansion without any observable retraction. This continuous bleb expansion might be attributed to the increased intracellular acidosis arising from accumulation of protons which have been reported to be involved in formation of membrane protrusions, enhanced invasive capacities and cell migration (Lagana et al., 2000; Paradiso et al., 2004). Furthermore, since EIPA was reported

to also inhibit the activity of the Ca^{2+}-activated cation channel, TRPP3 channel, the role of this channel was investigated by blocking its activity with phenamil, a TRPP3 channel selective inhibitor. In a manner similar to cariporide and zoniporide inhibition, use of different doses of phenamil showed no obvious inhibition of bleb retraction in both cell lines, ruling out the suspicion that the effect of EIPA inhibition was due to TRPP3 channel inhibition.

To further investigate the involvement of Na^+ influx in cell blebbing, the activity of NKCC1, which permits the cotransport of Na^+, K^+ and Cl^- was inhibited with the loop diuretic, bumetanide (BMT). Dose-dependent and cell-type specific effects were observed with the use of this drug. In HT1080 cells, use of 10 µM BMT induced significant increase in bleb size which remained stable across the different concentrations used up to maximum 100 µM; whereas in the ACHN cells, a stable dose-dependent significant increase in bleb size was found between 10 µM and 20 µM of BMT treatment. Another steady increase in bleb size occurred between 50 µM and 70 µM. Then another increase in bleb size occurred at the maximum dosage of 100 µM. To answer the question whether these blebs behaved like those in wild-type cells, a detailed analysis of bleb dynamics revealed that NKCC1 inhibition increased bleb lifespan in both cell lines, and this was in the case of the HT1080 cell line attributed to the prolonged increase in bleb retraction time, whereas in the ACHN cell line it was due to BMT-mediated increase in both bleb expansion and retraction time. It would be interesting in future to investigate the specific roles of K^+ and Cl^- ions in cell blebbing, which is also regulated by cell volume increase and swelling.

In mammalian tissues, cell swelling usually activates the volume-regulated anion channels (VRAC) to induce regulatory volume decrease (RVD). Thus, it was anticipated that VRAC could play a potential role in the AQP1-facilitated bleb retraction. Inhibition of cells with

DCPIB, a VRAC selective inhibitor could not shut bleb retraction as was observed with EIPA. However, there was significant increase in bleb size. Thus, it is obvious that cellular bleb formation is a process regulated by different plasma membrane ion transporters either acting alone or cooperating with AQPs, and these interactions could apparently impinge on plasma membrane architecture via perturbation of membrane lipid signaling molecules.

One of such membrane lipid signaling enzymes which is ubiquitously expressed in mammalian tissues is PLD. Specific cellular processes have been previously ascribed to the lipid signaling PLD isoforms, and they mediate these processes through one of three mechanisms: through their lipid-hydrolyzing lipase activity mediated through PA; through protein-protein interaction, or through their GEF activity in case of PLD2 (Gomez-Cambronero, 2014). For instance, actin reorganization, membrane trafficking, cell adhesion, tumour growth and metastasis have been attributed to the activities of the mammalian PLD1 (Chen et al., 2012; Selvy et al., 2011; Zouwail et al., 2005), whereas PLD2 has been shown to mediate cell spreading, endocytosis, cell growth, cell migration by acting as GEF to RhoA and Rac1, invasion and metastasis in lymphoma cells (Du et al., 2004; Henkels et al., 2013b; Jeon et al., 2011; Mahankali et al., 2011b; Zheng et al., 2006). Whereas PLD1 is known to have low basal activity which increases upon external stimulation, and localizes to perinuclear structures and golgi apparatus and endoplasmic reticulum; PLD2 has a higher basal activity and exclusively localizes to plasma membranes (Chen and Exton, 2004).

Therefore, this study started investigation of the involvement of the PLDs through pharmacological inhibition of the enzymes using FIPI, a potent inhibitor of both isoforms of PLD in vitro and in vivo (Chen et al., 2012). This drug inhibited bleb formation in both cell lines. Similar results were obtained when both PD1 and PLD2 were knocked down with specific siRNAs that targets the proteins from four different sequences. The inhibition of

blebbing by knockdown of both isoforms raised the question whether the siRNAs were specific to each isoforms. Determination of the specificity of the siRNAs identified PLD2 as being responsible for bleb formation as immunoblotting with human anti-PLD2 antibody of cell lysates in which the activity of PLD1 was knocked down revealed that PLD1 siRNA also negatively impacted on PLD2, whereas PLD2 siRNA has no effect on PLD1. It is worthy of note that this observation does not rule out the possibility that PLD1 could also regulate cell blebbing, as use of more PLD1-specific siRNA or gene knock out is required.

As most PLD-mediated cellular processes are through PA, the possibility of PLD2 signaling via this lipid second messenger in blebbing was tested with primary alcohol. Indeed, this report found that regulation of cell blebbing by PLD2 was through its enzymatic production of PA as inhibition of PA production with the primary alcohol, butan-1-ol ablated bleb formation. The present study investigated the mechanism of PA and its downstream signaling, and found that PLD2-derived PA mediates cell blebbing through LPA in the LPAR-Rho-ROCK-MLC signaling axis as pharmacological inhibition of this pathway strongly inhibited bleb formation in both HT1080 and ACHN cell lines. Interestingly, in a manner independent of its lipase activity, PLD2 has been reported to directly interact with and activate RhoA activity in HEK293 cells (Jeon et al., 2011). This further corroborates the finding that PLD2-derived PA via its product LPA, mediates bleb formation through the LPAR-Rho-ROCK signaling pathway. It was also reported that PLD-derived PA can interact with all PI5K isoforms to stimulate their activity thereby increasing cellular PIP_2 pool that regulate PLD activity via a feedback loop (Oude Weernink et al., 2007). PLD2 can act as a GEF, and as an upstream regulator of the small GTPase Rac1 to mediate membrane ruffling, and in this process, PA production was said to be necessary, but not sufficient for membrane ruffle formation (Mahankali et al., 2011a). Thus, it is unlikely that the GEF activity of PLD2

is required for bleb formation since increased Rac activity positively regulates lamellipodia formation, and is inversely correlated with actomyosin contractility and bleb formation (Sanz-Moreno et al., 2008).

The contribution of lipid signaling to cell blebbing was further assessed by probing key lipid signaling molecules. Cellular PIP_2 pool is regulated by PLC to yield DAG and IP_3 which activates PKC and intracellular Ca^{2+} release respectively. Similarly, PIP_2 can also be regulated by the activity of PI3K to generate PIP_3. PIP_2 levels usually bolsters the interaction between the plasma membrane and the cytoskeleton, and it also strengthens the activity of the ERM proteins. Consistent with this, depletion of PIP_2 levels enhanced fixation-induced blebbing of human umbilical vein endothelial cells (HUVEC) (Zhao et al., 2014). In the present study, accumulation of cellular PIP_2 levels by using U73122 and LY294002 to inhibit PLC and PI3K activities respectively, significantly suppressed the sizes of blebs formed in HT1080 cells, without any significant effect on bleb numbers. PKC has been previously shown to activate PLD2 activity (Foster and Xu, 2003). Inhibition of this kinase with Go6976 had similar effect as use of U73122 and LY294002. This again demonstrates that, cell blebbing is a complex cascade of events regulated by most of the numerous plasma membrane lipids and pathways that maintain the architectural integrity of the cell.

6.1 Proposed water and ion flow model of bleb regulation

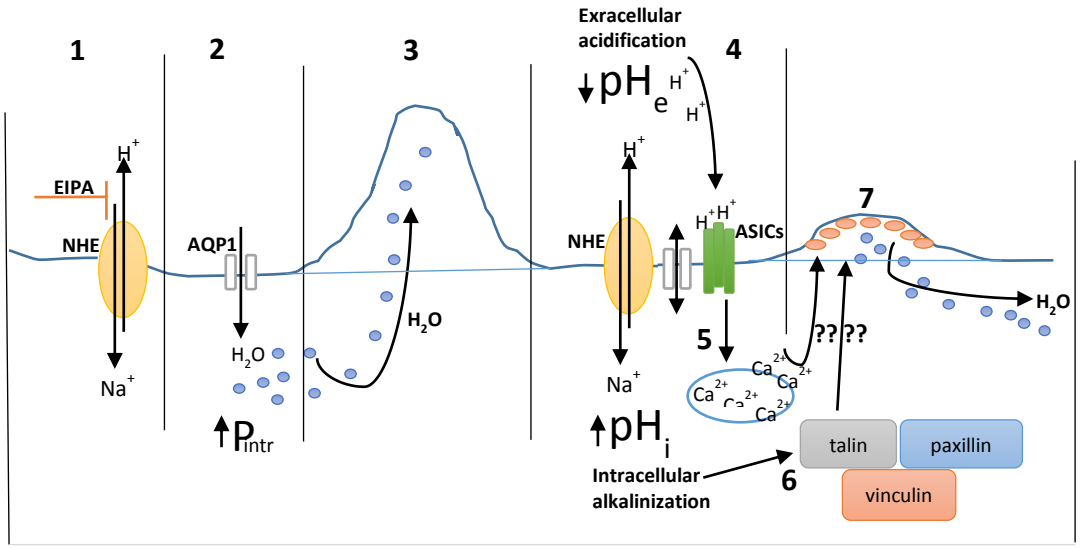

water Membrane-cortex linker proteins

Figure 6.1: Water and ion flow model of bleb regulation: 1. Influx of Na^+ through NHEs results in, **2.** influx of obligated water through AQP1 resulting in increased cytoplasmic pressure P_{intr}, **3.** The increased P_{intr} causes inflow of cytosolic water and fluids into a growing bleb thereby causing bleb expansion; **4.** pH gradient generated by Na^+/H^+ pump leads to extracellular acidosis (reduced extracellular pH) resulting in activation of plasma membrane acid-sensing ion channels (ASICs); **5.** Activated ASICs triggers release of Ca^{2+} from intracellular stores, and subsequent extrusion of Ca^{2+} via NCX1 facilitates actin polymerization resulting in bleb retraction. Similarly, intracellular alkalinization due to pH gradient generated by NHE could also leads to activation of pH-sensitive cytoskeletal proteins such as talin; **6.** Activated cytoskeletal proteins through unknown mechanisms stimulates recruitment of actin nucleation factors and other membrane-cortex proteins resulting in water outflow and bleb retraction.

Chapter 7. Conclusions and Future Directions

7.1 Final Conclusions

This study took an investigation into blebbing of cells in the extracellular matrix. Different studies have been conducted in the recent past to decipher the mechanisms underlying bleb-based migration. Although, some molecular mechanisms and signaling pathways have been postulated to mediate blebbing of cells, however, how blebbing is regulated in the ECM is not clearly understood. Therefore, the present study utilized 3D matrigel matrix as an in vitro model of the ECM, and investigated how bleb formation in cancer cells is regulated by the aquaporin water channels, transmembrane ion transporters and lipid signaling molecules. From the data presented in this study, it could be concluded that AQP1 promotes bleb formation as siRNA-mediated knockdown of the protein ablated cell blebbing, and that impairment of AQP1 activity increases bleb lifespan due to increased time of bleb expansion and retraction. AQP1 localizes to membrane blebs and its overexpression results in enlarged blebs that have relatively shorter lifespan due to much faster bleb retraction as compared to control blebs. This is consistent with the finding that AQP1 level accumulates to a peak during the retraction phase of bleb cycle. It is interesting to note that the endogenous expression level of AQP1 does not necessarily correlates with the capability of a cell to bleb. However, overexpression of AQP1 is sufficient to induce blebbing phenotype in non-blebbing cancer cell lines. As previously reported (Papadopoulos and Saadoun, 2014), AQP1 is involved in the lamellipodial-based, mesenchymal mode of cell migration as knockdown of the protein reduced migration of cells to cover up a scratched wound on flat surface. Moreover, there exists a differential regulation of blebbing by AQP isoforms as knockdown of AQP5 had no effect on cancer cell blebbing.

The novel discovery of AQP1 regulation of cell blebbing by increasing bleb retraction requires the activity of the Na^+/H^+ pump. Reduction in extracellular pH (extracellular acidosis) due to proton extrusion by the Na^+/H+ pump possibly activates plasma membrane acid-sensing ion channels (ASICs) which trigger calcium release from intracellular pools, and the subsequent efflux of Ca^{2+} via the NCX1 facilitates bleb retraction by causing rapid water outflow from the blebs through AQP1, or/and by stimulating actin nucleation factors as well as assembling the ERM proteins. Also, Na^+ influx could directly activate the NCX1 and then trigger Ca^{2+} to facilitate bleb retraction as explained above. On the other hand, accumulation of intracellular proton (intracellular acidification) due to inhibition of the Na^+/H^+ pump is thought to activate and disrupt interactions of cytoskeletal proteins like talin thereby causing rapid inflow of fluid and water through AQP1 resulting in continuous bleb expansion without any observable retraction. NHE1 localizes to intracellular vesicles, and that different Na^+ and other ion transporting channels such as the NKCC1 and VRAC are involved in regulation of blebbing.

Furthermore, the present study identified the lipid signaling PLD2 as a positive regulator of bleb formation. A proposed molecular mechanism for the PLD2-promoted cell blebbing is that the byproduct of PLD2 lipase action, phosphatidic acid PA, a versatile intracellular second messenger, is acted upon by phospholipase 2 (PLA_2) to produce lysophosphatidic acid LPA, another second messenger that binds its receptor, LPAR at plasma membranes. LPAR then stimulates Rho which in turn activates its downstream effector ROCK to phosphorylate and activate MLC to increase actomyosin contractility resulting in cell blebbing. Also, it was found that different modulators of membrane phospholipids level such as PLC, PI3K and PKC regulate bleb formation in cancer.

Therefore, the overall conclusion from this study is summarized as the 'water and ionic flow model' of cell blebbing (figure 6.1) which proposes that influx of obligated water through AQP1 due to influx of Na^+ into the cell by the Na^+/H^+ pump results in increased cytoplasmic pressure which leads to the subsequent flow of cytosolic fluids and water into a nucleated bleb thereby causing bleb expansion. On the other hand, extracellular acidosis (reduced pH) due to increased H^+ extrusion by the Na^+/H^+ pump activates plasma membrane acid-sensing ion channels (ASICs) to trigger increase of intracellular Ca^{2+} and their release through the NCX1, a process that facilitates actin filaments polymerization and subsequent retraction of blebs. Also, intracellular alkalinization due to pH gradient generated by proton and Na^+ fluxes activates pH-sensitive cytoskeletal proteins such as talin through mechanism(s) not yet known, and this then stimulates recruitment of actin nucleation factors and other membrane-cortex linker proteins which eventually results in rapid bleb retraction.

7.2 Future Directions

7.2.1 Aquaporins

This study investigated and identified AQP1 as a critical regulator of blebbing in the ECM. Specifically, overexpression of the protein resulted in increased bleb sizes, however, it is not known whether this increase in bleb size upon AQP1 overexpression correlates with increased membrane water permeability. Therefore, it would be interesting to perform water permeability measurement by using the calcein fluorescence quenching technique in which AQP1-transfected cells are loaded with calcein after which cells are subjected to osmotic challenges on a closed perfusion chamber in a microscope stage. Also more work is required to determine whether the accumulated fluorescence intensity observed during bleb retraction

monitoring AQP1 flow at the different phases of the bleb cycle by confocal microscopy was actually due to AQP1 accumulation or due to membrane curvature and thickening as the blebs retract. This could be achieved by labelling cells with plasma membrane dyes such as FM 4-64FX and CellMask Orange plasma membrane stains (Invitrogen) which will clearly distinguish the outer plasma membrane from blebs. It is also important to repeat AQP5 siRNA in the ACHN cell line as this will resolve whether AQP5 is not actually involved in cell blebbing or it regulates blebbing in a cell type-specific manner. Finally, it would be also interesting to determine by q-PCR the expression profile of all known thirteen AQP isoforms in the blebbing cells.

7.2.2 Ion channels

The actual mechanism(s) by which AQP1 facilitates bleb retraction is not clear, but data from this report implicated a requirement for Na^+/H^+ pump activity as inhibition of this antiporter inhibited bleb retraction. Almost all reported biological processes by the NHEs are mediated by NHE1, however, blocking the activity of this isoform with two known selective inhibitors, cariporide and zoniporide could not inhibit bleb retraction. Thus, before completely ruling out NHE1, it would be interesting to knockdown the gene by siRNA. Obviously, knockdown of some of the other isoforms is also required. The mechanism of the involvement of the NHEs in AQP1-facilitated bleb retraction requires further investigation to unravel whether influx of Na^+ with the accompanying increase in intracellular pH activate cytoskeletal and membrane proteins critical for bleb formation. How extracellular acidosis activates plasma membrane ASICs in the first place, and how activated ASICs further trigger intracellular signaling to regulate blebbing requires investigation. Immunoprecipitation and pulldown assays will be required to determine any kind of physical interaction between the AQPs and Na^+/H^+ pump

as well as with other Na^+ channels. It is also expedient to examine the role of Ca^{2+} by investigating the sodium-calcium exchanger 1 (NCX1) which regulates Ca^{2+} level in cells.

7.2.3 Lipid Signaling

As PLD siRNA knockdown was done on only the HT1080 cells, it is essential to repeat the experiment in future with the ACHN cell, and possibly with other blebbing cell lines. Similarly, it would be interesting to determine whether PIP_2 and PIP_3 are localize to bleb membranes.

References

Adamski, F.M., Timms, K.M., and Shieh, B.H. (1999). A unique isoform of phospholipase Cbeta4 highly expressed in the cerebellum and eye. Biochimica et biophysica acta *1444*, 55-60.

Aharonovitz, O., Zaun, H.C., Balla, T., York, J.D., Orlowski, J., and Grinstein, S. (2000). Intracellular pH regulation by Na(+)/H(+) exchange requires phosphatidylinositol 4,5-bisphosphate. The Journal of cell biology *150*, 213-224.

Algrain, M., Turunen, O., Vaheri, A., Louvard, D., and Arpin, M. (1993). Ezrin contains cytoskeleton and membrane binding domains accounting for its proposed role as a membrane-cytoskeletal linker. The Journal of cell biology *120*, 129-139.

Amith, S.R., and Fliegel, L. (2013). Regulation of the Na+/H+ Exchanger (NHE1) in Breast Cancer Metastasis. Cancer research *73*, 1259-1264.

Arpin, M., Chirivino, D., Naba, A., and Zwaenepoel, I. (2011). Emerging role for ERM proteins in cell adhesion and migration. Cell adhesion & migration *5*, 199-206.

Baeriswyl, V., and Christofori, G. (2009). The angiogenic switch in carcinogenesis. Seminars in cancer biology *19*, 329-337.

Barret, C., Roy, C., Montcourrier, P., Mangeat, P., and Niggli, V. (2000). Mutagenesis of the phosphatidylinositol 4,5-bisphosphate (PIP(2)) binding site in the NH(2)-terminal domain of ezrin correlates with its altered cellular distribution. The Journal of cell biology *151*, 1067-1080.

Barros, L.F., Kanaseki, T., Sabirov, R., Morishima, S., Castro, J., Bittner, C.X., Maeno, E., Ando-Akatsuka, Y., and Okada, Y. (2003). Apoptotic and necrotic blebs in epithelial cells display similar neck diameters but different kinase dependency. Cell death and differentiation *10*, 687-697.

Baumgartner, M., Patel, H., and Barber, D.L. (2004). Na(+)/H(+) exchanger NHE1 as plasma membrane scaffold in the assembly of signaling complexes. American journal of physiology Cell physiology *287*, C844-850.

Becchetti, A., and Arcangeli, A. (2010). Integrins and ion channels in cell migration: implications for neuronal development, wound healing and metastatic spread. Advances in experimental medicine and biology *674*, 107-123.

Becchetti, A., Munaron, L., and Arcangeli, A. (2013). The role of ion channels and transporters in cell proliferation and cancer. Frontiers in physiology *4*, 312.

Belbin, T.J., Singh, B., Smith, R.V., Socci, N.D., Wreesmann, V.B., Sanchez-Carbayo, M., Masterson, J., Patel, S., Cordon-Cardo, C., Prystowsky, M.B., *et al.* (2005). Molecular profiling of tumor progression in head and neck cancer. Archives of otolaryngology--head & neck surgery *131*, 10-18.

Belge, H., and Devuyst, O. (2006). Aquaporin-1--a water channel on the move. Nephrology, dialysis, transplantation : official publication of the European Dialysis and Transplant Association - European Renal Association *21*, 2069-2071.

Belvindrah, R., Hankel, S., Walker, J., Patton, B.L., and Muller, U. (2007). Beta1 integrins control the formation of cell chains in the adult rostral migratory stream. The Journal of neuroscience : the official journal of the Society for Neuroscience *27*, 2704-2717.

Bereiter-Hahn, J., Luck, M., Miebach, T., Stelzer, H.K., and Voth, M. (1990). Spreading of trypsinized cells: cytoskeletal dynamics and energy requirements. Journal of cell science *96 (Pt 1)*, 171-188.

Bhowmick, N.A., Neilson, E.G., and Moses, H.L. (2004). Stromal fibroblasts in cancer initiation and progression. Nature *432*, 332-337.

Bisi, S., Disanza, A., Malinverno, C., Frittoli, E., Palamidessi, A., and Scita, G. (2013). Membrane and actin dynamics interplay at lamellipodia leading edge. Current opinion in cell biology *25*, 565-573.

Blaser, H., Reichman-Fried, M., Castanon, I., Dumstrei, K., Marlow, F.L., Kawakami, K., Solnica-Krezel, L., Heisenberg, C.P., and Raz, E. (2006). Migration of zebrafish primordial germ cells: a role for myosin contraction and cytoplasmic flow. Developmental cell *11*, 613-627.

Bonilha, V.L. (2007). Focus on molecules: ezrin. Experimental eye research *84*, 613-614.

Boucrot, E., and Kirchhausen, T. (2007). Endosomal recycling controls plasma membrane area during mitosis. Proceedings of the National Academy of Sciences of the United States of America *104*, 7939-7944.

Bourguignon, L.Y., Singleton, P.A., Diedrich, F., Stern, R., and Gilad, E. (2004). CD44 interaction with Na+-H+ exchanger (NHE1) creates acidic microenvironments leading to hyaluronidase-2 and cathepsin B activation and breast tumor cell invasion. The Journal of biological chemistry *279*, 26991-27007.

Bovellan, M., Fritzsche, M., Stevens, C., and Charras, G. (2010). Death-associated protein kinase (DAPK) and signal transduction: blebbing in programmed cell death. The FEBS journal *277*, 58-65.

Bowens, N.H., Dohare, P., Kuo, Y.H., and Mongin, A.A. (2013). DCPIB, the proposed selective blocker of volume-regulated anion channels, inhibits several glutamate transport pathways in glial cells. Molecular pharmacology *83*, 22-32.

Brabletz, T., Jung, A., Reu, S., Porzner, M., Hlubek, F., Kunz-Schughart, L.A., Knuechel, R., and Kirchner, T. (2001). Variable beta-catenin expression in colorectal cancers indicates tumor progression driven by the tumor environment. Proceedings of the National Academy of Sciences of the United States of America *98*, 10356-10361.

Bravo-Cordero, J.J., Magalhaes, M.A., Eddy, R.J., Hodgson, L., and Condeelis, J. (2013). Functions of cofilin in cell locomotion and invasion. Nature reviews Molecular cell biology *14*, 405-415.

Bretscher, A. (1999). Regulation of cortical structure by the ezrin-radixin-moesin protein family. Current opinion in cell biology *11*, 109-116.

Brisson, L., Gillet, L., Calaghan, S., Besson, P., Le Guennec, J.Y., Roger, S., and Gore, J. (2011). Na(V)1.5 enhances breast cancer cell invasiveness by increasing NHE1-dependent H(+) efflux in caveolae. Oncogene *30*, 2070-2076.

Brooks, S.A., Lomax-Browne, H.J., Carter, T.M., Kinch, C.E., and Hall, D.M. (2010). Molecular interactions in cancer cell metastasis. Acta Histochem *112*, 3-25.

Bryan, T.M., and Cech, T.R. (1999). Telomerase and the maintenance of chromosome ends. Current opinion in cell biology *11*, 318-324.

Burkhart, D.L., and Sage, J. (2008). Cellular mechanisms of tumour suppression by the retinoblastoma gene. Nature reviews Cancer *8*, 671-682.

Burton, K., and Taylor, D.L. (1997). Traction forces of cytokinesis measured with optically modified elastic substrata. Nature *385*, 450-454.

Busco, G., Cardone, R.A., Greco, M.R., Bellizzi, A., Colella, M., Antelmi, E., Mancini, M.T., Dell'Aquila, M.E., Casavola, V., Paradiso, A., *et al.* (2010). NHE1 promotes invadopodial ECM proteolysis through acidification of the peri-invadopodial space. FASEB journal : official publication of the Federation of American Societies for Experimental Biology *24*, 3903-3915.

Cao, C., Sun, Y., Healey, S., Bi, Z., Hu, G., Wan, S., Kouttab, N., Chu, W., and Wan, Y. (2006). EGFR-mediated expression of aquaporin-3 is involved in human skin fibroblast migration. The Biochemical journal *400*, 225-234.

Cao, J.X., Koop, B.F., and Upton, C. (1997). A human homolog of the vaccinia virus HindIII K4L gene is a member of the phospholipase D superfamily. Virus research *48*, 11-18.

Carbrey, J.M., Gorelick-Feldman, D.A., Kozono, D., Praetorius, J., Nielsen, S., and Agre, P. (2003). Aquaglyceroporin AQP9: solute permeation and metabolic control of expression in liver. Proceedings of the National Academy of Sciences of the United States of America *100*, 2945-2950.

Carbrey, J.M., Song, L., Zhou, Y., Yoshinaga, M., Rojek, A., Wang, Y., Liu, Y., Lujan, H.L., DiCarlo, S.E., Nielsen, S., *et al.* (2009). Reduced arsenic clearance and increased toxicity in aquaglyceroporin-9-null mice. Proceedings of the National Academy of Sciences of the United States of America *106*, 15956-15960.

Cardone, R.A., Bellizzi, A., Busco, G., Weinman, E.J., Dell'Aquila, M.E., Casavola, V., Azzariti, A., Mangia, A., Paradiso, A., and Reshkin, S.J. (2007). The NHERF1 PDZ2 domain regulates PKA-RhoA-p38-mediated NHE1 activation and invasion in breast tumor cells. Molecular biology of the cell *18*, 1768-1780.

Cardone, R.A., Casavola, V., and Reshkin, S.J. (2005). The role of disturbed pH dynamics and the Na+/H+ exchanger in metastasis. Nature reviews Cancer *5*, 786-795.

Chae, Y.K., Woo, J., Kim, M.J., Kang, S.K., Kim, M.S., Lee, J., Lee, S.K., Gong, G., Kim, Y.H., Soria, J.C., *et al.* (2008). Expression of aquaporin 5 (AQP5) promotes tumor invasion in human non small cell lung cancer. PloS one *3*, e2162.

Chambers, A.F., Groom, A.C., and MacDonald, I.C. (2002). Dissemination and growth of cancer cells in metastatic sites. Nature reviews Cancer *2*, 563-572.

Chan, K.T., Bennin, D.A., and Huttenlocher, A. (2010). Regulation of adhesion dynamics by calpain-mediated proteolysis of focal adhesion kinase (FAK). The Journal of biological chemistry *285*, 11418-11426.

Charras, G., and Paluch, E. (2008). Blebs lead the way: how to migrate without lamellipodia. Nature reviews Molecular cell biology *9*, 730-736.

Charras, G.T. (2008). A short history of blebbing. Journal of microscopy *231*, 466-478.

Charras, G.T., Coughlin, M., Mitchison, T.J., and Mahadevan, L. (2008). Life and times of a cellular bleb. Biophysical journal *94*, 1836-1853.

Charras, G.T., Hu, C.K., Coughlin, M., and Mitchison, T.J. (2006). Reassembly of contractile actin cortex in cell blebs. The Journal of cell biology *175*, 477-490.

Charras, G.T., Yarrow, J.C., Horton, M.A., Mahadevan, L., and Mitchison, T.J. (2005). Non-equilibration of hydrostatic pressure in blebbing cells. Nature *435*, 365-369.

Chen, J.S., and Exton, J.H. (2004). Regulation of phospholipase D2 activity by protein kinase C alpha. The Journal of biological chemistry *279*, 22076-22083.

Chen, Q., Hongu, T., Sato, T., Zhang, Y., Ali, W., Cavallo, J.A., van der Velden, A., Tian, H., Di Paolo, G., Nieswandt, B., *et al.* (2012). Key roles for the lipid signaling enzyme phospholipase d1 in the tumor microenvironment during tumor angiogenesis and metastasis. Science signaling *5*, ra79.

Cheng, N., Chytil, A., Shyr, Y., Joly, A., and Moses, H.L. (2008). Transforming growth factor-beta signaling-deficient fibroblasts enhance hepatocyte growth factor signaling in mammary carcinoma cells to promote scattering and invasion. Molecular cancer research : MCR *6*, 1521-1533.

Chirivino, D., Del Maestro, L., Formstecher, E., Hupe, P., Raposo, G., Louvard, D., and Arpin, M. (2011). The ERM proteins interact with the HOPS complex to regulate the maturation of endosomes. Molecular biology of the cell *22*, 375-385.

Chu, X.P., and Xiong, Z.G. (2012). Physiological and pathological functions of acid-sensing ion channels in the central nervous system. Current drug targets *13*, 263-271.

Clement, D.L., Mally, S., Stock, C., Lethan, M., Satir, P., Schwab, A., Pedersen, S.F., and Christensen, S.T. (2013). PDGFRalpha signaling in the primary cilium regulates NHE1-

dependent fibroblast migration via coordinated differential activity of MEK1/2-ERK1/2-p90RSK and AKT signaling pathways. Journal of cell science *126*, 953-965.

Clements-Jewery, H., Sutherland, F.J., Allen, M.C., Tracey, W.R., and Avkiran, M. (2004). Cardioprotective efficacy of zoniporide, a potent and selective inhibitor of Na+/H+ exchanger isoform 1, in an experimental model of cardiopulmonary bypass. British journal of pharmacology *142*, 57-66.

Colley, W.C., Altshuller, Y.M., Sue-Ling, C.K., Copeland, N.G., Gilbert, D.J., Jenkins, N.A., Branch, K.D., Tsirka, S.E., Bollag, R.J., Bollag, W.B., *et al.* (1997). Cloning and expression analysis of murine phospholipase D1. The Biochemical journal *326 (Pt 3)*, 745-753.

Collins-Hooper, H., Woolley, T.E., Dyson, L., Patel, A., Potter, P., Baker, R.E., Gaffney, E.A., Maini, P.K., Dash, P.R., and Patel, K. (2012). Age-related changes in speed and mechanism of adult skeletal muscle stem cell migration. Stem Cells *30*, 1182-1195.

Colotta, F., Allavena, P., Sica, A., Garlanda, C., and Mantovani, A. (2009). Cancer-related inflammation, the seventh hallmark of cancer: links to genetic instability. Carcinogenesis *30*, 1073-1081.

Conner, A.C., Bill, R.M., and Conner, M.T. (2013). An emerging consensus on aquaporin translocation as a regulatory mechanism. Molecular membrane biology *30*, 1-12.

Conner, M.T., Conner, A.C., Bland, C.E., Taylor, L.H., Brown, J.E., Parri, H.R., and Bill, R.M. (2012). Rapid aquaporin translocation regulates cellular water flow: mechanism of hypotonicity-induced subcellular localization of aquaporin 1 water channel. The Journal of biological chemistry *287*, 11516-11525.

Conner, M.T., Conner, A.C., Brown, J.E.P., and Bill, R.M. (2010). Membrane Trafficking of Aquaporin 1 Is Mediated by Protein Kinase C via Microtubules and Regulated by Tonicity. Biochemistry *49*, 821-823.

Corrotte, M., Chasserot-Golaz, S., Huang, P., Du, G., Ktistakis, N.T., Frohman, M.A., Vitale, N., Bader, M.F., and Grant, N.J. (2006). Dynamics and function of phospholipase D and phosphatidic acid during phagocytosis. Traffic *7*, 365-377.

Cox, E.A., Sastry, S.K., and Huttenlocher, A. (2001). Integrin-mediated adhesion regulates cell polarity and membrane protrusion through the Rho family of GTPases. Molecular biology of the cell *12*, 265-277.

Crepaldi, T., Gautreau, A., Comoglio, P.M., Louvard, D., and Arpin, M. (1997). Ezrin is an effector of hepatocyte growth factor-mediated migration and morphogenesis in epithelial cells. The Journal of cell biology *138*, 423-434.

Cuddapah, V.A., and Sontheimer, H. (2011). Ion channels and transporters [corrected] in cancer. 2. Ion channels and the control of cancer cell migration. American journal of physiology Cell physiology *301*, C541-549.

Cui, Y., Wu, J., Zong, M., Song, G., Jia, Q., Jiang, J., and Han, J. (2009). Proteomic profiling in pancreatic cancer with and without lymph node metastasis. International journal of cancer Journal international du cancer *124*, 1614-1621.

Cunningham, C.C. (1995). Actin polymerization and intracellular solvent flow in cell surface blebbing. The Journal of cell biology *129*, 1589-1599.

Dai, X.Q., Ramji, A., Liu, Y., Li, Q., Karpinski, E., and Chen, X.Z. (2007). Inhibition of TRPP3 channel by amiloride and analogs. Molecular pharmacology *72*, 1576-1585.

Davies, M.A., and Samuels, Y. (2010). Analysis of the genome to personalize therapy for melanoma. Oncogene *29*, 5545-5555.

Deb, P., Pal, S., Dutta, V., Boruah, D., Chandran, V.M., and Bhatoe, H.S. (2012). Correlation of expression pattern of aquaporin-1 in primary central nervous system tumors with tumor type, grade, proliferation, microvessel density, contrast-enhancement and perilesional edema. Journal of cancer research and therapeutics *8*, 571-577.

Decher, N., Lang, H.J., Nilius, B., Bruggemann, A., Busch, A.E., and Steinmeyer, K. (2001). DCPIB is a novel selective blocker of I(Cl,swell) and prevents swelling-induced shortening of guinea-pig atrial action potential duration. British journal of pharmacology *134*, 1467-1479.

Deen, P.M., Verdijk, M.A., Knoers, N.V., Wieringa, B., Monnens, L.A., van Os, C.H., and van Oost, B.A. (1994). Requirement of human renal water channel aquaporin-2 for vasopressin-dependent concentration of urine. Science *264*, 92-95.

Denker, S.P., Huang, D.C., Orlowski, J., Furthmayr, H., and Barber, D.L. (2000). Direct binding of the Na--H exchanger NHE1 to ERM proteins regulates the cortical cytoskeleton and cell shape independently of H(+) translocation. Molecular cell *6*, 1425-1436.

Derivery, E., Fink, J., Martin, D., Houdusse, A., Piel, M., Stradal, T.E., Louvard, D., and Gautreau, A. (2008). Free Brick1 is a trimeric precursor in the assembly of a functional wave complex. PloS one *3*, e2462.

Deshpande, A., Sicinski, P., and Hinds, P.W. (2005). Cyclins and cdks in development and cancer: a perspective. Oncogene *24*, 2909-2915.

Di Fulvio, M., Lehman, N., Lin, X., Lopez, I., and Gomez-Cambronero, J. (2006). The elucidation of novel SH2 binding sites on PLD2. Oncogene *25*, 3032-3040.

Diz-Munoz, A., Krieg, M., Bergert, M., Ibarlucea-Benitez, I., Muller, D.J., Paluch, E., and Heisenberg, C.P. (2010). Control of directed cell migration in vivo by membrane-to-cortex attachment. PLoS biology *8*, e1000544.

Donowitz, M., Ming Tse, C., and Fuster, D. (2013). SLC9/NHE gene family, a plasma membrane and organellar family of Na(+)/H(+) exchangers. Mol Aspects Med *34*, 236-251.

Donowitz, M., Mohan, S., Zhu, C.X., Chen, T.E., Lin, R., Cha, B., Zachos, N.C., Murtazina, R., Sarker, R., and Li, X. (2009). NHE3 regulatory complexes. The Journal of experimental biology *212*, 1638-1646.

Dransfield, D.T., Bradford, A.J., Smith, J., Martin, M., Roy, C., Mangeat, P.H., and Goldenring, J.R. (1997). Ezrin is a cyclic AMP-dependent protein kinase anchoring protein. The EMBO journal *16*, 35-43.

Du, G., Altshuller, Y.M., Vitale, N., Huang, P., Chasserot-Golaz, S., Morris, A.J., Bader, M.F., and Frohman, M.A. (2003). Regulation of phospholipase D1 subcellular cycling through coordination of multiple membrane association motifs. The Journal of cell biology *162*, 305-315.

Du, G., and Frohman, M.A. (2009). A lipid-signaled myosin phosphatase surge disperses cortical contractile force early in cell spreading. Molecular biology of the cell *20*, 200-208.

Du, G., Huang, P., Liang, B.T., and Frohman, M.A. (2004). Phospholipase D2 localizes to the plasma membrane and regulates angiotensin II receptor endocytosis. Molecular biology of the cell *15*, 1024-1030.

Eisenmann, K.M., Harris, E.S., Kitchen, S.M., Holman, H.A., Higgs, H.N., and Alberts, A.S. (2007). Dia-interacting protein modulates formin-mediated actin assembly at the cell cortex. Current biology : CB *17*, 579-591.

Ellson, C.D., Andrews, S., Stephens, L.R., and Hawkins, P.T. (2002). The PX domain: a new phosphoinositide-binding module. Journal of cell science *115*, 1099-1105.

Estecha, A., Sanchez-Martin, L., Puig-Kroger, A., Bartolome, R.A., Teixido, J., Samaniego, R., and Sanchez-Mateos, P. (2009). Moesin orchestrates cortical polarity of melanoma tumour cells to initiate 3D invasion. Journal of cell science *122*, 3492-3501.

Ewald, A.J., Brenot, A., Duong, M., Chan, B.S., and Werb, Z. (2008). Collective epithelial migration and cell rearrangements drive mammary branching morphogenesis. Developmental cell *14*, 570-581.

Fackler, O.T., and Grosse, R. (2008). Cell motility through plasma membrane blebbing. The Journal of cell biology *181*, 879-884.

Falasca, M., Logan, S.K., Lehto, V.P., Baccante, G., Lemmon, M.A., and Schlessinger, J. (1998). Activation of phospholipase C gamma by PI 3-kinase-induced PH domain-mediated membrane targeting. The EMBO journal *17*, 414-422.

Fehon, R.G., McClatchey, A.I., and Bretscher, A. (2010). Organizing the cell cortex: the role of ERM proteins. Nature reviews Molecular cell biology *11*, 276-287.

Fievet, B.T., Gautreau, A., Roy, C., Del Maestro, L., Mangeat, P., Louvard, D., and Arpin, M. (2004). Phosphoinositide binding and phosphorylation act sequentially in the activation mechanism of ezrin. The Journal of cell biology *164*, 653-659.

Fiorio Pla, A., Avanzato, D., Munaron, L., and Ambudkar, I.S. (2012). Ion channels and transporters in cancer. 6. Vascularizing the tumor: TRP channels as molecular targets. American journal of physiology Cell physiology *302*, C9-15.

Foster, D.A. (2009). Phosphatidic acid signaling to mTOR: signals for the survival of human cancer cells. Biochimica et biophysica acta *1791*, 949-955.

Foster, D.A., and Xu, L. (2003). Phospholipase D in cell proliferation and cancer. Molecular cancer research : MCR *1*, 789-800.

Foster, F.M., Traer, C.J., Abraham, S.M., and Fry, M.J. (2003). The phosphoinositide (PI) 3-kinase family. Journal of cell science *116*, 3037-3040.

Franca-Koh, J., and Devreotes, P.N. (2004). Moving forward: mechanisms of chemoattractant gradient sensing. Physiology (Bethesda) *19*, 300-308.

Frantz, C., Barreiro, G., Dominguez, L., Chen, X., Eddy, R., Condeelis, J., Kelly, M.J., Jacobson, M.P., and Barber, D.L. (2008). Cofilin is a pH sensor for actin free barbed end formation: role of phosphoinositide binding. The Journal of cell biology *183*, 865-879.

Friedl, P. (2004). Prespecification and plasticity: shifting mechanisms of cell migration. Current opinion in cell biology *16*, 14-23.

Friedl, P., and Alexander, S. (2011). Cancer invasion and the microenvironment: plasticity and reciprocity. Cell *147*, 992-1009.

Friedl, P., Borgmann, S., and Brocker, E.B. (2001). Amoeboid leukocyte crawling through extracellular matrix: lessons from the Dictyostelium paradigm of cell movement. Journal of leukocyte biology *70*, 491-509.

Friedl, P., and Gilmour, D. (2009). Collective cell migration in morphogenesis, regeneration and cancer. Nature reviews Molecular cell biology *10*, 445-457.

Friedl, P., Maaser, K., Klein, C.E., Niggemann, B., Krohne, G., and Zanker, K.S. (1997). Migration of highly aggressive MV3 melanoma cells in 3-dimensional collagen lattices results in local matrix reorganization and shedding of alpha2 and beta1 integrins and CD44. Cancer research *57*, 2061-2070.

Friedl, P., and Wolf, K. (2003). Tumour-cell invasion and migration: diversity and escape mechanisms. Nature reviews Cancer *3*, 362-374.

Friedl, P., and Wolf, K. (2008). Tube travel: the role of proteases in individual and collective cancer cell invasion. Cancer research *68*, 7247-7249.

Friedl, P., and Wolf, K. (2009). Proteolytic interstitial cell migration: a five-step process. Cancer metastasis reviews *28*, 129-135.

Friedl, P., and Wolf, K. (2010). Plasticity of cell migration: a multiscale tuning model. The Journal of cell biology *188*, 11-19.

Frohman, M.A., and Morris, A.J. (1999). Phospholipase D structure and regulation. Chemistry and physics of lipids *98*, 127-140.

Fry, M.J. (2001). Phosphoinositide 3-kinase signalling in breast cancer: how big a role might it play? Breast cancer research : BCR *3*, 304-312.

Fu, D., Libson, A., and Stroud, R. (2002). The structure of GlpF, a glycerol conducting channel. Novartis Foundation symposium *245*, 51-61; discussion 61-55, 165-168.

Fujiyoshi, Y., Mitsuoka, K., de Groot, B.L., Philippsen, A., Grubmuller, H., Agre, P., and Engel, A. (2002). Structure and function of water channels. Current opinion in structural biology *12*, 509-515.

Fukata, Y., Kimura, K., Oshiro, N., Saya, H., Matsuura, Y., and Kaibuchi, K. (1998). Association of the myosin-binding subunit of myosin phosphatase and moesin: dual regulation of moesin phosphorylation by Rho-associated kinase and myosin phosphatase. The Journal of cell biology *141*, 409-418.

Gaggioli, C., Hooper, S., Hidalgo-Carcedo, C., Grosse, R., Marshall, J.F., Harrington, K., and Sahai, E. (2007). Fibroblast-led collective invasion of carcinoma cells with differing roles for RhoGTPases in leading and following cells. Nature cell biology *9*, 1392-1400.

Gao, L., Tsun, J., Sun, L., Kwan, J., Watson, A., Macdonald, P.S., and Hicks, M. (2011). Critical role of the STAT3 pathway in the cardioprotective efficacy of zoniporide in a model of myocardial preservation - the rat isolated working heart. British journal of pharmacology *162*, 633-647.

Gary, R., and Bretscher, A. (1995). Ezrin self-association involves binding of an N-terminal domain to a normally masked C-terminal domain that includes the F-actin binding site. Molecular biology of the cell *6*, 1061-1075.

Garzon-Muvdi, T., Schiapparelli, P., ap Rhys, C., Guerrero-Cazares, H., Smith, C., Kim, D.H., Kone, L., Farber, H., Lee, D.Y., An, S.S., *et al.* (2012). Regulation of brain tumor dispersal by NKCC1 through a novel role in focal adhesion regulation. PLoS biology *10*, e1001320.

Gavert, N., Ben-Shmuel, A., Lemmon, V., Brabletz, T., and Ben-Ze'ev, A. (2010). Nuclear factor-kappaB signaling and ezrin are essential for L1-mediated metastasis of colon cancer cells. Journal of cell science *123*, 2135-2143.

Gavert, N., Ben-Shmuel, A., Raveh, S., and Ben-Ze'ev, A. (2008). L1-CAM in cancerous tissues. Expert opinion on biological therapy *8*, 1749-1757.

Geiger, T.R., and Peeper, D.S. (2009). Metastasis mechanisms. Biochimica et biophysica acta *1796*, 293-308.

Giancotti, F.G., and Ruoslahti, E. (1999). Integrin signaling. Science *285*, 1028-1032.

Giannone, G., Ronde, P., Gaire, M., Beaudouin, J., Haiech, J., Ellenberg, J., and Takeda, K. (2004). Calcium rises locally trigger focal adhesion disassembly and enhance residency of focal adhesion kinase at focal adhesions. The Journal of biological chemistry *279*, 28715-28723.

Glinsky, G.V. (2006). Genomic models of metastatic cancer: functional analysis of death-from-cancer signature genes reveals aneuploid, anoikis-resistant, metastasis-enabling phenotype with altered cell cycle control and activated Polycomb Group (PcG) protein chromatin silencing pathway. Cell Cycle *5*, 1208-1216.

Glinsky, G.V., Berezovska, O., and Glinskii, A.B. (2005). Microarray analysis identifies a death-from-cancer signature predicting therapy failure in patients with multiple types of cancer. The Journal of clinical investigation *115*, 1503-1521.

Gomez-Cambronero, J. (2011). The exquisite regulation of PLD2 by a wealth of interacting proteins: S6K, Grb2, Sos, WASp and Rac2 (and a surprise discovery: PLD2 is a GEF). Cellular signalling *23*, 1885-1895.

Gomez-Cambronero, J. (2014). Phospholipase D in cell signaling: from a myriad of cell functions to cancer growth and metastasis. The Journal of biological chemistry *289*, 22557-22566.

Gonen, T., and Walz, T. (2006). The structure of aquaporins. Quarterly reviews of biophysics *39*, 361-396.

Gotoh, M., Fujiwara, Y., Yue, J., Liu, J., Lee, S., Fells, J., Uchiyama, A., Murakami-Murofushi, K., Kennel, S., Wall, J., *et al.* (2012). Controlling cancer through the autotaxin-lysophosphatidic acid receptor axis. Biochemical Society transactions *40*, 31-36.

Goudarzi, M., Banisch, T.U., Mobin, M.B., Maghelli, N., Tarbashevich, K., Strate, I., van den Berg, J., Blaser, H., Bandemer, S., Paluch, E., *et al.* (2012). Identification and regulation of a molecular module for bleb-based cell motility. Developmental cell *23*, 210-218.

Granes, F., Urena, J.M., Rocamora, N., and Vilaro, S. (2000). Ezrin links syndecan-2 to the cytoskeleton. Journal of cell science *113 (Pt 7)*, 1267-1276.

Grebecki, A., Grebecka, L., and Wasik, A. (2001). Minipodia and rosette contacts are adhesive organelles present in free-living amoebae. Cell biology international *25*, 1279-1283.

Gutjahr, M.C., Rossy, J., and Niggli, V. (2005). Role of Rho, Rac, and Rho-kinase in phosphorylation of myosin light chain, development of polarity, and spontaneous migration of Walker 256 carcinosarcoma cells. Experimental cell research *308*, 422-438.

Haas, B.R., and Sontheimer, H. (2010). Inhibition of the Sodium-Potassium-Chloride Cotransporter Isoform-1 reduces glioma invasion. Cancer research *70*, 5597-5606.

Habela, C.W., Ernest, N.J., Swindall, A.F., and Sontheimer, H. (2009). Chloride accumulation drives volume dynamics underlying cell proliferation and migration. Journal of neurophysiology *101*, 750-757.

Hamill, K.J., Hopkinson, S.B., Skalli, O., and Jones, J.C. (2013). Actinin-4 in keratinocytes regulates motility via an effect on lamellipodia stability and matrix adhesions. FASEB journal : official publication of the Federation of American Societies for Experimental Biology *27*, 546-556.

Han, Y., Eppinger, E., Schuster, I.G., Weigand, L.U., Liang, X., Kremmer, E., Peschel, C., and Krackhardt, A.M. (2009). Formin-like 1 (FMNL1) is regulated by N-terminal

myristoylation and induces polarized membrane blebbing. The Journal of biological chemistry *284*, 33409-33417.

Han, Z., and Patil, R.V. (2000). Protein kinase A-dependent phosphorylation of aquaporin-1. Biochemical and biophysical research communications *273*, 328-332.

Hanahan, D., and Folkman, J. (1996). Patterns and emerging mechanisms of the angiogenic switch during tumorigenesis. Cell *86*, 353-364.

Hanahan, D., and Weinberg, R.A. (2000). The hallmarks of cancer. Cell *100*, 57-70.
Hanahan, D., and Weinberg, R.A. (2011). Hallmarks of cancer: the next generation. Cell *144*, 646-674.

Hannemann, S., Madrid, R., Stastna, J., Kitzing, T., Gasteier, J., Schonichen, A., Bouchet, J., Jimenez, A., Geyer, M., Grosse, R., *et al.* (2008). The Diaphanous-related Formin FHOD1 associates with ROCK1 and promotes Src-dependent plasma membrane blebbing. The Journal of biological chemistry *283*, 27891-27903.

Hara-Chikuma, M., Sohara, E., Rai, T., Ikawa, M., Okabe, M., Sasaki, S., Uchida, S., and Verkman, A.S. (2005). Progressive adipocyte hypertrophy in aquaporin-7-deficient mice: adipocyte glycerol permeability as a novel regulator of fat accumulation. The Journal of biological chemistry *280*, 15493-15496.

Hara-Chikuma, M., and Verkman, A.S. (2006). Aquaporin-1 facilitates epithelial cell migration in kidney proximal tubule. Journal of the American Society of Nephrology : JASN *17*, 39-45.

Hara-Chikuma, M., and Verkman, A.S. (2008). Aquaporin-3 facilitates epidermal cell migration and proliferation during wound healing. J Mol Med (Berl) *86*, 221-231.

Hara, M., Ma, T., and Verkman, A.S. (2002). Selectively reduced glycerol in skin of aquaporin-3-deficient mice may account for impaired skin hydration, elasticity, and barrier recovery. The Journal of biological chemistry *277*, 46616-46621.

Harguindey, S., Arranz, J.L., Polo Orozco, J.D., Rauch, C., Fais, S., Cardone, R.A., and Reshkin, S.J. (2013). Cariporide and other new and powerful NHE1 inhibitors as potentially selective anticancer drugs--an integral molecular/biochemical/metabolic/clinical approach after one hundred years of cancer research. Journal of translational medicine *11*, 282.

Harguindey, S., Arranz, J.L., Wahl, M.L., Orive, G., and Reshkin, S.J. (2009). Proton transport inhibitors as potentially selective anticancer drugs. Anticancer research *29*, 2127-2136.

Harguindey, S., Orive, G., Luis Pedraz, J., Paradiso, A., and Reshkin, S.J. (2005). The role of pH dynamics and the Na+/H+ antiporter in the etiopathogenesis and treatment of cancer. Two faces of the same coin--one single nature. Biochimica et biophysica acta *1756*, 1-24.

Hegerfeldt, Y., Tusch, M., Brocker, E.B., and Friedl, P. (2002). Collective cell movement in primary melanoma explants: plasticity of cell-cell interaction, beta1-integrin function, and migration strategies. Cancer research *62*, 2125-2130.

Henkels, K.M., Boivin, G.P., Dudley, E.S., Berberich, S.J., and Gomez-Cambronero, J. (2013a). Phospholipase D (PLD) drives cell invasion, tumor growth and metastasis in a human breast cancer xenograph model. Oncogene *32*, 5551-5562.

Henkels, K.M., Mahankali, M., and Gomez-Cambronero, J. (2013b). Increased cell growth due to a new lipase-GEF (Phospholipase D2) fastly acting on Ras. Cellular signalling *25*, 198-205.

Hibuse, T., Maeda, N., Funahashi, T., Yamamoto, K., Nagasawa, A., Mizunoya, W., Kishida, K., Inoue, K., Kuriyama, H., Nakamura, T., *et al.* (2005). Aquaporin 7 deficiency is associated with development of obesity through activation of adipose glycerol kinase. Proceedings of the National Academy of Sciences of the United States of America *102*, 10993-10998.

Hidalgo-Carcedo, C., Hooper, S., Chaudhry, S.I., Williamson, P., Harrington, K., Leitinger, B., and Sahai, E. (2011). Collective cell migration requires suppression of actomyosin at cell-

cell contacts mediated by DDR1 and the cell polarity regulators Par3 and Par6. Nature cell biology *13*, 49-58.

Hoffmann, E.K., Lambert, I.H., and Pedersen, S.F. (2009). Physiology of cell volume regulation in vertebrates. Physiological reviews *89*, 193-277.

Hoffmann, E.K., and Pedersen, S.F. (2011). Cell volume homeostatic mechanisms: effectors and signalling pathways. Acta Physiol (Oxf) *202*, 465-485.

Homma, Y., Takenawa, T., Emori, Y., Sorimachi, H., and Suzuki, K. (1989). Tissue- and cell type-specific expression of mRNAs for four types of inositol phospholipid-specific phospholipase C. Biochemical and biophysical research communications *164*, 406-412.

Honda, A., Nogami, M., Yokozeki, T., Yamazaki, M., Nakamura, H., Watanabe, H., Kawamoto, K., Nakayama, K., Morris, A.J., Frohman, M.A., *et al.* (1999). Phosphatidylinositol 4-phosphate 5-kinase alpha is a downstream effector of the small G protein ARF6 in membrane ruffle formation. Cell *99*, 521-532.

Hoque, M.O., Soria, J.C., Woo, J., Lee, T., Lee, J., Jang, S.J., Upadhyay, S., Trink, B., Monitto, C., Desmaze, C., *et al.* (2006). Aquaporin 1 is overexpressed in lung cancer and stimulates NIH-3T3 cell proliferation and anchorage-independent growth. The American journal of pathology *168*, 1345-1353.

Hu, T., and Exton, J.H. (2003). Mechanisms of regulation of phospholipase D1 by protein kinase Calpha. The Journal of biological chemistry *278*, 2348-2355.

Huang, P., Altshuller, Y.M., Hou, J.C., Pessin, J.E., and Frohman, M.A. (2005). Insulin-stimulated plasma membrane fusion of Glut4 glucose transporter-containing vesicles is regulated by phospholipase D1. Molecular biology of the cell *16*, 2614-2623.

Huang, P., and Frohman, M.A. (2007). The potential for phospholipase D as a new therapeutic target. Expert opinion on therapeutic targets *11*, 707-716.

Hwang, J.I., Oh, Y.S., Shin, K.J., Kim, H., Ryu, S.H., and Suh, P.G. (2005). Molecular cloning and characterization of a novel phospholipase C, PLC-eta. The Biochemical journal *389*, 181-186.

Ikeda, T., Schmitt, B., Pouyssegur, J., Wakabayashi, S., and Shigekawa, M. (1997). Identification of cytoplasmic subdomains that control pH-sensing of the Na+/H+ exchanger (NHE1): pH-maintenance, ATP-sensitive, and flexible loop domains. Journal of biochemistry *121*, 295-303.

Ilina, O., and Friedl, P. (2009). Mechanisms of collective cell migration at a glance. Journal of cell science *122*, 3203-3208.

Illarionova, N.B., Gunnarson, E., Li, Y., Brismar, H., Bondar, A., Zelenin, S., and Aperia, A. (2010). Functional and molecular interactions between aquaporins and Na,K-ATPase. Neuroscience *168*, 915-925.

Isokpehi, R.D., Rajnarayanan, R.V., Jeffries, C.D., Oyeleye, T.O., and Cohly, H.H. (2009). Integrative sequence and tissue expression profiling of chicken and mammalian aquaporins. BMC genomics *10 Suppl 2*, S7.

Itoh, T., Koshiba, S., Kigawa, T., Kikuchi, A., Yokoyama, S., and Takenawa, T. (2001). Role of the ENTH domain in phosphatidylinositol-4,5-bisphosphate binding and endocytosis. Science *291*, 1047-1051.

Ivetic, A., and Ridley, A.J. (2004). Ezrin/radixin/moesin proteins and Rho GTPase signalling in leucocytes. Immunology *112*, 165-176.

Jelen, S., Parm Ulhoi, B., Larsen, A., Frokiaer, J., Nielsen, S., and Rutzler, M. (2013). AQP9 expression in glioblastoma multiforme tumors is limited to a small population of astrocytic cells and CD15(+)/CalB(+) leukocytes. PloS one *8*, e75764.

Jeon, H., Kwak, D., Noh, J., Lee, M.N., Lee, C.S., Suh, P.G., and Ryu, S.H. (2011). Phospholipase D2 induces stress fiber formation through mediating nucleotide exchange for RhoA. Cellular signalling *23*, 1320-1326.

Jeong, K.J., Cho, K.H., Panupinthu, N., Kim, H., Kang, J., Park, C.G., Mills, G.B., and Lee, H.Y. (2013). EGFR mediates LPA-induced proteolytic enzyme expression and ovarian cancer invasion: inhibition by resveratrol. Molecular oncology *7*, 121-129.

Jeong, K.J., Park, S.Y., Cho, K.H., Sohn, J.S., Lee, J., Kim, Y.K., Kang, J., Park, C.G., Han, J.W., and Lee, H.Y. (2012). The Rho/ROCK pathway for lysophosphatidic acid-induced proteolytic enzyme expression and ovarian cancer cell invasion. Oncogene *31*, 4279-4289.

Jhon, D.Y., Lee, H.H., Park, D., Lee, C.W., Lee, K.H., Yoo, O.J., and Rhee, S.G. (1993). Cloning, sequencing, purification, and Gq-dependent activation of phospholipase C-beta 3. The Journal of biological chemistry *268*, 6654-6661.

Jiang, Y. (2009). Aquaporin-1 activity of plasma membrane affects HT20 colon cancer cell migration. IUBMB life *61*, 1001-1009.

Jin, C., Ye, Q.H., Yuan, F.L., Gu, Y.L., Li, J.P., Shi, Y.H., Shen, X.M., Bo, L., and Lin, Z.H. (2015). Involvement of acid-sensing ion channel 1alpha in hepatic carcinoma cell migration and invasion. Tumour biology : the journal of the International Society for Oncodevelopmental Biology and Medicine.

Jung, H.J., Park, J.Y., Jeon, H.S., and Kwon, T.H. (2011). Aquaporin-5: a marker protein for proliferation and migration of human breast cancer cells. PloS one *6*, e28492.

Junttila, M.R., and Evan, G.I. (2009). p53-a Jack of all trades but master of none. Nature Reviews Cancer *9*, 821-829.

Kahsai, A.W., Zhu, S., and Fenteany, G. (2010). G protein-coupled receptor kinase 2 activates radixin, regulating membrane protrusion and motility in epithelial cells. Biochimica et biophysica acta *1803*, 300-310.

Kang, D.W., Park, M.H., Lee, Y.J., Kim, H.S., Kwon, T.K., Park, W.S., and Min do, S. (2008a). Phorbol ester up-regulates phospholipase D1 but not phospholipase D2 expression through a PKC/Ras/ERK/NFkappaB-dependent pathway and enhances matrix metalloproteinase-9 secretion in colon cancer cells. The Journal of biological chemistry *283*, 4094-4104.

Kang, S.K., Chae, Y.K., Woo, J., Kim, M.S., Park, J.C., Lee, J., Soria, J.C., Jang, S.J., Sidransky, D., and Moon, C. (2008b). Role of human aquaporin 5 in colorectal carcinogenesis. The American journal of pathology *173*, 518-525.

Kantonen, S., Hatton, N., Mahankali, M., Henkels, K.M., Park, H., Cox, D., and Gomez-Cambronero, J. (2011). A novel phospholipase D2-Grb2-WASp heterotrimer regulates leukocyte phagocytosis in a two-step mechanism. Molecular and cellular biology *31*, 4524-4537.

Kapoor, N., Bartoszewski, R., Qadri, Y.J., Bebok, Z., Bubien, J.K., Fuller, C.M., and Benos, D.J. (2009). Knockdown of ASIC1 and epithelial sodium channel subunits inhibits glioblastoma whole cell current and cell migration. The Journal of biological chemistry *284*, 24526-24541.

Kawaguchi, K., Saito, K., Asami, H., and Ohta, Y. (2014). ADP ribosylation factor 6 (Arf6) acts through FilGAP protein to down-regulate Rac protein and regulates plasma membrane blebbing. The Journal of biological chemistry *289*, 9675-9682.

Khaled, A.R., Moor, A.N., Li, A., Kim, K., Ferris, D.K., Muegge, K., Fisher, R.J., Fliegel, L., and Durum, S.K. (2001). Trophic factor withdrawal: p38 mitogen-activated protein kinase activates NHE1, which induces intracellular alkalinization. Molecular and cellular biology *21*, 7545-7557.

Khalil, A.A., and Friedl, P. (2010). Determinants of leader cells in collective cell migration. Integrative biology : quantitative biosciences from nano to macro *2*, 568-574.

Khan, K., Hardy, R., Haq, A., Ogunbiyi, O., Morton, D., and Chidgey, M. (2006). Desmocollin switching in colorectal cancer. British journal of cancer *95*, 1367-1370.

Khanna, A. (2006). Acquired nephrogenic diabetes insipidus. Seminars in nephrology *26*, 244-248.

Klein, R.R., Bourdon, D.M., Costales, C.L., Wagner, C.D., White, W.L., Williams, J.D., Hicks, S.N., Sondek, J., and Thakker, D.R. (2011). Direct activation of human phospholipase C by its well known inhibitor u73122. The Journal of biological chemistry *286*, 12407-12416.

Knoepp, S.M., Chahal, M.S., Xie, Y., Zhang, Z., Brauner, D.J., Hallman, M.A., Robinson, S.A., Han, S., Imai, M., Tomlinson, S., *et al.* (2008). Effects of active and inactive phospholipase D2 on signal transduction, adhesion, migration, invasion, and metastasis in EL4 lymphoma cells. Molecular pharmacology *74*, 574-584.

Kolyada, A.Y., Riley, K.N., and Herman, I.M. (2003). Rho GTPase signaling modulates cell shape and contractile phenotype in an isoactin-specific manner. American journal of physiology Cell physiology *285*, C1116-1121.

Krane, C.M., and Goldstein, D.L. (2007). Comparative functional analysis of aquaporins/glyceroporins in mammals and anurans. Mammalian genome : official journal of the International Mammalian Genome Society *18*, 452-462.

Krieg, J., and Hunter, T. (1992). Identification of the two major epidermal growth factor-induced tyrosine phosphorylation sites in the microvillar core protein ezrin. The Journal of biological chemistry *267*, 19258-19265.

Kruse, E., Uehlein, N., and Kaldenhoff, R. (2006). The aquaporins. Genome biology *7*, 206.

Kubota, H.Y. (1981). Creeping locomotion of the endodermal cells dissociated from gastrulae of the Japanese newt, Cynops pyrrhogaster. Experimental cell research *133*, 137-148.

Lagana, A., Vadnais, J., Le, P.U., Nguyen, T.N., Laprade, R., Nabi, I.R., and Noel, J. (2000). Regulation of the formation of tumor cell pseudopodia by the Na(+)/H(+) exchanger NHE1. Journal of cell science *113 (Pt 20)*, 3649-3662.

Lammermann, T., and Sixt, M. (2009). Mechanical modes of 'amoeboid' cell migration. Current opinion in cell biology *21*, 636-644.

Lauffenburger, D.A., and Horwitz, A.F. (1996). Cell migration: a physically integrated molecular process. Cell *84*, 359-369.

Lauritzen, G., Stock, C.M., Lemaire, J., Lund, S.F., Jensen, M.F., Damsgaard, B., Petersen, K.S., Wiwel, M., Ronnov-Jessen, L., Schwab, A., *et al.* (2012). The Na+/H+ exchanger NHE1, but not the Na+, HCO3(-) cotransporter NBCn1, regulates motility of MCF7 breast cancer cells expressing constitutively active ErbB2. Cancer letters *317*, 172-183.

Le Clainche, C., and Carlier, M.F. (2008). Regulation of actin assembly associated with protrusion and adhesion in cell migration. Physiological reviews *88*, 489-513.

Lecaudey, V., Cakan-Akdogan, G., Norton, W.H., and Gilmour, D. (2008). Dynamic Fgf signaling couples morphogenesis and migration in the zebrafish lateral line primordium. Development *135*, 2695-2705.

Lecaudey, V., and Gilmour, D. (2006). Organizing moving groups during morphogenesis. Current opinion in cell biology *18*, 102-107.

Lee, C.H., Cragoe, E.J., Jr., and Edwards, A.M. (2003). Control of hepatocyte DNA synthesis by intracellular pH and its role in the action of tumor promoters. Journal of cellular physiology *195*, 61-69.

Lee, G.Y., Kenny, P.A., Lee, E.H., and Bissell, M.J. (2007). Three-dimensional culture models of normal and malignant breast epithelial cells. Nature methods *4*, 359-365.

Lee, S.B., and Rhee, S.G. (1996). Molecular cloning, splice variants, expression, and purification of phospholipase C-delta 4. The Journal of biological chemistry *271*, 25-31.

Lee, S.J., Chae, Y.S., Kim, J.G., Kim, W.W., Jung, J.H., Park, H.Y., Jeong, J.Y., Park, J.Y., Jung, H.J., and Kwon, T.H. (2014). AQP5 expression predicts survival in patients with early breast cancer. Annals of surgical oncology *21*, 375-383.

Lee, W.K., Kim, J.K., Seo, M.S., Cha, J.H., Lee, K.J., Rha, H.K., Min, D.S., Jo, Y.H., and Lee, K.H. (1999). Molecular cloning and expression analysis of a mouse phospholipase C-delta1. Biochemical and biophysical research communications *261*, 393-399.

Legg, J.W., Lewis, C.A., Parsons, M., Ng, T., and Isacke, C.M. (2002). A novel PKC-regulated mechanism controls CD44 ezrin association and directional cell motility. Nature cell biology *4*, 399-407.

Lehen'kyi, V., Shapovalov, G., Skryma, R., and Prevarskaya, N. (2011). Ion channnels and transporters in cancer. 5. Ion channels in control of cancer and cell apoptosis. American journal of physiology Cell physiology *301*, C1281-1289.

Lehoux, S., Abe, J., Florian, J.A., and Berk, B.C. (2001). 14-3-3 Binding to Na+/H+ exchanger isoform-1 is associated with serum-dependent activation of Na+/H+ exchange. The Journal of biological chemistry *276*, 15794-15800.

Lemmon, M.A., and Schlessinger, J. (2010). Cell signaling by receptor tyrosine kinases. Cell *141*, 1117-1134.

Levin, M.H., and Verkman, A.S. (2006). Aquaporin-3-dependent cell migration and proliferation during corneal re-epithelialization. Investigative ophthalmology & visual science *47*, 4365-4372.

Levine, A.J. (1997). p53, the cellular gatekeeper for growth and division. Cell *88*, 323-331.

Li, J., and Verkman, A.S. (2001). Impaired hearing in mice lacking aquaporin-4 water channels. The Journal of biological chemistry *276*, 31233-31237.

Li, X., Liu, Y., Alvarez, B.V., Casey, J.R., and Fliegel, L. (2006). A novel carbonic anhydrase II binding site regulates NHE1 activity. Biochemistry *45*, 2414-2424.

Lin, F.G., Cheng, H.F., Lee, I.F., Kao, H.J., Loh, S.H., and Lee, W.H. (2001). Downregulation of phospholipase C delta3 by cAMP and calcium. Biochemical and biophysical research communications *286*, 274-280.

Ling, K., Schill, N.J., Wagoner, M.P., Sun, Y., and Anderson, R.A. (2006). Movin' on up: the role of PtdIns(4,5)P(2) in cell migration. Trends in cell biology *16*, 276-284.

Liu, M.Y., Gutowski, S., and Sternweis, P.C. (2001). The C terminus of mammalian phospholipase D is required for catalytic activity. The Journal of biological chemistry *276*, 5556-5562.

Liu, Y.L., Matsuzaki, T., Nakazawa, T., Murata, S., Nakamura, N., Kondo, T., Iwashina, M., Mochizuki, K., Yamane, T., Takata, K., *et al.* (2007). Expression of aquaporin 3 (AQP3) in normal and neoplastic lung tissues. Human pathology *38*, 171-178.

Loitto, V.M., Huang, C., Sigal, Y.J., and Jacobson, K. (2007). Filopodia are induced by aquaporin-9 expression. Experimental cell research *313*, 1295-1306.

Lopez, I., Arnold, R.S., and Lambeth, J.D. (1998). Cloning and initial characterization of a human phospholipase D2 (hPLD2). ADP-ribosylation factor regulates hPLD2. The Journal of biological chemistry *273*, 12846-12852.

Lopez, I., Mak, E.C., Ding, J., Hamm, H.E., and Lomasney, J.W. (2001). A novel bifunctional phospholipase c that is regulated by Galpha 12 and stimulates the Ras/mitogen-activated protein kinase pathway. The Journal of biological chemistry *276*, 2758-2765.

Lorentzen, A., Bamber, J., Sadok, A., Elson-Schwab, I., and Marshall, C.J. (2011). An ezrin-rich, rigid uropod-like structure directs movement of amoeboid blebbing cells. Journal of cell science *124*, 1256-1267.

Louvet-Vallee, S. (2000). ERM proteins: from cellular architecture to cell signaling. Biology of the cell / under the auspices of the European Cell Biology Organization *92*, 305-316.

Lucien, F., Brochu-Gaudreau, K., Arsenault, D., Harper, K., and Dubois, C.M. (2011). Hypoxia-induced invadopodia formation involves activation of NHE-1 by the p90 ribosomal S6 kinase (p90RSK). PloS one *6*, e28851.

Ludwig, F.T., Schwab, A., and Stock, C. (2013). The Na+ /H+ -exchanger (NHE1) generates pH nanodomains at focal adhesions. Journal of cellular physiology *228*, 1351-1358.

Ma, T., Hara, M., Sougrat, R., Verbavatz, J.M., and Verkman, A.S. (2002). Impaired stratum corneum hydration in mice lacking epidermal water channel aquaporin-3. The Journal of biological chemistry *277*, 17147-17153.

Ma, T., Song, Y., Yang, B., Gillespie, A., Carlson, E.J., Epstein, C.J., and Verkman, A.S. (2000). Nephrogenic diabetes insipidus in mice lacking aquaporin-3 water channels. Proceedings of the National Academy of Sciences of the United States of America *97*, 4386-4391.

Madsen, C.D., Hooper, S., Tozluoglu, M., Bruckbauer, A., Fletcher, G., Erler, J.T., Bates, P.A., Thompson, B., and Sahai, E. (2015). STRIPAK components determine mode of cancer cell migration and metastasis. Nature cell biology *17*, 68-80.

Maeda, N., Hibuse, T., and Funahashi, T. (2009). Role of aquaporin-7 and aquaporin-9 in glycerol metabolism; involvement in obesity. Handbook of experimental pharmacology, 233-249.

Magalhaes, M.A., Larson, D.R., Mader, C.C., Bravo-Cordero, J.J., Gil-Henn, H., Oser, M., Chen, X., Koleske, A.J., and Condeelis, J. (2011). Cortactin phosphorylation regulates cell invasion through a pH-dependent pathway. The Journal of cell biology *195*, 903-920.

Mahankali, M., Peng, H.J., Cox, D., and Gomez-Cambronero, J. (2011a). The mechanism of cell membrane ruffling relies on a phospholipase D2 (PLD2), Grb2 and Rac2 association. Cellular signalling *23*, 1291-1298.

Mahankali, M., Peng, H.J., Henkels, K.M., Dinauer, M.C., and Gomez-Cambronero, J. (2011b). Phospholipase D2 (PLD2) is a guanine nucleotide exchange factor (GEF) for the GTPase Rac2. Proceedings of the National Academy of Sciences of the United States of America *108*, 19617-19622.

Majerus, P.W., Kisseleva, M.V., and Norris, F.A. (1999). The role of phosphatases in inositol signaling reactions. The Journal of biological chemistry *274*, 10669-10672.

Malawista, S.E., de Boisfleury Chevance, A., and Boxer, L.A. (2000). Random locomotion and chemotaxis of human blood polymorphonuclear leukocytes from a patient with leukocyte adhesion deficiency-1: normal displacement in close quarters via chimneying. Cell motility and the cytoskeleton *46*, 183-189.

Mari, Y., Katnik, C., and Cuevas, J. (2010). ASIC1a channels are activated by endogenous protons during ischemia and contribute to synergistic potentiation of intracellular Ca(2+) overload during ischemia and acidosis. Cell calcium *48*, 70-82.

Mari, Y., Katnik, C., and Cuevas, J. (2014). sigma-1 Receptor Inhibition of ASIC1a Channels is Dependent on a Pertussis Toxin-Sensitive G-Protein and an AKAP150/Calcineurin Complex. Neurochemical research.

Markadieu, N., and Delpire, E. (2014). Physiology and pathophysiology of SLC12A1/2 transporters. Pflugers Archiv : European journal of physiology *466*, 91-105.

Martin, C., Pedersen, S.F., Schwab, A., and Stock, C. (2011). Intracellular pH gradients in migrating cells. American journal of physiology Cell physiology *300*, C490-495.

Matsui, T., Maeda, M., Doi, Y., Yonemura, S., Amano, M., Kaibuchi, K., and Tsukita, S. (1998). Rho-kinase phosphorylates COOH-terminal threonines of ezrin/radixin/moesin

(ERM) proteins and regulates their head-to-tail association. The Journal of cell biology *140*, 647-657.

Meima, M.E., Mackley, J.R., and Barber, D.L. (2007). Beyond ion translocation: structural functions of the sodium-hydrogen exchanger isoform-1. Current opinion in nephrology and hypertension *16*, 365-372.

Meima, M.E., Webb, B.A., Witkowska, H.E., and Barber, D.L. (2009). The sodium-hydrogen exchanger NHE1 is an Akt substrate necessary for actin filament reorganization by growth factors. The Journal of biological chemistry *284*, 26666-26675.

Miller, E.W., Dickinson, B.C., and Chang, C.J. (2010). Aquaporin-3 mediates hydrogen peroxide uptake to regulate downstream intracellular signaling. Proceedings of the National Academy of Sciences of the United States of America *107*, 15681-15686.

Mills, J.C., Stone, N.L., and Pittman, R.N. (1999). Extranuclear apoptosis. The role of the cytoplasm in the execution phase. The Journal of cell biology *146*, 703-708.

Min, D.S., Ahn, B.H., and Jo, Y.H. (2001). Differential tyrosine phosphorylation of phospholipase D isozymes by hydrogen peroxide and the epidermal growth factor in A431 epidermoid carcinoma cells. Molecules and cells *11*, 369-378.

Min, X.J., Li, H., Hou, S.C., He, W., Liu, J., Hu, B., and Wang, J. (2011). Dysfunction of volume-sensitive chloride channels contributes to cisplatin resistance in human lung adenocarcinoma cells. Exp Biol Med (Maywood) *236*, 483-491.

Mizuguchi, M., Yamada, M., Kim, S.U., and Rhee, S.G. (1991). Phospholipase C isozymes in neurons and glial cells in culture: an immunocytochemical and immunochemical study. Brain research *548*, 35-40.

Moon, C., Soria, J.C., Jang, S.J., Lee, J., Obaidul Hoque, M., Sibony, M., Trink, B., Chang, Y.S., Sidransky, D., and Mao, L. (2003). Involvement of aquaporins in colorectal carcinogenesis. Oncogene *22*, 6699-6703.

Morris, A.J., Frohman, M.A., and Engebrecht, J. (1997). Measurement of phospholipase D activity. Analytical biochemistry *252*, 1-9.

Musa-Aziz, R., Chen, L.M., Pelletier, M.F., and Boron, W.F. (2009). Relative CO2/NH3 selectivities of AQP1, AQP4, AQP5, AmtB, and RhAG. Proceedings of the National Academy of Sciences of the United States of America *106*, 5406-5411.

Naba, A., Reverdy, C., Louvard, D., and Arpin, M. (2008). Spatial recruitment and activation of the Fes kinase by ezrin promotes HGF-induced cell scattering. The EMBO journal *27*, 38-50.

Nakamura, F., Amieva, M.R., and Furthmayr, H. (1995). Phosphorylation of threonine 558 in the carboxyl-terminal actin-binding domain of moesin by thrombin activation of human platelets. The Journal of biological chemistry *270*, 31377-31385.

Nakamura, F., Huang, L., Pestonjamasp, K., Luna, E.J., and Furthmayr, H. (1999). Regulation of F-actin binding to platelet moesin in vitro by both phosphorylation of threonine 558 and polyphosphatidylinositides. Molecular biology of the cell *10*, 2669-2685.

Nakamura, N., Oshiro, N., Fukata, Y., Amano, M., Fukata, M., Kuroda, S., Matsuura, Y., Leung, T., Lim, L., and Kaibuchi, K. (2000). Phosphorylation of ERM proteins at filopodia induced by Cdc42. Genes to cells : devoted to molecular & cellular mechanisms *5*, 571-581.

Nakashima, S., Banno, Y., Watanabe, T., Nakamura, Y., Mizutani, T., Sakai, H., Zhao, Y., Sugimoto, Y., and Nozawa, Y. (1995). Deletion and site-directed mutagenesis of EF-hand domain of phospholipase C-delta 1: effects on its activity. Biochemical and biophysical research communications *211*, 365-369.

Negrini, S., Gorgoulis, V.G., and Halazonetis, T.D. (2010). Genomic instability--an evolving hallmark of cancer. Nature reviews Molecular cell biology *11*, 220-228.

Nejsum, L.N., Kwon, T.H., Jensen, U.B., Fumagalli, O., Frokiaer, J., Krane, C.M., Menon, A.G., King, L.S., Agre, P.C., and Nielsen, S. (2002). Functional requirement of aquaporin-5

in plasma membranes of sweat glands. Proceedings of the National Academy of Sciences of the United States of America *99*, 511-516.

Ng, T., Parsons, M., Hughes, W.E., Monypenny, J., Zicha, D., Gautreau, A., Arpin, M., Gschmeissner, S., Verveer, P.J., Bastiaens, P.I., *et al.* (2001). Ezrin is a downstream effector of trafficking PKC-integrin complexes involved in the control of cell motility. The EMBO journal *20*, 2723-2741.

Nico, B., and Ribatti, D. (2010). Aquaporins in tumor growth and angiogenesis. Cancer letters *294*, 135-138.

Niggli, V. (2005). Regulation of protein activities by phosphoinositide phosphates. Annual review of cell and developmental biology *21*, 57-79.

Norman, L., Sengupta, K., and Aranda-Espinoza, H. (2011). Blebbing dynamics during endothelial cell spreading. European journal of cell biology *90*, 37-48.

Norman, L.L., Brugues, J., Sengupta, K., Sens, P., and Aranda-Espinoza, H. (2010). Cell blebbing and membrane area homeostasis in spreading and retracting cells. Biophysical journal *99*, 1726-1733.

Oude Weernink, P.A., Lopez de Jesus, M., and Schmidt, M. (2007). Phospholipase D signaling: orchestration by PIP2 and small GTPases. Naunyn-Schmiedeberg's archives of pharmacology *374*, 399-411.

Oude Weernink, P.A., Schmidt, M., and Jakobs, K.H. (2004). Regulation and cellular roles of phosphoinositide 5-kinases. European journal of pharmacology *500*, 87-99.

Padan, E., Kozachkov, L., Herz, K., and Rimon, A. (2009). NhaA crystal structure: functional-structural insights. The Journal of experimental biology *212*, 1593-1603.

Paluch, E., Piel, M., Prost, J., Bornens, M., and Sykes, C. (2005). Cortical actomyosin breakage triggers shape oscillations in cells and cell fragments. Biophysical journal *89*, 724-733.

Paluch, E., Sykes, C., Prost, J., and Bornens, M. (2006). Dynamic modes of the cortical actomyosin gel during cell locomotion and division. Trends in cell biology *16*, 5-10.
Paluch, E.K., and Raz, E. (2013). The role and regulation of blebs in cell migration. Current opinion in cell biology.

Pang, T., Su, X., Wakabayashi, S., and Shigekawa, M. (2001). Calcineurin homologous protein as an essential cofactor for Na+/H+ exchangers. The Journal of biological chemistry *276*, 17367-17372.

Panupinthu, N., Zhao, L., Possmayer, F., Ke, H.Z., Sims, S.M., and Dixon, S.J. (2007). P2X7 nucleotide receptors mediate blebbing in osteoblasts through a pathway involving lysophosphatidic acid. The Journal of biological chemistry *282*, 3403-3412.

Papadopoulos, M.C., and Saadoun, S. (2014). Key roles of aquaporins in tumor biology. Biochimica et biophysica acta.

Papadopoulos, M.C., Saadoun, S., and Verkman, A.S. (2008). Aquaporins and cell migration. Pflugers Archiv : European journal of physiology *456*, 693-700.

Paradise, R.K., Whitfield, M.J., Lauffenburger, D.A., and Van Vliet, K.J. (2013). Directional cell migration in an extracellular pH gradient: a model study with an engineered cell line and primary microvascular endothelial cells. Experimental cell research *319*, 487-497.

Paradiso, A., Cardone, R.A., Bellizzi, A., Bagorda, A., Guerra, L., Tommasino, M., Casavola, V., and Reshkin, S.J. (2004). The Na+-H+ exchanger-1 induces cytoskeletal changes involving reciprocal RhoA and Rac1 signaling, resulting in motility and invasion in MDA-MB-435 cells. Breast cancer research : BCR *6*, R616-628.

Park, J.I., Venteicher, A.S., Hong, J.Y., Choi, J., Jun, S., Shkreli, M., Chang, W., Meng, Z., Cheung, P., Ji, H., *et al.* (2009). Telomerase modulates Wnt signalling by association with target gene chromatin. Nature *460*, 66-72.

Park, S.K., Min, D.S., and Exton, J.H. (1998). Definition of the protein kinase C interaction site of phospholipase D. Biochemical and biophysical research communications *244*, 364-367.

Pearson, M.A., Reczek, D., Bretscher, A., and Karplus, P.A. (2000). Structure of the ERM protein moesin reveals the FERM domain fold masked by an extended actin binding tail domain. Cell *101*, 259-270.

Pelham, R.J., Jr., and Wang, Y. (1997). Cell locomotion and focal adhesions are regulated by substrate flexibility. Proceedings of the National Academy of Sciences of the United States of America *94*, 13661-13665.

Pinner, S., and Sahai, E. (2008). PDK1 regulates cancer cell motility by antagonising inhibition of ROCK1 by RhoE. Nature cell biology *10*, 127-137.

Poincloux, R., Collin, O., Lizarraga, F., Romao, M., Debray, M., Piel, M., and Chavrier, P. (2011). Contractility of the cell rear drives invasion of breast tumor cells in 3D Matrigel. Proceedings of the National Academy of Sciences of the United States of America *108*, 1943-1948.

Pollard, T.D., and Borisy, G.G. (2003). Cellular motility driven by assembly and disassembly of actin filaments. Cell *112*, 453-465.

Polte, T.R., Eichler, G.S., Wang, N., and Ingber, D.E. (2004). Extracellular matrix controls myosin light chain phosphorylation and cell contractility through modulation of cell shape and cytoskeletal prestress. American journal of physiology Cell physiology *286*, C518-528.

Porporato, P.E., Dhup, S., Dadhich, R.K., Copetti, T., and Sonveaux, P. (2011). Anticancer targets in the glycolytic metabolism of tumors: a comprehensive review. Frontiers in pharmacology *2*, 49.

Prevarskaya, N., Skryma, R., and Shuba, Y. (2010). Ion channels and the hallmarks of cancer. Trends in molecular medicine *16*, 107-121.

Provost, J.J., Rastedt, D., Canine, J., Ngyuen, T., Haak, A., Kutz, C., Berthelsen, N., Slusser, A., Anderson, K., Dorsam, G., *et al.* (2012). Urokinase plasminogen activator receptor induced non-small cell lung cancer invasion and metastasis requires NHE1 transporter expression and transport activity. Cell Oncol (Dordr).

Qiu, Z., Dubin, A.E., Mathur, J., Tu, B., Reddy, K., Miraglia, L.J., Reinhardt, J., Orth, A.P., and Patapoutian, A. (2014). SWELL1, a plasma membrane protein, is an essential component of volume-regulated anion channel. Cell *157*, 447-458.

Reczek, D., Berryman, M., and Bretscher, A. (1997). Identification of EBP50: A PDZ-containing phosphoprotein that associates with members of the ezrin-radixin-moesin family. The Journal of cell biology *139*, 169-179.

Renkawitz, J., Schumann, K., Weber, M., Lammermann, T., Pflicke, H., Piel, M., Polleux, J., Spatz, J.P., and Sixt, M. (2009). Adaptive force transmission in amoeboid cell migration. Nature cell biology *11*, 1438-1443.

Reshkin, S.J., Bellizzi, A., Albarani, V., Guerra, L., Tommasino, M., Paradiso, A., and Casavola, V. (2000a). Phosphoinositide 3-kinase is involved in the tumor-specific activation of human breast cancer cell Na(+)/H(+) exchange, motility, and invasion induced by serum deprivation. The Journal of biological chemistry *275*, 5361-5369.

Reshkin, S.J., Bellizzi, A., Caldeira, S., Albarani, V., Malanchi, I., Poignee, M., Alunni-Fabbroni, M., Casavola, V., and Tommasino, M. (2000b). Na+/H+ exchanger-dependent intracellular alkalinization is an early event in malignant transformation and plays an essential role in the development of subsequent transformation-associated phenotypes.

FASEB journal : official publication of the Federation of American Societies for Experimental Biology *14*, 2185-2197.

Reshkin, S.J., Cardone, R.A., and Harguindey, S. (2013). Na+-H+ exchanger, pH regulation and cancer. Recent patents on anti-cancer drug discovery *8*, 85-99.

Rich, I.N., Worthington-White, D., Garden, O.A., and Musk, P. (2000). Apoptosis of leukemic cells accompanies reduction in intracellular pH after targeted inhibition of the Na(+)/H(+) exchanger. Blood *95*, 1427-1434.

Ridley, A.J. (2011). Life at the leading edge. Cell *145*, 1012-1022.

Ridley, A.J., Schwartz, M.A., Burridge, K., Firtel, R.A., Ginsberg, M.H., Borisy, G., Parsons, J.T., and Horwitz, A.R. (2003). Cell migration: integrating signals from front to back. Science *302*, 1704-1709.

Rossy, J., Gutjahr, M.C., Blaser, N., Schlicht, D., and Niggli, V. (2007). Ezrin/moesin in motile Walker 256 carcinosarcoma cells: signal-dependent relocalization and role in migration. Experimental cell research *313*, 1106-1120.

Saadoun, S., Papadopoulos, M.C., Davies, D.C., Bell, B.A., and Krishna, S. (2002a). Increased aquaporin 1 water channel expression in human brain tumours. British journal of cancer *87*, 621-623.

Saadoun, S., Papadopoulos, M.C., Davies, D.C., Krishna, S., and Bell, B.A. (2002b). Aquaporin-4 expression is increased in oedematous human brain tumours. Journal of neurology, neurosurgery, and psychiatry *72*, 262-265.

Saadoun, S., Papadopoulos, M.C., Hara-Chikuma, M., and Verkman, A.S. (2005a). Impairment of angiogenesis and cell migration by targeted aquaporin-1 gene disruption. Nature *434*, 786-792.

Saadoun, S., Papadopoulos, M.C., Watanabe, H., Yan, D., Manley, G.T., and Verkman, A.S. (2005b). Involvement of aquaporin-4 in astroglial cell migration and glial scar formation. Journal of cell science *118*, 5691-5698.

Saadoun, S., Tait, M.J., Reza, A., Davies, D.C., Bell, B.A., Verkman, A.S., and Papadopoulos, M.C. (2009). AQP4 gene deletion in mice does not alter blood-brain barrier integrity or brain morphology. Neuroscience *161*, 764-772.

Sabatini, D.M. (2006). mTOR and cancer: insights into a complex relationship. Nature reviews Cancer *6*, 729-734.

Sahai, E. (2002). p53 moves into control of cell morphology. Molecular interventions *2*, 286-289.

Sahai, E. (2005). Mechanisms of cancer cell invasion. Current opinion in genetics & development *15*, 87-96.

Sahai, E., and Marshall, C.J. (2003). Differing modes of tumour cell invasion have distinct requirements for Rho/ROCK signalling and extracellular proteolysis. Nature cell biology *5*, 711-719.

Saito, K., Ozawa, Y., Hibino, K., and Ohta, Y. (2012). FilGAP, a Rho/Rho-associated protein kinase-regulated GTPase-activating protein for Rac, controls tumor cell migration. Molecular biology of the cell *23*, 4739-4750.

Santarius, M., Lee, C.H., and Anderson, R.A. (2006). Supervised membrane swimming: small G-protein lifeguards regulate PIPK signalling and monitor intracellular PtdIns(4,5)P2 pools. The Biochemical journal *398*, 1-13.

Sanz-Moreno, V., Gadea, G., Ahn, J., Paterson, H., Marra, P., Pinner, S., Sahai, E., and Marshall, C.J. (2008). Rac activation and inactivation control plasticity of tumor cell movement. Cell *135*, 510-523.

Sanz-Moreno, V., Gaggioli, C., Yeo, M., Albrengues, J., Wallberg, F., Viros, A., Hooper, S., Mitter, R., Feral, C.C., Cook, M., *et al.* (2011). ROCK and JAK1 signaling cooperate to control actomyosin contractility in tumor cells and stroma. Cancer cell *20*, 229-245.

Sanz-Moreno, V., and Marshall, C.J. (2010). The plasticity of cytoskeletal dynamics underlying neoplastic cell migration. Current opinion in cell biology *22*, 690-696.

Sarbassov, D.D., Ali, S.M., and Sabatini, D.M. (2005). Growing roles for the mTOR pathway. Current opinion in cell biology *17*, 596-603.

Sarrio, D., Rodriguez-Pinilla, S.M., Dotor, A., Calero, F., Hardisson, D., and Palacios, J. (2006). Abnormal ezrin localization is associated with clinicopathological features in invasive breast carcinomas. Breast cancer research and treatment *98*, 71-79.

Saunders, C.M., Larman, M.G., Parrington, J., Cox, L.J., Royse, J., Blayney, L.M., Swann, K., and Lai, F.A. (2002). PLC zeta: a sperm-specific trigger of Ca(2+) oscillations in eggs and embryo development. Development *129*, 3533-3544.

Schmidt, S., and Friedl, P. (2010). Interstitial cell migration: integrin-dependent and alternative adhesion mechanisms. Cell and tissue research *339*, 83-92.

Schwab, A., Nechyporuk-Zloy, V., Fabian, A., and Stock, C. (2007). Cells move when ions and water flow. Pflugers Archiv : European journal of physiology *453*, 421-432.

Schwab, A., and Stock, C. (2014). Ion channels and transporters in tumour cell migration and invasion. Philosophical transactions of the Royal Society of London Series B, Biological sciences *369*, 20130102.

Scott, S.A., Selvy, P.E., Buck, J.R., Cho, H.P., Criswell, T.L., Thomas, A.L., Armstrong, M.D., Arteaga, C.L., Lindsley, C.W., and Brown, H.A. (2009). Design of isoform-selective phospholipase D inhibitors that modulate cancer cell invasiveness. Nature chemical biology *5*, 108-117.

Selvy, P.E., Lavieri, R.R., Lindsley, C.W., and Brown, H.A. (2011). Phospholipase D: enzymology, functionality, and chemical modulation. Chemical reviews *111*, 6064-6119.

Shaw, R.J., Henry, M., Solomon, F., and Jacks, T. (1998). RhoA-dependent phosphorylation and relocalization of ERM proteins into apical membrane/actin protrusions in fibroblasts. Molecular biology of the cell *9*, 403-419.

Shcherbina, A., Bretscher, A., Kenney, D.M., and Remold-O'Donnell, E. (1999). Moesin, the major ERM protein of lymphocytes and platelets, differs from ezrin in its insensitivity to calpain. FEBS letters *443*, 31-36.

Sheetz, M.P. (2001). Cell control by membrane-cytoskeleton adhesion. Nature reviews Molecular cell biology *2*, 392-396.

Sheetz, M.P., Felsenfeld, D., Galbraith, C.G., and Choquet, D. (1999). Cell migration as a five-step cycle. Biochemical Society symposium *65*, 233-243.

Shen, Y., Xu, L., and Foster, D.A. (2001). Role for phospholipase D in receptor-mediated endocytosis. Molecular and cellular biology *21*, 595-602.

Shen, Y., Zheng, Y., and Foster, D.A. (2002). Phospholipase D2 stimulates cell protrusion in v-Src-transformed cells. Biochemical and biophysical research communications *293*, 201-206.

Shiozaki, A., Nako, Y., Ichikawa, D., Konishi, H., Komatsu, S., Kubota, T., Fujiwara, H., Okamoto, K., Kishimoto, M., Marunaka, Y., *et al.* (2014). Role of the Na (+)/K (+)/2Cl(-) cotransporter NKCC1 in cell cycle progression in human esophageal squamous cell carcinoma. World journal of gastroenterology : WJG *20*, 6844-6859.

Sidhaye, V.K., Chau, E., Srivastava, V., Sirimalle, S., Balabhadrapatruni, C., Aggarwal, N.R., D'Alessio, F.R., Robinson, D.N., and King, L.S. (2012). A novel role for aquaporin-5 in enhancing microtubule organization and stability. PloS one *7*, e38717.

Simonin, A., and Fuster, D. (2010). Nedd4-1 and beta-arrestin-1 are key regulators of Na+/H+ exchanger 1 ubiquitylation, endocytosis, and function. The Journal of biological chemistry *285*, 38293-38303.

Small, J.V., Stradal, T., Vignal, E., and Rottner, K. (2002). The lamellipodium: where motility begins. Trends in cell biology *12*, 112-120.

Srivastava, J., Barreiro, G., Groscurth, S., Gingras, A.R., Goult, B.T., Critchley, D.R., Kelly, M.J., Jacobson, M.P., and Barber, D.L. (2008). Structural model and functional significance of pH-dependent talin-actin binding for focal adhesion remodeling. Proceedings of the National Academy of Sciences of the United States of America *105*, 14436-14441.

Sroka, J., von Gunten, M., Dunn, G.A., and Keller, H.U. (2002). Phenotype modulation in non-adherent and adherent sublines of Walker carcinosarcoma cells: the role of cell-substratum contacts and microtubules in controlling cell shape, locomotion and cytoskeletal structure. The international journal of biochemistry & cell biology *34*, 882-899.

Stahelin, R.V., Ananthanarayanan, B., Blatner, N.R., Singh, S., Bruzik, K.S., Murray, D., and Cho, W. (2004). Mechanism of membrane binding of the phospholipase D1 PX domain. The Journal of biological chemistry *279*, 54918-54926.

Steed, P.M., Clark, K.L., Boyar, W.C., and Lasala, D.J. (1998). Characterization of human PLD2 and the analysis of PLD isoform splice variants. FASEB journal : official publication of the Federation of American Societies for Experimental Biology *12*, 1309-1317.

Steeg, P.S. (2006). Tumor metastasis: mechanistic insights and clinical challenges. Nature medicine *12*, 895-904.

Stock, C., Ludwig, F.T., and Schwab, A. (2012). Is the multifunctional Na(+)/H(+) exchanger isoform 1 a potential therapeutic target in cancer? Current medicinal chemistry *19*, 647-660.

Stockem, W., Hoffmann, H.U., and Gawlitta, W. (1982). Spatial organization and fine structure of the cortical filament layer in normal locomoting Amoeba proteus. Cell and tissue research *221*, 505-519.

Stoddard, N.C., and Chun, J. (2015). Promising pharmacological directions in the world of lysophosphatidic Acid signaling. Biomolecules & therapeutics *23*, 1-11.

Stroka, K.M., Jiang, H., Chen, S.H., Tong, Z., Wirtz, D., Sun, S.X., and Konstantopoulos, K. (2014). Water permeation drives tumor cell migration in confined microenvironments. Cell *157*, 611-623.

Su, W., Chen, Q., and Frohman, M.A. (2009a). Targeting phospholipase D with small-molecule inhibitors as a potential therapeutic approach for cancer metastasis. Future Oncol *5*, 1477-1486.

Su, W., Yeku, O., Olepu, S., Genna, A., Park, J.S., Ren, H., Du, G., Gelb, M.H., Morris, A.J., and Frohman, M.A. (2009b). 5-Fluoro-2-indolyl des-chlorohalopemide (FIPI), a phospholipase D pharmacological inhibitor that alters cell spreading and inhibits chemotaxis. Molecular pharmacology *75*, 437-446.

Sugars, J.M., Cellek, S., Manifava, M., Coadwell, J., and Ktistakis, N.T. (1999). Fatty acylation of phospholipase D1 on cysteine residues 240 and 241 determines localization on intracellular membranes. The Journal of biological chemistry *274*, 30023-30027.

Suh, B.C., and Hille, B. (2005). Regulation of ion channels by phosphatidylinositol 4,5-bisphosphate. Current opinion in neurobiology *15*, 370-378.

Suh, P.G., Park, J.I., Manzoli, L., Cocco, L., Peak, J.C., Katan, M., Fukami, K., Kataoka, T., Yun, S., and Ryu, S.H. (2008). Multiple roles of phosphoinositide-specific phospholipase C isozymes. BMB reports *41*, 415-434.

Sun, L., Mao, G., Kunapuli, S.P., Dhanasekaran, D.N., and Rao, A.K. (2007). Alternative splice variants of phospholipase C-beta2 are expressed in platelets: effect on Galphaq-dependent activation and localization. Platelets *18*, 217-223.

Svitkina, T.M., Verkhovsky, A.B., McQuade, K.M., and Borisy, G.G. (1997). Analysis of the actin-myosin II system in fish epidermal keratocytes: mechanism of cell body translocation. The Journal of cell biology *139*, 397-415.

Takahashi, E., Abe, J., Gallis, B., Aebersold, R., Spring, D.J., Krebs, E.G., and Berk, B.C. (1999). p90(RSK) is a serum-stimulated Na+/H+ exchanger isoform-1 kinase. Regulatory phosphorylation of serine 703 of Na+/H+ exchanger isoform-1. The Journal of biological chemistry *274*, 20206-20214.

Takesono, A., Heasman, S.J., Wojciak-Stothard, B., Garg, R., and Ridley, A.J. (2010). Microtubules regulate migratory polarity through Rho/ROCK signaling in T cells. PloS one *5*, e8774.

Tanaka, O., and Kondo, H. (1994). Localization of mRNAs for three novel members (beta 3, beta 4 and gamma 2) of phospholipase C family in mature rat brain. Neuroscience letters *182*, 17-20.

Tinevez, J.Y., Schulze, U., Salbreux, G., Roensch, J., Joanny, J.F., and Paluch, E. (2009). Role of cortical tension in bleb growth. Proceedings of the National Academy of Sciences of the United States of America *106*, 18581-18586.

Tominaga, T., and Barber, D.L. (1998). Na-H exchange acts downstream of RhoA to regulate integrin-induced cell adhesion and spreading. Molecular biology of the cell *9*, 2287-2303.

Tominaga, T., Ishizaki, T., Narumiya, S., and Barber, D.L. (1998). p160ROCK mediates RhoA activation of Na-H exchange. The EMBO journal *17*, 4712-4722.

Tournaviti, S., Hannemann, S., Terjung, S., Kitzing, T.M., Stegmayer, C., Ritzerfeld, J., Walther, P., Grosse, R., Nickel, W., and Fackler, O.T. (2007). SH4-domain-induced plasma

membrane dynamization promotes bleb-associated cell motility. Journal of cell science *120*, 3820-3829.

Trinkaus, J.P. (1973). Surface activity and locomotion of Fundulus deep cells during blastula and gastrula stages. Developmental biology *30*, 69-103.

Tsukaguchi, H., Shayakul, C., Berger, U.V., Mackenzie, B., Devidas, S., Guggino, W.B., van Hoek, A.N., and Hediger, M.A. (1998). Molecular characterization of a broad selectivity neutral solute channel. The Journal of biological chemistry *273*, 24737-24743.

Vahle, A.K., Domikowsky, B., Schwoppe, C., Krahling, H., Mally, S., Schafers, M., Hermann, S., Shahin, V., Haier, J., Schwab, A., *et al.* (2014). Extracellular matrix composition and interstitial pH modulate NHE1-mediated melanoma cell motility. International journal of oncology *44*, 78-90.

Valastyan, S., and Weinberg, R.A. (2011). Tumor metastasis: molecular insights and evolving paradigms. Cell *147*, 275-292.

Valentin, G., Haas, P., and Gilmour, D. (2007). The chemokine SDF1a coordinates tissue migration through the spatially restricted activation of Cxcr7 and Cxcr4b. Current biology : CB *17*, 1026-1031.

van Kempen, L.C., van den Oord, J.J., van Muijen, G.N., Weidle, U.H., Bloemers, H.P., and Swart, G.W. (2000). Activated leukocyte cell adhesion molecule/CD166, a marker of tumor progression in primary malignant melanoma of the skin. The American journal of pathology *156*, 769-774.

Verkman, A.S. (2008). Mammalian aquaporins: diverse physiological roles and potential clinical significance. Expert reviews in molecular medicine *10*, e13.

Verkman, A.S. (2011). Aquaporins at a glance. Journal of cell science *124*, 2107-2112.

Verkman, A.S. (2012). Aquaporins in clinical medicine. Annual review of medicine *63*, 303-316.

Verkman, A.S., Anderson, M.O., and Papadopoulos, M.C. (2014). Aquaporins: important but elusive drug targets. Nature reviews Drug discovery *13*, 259-277.

Verkman, A.S., Hara-Chikuma, M., and Papadopoulos, M.C. (2008). Aquaporins--new players in cancer biology. J Mol Med (Berl) *86*, 523-529.

Vial, E., Sahai, E., and Marshall, C.J. (2003). ERK-MAPK signaling coordinately regulates activity of Rac1 and RhoA for tumor cell motility. Cancer cell *4*, 67-79.

Vitorino, P., and Meyer, T. (2008). Modular control of endothelial sheet migration. Genes & development *22*, 3268-3281.

Wagner, K., and Brezesinski, G. (2007). Phospholipase D activity is regulated by product segregation and the structure formation of phosphatidic acid within model membranes. Biophysical journal *93*, 2373-2383.

Wakabayashi, S., Ikeda, T., Iwamoto, T., Pouyssegur, J., and Shigekawa, M. (1997). Calmodulin-binding autoinhibitory domain controls "pH-sensing" in the Na+/H+ exchanger NHE1 through sequence-specific interaction. Biochemistry *36*, 12854-12861.

Wakayama, T., Nakata, H., Kurobo, M., Sai, Y., and Iseki, S. (2009). Expression, localization, and binding activity of the ezrin/radixin/moesin proteins in the mouse testis. The journal of histochemistry and cytochemistry : official journal of the Histochemistry Society *57*, 351-362.

Wang, W., Goswami, S., Sahai, E., Wyckoff, J.B., Segall, J.E., and Condeelis, J.S. (2005). Tumor cells caught in the act of invading: their strategy for enhanced cell motility. Trends in cell biology *15*, 138-145.

Wang, X. (2002). Phospholipase D in hormonal and stress signaling. Current opinion in plant biology *5*, 408-414.

Wang, X. (2004). Lipid signaling. Current opinion in plant biology *7*, 329-336.

Wang, Y., Litvinov, R.I., Chen, X., Bach, T.L., Lian, L., Petrich, B.G., Monkley, S.J., Kanaho, Y., Critchley, D.R., Sasaki, T., *et al.* (2008). Loss of PIP5KIgamma, unlike other PIP5KI isoforms, impairs the integrity of the membrane cytoskeleton in murine megakaryocytes. The Journal of clinical investigation *118*, 812-819.

Wang, Z., and Schey, K.L. (2011). Aquaporin-0 interacts with the FERM domain of ezrin/radixin/moesin proteins in the ocular lens. Investigative ophthalmology & visual science *52*, 5079-5087.

Ward, P.D., Ouyang, H., and Thakker, D.R. (2003). Role of phospholipase C-beta in the modulation of epithelial tight junction permeability. The Journal of pharmacology and experimental therapeutics *304*, 689-698.

Warth, A., Kroger, S., and Wolburg, H. (2004). Redistribution of aquaporin-4 in human glioblastoma correlates with loss of agrin immunoreactivity from brain capillary basal laminae. Acta neuropathologica *107*, 311-318.

Webb, B.A., Chimenti, M., Jacobson, M.P., and Barber, D.L. (2011). Dysregulated pH: a perfect storm for cancer progression. Nature reviews Cancer *11*, 671-677.

Weidinger, G., Stebler, J., Slanchev, K., Dumstrei, K., Wise, C., Lovell-Badge, R., Thisse, C., Thisse, B., and Raz, E. (2003). dead end, a novel vertebrate germ plasm component, is required for zebrafish primordial germ cell migration and survival. Current biology : CB *13*, 1429-1434.

Weigelt, B., and Downward, J. (2012). Genomic Determinants of PI3K Pathway Inhibitor Response in Cancer. Frontiers in oncology *2*, 109.

Weigelt, B., Peterse, J.L., and van 't Veer, L.J. (2005). Breast cancer metastasis: markers and models. Nature reviews Cancer *5*, 591-602.

Weinman, E.J., Hall, R.A., Friedman, P.A., Liu-Chen, L.Y., and Shenolikar, S. (2006). The association of NHERF adaptor proteins with g protein-coupled receptors and receptor tyrosine kinases. Annual review of physiology *68*, 491-505.

Wen, W., Yan, J., and Zhang, M. (2006). Structural characterization of the split pleckstrin homology domain in phospholipase C-gamma1 and its interaction with TRPC3. The Journal of biological chemistry *281*, 12060-12068.

Wicha, M.S., Liu, S., and Dontu, G. (2006). Cancer stem cells: an old idea--a paradigm shift. Cancer research *66*, 1883-1890; discussion 1895-1886.

Wolf, K., Mazo, I., Leung, H., Engelke, K., von Andrian, U.H., Deryugina, E.I., Strongin, A.Y., Brocker, E.B., and Friedl, P. (2003). Compensation mechanism in tumor cell migration: mesenchymal-amoeboid transition after blocking of pericellular proteolysis. The Journal of cell biology *160*, 267-277.

Wolf, K., Wu, Y.I., Liu, Y., Geiger, J., Tam, E., Overall, C., Stack, M.S., and Friedl, P. (2007). Multi-step pericellular proteolysis controls the transition from individual to collective cancer cell invasion. Nature cell biology *9*, 893-904.

Wymann, M.P., and Schneiter, R. (2008). Lipid signalling in disease. Nature reviews Molecular cell biology *9*, 162-176.

Yan, W., Nehrke, K., Choi, J., and Barber, D.L. (2001). The Nck-interacting kinase (NIK) phosphorylates the Na+-H+ exchanger NHE1 and regulates NHE1 activation by platelet-derived growth factor. The Journal of biological chemistry *276*, 31349-31356.

Yang, B., Gillespie, A., Carlson, E.J., Epstein, C.J., and Verkman, A.S. (2001). Neonatal mortality in an aquaporin-2 knock-in mouse model of recessive nephrogenic diabetes insipidus. The Journal of biological chemistry *276*, 2775-2779.

Yang, B., and Verkman, A.S. (1997). Water and glycerol permeabilities of aquaporins 1-5 and MIP determined quantitatively by expression of epitope-tagged constructs in Xenopus oocytes. The Journal of biological chemistry *272*, 16140-16146.

Yang, B., Zador, Z., and Verkman, A.S. (2008a). Glial cell aquaporin-4 overexpression in transgenic mice accelerates cytotoxic brain swelling. The Journal of biological chemistry *283*, 15280-15286.

Yang, H.S., and Hinds, P.W. (2003). Increased ezrin expression and activation by CDK5 coincident with acquisition of the senescent phenotype. Molecular cell *11*, 1163-1176.

Yang, J.S., Gad, H., Lee, S.Y., Mironov, A., Zhang, L., Beznoussenko, G.V., Valente, C., Turacchio, G., Bonsra, A.N., Du, G., *et al.* (2008b). A role for phosphatidic acid in COPI vesicle fission yields insights into Golgi maintenance. Nature cell biology *10*, 1146-1153.

Yap, A.S., and Kovacs, E.M. (2003). Direct cadherin-activated cell signaling: a view from the plasma membrane. The Journal of cell biology *160*, 11-16.

Yasui, M., Hazama, A., Kwon, T.H., Nielsen, S., Guggino, W.B., and Agre, P. (1999). Rapid gating and anion permeability of an intracellular aquaporin. Nature *402*, 184-187.

Yi, Y.H., Chang, Y.S., Lin, C.H., Lew, T.S., Tang, C.Y., Tseng, W.L., Tseng, C.P., and Lo, S.J. (2012). Integrin-mediated membrane blebbing is dependent on sodium-proton exchanger 1 and sodium-calcium exchanger 1 activity. The Journal of biological chemistry *287*, 10316-10324.

Yi, Y.H., Ho, P.Y., Chen, T.W., Lin, W.J., Gukassyan, V., Tsai, T.H., Wang, D.W., Lew, T.S., Tang, C.Y., Lo, S.J., *et al.* (2009). Membrane targeting and coupling of NHE1-integrinalphaIIbbeta3-NCX1 by lipid rafts following integrin-ligand interactions trigger Ca2+ oscillations. The Journal of biological chemistry *284*, 3855-3864.

Yonemura, S., Hirao, M., Doi, Y., Takahashi, N., Kondo, T., and Tsukita, S. (1998). Ezrin/radixin/moesin (ERM) proteins bind to a positively charged amino acid cluster in the

juxta-membrane cytoplasmic domain of CD44, CD43, and ICAM-2. The Journal of cell biology *140*, 885-895.

Yonemura, S., Matsui, T., and Tsukita, S. (2002). Rho-dependent and -independent activation mechanisms of ezrin/radixin/moesin proteins: an essential role for polyphosphoinositides in vivo. Journal of cell science *115*, 2569-2580.

Yoshida, K., and Soldati, T. (2006). Dissection of amoeboid movement into two mechanically distinct modes. Journal of cell science *119*, 3833-3844.

Zeng, X.X., Zheng, X., Xiang, Y., Cho, H.P., Jessen, J.R., Zhong, T.P., Solnica-Krezel, L., and Brown, H.A. (2009). Phospholipase D1 is required for angiogenesis of intersegmental blood vessels in zebrafish. Developmental biology *328*, 363-376.

Zeniou-Meyer, M., Zabari, N., Ashery, U., Chasserot-Golaz, S., Haeberle, A.M., Demais, V., Bailly, Y., Gottfried, I., Nakanishi, H., Neiman, A.M., *et al.* (2007). Phospholipase D1 production of phosphatidic acid at the plasma membrane promotes exocytosis of large dense-core granules at a late stage. The Journal of biological chemistry *282*, 21746-21757.

Zhang, J., Xiong, Y., Lu, L.X., Wang, H., Zhang, Y.F., Fang, F., Song, Y.L., and Jiang, H. (2013). AQP1 expression alterations affect morphology and water transport in Schwann cells and hypoxia-induced up-regulation of AQP1 occurs in a HIF-1alpha-dependent manner. Neuroscience *252*, 68-79.

Zhang, Z., Chen, Z., Song, Y., Zhang, P., Hu, J., and Bai, C. (2010). Expression of aquaporin 5 increases proliferation and metastasis potential of lung cancer. The Journal of pathology *221*, 210-220.

Zhao, C., Du, G., Skowronek, K., Frohman, M.A., and Bar-Sagi, D. (2007). Phospholipase D2-generated phosphatidic acid couples EGFR stimulation to Ras activation by Sos. Nature cell biology *9*, 706-712.

Zhao, S., Liao, H., Ao, M., Wu, L., Zhang, X., and Chen, Y. (2014). Fixation-induced cell blebbing on spread cells inversely correlates with phosphatidylinositol 4,5-bisphosphate level in the plasma membrane. FEBS open bio *4*, 190-199.

Zheng, Y., Rodrik, V., Toschi, A., Shi, M., Hui, L., Shen, Y., and Foster, D.A. (2006). Phospholipase D couples survival and migration signals in stress response of human cancer cells. The Journal of biological chemistry *281*, 15862-15868.

Zhou, Y., Wing, M.R., Sondek, J., and Harden, T.K. (2005). Molecular cloning and characterization of PLC-eta2. The Biochemical journal *391*, 667-676.

Zouwail, S., Pettitt, T.R., Dove, S.K., Chibalina, M.V., Powner, D.J., Haynes, L., Wakelam, M.J., and Insall, R.H. (2005). Phospholipase D activity is essential for actin localization and actin-based motility in Dictyostelium. The Biochemical journal *389*, 207-214.